Measurement and Modelling of Phase Equilibrium of Oil - Water - Polar Chemicals

Frost, Michael Grynnerup

Publication date:
2014

Document Version
Publisher's PDF, also known as Version of record

Measurement and Modelling of Phase Equilibrium of Oil - Water - Polar Chemicals

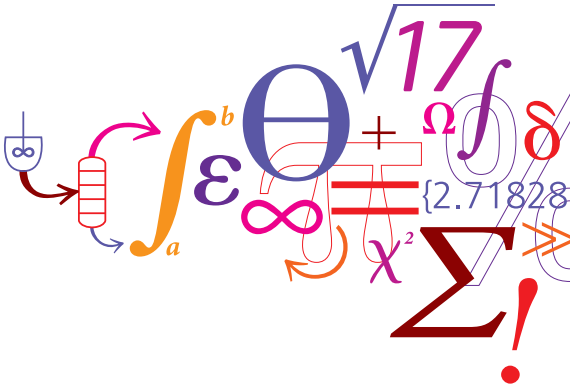

Michael Frost
Ph.D. Thesis
November 2014

Measurement and Modelling of Phase Equilibrium of Oil – Water - Polar Chemicals

Ph.D. Thesis

Michael Frost

November 2014

Supervisors:

Professor Georgios M. Kontogeorgis

Associate Professor Nicolas von Solms

Center for Energy Resources Engineering

Department of Chemical and Biochemical Engineering

Technical University of Denmark (DTU)

DK-2800 Lyngby, Denmark

Address: Center for Energy Resources Engineering
Department of Chemical and
Biochemical Engineering
Technical University of Denmark
Søltofts Plads, Building 229
DK-2800 Kgs. Lyngby
Denmark
Phone: +45 4525 2800
Fax: +45 4525 4588
Web: www.cere.dtu.dk

Print: J&R Frydenberg A/S
København
March 2015

ISBN: 978-87-93054-63-9

Preface

This thesis is submitted in partial fulfillment of the requirements for the Ph.D. degree at the Technical University of Denmark (DTU). The work was carried out at the Department of Chemical and Biochemiocal Engineering, DTU, from June 2011 to November 2014 under the supervision of Professor Georgios M. Kontogeorgis and Associate Professor Nicolas von Solms. The project was funded by Statoil, and the work has been carried out in close collaboration with Statoil, including an external stay at Statoil Research and Development Center, Trondheim, Norway.

I wish to thank my supervisors for supporting me throughout the project and their guidance and support on the research presented in this thesis. Your deep involvement has been very helpful in this project. You have been a source of inspiration for me throughout this project due to your passion and dedication towards research. I am very grateful for the opportunity to do this project, which has been a great experience for me. Thank you for giving me the possibility and the free hands to involve myself into experimental work, an area that has truly captured me. I would like to thank the technicians for all the help and assistance when working in the lab, this work would not have been possible without you. A special thanks to Professor Dominique Richon, who stayed at our research center as an Otto Mønsted visiting Professor. You were a great inspiration, your training and guidance gave me enthusiasm for instrumentation and design of new experimental equipment.

My thanks to co-workers at the Statoil Research Centre who helped me with the experimental part of this work regarding oil mixtures. Thanks to Toril Haugum and Ingunn Tanem for help regarding work in the lab and training me in SimDist analysis. Big thanks to Dr. Even Solbraa, for guidance and input during this project. I wish to acknowledge Statoil for the financial support of this work and for giving permission to publish all the experimental results I obtained during my stay in Trondheim.

I would like to thank all the colleagues who have helped me throughout this project, from top management to secretaries, professors, researches and Ph.D. students. A special thanks to my fellow colleagues in the CHIGP project, Ioannis, Bjørn, Xiadong and Martin, for many fruitful discussions, exiting project meetings and participation in international conferences. I would like to thank Louise and Patricia for all the practical assistance during my Ph.D., your help has been very valuable.

A special thank you goes to my wife Signe, for your love, care and understanding throughout this project. You always encouraged me in the challenging moments of life. Thank you for our wonderful daughter, Sofie, who was born during this Ph.D., you are both always in my thoughts.

November 07, 2014

Michael Frost

Summary

As the exploitable resources decrease, more sophisticated recovery methods are employed in the oil industry to produce the remaining resources. A result of using more sophisticated recovery methods is that oil field chemicals are more widely used, especially in the offshore oil production. These chemicals belong to different families like alcohols, glycols, alkanolamines, surfactants and polymers. They have various functions, e.g., methanol and MEG are used as gas hydrate inhibitors, surfactants are used to lower interfacial tension between crude oil and microemulsion and polymers in a polymer-waterflooding process act primarily as thickeners.

The main purpose of this work, focusing on the phase equilibrium of complex systems containing thermodynamic gas hydrate inhibitors, is to give a solid contribution in bridging the existing gaps in what experimental data is concerned. This was achieved not just with the measurement of new experimental data, but through the development of new experimental equipment for the study of multi-phase equilibrium. In addition to measurement of well-defined systems, LLE have been measured for North Sea oils with MEG and water.

The work can be split up into two parts:

- Experimental
    - VLE, LLE and VLLE
- Modeling
    - Well-defined systems
    - Oil systems

In the first part, an existing experimental set-up is described and the investigation of limitations and optimizations needed for optimal use. A complete description of the equipment is made, and the results obtained in the study of reference systems presented, confirming the quality of the equipment. The equipment is used for measurement of VLE for several systems of interest; methane + water, methane + methanol, methane + methanol + water and methane + MEG.
Details dealing with the design, assembling and testing of new experimental equipment for measuring VLLE are given in chapter 3. A general insight on the processes behind the development of new equipment is given, followed by the complete description of the set-up developed in this work. The results obtained in the study of reference systems are also presented, confirming the

quality of the equipment and its potential for the attainment of high quality data. Measurements were performed for VLLE of a multicomponent system consisting of methane + n-hexane + methanol + water.

In order to develop a thermodynamic model for the distribution of chemicals in oil-water systems experimental data are required, but such data with oil systems are very rare in the literature. In this project experimental work has been carried out at Statoil R&D and an experimental method has been established and tested for such measurements. The mutual solubility of two North Sea oils, MEG and water has been measured in the temperature range of 303-323 K at atmospheric pressure.

In the second part of this work, the CPA EoS has been used for modeling hydrocarbon system containing polar chemicals, such as water and gas hydrate inhibitor MEG or methanol. All the experimental data measured in this work have been investigated using CPA, with satisfactory results. A single temperature independent k_{ij} between the components present in the system, is usually enough to describe the solubility of all phases. Accurate predictions are made for VLLE of a quaternary system of methane + n-hexane + methanol + water, using the CPA EoS with binary interaction parameters taken from binary systems. Predictions are in good agreement with the experimental data, even for very low solubility, such as n-hexane in aqueous phase. In conclusion, the CPA EoS predicts satisfactorily the multiphase equilibrium of multicomponent water – alcohol – aliphatic hydrocarbon systems, based solely on the binary interaction parameters taken from binary systems, using the 2B association scheme for methanol and the 4C association scheme for water.

Finally, CPA has been extended to reservoir-fluid + MEG and reservoir-fluid + MEG + water systems. The reservoir fluid consists of three condensates and four oils from fields in the North Sea. The mutual solubility of oil and MEG is satisfactorily correlated using correlations for estimating k_{ij} for all MEG-HC pairs. Similarly the mutual solubility of condensate/oil, MEG and water is predicted satisfactorily using correlations for k_{ij} of all MEG-HC pairs and water-HC pairs, as a function of molecular weight. The experimental trends in mutual solubility as a function of temperature and MEG content in polar phase are predicted satisfactorily which are correct in order of magnitude according to the industrial requirements.

Resumé

I forbindelse med at verdens olie og gas ressourcer formindskes, introducerer olie industrien flere avancerede produktions metoder for at øge indvindingen af de resterende ressourcer. Resultatet af anvendelsen af nye avancerede metoder, er at olieudvindingskemikalier bliver brugt i en meget højere grad, især ved olieproduktion offshore. Disse kemikalier tilhører forskellige familier, såsom alkoholer, alkanolaminer, polymerer og mere. De har forskellige funktioner, f.eks. anvendes kemikalier som metanol og MEG som gas hydrat inhibitorer.

Hovedformålet med dette projekt, hvis fokus ligger på kemiske fase-ligevægte af komplekse blandinger indeholdende gas hydrat inhibitorer, er at give et solidt bidrag til de huller der findes blandt eksperimentelle data. Dette blev opnået, ikke blot ved måling af nye eksperimentelle data, men med udvikling og konstruktion af nyt udstyr, der kan anvendes til målinger af flere fase ligevægte. Ud over eksperimentelle data for veldefinerede systemer, er der blevet målt væske-væske ligevægt for olieblandinger fra Nordsøen, med MEG og vand.

Arbejdet kan deles op i to dele:

- Eksperimentelt
    - VLE, LLE og VLLE
- Modellering
    - Veldefinerede systemer
    - Olieblandinger

I første del beskrives et eksisterende udstyr, samt analyse af dens begrænsninger og nødvendige optimeringer for optimal anvendelse. Der bliver givet en komplet beskrivelse af udstyret, samt resultater for analyse af et reference system, som er med til at bevise kvaliteten af det eksperimentelle udstyr. Udstyret er anvendt til at måle VLE (gas-væske ligevægt) for flere kemiske blandinger af interesse for olie industrien; metan + vand, metan + metanol, metan + metanol + vand og metan + MEG.
Detaljer vedrørende design, konstruktion og test af nyudviklet udstyr anvendt til eksperimentel måling er af VLLE (gas-væske-væske ligevægt) beskrives i kapitel 3. Her gives en generel indsigt i de processer der finder sted ved udviklingen af denne type nyt udstyr, samt en beskrivelse af det udstyr som er blevet designet og konstrueret i dette arbejde. I dette kapitel vises ligeledes

eksperimentelle resultater der er opnået på et reference system, som er med til at validere kvaliteten af udstyret og dens potentiale for at producere data af høj kvalitet. Ved brug af dette udstyr, er der blevet målt VLLE for et flerkomponent system bestående af metan + n-hexan + metanol + vand. For at kunne udvikle en termodynamisk model, som er i stand til at forudsige fordelingen af kemikalier i oliesystemer, har man brug for eksperimentelle data. Denne type data er dog meget sjælden i litteraturen. I dette projekt er denne type eksperimenter udført i forbindelse med et ophold på Statoil R&D i Norge. Her blev der udviklet en eksperimentel metode, som viste sig anvendelig for denne type olieblandinger. Ligevægte mellem to Nordsø olie og MEG/vand er blevet målt i temperatur området 303-323 K og ved atmosfærisk tryk.
I anden halvdel af denne afhandling anvendes tilstandsligningen CPA (Cubic-Plus-Association), til at modellere systemer bestående af kulbrinter og polære kemikalier som vand og gas hydrat inhibitorer (MEG/metanol). CPA er blevet anvendt for alle eksperimentelle data produceret i dette projekt, med tilfredsstillende resultater. Der anvendes en enkelt temperatur uafhængig k_{ij} mellem de komponenter der er til stede, som ofte er nok til korrekt beskrivelse af alle tilstedeværende faser. Gode forudsigelser er opnået for VLLE af flerkomponent systemet metan + n-hexan + metanol + vand, ved anvendelsen af CPA med binære interaktions parametre taget fra binære systemer. Forudsigelserne stemmer godt overens med de eksperimentelle data, selv for meget lav opløselighed, såsom n-hexan i væskefasen. Konkluderende, CPA kan tilfredsstillende forudsige flerfase ligevægt i flerkomponentblandinger med vand – alkohol – alifatiske kulbrinter, ved anvendelsen af binære interaktions parametre taget fra de binære systemer og brugen af 2B association ordning for metanol, samt 4C association ordning for vand.

Afsluttende er CPA blevet forlænget til anvendelse for olieblandinger med polære kemikalier (MEG/vand). Disse olieblandinger består af tre gas kondensater og fire olier fra Nordsøen. Den kemiske ligevægt mellem olie og MEG beskrives tilfredsstillende, ved brugen af korrelationer til at estimere k_{ij} mellem MEG of kulbrinter. Ligeledes opnås tilfredsstillende forudsigelser for ligevægten mellem olie, MEG og vand, ved brugen af korrelationer til at estimere k_{ij} mellem MEG-kulbrinter og vand-kulbrinter, som funktion af kulbrintens molekylvægt. De eksperimentelle tendenser i opløseligheden som funktion af temperaturen, og MEG opløselighed i den polære fase, er fanget med god nøjagtighed, som ligger i en korrekt størrelsesorden ifølge de industrielle krav.

Table of Contents

Chapter 1 – Introduction

As the deep water oil and gas exploration are continuously increasing, the complex phase behavior between petroleum fluids and polar chemicals such as water, methanol or glycols has gained increasing attention. Vast quantities of so-called "production chemicals" are introduced to the systems, in order to facilitate production from reservoirs and transport in pipelines. Examples of such chemicals are hydrate inhibitors, such as methanol or glycols, which are injected to the natural gas well stream, in order to prevent the formation of gas hydrates during transportation and further processing. The trend towards long distance multiphase flow pipelines, which are based on the seabed, increases the need for accurate calculations of mixtures containing water, an inhibitor, a gas phase and a condensed phase.

Hydrates, or clathrates, are crystalline solid compounds formed when water assumes a cage-like structure around smaller guest molecules such as the ones present in natural gas, and their discovery is usually credited to Sir Humphrey Davy, in 1810 [1]. The relevance of the problem is increasing with the exploration of arctic fields and the tendency towards longer offshore pipelines, placed on the seabed. The blocking of a pipeline due to the formation of hydrates translates into high economic losses, not only due to the need to remediate the situation, but also due to the consequent disruption in the production.
Compounds like methanol or ethylene glycol are good thermodynamic inhibitors, lowering the temperature of hydrate formation for a given pressure. But due to the occurrence of problems with the formation of hydrates under conditions in which problem-free operation would be expected, especially in places of peaks of flow such as choke valves, the tendency in the use of hydrate inhibitors has gone in the direction of applying considerable safety margins, with an excess of inhibitors being regularly used in the processes, with economical and environmental consequences. This increase in production chemicals is not only due to the fact that new fields are brought to production. But also due to the new solutions which have been applied, for instance the use of methanol for multiphase well stream transport from subsea wells. In addition mature fields (e.g.

Gullfaks and Statfjord in the North Sea) have increased needs for chemical based treatments like well treatment or water treatment [2].

Different methods and software can be used to obtain more or less accurate predictions of the conditions for hydrate formation, even for some complex systems, but the results are still poor for high pressure systems (above 30 MPa), systems with high concentrations of acid gas or for estimating the partition of the inhibitor between the aqueous and the organic phases [3]. In the prediction of phase equilibrium, there is still much room for improvement in the different methods, especially concerning the characterization of complex systems. In some cases, only precise and accurate experimental data from "real-life" systems can provide the necessary basis, not only to optimize the different processes, but also to reduce safety margins, leading to a reduction in the amounts of inhibitors used. Using only the amount of inhibitor that is strictly necessary for risk-free operation has inherent economic and environmental advantages.
The need for high-quality experimental phase equilibria data is true for the chemical industry in general. Examples include pharmaceutical processes, the food industry, chemical separation processes, refrigeration, reservoir simulation, gas processing, applications involving supercritical fluids or chromatography, and new fields such as ionic liquids, carbon dioxide sequestration and storage or "green solvents". All these areas deal with processes whose optimization is dependent on phase equilibria data. The importance of reliable and precise experimental phase equilibrium data is recognized by the scientific community as well as by industry. Richon [4] has documented statements by several prominent scientists and engineers, unanimously of the opinion that more high quality data is necessary. Even for simpler systems, which have been studied at various times over the years by different researchers, the data is sometimes scarce in particular ranges of pressure and temperature. In other cases, the abundance of data reveals considerable discrepancies in the results obtained by different research groups, as recently demonstrated for example by Folas et al. [5], who gathered several published values concerning the solubility of methane in water.

Despite the overwhelming importance of experimental data, reliable and precise measurements can be difficult to achieve and are often expensive and relatively slow, representing a serious investment, not only concerning the acquisition of equipment or the development of custom-made experimental set-ups, but also regarding human resources.

However, the costs for a company of using imprecise data can be much higher, and may have serious consequences where safety is concerned. Also, young researchers are sometimes influenced by the idea that performing calculations or simulations in an office is more comfortable than tedious hours spent in the lab, and that theoretical work will bring them more recognition and possibly publishable results at a faster rate. This may be the cause of the worrying lack of experimentalists, lamented in some of the cited statements in the article by Richon [4].
Another serious problem is the existence of experimental data of dubious quality. Either because the lack of experimental data prompts researchers with little or no experimental experience to go into the laboratory in order to produce data which they can use to back-up their models, or because of a lack of understanding of the sensitivity of some experimental aspects.

It is important to know the distribution of production chemicals in oil, water and gas streams because it is a key to the calculation of the amounts of chemicals required for a specific facility. It is also important information to fulfill the demand from the environmental perspective in order to know the amount of chemicals and hydrocarbons (HC) in a processed water stream for ensuring minimal impact on marine life. Furthermore, it is important for design and operation of separation equipment as well as to report the chemicals and water contents of fuel oil which may be crucial for downstream processing [6,7].
The distribution of the chemicals can either be measured experimentally or predicted using a suitable thermodynamic model. The experimental method is expensive and challenging, partly due to the difficulties involved in measurements of such low solubilities. An evidence for this is the scarcity of such experimental data (with natural gas condensate and oil) in the literature. Data are available for only few binaries and ternaries dealing with well-defined hydrocarbons, MEG and water systems [8-11]. However for the development and validation of a thermodynamic model, experimental data are required. Those data are scarce in general, especially for gas-condensates and oil mixtures.

The work presented in this dissertation, sets out to provide a modest yet solid contribution to bridging the gaps in experimental data, not only by measuring new data, but by developing new experimental equipment for the study of phase equilibria through the use of different methods. Beside the work on measurement of phase equilibria of well-defined systems (VLE/VLLE), work was carried out at Statoil Research Center in Norway, in order to measure mutual solubility data for

oil systems containing MEG and MEG + water. These systems of water, hydrocarbons and chemicals represent complex mixtures containing associating /polar and non-associating compounds.

Parallel to the experimental work, the Cubic Plus Association (CPA) equation of state (EoS) proposed by Kontogeorgis et al. [12], which has been shown previously is a suitable model for such mixtures [11], was used in the modelling of mixtures containing hydrocarbons, water and thermodynamic hydrate inhibitors. Such systems, containing associating compounds, are challenging from a theoretical point of view since the components form hydrogen bonds and often exhibit an unusual thermodynamic behavior.

References

[1] H. Davy, Philos Trans R Soc London 101 (**1811**) 1-35.

[2] Knudsen, B. L. 8th *International Oil Field Chemical Symbosium*, Geilo, **1997**.

[3] E. D. Sloan, *Fluid Phase Equilib.* 228-229 (**2005**) 67-74.

[4] D. Richon, *Pure Appl. Chem.* 81 (**2009**) 1769-1782.

[5] G. K. Folas, E. W. Froyna, J. Lovland, G. M. Kontogeorgis, E. Solbraa, *Fluid Phase Equilib.* 252 (**2007**) 162-174.

[6] Wei, Y. S. Sadus, R. J. *AIChE Journal,* 46 (**2000**) 169-196.

[7] Oliveira, M. B. Coutinho, J. A. P. Queimada, A. J. *Fluid Phase Equilibria* 258 (**2007**) 58-66.

[8] Folas, G. K. Kontogeorgis, G. M. Michelsen, M. L. Stenby, E. H. Solbraa, E. *Journal of Chemical & Engineering Data*, 51 (**2006)** 977-983.

[9] Derawi, S. O. Kontogeorgis, G. M. Stenby, E. H. Haugum, T. Fredheim, A. O. *Journal of Chemical & Engineering Data,* 47 (**2002)** 169-173.

[10] Razzouk, A. Naccoul, R. A. Mokbel, I. Duchet-Suchaux, P. Jose, J. Rauzy, E. Berro, C. *Journal of Chemical & Engineering Data,* 55 (**2010**) 1468-1472.

[11] Kontogeorgis, G. M. Folas, G. K. *Thermodynamic Models for Industrial Applications: From Classical and Advanced Mixing Rules to Association Theories*, 1st ed. Wiley, **2010**.

[12] Kontogeorgis, G. M. Voutsas, E. C. Yakoumis, I. V. Tassios, D. P. *Industrial & Engineering Chemistry Research*, 35 (**1996**) 4310-4318.

Chapter 2 – Experimental study of VLE of methane with gas hydrate inhibitors

There is a need for high-quality experimental phase equilibrium data in the chemical industry. This includes a wide range of different subjects, which all deal with processes that rely on phase equilibrium data for optimization. The importance of reliable and precise experimental phase equilibrium data is recognized by the scientific community as well as by industry, as it is also mentioned by Richon et. al. [1] "It is of utmost importance to have accurate experimental data available in order to develop accurate modeling for scientific and engineering purposes".
Despite the overwhelming importance of experimental data, reliable and precise measurements can be difficult to achieve and are often expensive and relatively slow, representing a serious investment. Computational models, molecular simulations and correlation methods can however be used in order to reduce the number of experimental data points to be measured. Ultimately, a combination of both experimental measurements and computational methods is desirable, but experimental data will always have a decisive role in the validation of theoretical methods and in the adjustment of parameters in correlations.

2.1 Introduction

A review of existing phase equilibrium data for the systems under consideration in this work reveals the need for new accurate and reliable data, preferably with full characterization of all the phases present in equilibrium.
While for some systems the data is very scarce, especially in particular ranges of pressure and temperature, for some better studied systems there are still considerable divergences in the results obtained by different research groups, as it was recently demonstrated in the work of Folas et al. [2], for the solubility of methane in water. In the analysis of articles in the literature, it was also found that often, a considerable part of the information available from the experiments is simply disregarded. Examples of this are several studies of solubility of one compound in another phase,

disregarding the determination of mutual solubilities, sometimes easily available with small changes in the experimental setup and in the procedure.
Other problems are related to experimental limitations in the complete analysis of some of the phases, mostly due to very low concentrations, such as in the determination of the water and glycol content in the gas phase. But as in many other areas, continuous technological developments have led to significant advances in the available instrumentation, with increased sensitivity, promoting the development of new methods and the enhancement of the existing ones, thus allowing not only the measurement of new data but also the evaluation of the existing values.
In this work, we set out to re-commission and optimize existing equipment with the purpose of measurement of multiphase equilibrium, described in 2012 by Fonseca et al. [3]. This chapter gives and introduction to the analytical isothermal cell (AnT Cell), which is used for vapor – liquid equilibrium measurements. The AnT Cell is optimized and tested on various systems of interest, where we tackle many of the issues that are present when measuring complex phase equilibrium. New experimental data are presented over a wide range of temperatures and pressures.

2.2 Experimental section

2.2.1 Description of the equipment

In this section of the work, the experimental set-up is presented. The set-up was specially designed for the measurement of multi-phase equilibria in hydrocarbon-water-hydrate inhibitor systems, at temperatures ranging from 213 K to 353 K and at pressures up to 40 MPa. A complete description of the design and construction of the equipment was given in the PhD by Fonseca [4]. The set-up is depicted in figure 2.1 and presented with schematics in figure 2.2. According to the classification proposed and described in two recent works [5,6], this method uses an isothermal analytical method, where special capillary valves are used for sampling, from a cell of variable volume, with a view window.

Figure 2.1: General aspect of the experimental set-up for the measurement of multi-phase equilibria, showing the cell inside the temperature chamber and the GC unit. Photo is taken at CERE labs.

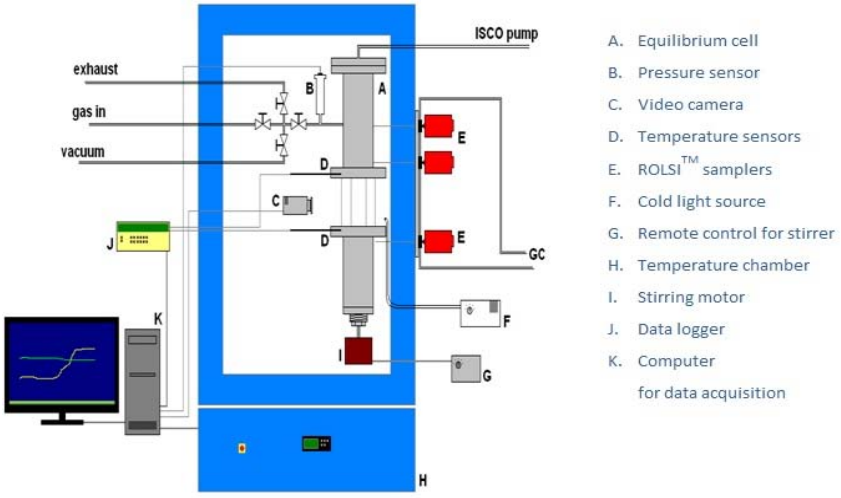

Figure 2.2: Schematic representation of the experimental set-up for the measurement of multiphase equilibria. – A: High pressure cell with 360º sapphire window. B: Temperature compensated high precision pressure sensor. C: Video camera. D: Platinum resistance thermometers Pt100. E: ROLSI™ samplers. F: Cold light source with optical fibre. G: Remote control for the stirring motor. H: Low temperature chamber. I: Stirring motor. J: Data logger. K: Computer.

The main part of the set-up is the variable-volume high-pressure equilibrium cell, specially designed for this application and equipped with a 360º sapphire window. The volume of the cell can be varied manually and automatically by means of a high pressure syringe pump. The temperature, measured in different points of the cell by platinum resistance thermometers is monitored and recorded over time through a computer, to which is also connected the temperature compensated pressure sensor.

Connected to the cell are three automatic Rapid On-Line Sampler Injectors (ROLSI™), which allow the withdrawing of very small samples from the different phases directly to the carrier gas stream. In the current configuration, the GC analysis is made using an Agilent 6890 GC System, equipped with an Agilent 7683B automatic injector, a HP-PLOT Q capillary column, and a thermal conductivity detector (TCD) coupled in series with a flame ionization detector (FID). A second computer using the software GC ChemStation is used for the acquisition and treatment of the GC data.

The cell is positioned close to the side wall of the temperature chamber, which is necessary due to the sampling system, in order to keep the connections to the ROLSI™ samplers, placed outside the chamber, as short as possible, since the thickness of the temperature chamber is already considerable, around 150 mm.

2.2.1.1 The equilibrium cell

The core part is the high pressure cell, equipped with a 360º sapphire window, and with an operating volume variable from approximately 116 cm^3 to 207 cm^3. The body of the cell can be seen in more detail in Figure 2.3 and 2.4, where a three dimensional computer generated image is presented, as well as an image with a cut of the cell, showing its interior.

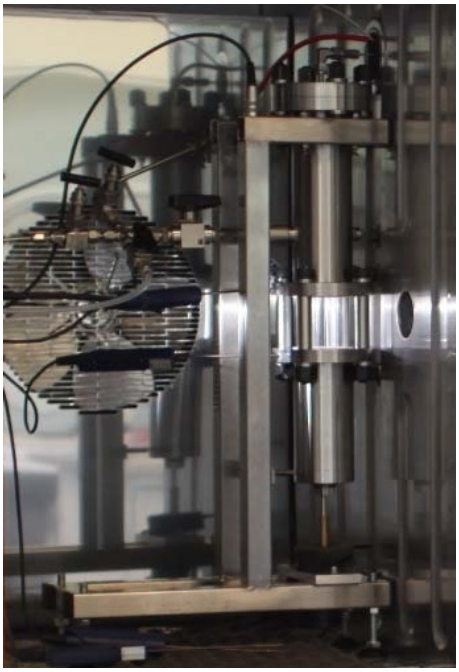

Figure 2.3: Image of the equilibrium cell mounted on a structure specially designed and constructed for this application, inside the temperature chamber. Photo is taken at CERE labs.

Figure 2.4: Three-dimensional computer generated images of the high pressure cell. – On the left: View of the cell. On the right: Cut of the cell showing its interior.

The cell is constituted by two stainless steel segments connected through a tube of sapphire that acts as a 360º window. The inner diameter of the cell varies from a maximum of 40 mm for the stainless steel segments to a minimum of 20 mm for the inner diameter of the sapphire tube. The sapphire has a wall thickness of 15 mm and it was dimensioned according to the properties of the material provided by the supplier, to cope with pressures of 40 MPa for extended periods of time, but also to pass the safety tests imposed by the internal rules at the department, according to which, the cell had to be tested for a pressure of approximately 133% of the maximum operating pressure (54 MPa).

Each of the stainless steel segments contains a piston in its interior, for regulation of the volume of the cell. This piston, of manual operation, is capable of inducing a 24 cm^3 difference in the volume of the cell, and it is intended to be adjusted in the beginning of a series of experiments, influencing the range of volumes available for those experiments. It can, however, be regulated at any time, allowing for example the height of the interface between two phases to be conveniety positioned on the sapphire window, or the adjustment of the position of the sampling points relatively to the different phases.

The piston has the purpose of compensating for any pressure drops that might result from the sampling process, although it can also be used to set a specific value of pressure in the cell, for example to promote the appearance of a new phase, or the observation of critical phenomena. The position of the piston is set by the balance between the pressure inside the cell and the pressure imposed by a high pressure syringe pump ISCO 100DX (Teledyne Isco, Inc., USA), using as pressure transmitting medium the thermal fluid Julabo Thermal HL80 (JULABO Labortechnik GmbH, Germany).

The total weight of the cell, including bolts and nuts, is over 15 kg, and although this affects its practicality, it provides the cell a high thermal inertia, related directly to the mass of the cell and the heat capacity of its constituent materials. A higher thermal inertia will contribute to a slower achievement of the programmed temperature, but this is largely compensated by the fact that once in equilibrium, the cell will attenuate the inevitable temperature oscillations inside the temperature chamber, especially when working at temperatures that differ greatly from the ambient temperature.

2.2.1.2 Temperature and pressure measurements

One of the main goals for this equipment is its extensive temperature range of operation, reaching values as low as 213 K. To accomplish this, the thermostatisation of the equilibrium cell was done using a temperature chamber WEISS WT 240/70, specially customized by the manufacturer, Weiss Umwelttechnik GmbH, Germany, for this application. With an internal working volume of 240 dm3 and equipped with a relatively large window in its front, this temperature chamber is designed to promote a stable temperature on its interior, in the range from 203 K to 453 K with temperature constancy better than ±0.7 K over time, according to the manufacturer.

Probably the most important parameters in any thermodynamic measurement are temperature and pressure. In phase equilibrium this is evident, regardless of the experimental method used.

The temperature of the cell is monitored with a resolution of 0.001 K and a precision of 0.01 K, through two four-wire platinum resistance thermometers Pt100 class 1/10 DIN, acquired from Dostmann Electronic GmbH, Germany, placed horizontally over and under the sapphire window, perpendicularly to each other, meaning that one of the sensors has its tip in the front side of the cell, while the other sensor has its tip in the back of the cell. This configuration is intended to readily detect any problems with the temperature uniformity in the cell. The thermometers, with a diameter of 3 mm, are inserted in specially cavities with thermal paste, in order to improve the thermal contact. In the absence of standard thermometry equipment in the laboratory, the temperature sensors were calibrated according to the International Temperature Scale ITS-90, at the triple point of water, through the careful measurement of their electrical resistance at that temperature. The thermometers are connected to a data acquisition system Agilent 34970A (Agilent Technologies, Inc., USA) which is in turn connected to a computer via a RS-232 connection, for monitoring and recording of the experimental conditions through the software Agilent BenchLink Data Logger 3 from the same manufacturer.

The pressure inside the cell is monitored by means of a temperature compensated, high precision, pressure transmitter Keller 33X (KELLER AG für Druckmesstechnik, Switzerland), for measurements up to 50 MPa with an accuracy of 0.1% of the full scale (0.05 MPa) over the whole temperature range of operation. This transmitter is equipped with a floating piezoresistive transducer and an internal microprocessor with an integrated 16-bit A/D converter. The zero of the sensor was adjusted against a Crouzet quartz mano 2100, calibrated by Buhl & Bønsøe A/S, a company accredited by DANAK, The Danish Accreditation and Metrology Fund.

2.2.1.3 Sampling

The sampling system consists of two automatic electromagnetic capillary ROLSI™ samplers, a product developed by the CENERG-TEP laboratory of the ENSMP (École Nationale Supérieure des Mines de Paris).

Developed specifically for phase equilibrium studies, The ROLSI™ samplers have been established as a reference worldwide, being currently used in many universities as well as in industry, in many research groups considered as a reference for phase equilibria and petroleum related studies [7-16].

These sampler-injectors, illustrated in Figure 2.5, are electromagnetic valves that allow taking samples from each of the phases without the disturbance of the other phases in equilibrium, and vaporizing them directly to the carrier gas stream of a gas chromatograph, without any manipulation of the samples.

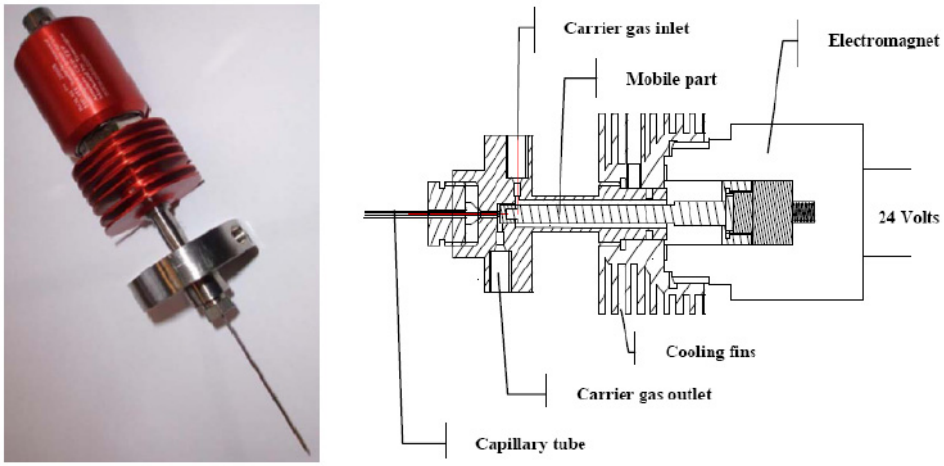

Figure 2.5: Electromagnetic ROLSI™ sampler [4]. – On the left: picture of the sampler. On the right: Schematic drawing of a sampler.

The samplers are designed to reduce the possibility of eventual pressure drops in the cell, by using tubes with an internal diameter varying from 0.10 mm to 0.15 mm. This increases the number of samples that can be taken for each equilibrium stage, before the equilibrium is changed.

Another parameter to influence the amount of withdrawn sample is the internal diameter of the capillaries tubes. Very thin capillaries, appropriate for sampling at pressures around 40 MPa, will not be adequate for sampling at pressures less than 1 MPa. Currently the setup is using capillaries that can be used with pressures between 5 MPa and 40 MPa.

The opening time of the samplers is controlled by a Crouzet Top 948 timer (Crouzet Automatismes SAS, France), and can be reduced to a minimum of 0.05 seconds. When a sample is withdrawn, an electronic signal is sent to the gas chromatograph in order for this unit to start recording a new chromatogram. The time between samplings can also be programmed so that a series of samplings can be programmed and run in a fully automated way. Both the ROLSITM samplers and the GC carrier gas line can be heated up to 523 K, through the use of West P6100 1/16 Din process controllers (West Instruments, UK).

Besides promoting the immediate vaporization of the samples, the heating has also the purpose of avoiding, or at least minimizing, the possible adsorption of the analytes in the carrier gas line, which would constitute a serious source of errors in the analysis, especially when dealing with samples containing very low amounts of some compounds. The segment of tubing that conducts the samples to the GC unit is made of deactivated fused-silica, much like an empty GC column, in an attempt to further minimize possible adsorption problems. Both the timer and the PID temperature controllers are supplied together with the samplers, in a control box whose front panel is shown in Figure 2.6.

Figure 2.6: Control panel for the ROLSI™ samplers, with the timer, the temperature controllers, and additional switches to choose from which valve to use at a given time.

2.2.2 Test and optimization

Due to many issues regarding difficult phase equilibrium measurements, equipment should often be tested very thoroughly and optimized accordingly. Ideally new equipment should always be designed and constructed for a specific purpose. However, since this is very expensive and time consuming, existing equipment is often re-commissioned, in order account for new systems.

Before running new experiments on this existing equipment, a series of test was performed, in order to validate and optimize. During these tests, several issues was found and solved.

2.2.2.1 Limitations of the existing equipment

Before running new experiments on this existing equipment, a series of tests were performed, in order to validate its effectiveness and capabilities/limitations. During these tests, several issues were encountered.

In order to obtain accurate results, carrier gas lines from the ROLSI™ samplers to the GC, needs to be properly heated to negate condensation in the lines. The equipment was tested using a volatile component (n-heptane), from which samples was withdrawn using the ROLSI™ and sent to the GC for analysis. This resulted in condensation of the n-heptane, which was observed as fluctuation of peak size (random sizes or completely missing) and changing retention times on the gas chromatograph. In the existing equipment, cold spots within the transfer lines were observed, which is a large factor in phase equilibrium measurements, and is often reason for acquiring wrong results.

Continuous control of ROLSI™ samplers is important, as they can be a large source of error. It is important to maintain a proper sampling size, and remove any leak that might occur. The ROLSI™ samplers are using a polymer seal, which can be subject for leaks, if not handled properly. Furthermore, the low internal diameter of the capillary tubes, used by the ROLSI™ samplers, can be the subject of contamination and blockage. An important factor when using the ROLSI™ samplers for phase equilibrium measurements is the ability to perform proper maintenance of the samplers. Especially due to the small samples withdrawn, any contaminations or blockages can contribute to large errors.

The existing equipment is fitted with three ROLSI™ samplers, as can be seen in figure 2.2, situated with bolts into the heating cabinet. In order to properly investigate leaks, it is important to test the

ROLSI™ samplers individually. No effective method was established for testing the ROLSI™ for leaks (contributing a considerable amount of time and effort).

The analytical isothermal cell was originall designed for measurement of multiphase equilibrium, VLE/VLLE. In order to obtain accurate results, the mixture needs to be in equilibrium. This is usually done by stirring the mixture, until the pressure is constant; indicating that no more is being transferred between phases. This is obviously very important in phase equilibrium measurements, and is an effect which is not always taken into account. Many discrepancies in phase equilibrium data can be contributed to the mixture not being completely in equilibrium. A thorough test has been performed on the existing equipment, for testing the stirring efficiency for both VLE and VLLE.

A test was performed on the binary system of nitrogen + n-heptane (VLE), in order to observe, how efficient equilibrium is achieved when two phases are present. It can be seen from figures 2.7 and 2.8 that equilibrium occurs within 500-1000 seconds after starting the stirring, which is considered to be efficient. The figures present the pressure within the equilibrium cell as a function of time (in s), with and without stirring. From figure 2.7, it can be seen why proper stirring is important, as equilibrium would not be obtained in reasonable time without it.

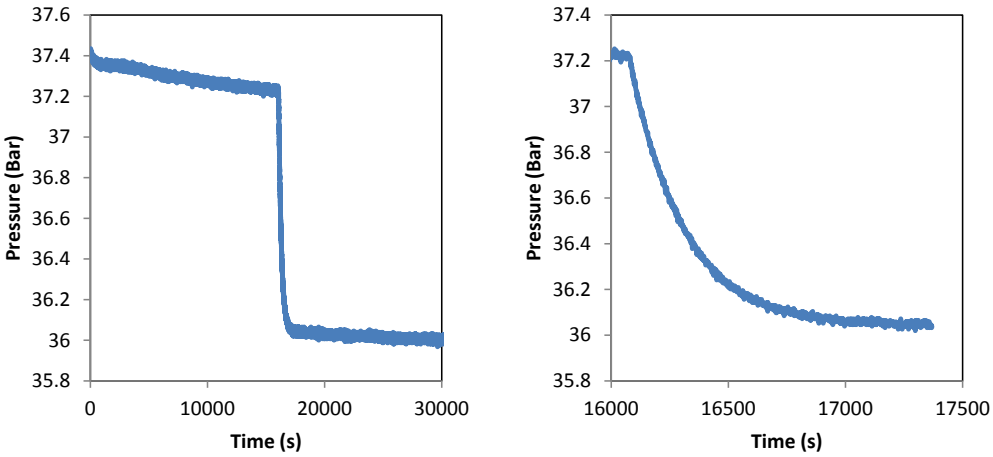

Figure 2.7: Measured pressure inside the equilibrium cell for the binary system of nitrogen and n-heptane. The pressure was measured before and after stirring was initiated.

The importance of proper stirring is increased, when adding to the amount of phases present in the mixture. Performing test on the VLLE system of carbon dioxide + water + bromododecane, the pressure was investigated as a function of time, with and without stirring. With this ternary mixture, a lot of issues regarding the stirring have been observed. A schematic of the stirring can be seen in figure 2.9. For proper stirring of a VLLE mixture, a good vortex is desired between all the phases (L1+L2 and L2+V), however, this is not the case for the existing equipment. It was seen that proper stirring only occurred between the two liquid phases. The right side of Figure 2.9 shows the observed vortex during experiment. Here only vortex between the lower phases is present.

The issue with stirring becomes even more evident, when we look at the equilibrium time, as seen in figure 2.8. For this specific mixture, more than one day of stirring was needed, before any signs of constant pressure were seen. Even after the end of stirring, pressure drops are observed, indicating that equilibrium was not completely achieved. The stirring is an integrated part of the equipment, and it is a complicated task to optimize this part, without completely changing the design. It is therefore advised, not to use the equipment in its current form for VLLE measurements.

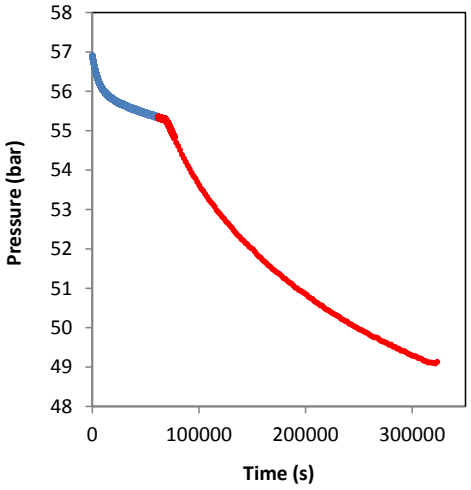

Figure 2.8: Measured pressure inside the equilibrium cell for the ternary system of carbon dioxide, water and bromododecane. The pressure was measured before (blue line) and after stirring was initiated (red line).

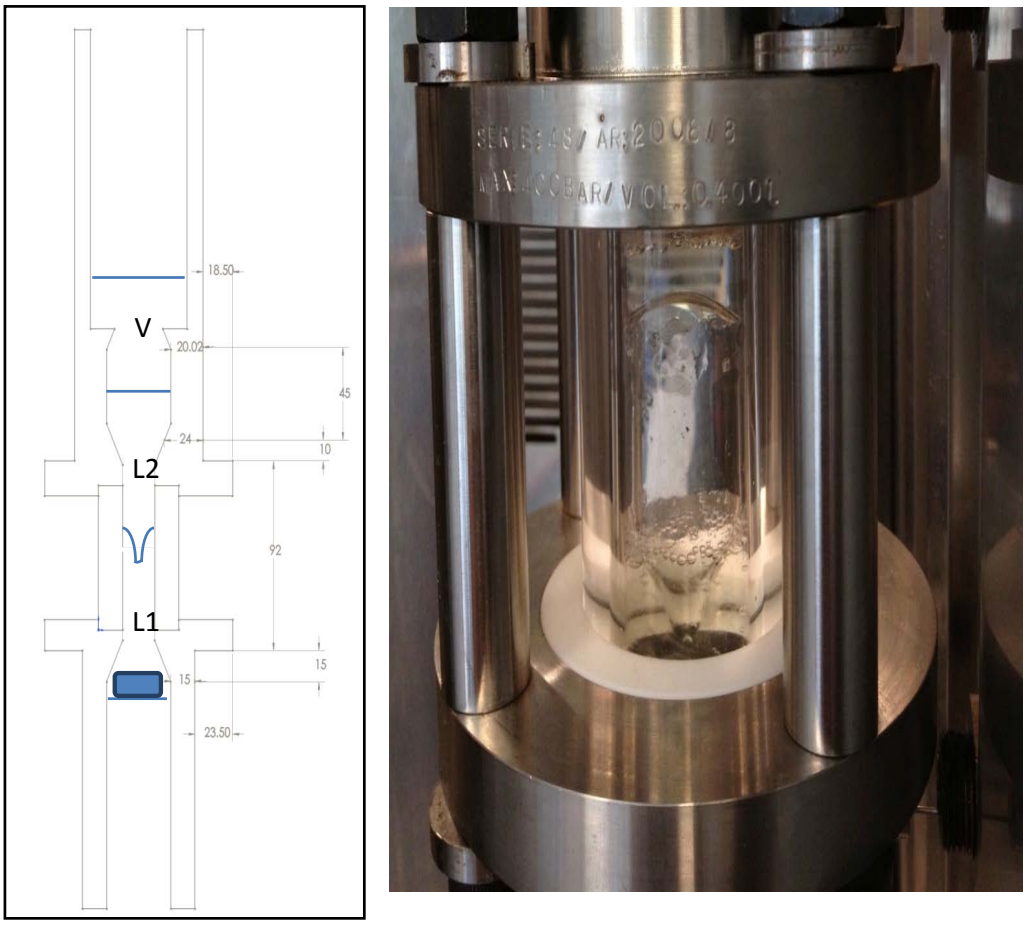

Figure 2.9: On the left - A schematic of the stirring inside the equilibrium cell. On the right – A picture of the stirring inside the cell.

2.2.2.2 Improvements of existing equipment

In addition to the mentioned limitations, the set-up was not in use for a long period of time, and several parts needed repair. It was therefore decided to make some small changes to the equipment, in order to, at least, overcome or minimize some of the perceived limitations.

The carrier gas lines has been improved by reducing the travel length (Distance between ROLSI™ and GC), while getting rid of the cold spots. Cold spots were observed, especially for the contact between transfer line and the gas chromatograph. The optimization of the transfer lines, with regards to length, will improve the quality of the analysis, since there is less travel distance (less

loss of components, due to the small samples withdrawn). Furthermore, the velocity of the gas flow is increased, which will greatly improve the peak sizes and general analysis on the gas chromatograph. Improvement of the transfer lines was performed, improving on both thermal and electrical coating for the transfer lines, as well as improving the fittings, by using special ordered Teflon fittings. This will ensure that the heating is uniform across the entire transfer line. Having uniform heating across the entire transfer will ensure that condensation of light components due to temperature changes is prevented. Using these improvements, the analysis on the gas chromatograph has been greatly improved. An example of this is the analysis of pure nitrogen, as seen in figure 2.10, where samples are drawn repeatedly from the equilibrium cell using the ROLSI™ samplers. High accuracy and reproducibility were observed with continuous sampling, which is one of the strengths of using the ROLSI™ samplers.

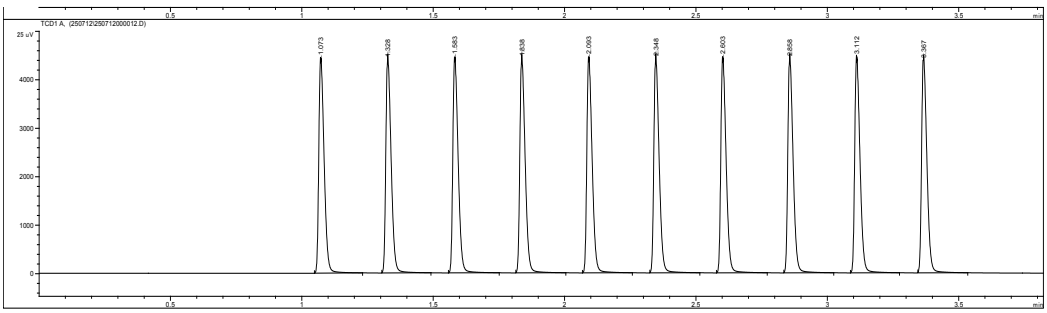

Figure 2.10: Peaks on the GC during continues sampling of pure nitrogen using the ROLSI™ samplers.

Continuous control of ROLSI™ samplers is important, as they can be a large source of error. It is important to maintain a proper sampling size, and remove any leak that might occur. The ROLSI™ samplers are using a polymer seal, which can be subject of large leaks, if not handled properly.

In order to optimize this equipment further, a large improvement has been put into handling these ROLSI™ samplers.

1. Disassembling and test of ROLSI™: By adding new mounting system, we have greatly improved the possibility of disassembling the ROLSI™ from the setup, which will save a lot of time and make it much easier to test individual samplers. (Makes it possible to remove the samplers individually, instead of having to dismount all of them each time)

2. Improving the testing of ROLSI™, by getting proper equipment (See figure 2.11): It is now possible to test the ROLSI™ samplers for leaking and clogging, without having to use the entire setup each time. Furthermore, it is possible to test them individually, which is important for detecting errors.

Figure 2.11: Equipment created for testing of ROLSI™ samplers. Allowing for pressure testing individual samplers.

In conclusion, additional modifications are imperative in order to deal with the existing problems, preferably involving not only simple changes in the configuration of the set-up, but also a strong effort in the modernization of the whole set-up, with the purpose of increasing the quality and precision of the results it could produce.

2.2.3 Experimental procedure

In the following description, the schematic diagram of Figure 2.2 should be considered. One of the first steps is the loading of the cell, with the different components to be studied. This can be performed using a syringe with a long needle through the valve, making it possible to determine the volume of the liquid compounds injected, either volumetrically, through the graduation in the syringe, or gravimetrically, by weighing the cell before and after the injection of the compound. After this, the degassing of the components can be performed, by connecting the valve system to

vacuum. In normal conditions of operation, the cell will be operated at high pressure, in order to allow the operation of the sampling system. This means that almost invariably, a pressurized gas will be loaded into the equilibrium cell. Once the interior of the cell is free from any air, the compressed gas can be loaded.

After loading the cell, the equilibration process can take place, after programming the temperature of the chamber in the computer. The collection and recording of temperature and pressure values over time can be done with any desired frequency. However it should be considered that some studies may last for several days, and that a high frequency in the collection of values may lead to a substantial amount of data, and consequently to files that will be more difficult to handle in a posterior analysis. In general, in this work, values of pressure and temperature were collected for recording every 10 minutes. In order to improve simplicity in a later analysis of the experiment conditions, it is useful if pressure and temperature are recorded in coincident points in time.
In the end of an experiment, the valves can be opened slowly for depressurization of the system. After depressurization, the liquid phases can be pumped out through a thin flexible tube.
Before further experiments, the cell should be carefully cleaned several times with an adequate solvent(s), and placed under vacuum for some hours, in order to evaporate possible traces of solvent before the preparation of a new experiment.

2.2.3.1 Chemical analysis using gas chromatography

Gas chromatography is a powerful and versatile method, well established in the petroleum industry, which has proven its effectiveness in the study of the type of systems considered in this project. Two different aspects of the application of gas chromatography should be considered. Firstly, it is necessary to achieve a good separation between the different components of the systems under study, which on its own allows only a qualitative analysis. This is related to the development of an appropriate chromatographic method, through the selection of an adequate column and the optimization of a number of experimental parameters. After this first stage, with the development of the separation process, it is then necessary to establish the relations between the area of the chromatographic peaks and the amount of each substance injected in the GC column, in order to create the basis for the desired quantitative analysis. These relations, usually linear in a specific range of conditions, are dependent on the nature of the compounds to be analyzed and on the type of detector installed on the GC. These relations can be determined by means of calibrations, which

can be performed in relative or absolute terms, giving rise respectively, to more restricted or more universal calibrations.

For a typical ternary system of interest for this work, containing water, a hydrocarbon and either methanol or glycol, the choice of the right column already entails a certain degree of complexity, since although relatively simple, such a system contains both polar and nonpolar compounds, and usually the columns adequate for the first type of compounds are not suitable for the second.
In this work, analysis of each phase was done using an Agilent 6890 GC System, fitted with a HP-PLOT Q capillary column, without the use of another column in parallel, a solution adopted in some of the works found in the literature [17-21]. As for detection, a flame ionization detector (FID) and a thermal conductivity detector (TCD) are used in series (FID detector being last). The flame ionisation detector (FID) is the most widely used and presents a very good sensibility to hydrocarbons. The thermal conductivity detector (TCD), in principle, a universal detector based on the difference in the thermal conductivities of the analytes and that of the carrier gas, at the temperature of the detector, is essential in this work for the detection of water. Information of the GC used in this work can be seen in table 2.1.

Table 2.1: Information on the gas chromatograph used for chemical analysis.

Characteristic	Agilent 6890 GC
Type	HP-PLOT/Q
Manufacturer	Agilent
Column Length	30 m
Column Internal Diameter	0.320 mm
Column Film Thickness	20 µm
Injector	0.1 µl
Carrier Gas	Helium
Detector Type	FID/TCD

The development of the chromatographic method consisted not only in the experimentation of different columns, but also in the development and testing of different experimental conditions such as the inlet temperature, detector temperature, column temperature and temperature program, nature of the carrier gas, carrier gas flow rates, etc., in order to optimize the separation of all the compounds in a typical multi-component system. The aim of this optimisation is to obtain well defined, narrow and symmetrical peaks for all the compounds involved. In addition to this, it is

desirable to reduce as much as possible the time necessary for each analysis, meaning that the retention times for all the components should be as low as possible, without causing an overlapping of the respective peaks in the chromatogram.

The generic chromatographic method used in this work is presented in table 2.2.

Table 2.2: List of parameters used for the generic chromatographic method used for analysis of the mixtures in this work.

Parameters	Setting
Temperature of the injector	200 °C / 473 K
Split ratio	25:1
Total flow	53 mL/min
Carrier gas	He
Temperature of TCD	250 °C / 523 K
Temperature of FID	250 °C / 523 K

The temperature program consisted in a 5 minutes plateau at a temperature of 60 ºC (333 K), followed by an increase in the temperature, at 20 K/min (9.5 minutes), before a new plateau at 250 ºC (523 K) for another 15 minutes, accounting for a total time of approximately 30 minutes. The temperature program is presented in figure 2.12.

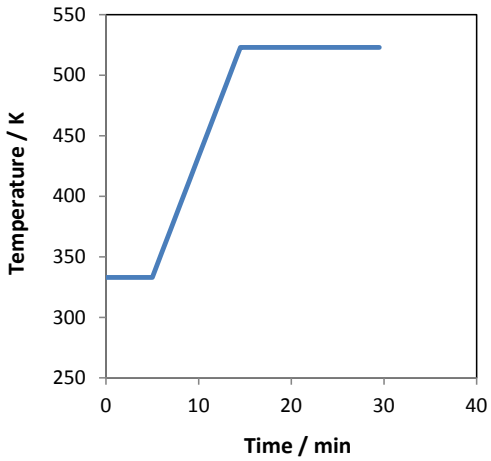

Figure 2.12: Temperature profile used on the gas chromatograph.

This analysis time can obviously still be reduced, just by changing the temperature program. This would be especially useful in studies of only two or three compounds. However, it should be taken into consideration that the chromatographic method presented is a generic method, developed to provide a basis for the generality of the analysis to be performed in the study of the type of systems under consideration in this work.

2.2.3.2 Calibration of the gas chromatograph

It is necessary to perform a calibration, in order to perform quantitative analyses from the phases in equilibrium in the cell. Often in phase equilibrium studies, the knowledge of the mole fractions in each phase is sufficient to characterize the system. In order to obtain such information from a chromatogram, it is only necessary to know the relative sensibility of the detectors to each of the components, and the information of the mole fraction is given by the ratio between the areas of the peaks. For such measurements, a calibration can be easily performed by calibrating independently each compound, obtaining a relation between the area of the peak in the chromatogram and the amount of compound injected. These calibrations are recommended, being valid for that particular compound regardless of the system under study. This means that, when a new system is placed under study, containing one or more components for which a calibration was previously made, a considerable amount of time can be saved since there is no need to calibrate for those compounds. It should be understood however, that a few injections of standard solutions should always be performed, in order to confirm that the previously made calibration is still valid. During experiments, the calibration is continuously tested.

Performing the calibrations, different amounts of a compound are injected, usually using diluted solutions with a precisely known concentration so that smaller amounts of the component of interest can be injected. To increase the quality of the calibration, the volume of each injection is precisely known, and the same exact volume is injected a number of times, in order to increase the accuracy. For liquid compounds, an automatic injector is used (Agilent 7683B), which makes it easy to reproduce the calibrations and increases accuracy. The calibration for gaseous compounds is performed manually by the use of gas-tight syringes, and is done by injecting a given volume.

2.2.4 Testing of equipment: Reference system

An important step in the validation of any experimental set-up, involves the study of reference systems or of other systems that have been studied frequently and by different authors.
The binary system nitrogen +n-heptane were selected for the first measurements. Although being a simple system, its study entails a number of challenges. Previous to the actual measurements, it is necessary to perform a calibration for the two components involved. This involves the calibration for a liquid and the calibration for a gas. Additionally to this, the study of the samples withdrawn during the measurements on this binary system will involve the analysis of very low concentrations, constituting a serious test for the capability of the gas chromatography, in terms of detection limits, the influence of noise in the signals, repeatability of the values, etc.

2.2.4.1 Calibration for nitrogen and n-heptane

Following is a description of the process of calibration for nitrogen and n-heptane, a system that has been measured various times by different authors [22,23], and which will be used in the validation of the current experimental analytical method.
The calibration process started with the calibration for Nitrogen. Regarding the calibration for nitrogen, the procedure consisted in the manual injection of different volumes of the pure gas, using gas-tight syringes of different volumes. Nitrogen was initially transferred from the pressurized bottle to a sampling bag, of one liter of capacity and equipped with a valve and a septum containing a syringe port. The film is composed mostly from polyvinyl fluoride, and it is characterized by a high chemical inertia and resistance to gas permeation, assuring the sample integrity. From the sample bag, a number of samples of different volumes, between 50 μL and 400 μL were withdrawn for injection. The amount of substance injected, was calculated using values for the density of the gas at the temperature of the room and at atmospheric pressure [24].
A minimum of five injections were performed for each volume. The results are presented in Figure 2.13, where the areas of the chromatographic peaks yielded by the TCD detector are represented as a function of the volume of nitrogen injected and the corresponding correlation as a function of number of moles nitrogen.

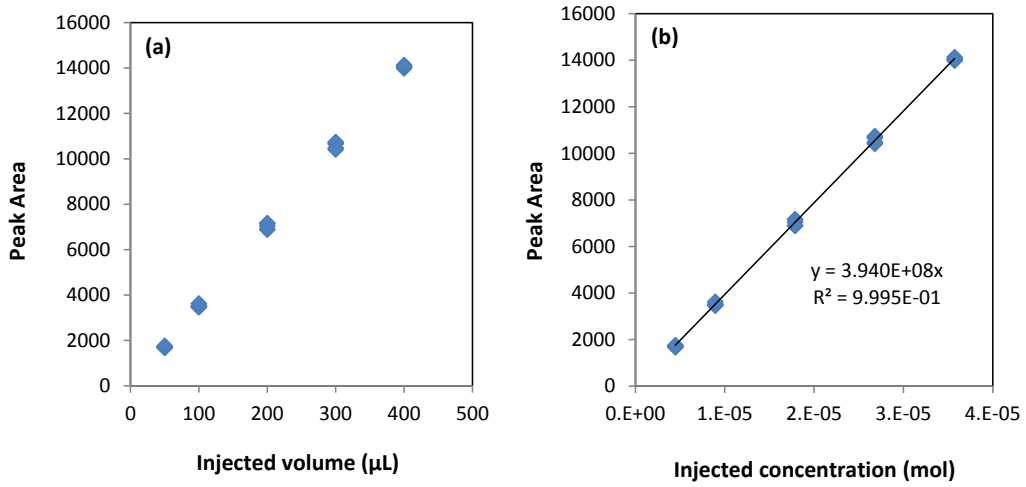

Figure 2.13: Areas of the chromatographic peaks as a function of: (a) the volume of nitrogen injected and (b) the number of moles of nitrogen injected. Trend line added to gain correlation.

The average areas of the chromatographic peaks obtained during the calibrations, and the corresponding number of moles injected are given in Table 2.3.

Table 2.3: Average areas of the chromatographic peaks obtained in the calibration of the GC for nitrogen, and number of moles injected.

Average Area µV*s	Moles injected
1707	4.46E-06
3515	8.93E-06
7026	1.79E-05
10596	2.68E-05
14053	3.57E-05

This leads to an expression where the area is a function of nitrogen concentration, with a square linear correlation coefficient for the equation is given by $r^2 = 0.9995$.

$$Area = 3.94 \cdot 10^8 \cdot n_{nitrogen} \quad (2.1)$$

Where $n_{nitrogen}$ is the amount of nitrogen in moles.

A constraint has been implemented in equation 2.1, that the area should be 0 when no nitrogen is present. However, this does not affect the accuracy ($r^2 - value$) by any significance. In order to validate the calibrations, we take a look at the variance in peak area. Figure 2.14 presents the difference in peak area compared to calculated area using equation 3.1. Since we have a nice displacement on both sides, the calibration is assumed to be accurate within an area of ± 200.

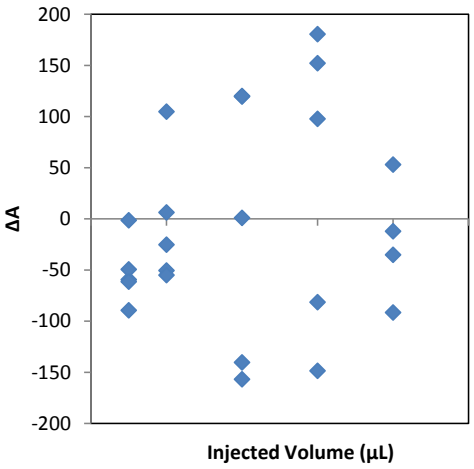

Figure 2.14: The difference in calculated area using equation 2.1 and actual area gained from gas chromatograph, for the calibration of nitrogen.

Calibration for n-heptane was done by manual injection, using low volume liquid syringes. A series of injections was performed, using various volumes between 0.5 – 1 µL.
The results are presented in Figure 2.15, where the areas of the chromatographic peaks yielded by the FID detector are represented as a function of the volume of n-heptane injected and the corresponding correlation as a function of number of moles n-heptane. Calibration is only presented for the FID detector, since the accuracy is better for hydrocarbons than the TCD detector.

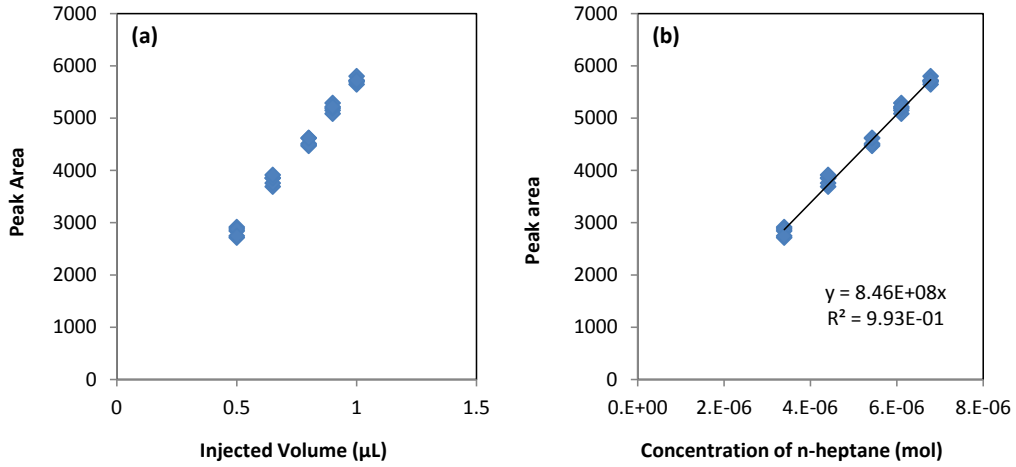

Figure 2.15: Areas of the chromatographic peaks as a function of: (a) the volume of n-heptane injected and (b) the number of moles of n-heptane injected.

The average areas of the chromatographic peaks obtained during the calibrations, and the corresponding number of moles injected are given in Table 2.4.

Table 2.4: Average areas of the chromatographic peaks obtained in the calibration of the GC for n-heptane, and number of moles injected.

Average Area µV*s	Moles injected
2819	3.391E-06
3813	4.408E-06
4541	5.425E-06
5186	6.103E-06
5716	6.781E-06

The lines shown in the graph are considered as the calibration lines for n-heptane. As before, a constraint was imposed forcing the equations to an intercept of zero, therefore yielding a value of zero for the area when no n-heptane is injected, for the reasons explained previously. The resulting equations, relative to the FID detector, are given by the following expression, with a square linear correlation coefficient for the equation is given by $r^2 = 0.9930$.

$$Area = 8.46 \cdot 10^8 \cdot n_{heptane} \quad (2.2)$$

Where $n_{heptane}$ is the amount of n-heptane in mol.

Figure 2.16 presents the difference in peak area compared to calculated area using equation 3.2. An even displacement is seen on both sides of the center, hence the calibration is assumed to be accurate within an area of ± 200.

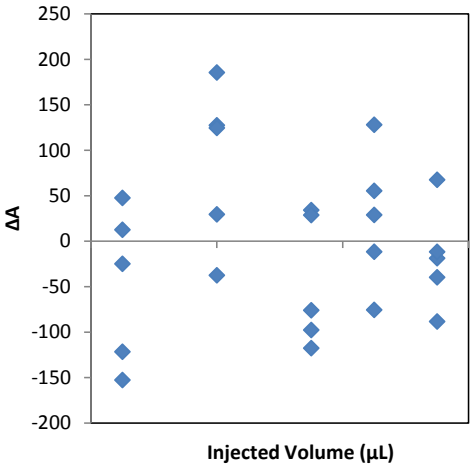

Figure 2.16: The difference in calculated area using equation 2.2 and actual area gained from gas chromatograph, for the calibration of n-heptane.

2.2.4.2 Analytical results for the reference system nitrogen + n-heptane

After completing the calibrations for both components, measurements on the binary system of nitrogen + n-heptane were performed at temperatures of 305 K, and pressures between 5 MPa and 20 MPa. Firstly, the equilibrium cell was cleaned with toluene, water and ethanol several times, before being placed under vacuum for a period of 24 hours. The cell was then re-opened, and n-heptane was placed inside for degassing. After the successful degassing, nitrogen was added to the cell directly from a high pressure bottle, taking care to rinse the previously evacuated tubing. After equilibration through stirring, samples from the gas and liquid phases were withdrawn and analyzed. A series of 6 measurements were made for each of the experimental conditions studied, in order to evaluate the repeatability of the sampling and of the analysis.

Concerning the opening times of the samplers, a balance has to be reached. Low opening times allow sharper chromatographic peaks and a chromatogram with a better definition, but of lower area and therefore more susceptible of being affected by errors in the integration of the peaks, which in the determination of lower concentrations can be critical. On the other hand, larger sampling times help reduce this problem and permit the measurement of lower concentrations, but can lead to a significant broadening of the peaks. The results obtained in the analytical study of VLE in the binary system nitrogen + heptane are presented in Table 2.5, where $x_{nitrogen}$ and $y_{heptane}$ correspond to the molar fractions of nitrogen in the liquid phase, and of n-heptane in the gas phase, respectively. The temperature is kept at 305K (± 1K).

Table 2.5: Results obtained in the analytical study of the system nitrogen + n-heptane. $\boldsymbol{x_{nitrogen}}$ and $\boldsymbol{y_{heptane}}$ correspond to the molar fractions of nitrogen in the liquid phase, and of n-heptane in the gas phase, respectively

T / K	P / MPa	$x_{nitrogen}$	$y_{heptane}$
305	5.43	0.0680	0.0022
305	7.11	0.0780	0.0038
305	8.79	0.0987	0.0074
305	10.10	0.1210	0.0050
305	13.07	0.1540	0.0067
305	15.21	0.1730	0.0070
305	17.09	0.1890	0.0065
305	18.71	0.2010	0.0066

The results obtained in the analysis of the different phases are compared with values found in literature. All values are averaged over several samples taken for each condition. Figure 2.17 presents the values relative to the solubility of nitrogen in heptane and the solubility of n-heptane in nitrogen, making a comparison to literature sources [22-23]. In the plot each point represents the average values for each series. A good agreement between the results obtained in this work and the literature values can be observed, even taking into account the dispersion between the different data sources available under the operating conditions, confirming not only the quality of the equipment developed, but also the validity of the performed calibrations.

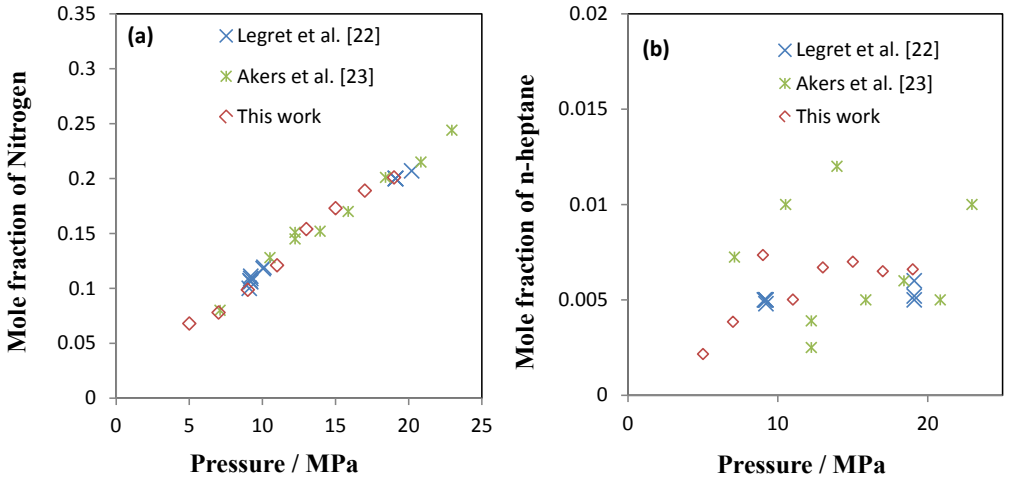

Figure 2.17: Solubility mole fraction of: (a) nitrogen in the aqueous phase, (b) n-heptane in the gas phase, and comparison with literature data [22,23] at 305 K. Each data point presented in this work is the average value obtained at the specific condition.

In the analysis of both phases, it was noticed that the integration of the chromatographic peaks is a critical step, which can have a serious influence on the final results. The combination of low sample volumes with low concentrations, result in an extremely small peak for the solute, where a small error in the integration translates into a considerable relative error in the mole fraction value.
The results gathered in the analytical study of this binary system confirm the correct performance of the analytical part of the set-up, even in challenging conditions such as these, with the determination of very low concentrations.

2.3 Experimental results

The analytical isothermal cell (AnT Cell) has been proven to effectively produce accurate VLE results, and is therefore used in this project to further investigate VLE for several systems of interest. A focus has been put towards hydrocarbon systems in the presence of polar chemicals (Water/MEG/Methanol), used for gas hydrate inhibition. All systems are compared against appropriate literature data, in order to validate the accuracy. Systems investigated are in many cases well described in literature, however, the results are often subject to inconsistencies or a lack of data in certain pressure and temperature ranges. The quantification of methane, methanol, MEG and water from the chromatograms was performed according to the procedure presented for calibration

of gas chromatograph. Calibrating for each individual component, relation between peak area and concentration are obtained for all necessary components.

2.3.1 VLE for the binary system methane + water

The binary system of methane and water is investigated over a wide range of temperatures (283-323 K) and pressures (5-20 MPa). Although being a simple system, its study entails a number of challenges. The study of the samples withdrawn during the measurements on this binary system will involve the analysis of very low concentrations, constituting a serious test for the capability of the gas chromatography, in terms of detection limits, the influence of noise in the signals, reproducibility of the values, etc. The results obtained in the analysis of the different phases are compared against literature data, at two different temperatures. Figure 2.18 presents the solubility of methane in water at 298 K and 283 K, compared to several literature sources [4,25-29]. In the plot, the points represent the average value for at least 6 measurements.

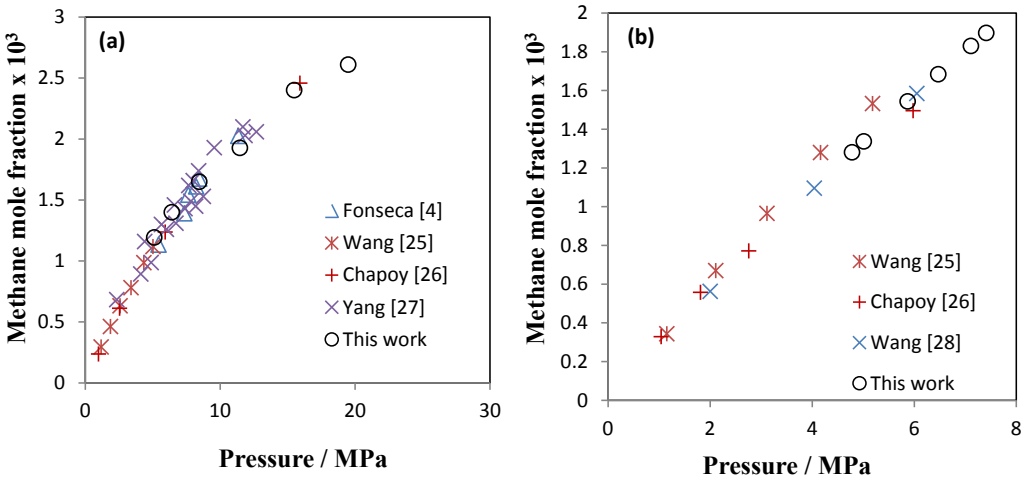

Figure 2.18: Solubility mole fraction of methane in water and comparison with literature data [4, 25-28] at: (a) 298 K and (b) 283 K. Each data point presented in this work is the average values obtained at the specific condition.

For the temperatures 298 K and 283 K, the agreement is close to perfect. The agreement can be considered good, especially when taking into account the dispersion between the different data sources observable for the temperature of 298 K.

Figure 2.19 present the solubility of water in methane, compared to literature sources. In the plots, the points represent the average value for each series of results. Once again we have excellent agreement between the data from this work and the literature. It should be noticed, that the measurement of water in gas phase is considered to be difficult, due to the very low concentration. This can be seen by the low amount of experimental data available in literature, where many sources only present the solubility data for one phase. The results obtained in this work are quite satisfactory, even at the low temperature (T = 283 K), where the concentration of water in the gas phase is low.

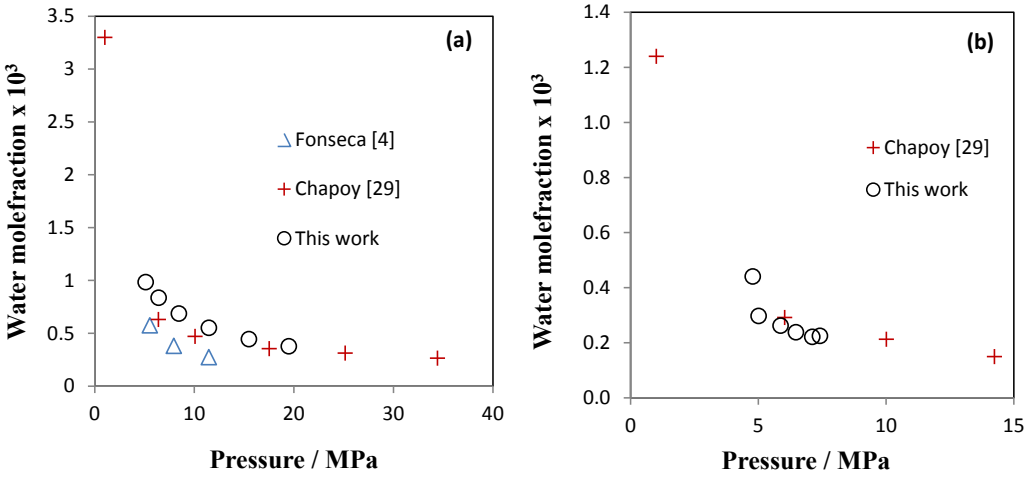

Figure 2.19: Solubility in mole fraction of water in the gas phase and comparison with literature data [4, 29] at: (a) 298 K and (b) 283 K. Each data point presented in this work is the average value obtained at the specific condition.

One of the major concerns in this type of analysis was the possibility of adsorption of traces of water in the transfer lines, occurring in the connection between the sample-injectors and the GC unit. The transfer line is made of deactivated fused-silica, much like an empty GC column, in order to minimise adsorption problems, and it was heated up to 523 K.

The results obtained in the VLE study for the binary system methane + water are presented in Table 2.6. All results are averaged values, from at least 6 samples at each condition.

Table 2.6: Results obtained in the analytical study of the system methane + water. $\boldsymbol{x_{methane}}$ and $\boldsymbol{y_{water}}$ correspond to the mole fractions of methane in the liquid phase, and of water in the gas phase, respectively.

T / K	P / MPa	$x_{methane}$ x 10^3	y_{water} x 10^3
283	5.01	1.3375	0.2976
283	5.87	1.5441	0.2624
283	4.78	1.2812	0.4409
283	6.47	1.6844	0.2384
283	7.41	1.8978	0.2254
283	7.11	1.8306	0.2218
298	5.11	1.1938	0.9846
298	6.41	1.4002	0.8369
298	8.45	1.6507	0.6871
298	11.46	1.9281	0.5523
298	15.48	2.4017	0.4452
298	19.49	2.6111	0.3776
313	5.48	0.6710	1.5954
313	6.78	0.9145	1.3571
313	8.15	1.2340	1.1800
313	12.46	1.8870	0.8547
313	16.78	2.3480	0.6816
323	4.98	0.6039	3.8748
323	6.49	0.8231	3.3474
323	8.48	1.1106	2.6518
323	11.49	1.6983	2.2427
323	14.48	2.1132	1.9736
323	18.48	1.9843	1.7250

2.3.2 VLE for the binary system methane + methanol

The system of methane and methanol is investigated at the temperature of 298 K and different pressures. The results obtained in the analysis of the different phases are compared against literature data. Figure 2.20 presents the solubility of methane in methanol and the solubility of methanol in the gas phase, compared to literature data [28,30]. Excellent agreement between the obtained solubility data and literature data are observed. The data available in literature are at different temperatures; however, it is observed that we correctly see an influence in the solubility as a function of temperature.

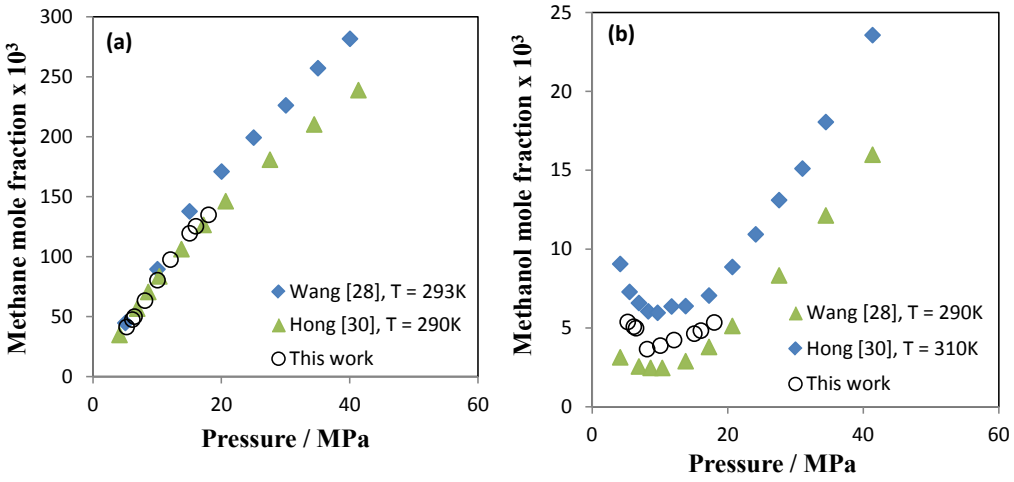

Figure 2.20: Solubility mole fraction of: (a) methane in methanol, (b) methanol in the gas phase, and comparison with literature data [28,30] at 298 K. Each data point presented in this work is the average value obtained at the specific condition.

The results for methanol in the gas phase are in good agreement with the existing trends, both pressure and temperature. Of particularly interest is the minimum solubility, which is also found in this work. The literature data [28,30] was available only at higher and lower temperatures. The obtained solubility data of methane in methanol in this work is correctly positioned between the data points found in literature. Again we can observe the effect of temperature on the solubility, where the concentration of methanol in the gas phase is increasing with increasing temperature.

The results obtained in this study are shown in Table 2.7. All values are average of at least 6 measurements.

Table 2.7: Results obtained in the analytical study of the system methane + methanol. $\boldsymbol{x_{methane}}$ and $\boldsymbol{y_{methanol}}$ correspond to the molar fractions of methane in the liquid phase, and of methanol in the gas phase, respectively.

T / K	P / MPa	$x_{methane}$ x 10^3	$y_{methanol}$ x 10^3
298	5.24	41.26	5.38
298	6.14	47.47	5.08
298	6.47	49.95	4.98
298	8.102	63.29	3.65
298	10.054	80.32	3.88
298	12.074	97.49	4.23
298	15.068	119.41	4.63
298	16.04	125.25	4.83
298	18.01	134.83	5.34

2.3.3 VLE for the ternary system methane + methanol + water

The system of methane + methanol + water is investigated over a range of temperature (280 – 313 K) and pressure (5-13MPa). In preparing this multicomponent mixture, a composition of 0.25 mol% methane, 0.463 mol% water and 0.287 mol% methanol was used.

The results obtained in the analysis of the different phases are compared against literature data. Figure 2.21 presents the solubility of (a) methane in aqueous phase, (b) methanol in the gas phase, (c) water in the gas phase; at 298K, making a comparison to literature sources [28, 31-32]. In the plot, the points represent the average value for each series of results. The comparison is made on the basis of methanol concentration (wt%) in the aqueous phase. Different literature data are available, with varying concentration of methanol. The mixture investigated in this work has a 52wt% of methanol in the aqueous phase. The results are in good agreement with literature data, and exhibit similar trends. It can be seen that there is an increase in methane solubility with increasing methanol concentration.

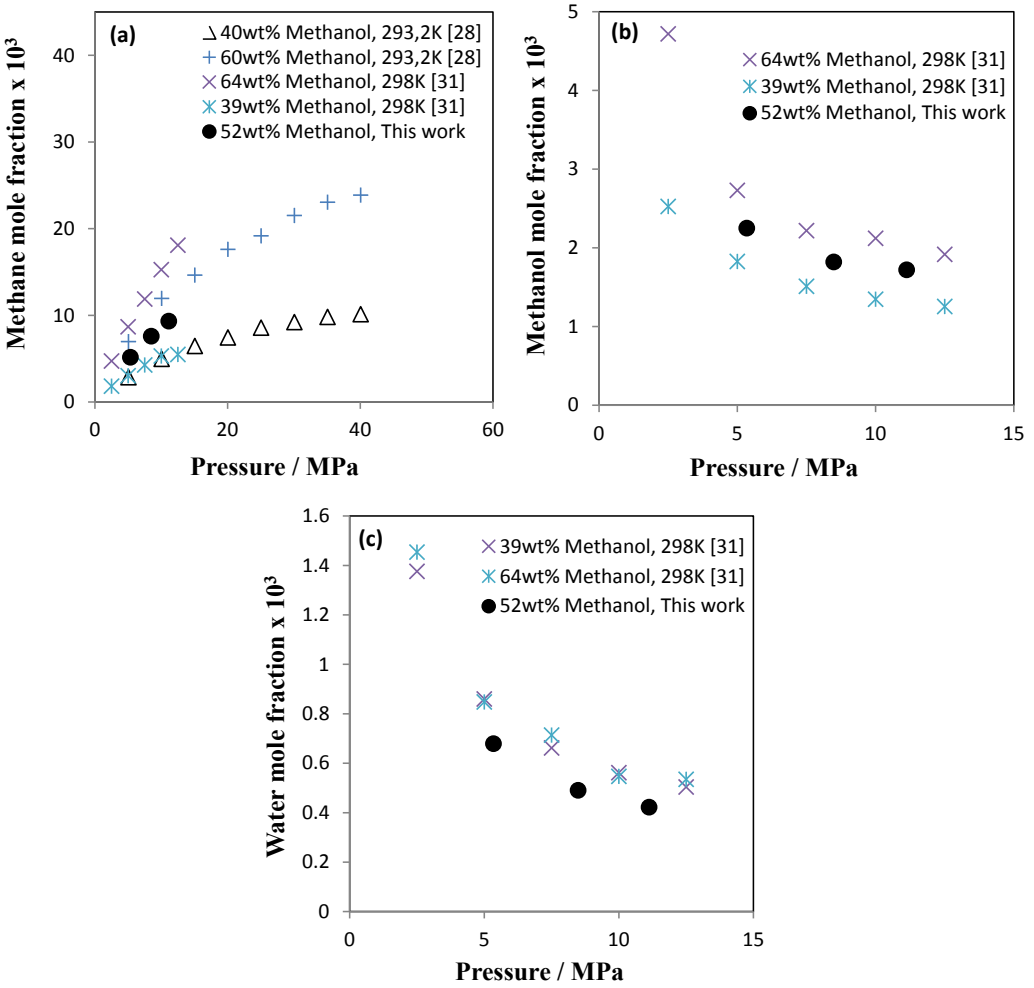

Figure 2.21: Solubility mole fraction of: (a) methane in methanol/water, (b) methanol in the gas phase, (c) water in the gas phase and comparison with literature data [28,31] at 298 K. Each data point presented in this work is the average value obtained at the specific condition.

The results are compared against literature data, which have similar methanol concentration. We observe a good agreement with literature data for methanol content in the gas phase, where our measured data correctly decreases with increasing pressure and is have values between the literature data, which have higher and lower amount of methanol present in the feed.

The results show slightly lower water concentration in this work, but are in the same order of magnitude, and exhibit correct trend. Difference can be explained by differences in feed composition.

The results obtained for the system of methane (1) + water (2) + methanol (3) can be seen in Table 2.8. All values are average for at least 6 measurements at the given conditions.

Table 2.8: Results obtained in the analytical study of the system methane (1) + water (2) + methanol (3).

T / K	P / MPa	x_1 x 10^3	x_2	x_3	y_1	y_2 x 10^3	y_3 x 10^3
280	5.1	5.14	0.6126	0.3823	0.9989	0.2249	0.8923
280	9.8	8.50	0.6096	0.3819	0.9992	0.1499	0.7297
280	13.1	10.34	0.6080	0.3817	0.9991	0.1341	0.7514
298	5.3	5.17	0.6128	0.3820	0.9973	0.6793	2.2496
298	8.5	7.60	0.6106	0.3818	0.9978	0.4907	1.8199
298	11.1	9.34	0.6090	0.3816	0.9980	0.4225	1.7199
313	5.6	5.37	0.6130	0.3817	0.9945	1.5002	4.3658
313	8.1	7.37	0.6111	0.3816	0.9955	1.1457	3.6045
313	12.1	10.07	0.6086	0.3813	0.9961	0.9082	3.2158

2.3.4 VLE for the binary system methane + MEG

An initial study was performed, to test the limits of the GC, with regards to very low concentrations. Systems such as methane + glycols are considered among the most difficult to measure, since the solubility of glycols in the gas phase is usually very low. This has a large impact on the chemical analysis methods used in this work. Very small amount of sample is withdrawn using the ROLSI™ samplers, which leads to small or no peaks on the gas chromatograph, when concentrations are very low. This puts a lot of focus on the calibrations of components and the integration of peaks on the GC. For this kind of systems, it is important that the amount of noise (column contamination etc.) is as low as possible.

The system of methane and MEG has been investigated at two different temperatures (298 K and 323 K) and over a range of pressures (5 – 20 MPa). Figures 2.22 and 2.23 present the mutual solubility of methane + MEG at 323 K and 298 K, together with literature data. It can be seen, that there is a good agreement with literature data, even down to low concentrations (30 – 40 mole ppm) of MEG in gas phase. At these small concentrations, it was found, that even the smallest change in integration could yield large differences in the obtained solubility. In order to try and get the most accurate results, at least 15 samples were withdrawn under each conditions.
At the lower temperature (298 K), the concentration of MEG in the gas phase becomes very difficult to detect. This is seen by a large scatter in GC peaks, or in some cases, no peaks are seen at

all. The solubility of methane in liquid phase at 298 K, is in good agreement with literature data over the entire pressure range. For the solubility of MEG in the gas phase, the few points able to be measured seem to be in the same order of magnitude of the data presented in literature. However, the experimental uncertainty for these low concentration data points is much higher.

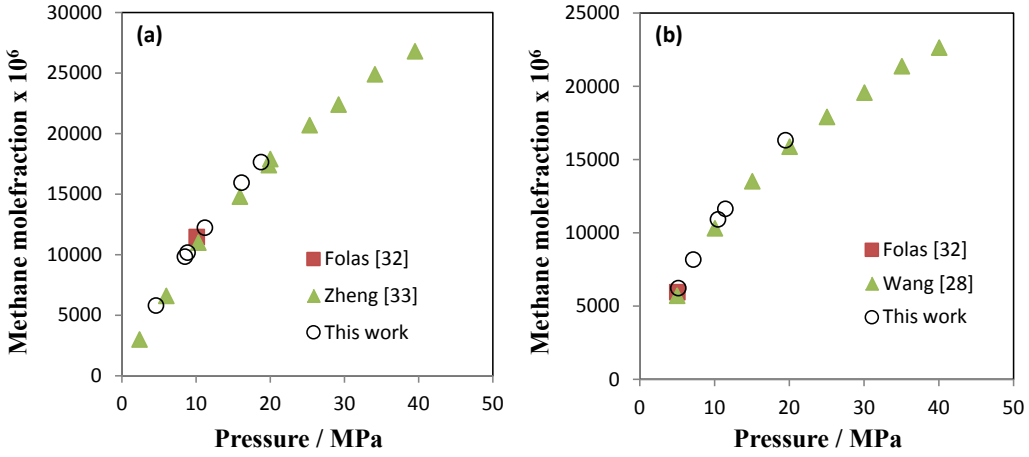

Figure 2.22: Solubility mole fraction of methane in MEG and comparison with literature data [28,32,33] at: (a) 323 K and (b) 298 K. Each data point presented in this work is the average value obtained at the specific condition.

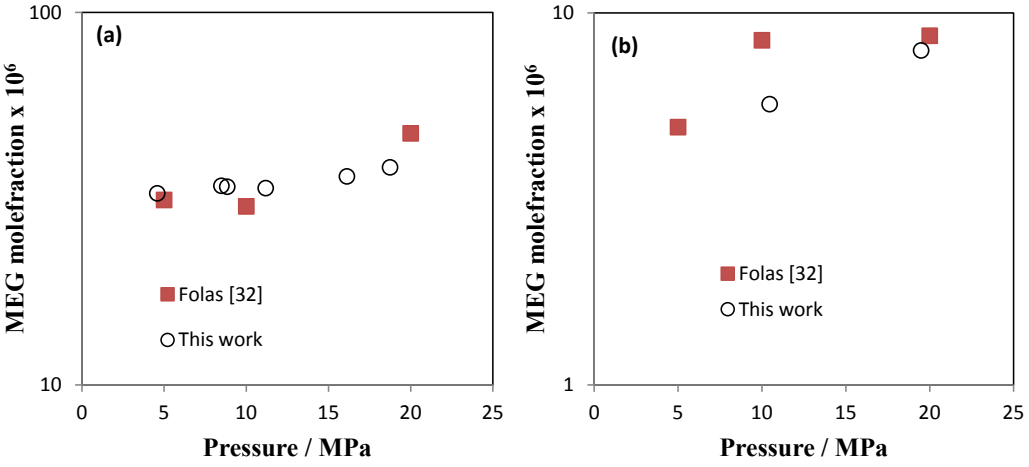

Figure 2.23: Solubility mole fraction of MEG in the gas phase and comparison with literature data [32] at: (a) 323 K and (b) 298 K. Each data point presented in this work is the average value obtained at the specific condition.

The experimental results obtained for the system of methane + MEG can be seen in Table 2.9. All values are the average of 15 samples under the given condition.

Table 2.9: Results obtained in the analytical study of the system methane + MEG. $\boldsymbol{x_{methane}}$ and $\boldsymbol{y_{MEG}}$ correspond to the molar fractions of methane in the liquid phase, and of MEG in the gas phase, respectively.

T / K	P / MPa	$x_{methane}$ x 10^6	y_{MEG} x 10^6
298	5.2	6228	---
298	7.2	8177	---
298	10.5	10918	6
298	11.4	11639	---
298	19.5	16320	8
323	4.6	5802	33
323	8.5	9840	34
323	8.8	10173	34
323	11.2	12232	34
323	16.1	15950	36
323	18.7	17648	38

The results gathered in the analytical study of this binary system confirm the correct performance of the analytical part of the set-up, even in challenging conditions such as these, with the determination of very low concentrations. In combination with the tests previously presented, these results confirm the high quality of the analytical equipment.

2.4 Conclusions

In this chapter, the quality of the equipment designed and constructed by Fonseca et al. [3,4] was confirmed by the extensive testing performed to all the systems involved, from the temperature and pressure measurements to the analytical aspects.

A description of the set-up was given, including the analytical procedures used, and the importance of these in order to gain accurate results. Limitations of the existing equipment have been investigated, resulting in several major issues, such as unsatisfactory stirring for VLLE and condensation in transfer lines. The optimization and changes to the original design are described.

New high quality vapour-liquid equilibrium data have been obtained for methane with methanol and water. The obtained data are in good agreement with literature data, where data was possible to

obtain. Experimental data are presented for the system MEG + methane, which are in good agreement with literature data. These data help prove the high quality of the equipment, and the experimental procedures adopted in this work.

References

[1] D. Richon, *Pure Appl. Chem.* 81 (**2009**) 1769-1782

[2] G. K. Folas, E. W. Froyna, J. Lovland, G. M. Kontogeorgis, E. Solbraa, *Fluid Phase Equilib.* 252 (**2007**) 162-174

[3] J. M. S. Fonseca, N. von Solms, *Fluid Phase Equilibria* 329 (**2012**) 55-62

[4] Ph.D. Thesis, José M. S. Fonseca, **2010**, Danmarks Tekniske Universitet (CERE)

[5] R. Dohrn, S. Peper, J. M. S. Fonseca, *Fluid Phase Equilib.* 288 (**2010**) 1-54

[6] J. M. S. Fonseca, S. Peper, R. Dohrn, *Fluid Phase Equilib.* 300 (**2011**) 1-69

[7] H. Madani, A. Valtz, C. Coquelet, A. H. Meniai, D. Richon, *J. Chem. Thermodyn.* 40 (**2008**) 1490-1494

[8] F. Garcia-Sánchez, G. Eliosa-Jiménez, G. Silva-Oliver, A. Godínez-Silva, *J. Chem. Thermodyn.* 39 (**2007**) 893-905

[9] M. Grigiante, P. Stringari, G. Scalabrin, E. C. Ihmels, K. Fischer, J. Gmehling, *J. Chem. Thermodyn.* 40 (**2008**) 537-548

[10] O. Elizalde-Solis, L. A. Galicia-Luna, S. I. Sandler, J. G. Sampayo-Hernández, *Fluid Phase Equilib.* 210 (**2003**) 215-227

[11] A. Valtz, C. Coquelet, A. Baba-Ahmed, D. Richon, *Fluid Phase Equilib.* 207 (**2003**) 53-67

[12] S. Mokraoui, C. Coquelet, A. Valtz, P. E. Hegel, D. Richon, *Ind. Eng. Chem. Res.*

46 (**2007**) 9257-9262

[13] D. Seredynska, G. Ullrich, G. Wiegand, N. Dahmen, E. Dinjus, *J. Chem. Eng. Data* 52 (**2007**) 2284-2287

[14] Catinca Secuianu, Department of Applied Physical Chemistry and Electrochemistry, "Politehnica" University of Bucharest, Romania, Personal Communication, **2009**

[15] Even Solbraa, Statoil ASA, Research and Development Centre, Trondheim, Norway, Personal Communication, **2013**

[16] D. Richon, *Pure Appl. Chem.* 81 (**2009**) 1769-1782

[17] T. Jiang, C. J. Liu, M. F. Rao, C. D. Yao, G. L. Fan, *Fuel Process. Technol.* 73 (**2001**) 143-152

[18] M. Jia, W. Li, H. Xu, S. Hou, Q. Ge, *Appl. Catal.* , A 233 (**2002**) 7-12

[19] R. Susilo, J. D. Lee, P. Englezos, *Fluid Phase Equilib.* 231 (**2005**) 20-26

[20] S. O. Derawi, G. M. Kontogeorgis, E. H. Stenby, T. Haugum, A. O. Fredheim, *J. Chem. Eng. Data* 47 (**2002**) 169-173

[21] G. K. Folas, G. M. Kontogeorgis, M. L. Michelsen, E. H. Stenby, E. Solbraa, *J. Chem. Eng. Data* 51 (**2006**) 977-983

[22] Legret, D., Richon, D. and Renon, H., *AIChE J.,* 27 (**1981**) 203–207

[23] W. W. Akers, D. M. Kehn, and C. H. Kilgore, *Industrial & Engineering Chemistry* , 12, 2536-2539.

[24] NIST Chemistry WebBook, NIST Standard Reference Database Number 69*,* National, Institute of Standards and Technology, Gaithersburg MD, 20899, http://webbook.nist.gov, **2009**

[25] Y. Wang, B. Han. H. Yan, R. Liu, *Thermochim. Acta* 253 (**1995**) 327-334

[26] A. Chapoy, A. H. Mohammadi, D. Richon, B. Tohidi, *Fluid Phase Equilib.* 220 (**2004**) 111-119

[27] S. O. Yang, S. H. Cho, H. Lee, C. S. Lee, *Fluid Phase Equilib.* 185 (**2001**) 53-63

[28] L. K. Wang, G. J. Chen, G. H. Han, X. Q. Guo, T. M. Guo, *Fluid Phase Equilib.* 207 (**2003**) 143-154

[29] A.Chapoy, C.Coquelet, D.Richon, *FPE* 230 (**2005**) 210-214

[30] J. H. Hong, P. V. Malone, M. D. Jett and R. Kobayashi, *Fluid Phase Equilib.* 38 (**1987**) 83-96

[31] Sinyavskaya R.P. et al., *Gazovaya Prom.* V1 (**1984**) 39-40

[32] G. Folas, O.J. Berg, E. Solbraa, A. Fredheim, G. Kontogeorgis, M.L. Michelsen and E.H. Stenby, *Fluid Phase Equilib.* 251 (**2007**) 52-58

[33] D. Zheng, W. Ma, R. Wei, T. Guo, , *Fluid Phase Equilib.* 155 (**1999**) 277-286

Chapter 3 – New experimental set-up for measurements of Vapor-Liquid-Liquid equilibrium

The review of existing phase equilibria data for the systems under consideration in this work, presented in Chapter 2, revealed the need for new accurate and reliable data, preferably with full characterization of all the phases present in equilibrium. The need for high-quality experimental phase equilibria data is true for the chemical industry in general. Examples include pharmaceutical processes, the food industry, chemical separation processes, refrigeration, reservoir simulation, gas processing, applications involving supercritical fluids or chromatography, and new fields such as ionic liquids, carbon dioxide sequestration and storage or "green solvents". All these areas deal with processes whose optimization is dependent on phase equilibria data

Despite the overwhelming importance of experimental data, reliable and precise measurements can be difficult to achieve and are often expensive and relatively slow, representing a serious investment, not only concerning the acquisition of equipment or the development of custom-made experimental set-ups, but also regarding human resources. Another serious problem is the existence of experimental data of dubious quality. Either because the lack of experimental data prompts researchers with little or no experimental experience to go into the laboratory in order to produce data which they can use to back-up their models, or because of a lack of understanding of the sensitivity of some experimental aspects.

With this as motivation, we set out to develop a new experimental set-up, to measure VLLE of mixtures of interest to the chemical and oil & gas industry. This chapter focuses on the description of the design and construction of the experimental set-up, and presents initial results for a multicomponent mixture.

3.1 New experimental set-up – Before you begin

The development of a new experimental set-up entails a series of preliminary steps which usually go unnoticed when looking at the final result. These preliminary studies are often time consuming, however, they should not be disregarded, as they are of great importance for the success of the experimental equipment.

The initial step is a simple one, but an important part to consider, before beginning designing and constructing new equipment. It is important to consider which goals you want to achieve, what properties are to be measured, which chemicals are involved, temperature and pressure ranges. Taking your goals into account as early as possible, can prevent having to change the design, after construction has started and prevent errors later in the process.

When this is done, the creative part of designing the equipment itself can take place. In this part inspiration and discussion with specialists from different areas, about what materials to use, the difficulty involved in machining the necessary parts, etc. can be invaluable.

If the planning was careful, and the necessary parts were manufactured according to the design, the stage of assembly of all the parts should proceed without further complications. In this aspect, computer-aided design (CAD) has become an invaluable tool, allowing to virtually build the equipment and to "travel" through it using three dimensional applications, even before the parts have been manufactured of acquired. Currently, modern equipment used by workshops in the machining of parts also uses this type of software, making the process easier and less susceptible of errors.

In summary, the development of a new experimental set-up is a multidisciplinary process, requiring knowledge in different areas, from metrology to material science, electronics or CAD software, in addition to the necessary knowledge in the area of application of the equipment.

3.2 New experimental equipment

There exist a need for accurate and reliable data, which includes the demand for characterization of all phases which are present in a system [1]. Of particular interest are the quantification of residual amounts of non-volatile compounds in the gas phase.

In this project, equipment of higher complexity was chosen, with the necessary development of a sampling procedure, as well as of an analytical method for the analysis of all phases. An analytical method allow for a good understanding of the equilibrium, with proper quantification of all the

phases involved, without referring to mass balances, use of equations of state or other approximations. These methods also allow the study of more complex systems, analogous to the "real-life" systems typical of industrial problems.

An advantage in an equilibrium cell is the use of windows, for visual observation of the contents of the cell, interfaces between phases, among other phenomena. Among possible materials, sapphire is likely to be the most obvious choice. It possesses a high mechanical strength, chemical resistance, thermal conductivity and thermal stability. Rondinone et al. [2] developed a sapphire cell for the study of gas hydrates using neutron-scattering experiments, taking advantage of the special characteristics of this material. Gorbaty and Bondarenko [3] presented an equipment for Raman studies in corrosive liquids suitable for measurements at pressures up to 100 MPa and temperatures up to 800 K, in which the liquids under study could only come in contact with sapphire and gold. Several examples of experimental set-up's specially designed for operation at low temperatures and high pressures can be found in the literature [2,4,5]. The purchase of an equilibrium cell by the use of a commercial model will usually imply some limitations, either in the temperature range of application, in the selection of parts, in the quality of the instrumentation, or in the main characteristics of the cell itself.
During the summer of 2012, Professor Dominique Richon was a visitor (Otto Mønsted visiting professor) at our research center. Taking advantage of his experience in the field of experimental thermodynamics, we set out to design new equipment for VLLE study, which was constructed completely in-house. The resulting set-up is presented in this chapter, including the first results.

3.2.1 The equipment

In this section, the new experimental set-up is presented, that although priming for its versatility, was specially designed for the measurement of multi-phase equilibria in hydrocarbon-water-hydrate inhibitor systems, at temperatures ranging from 283 K to 353 K and at pressures up to 30 MPa. The experimental set-up can be seen in Figures 3.1 and 3.2.

Figure 3.1: General aspect of the experimental set-up for the measurement of multi-phase equilibria. Photo is taken at CERE labs.

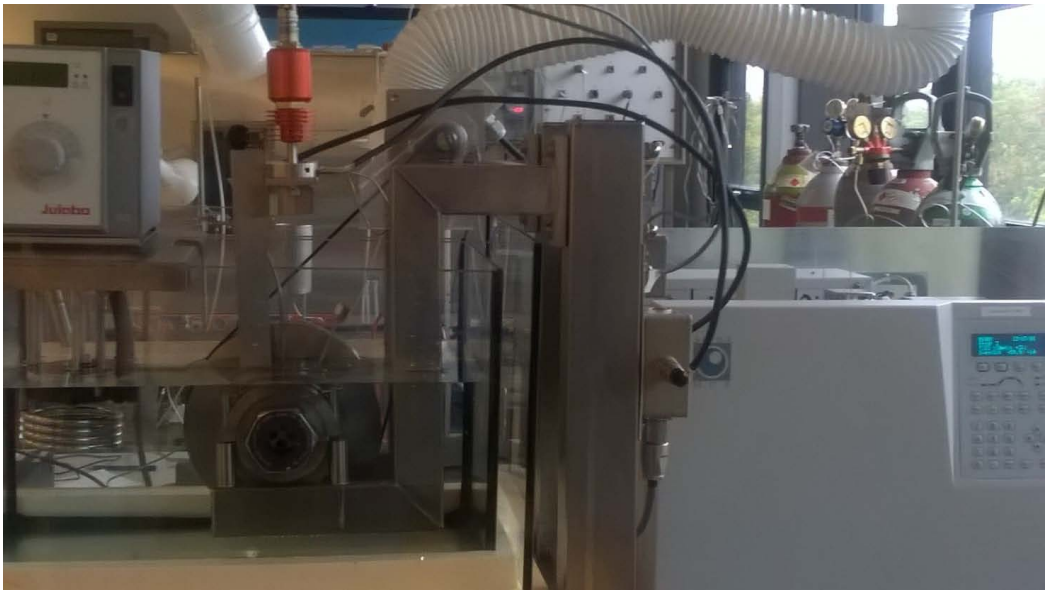

Figure 3.2: General aspect of the experimental set-up for the measurement of multi-phase equilibria. Photo is taken at CERE labs.

The main part of the equipment is the high-pressure equilibrium cell, specially designed for this application. The cell is fitted with sapphire windows in each end, which allows for viewing of all phases and any phenomena appearing during experiments. The temperature, measured by platinum resistance thermometers, is monitored and recorded over time through a computer, to which is also connected the temperature compensated pressure sensor. The equilibrium cell is situated in a liquid bath (water or glycol dependent on temperature range), where the temperature is regulated by external liquid circulation thermostat, enabling temperature to be held constant within 0.5 K Connected to the cell are two automatic ROLSI™ sampler-injectors, which allow the withdrawing of very small samples from the different phases directly to the carrier gas stream of a gas chromatograph (GC), where the samples are then analysed. This is similar to the procedure described earlier in Chapter 2, where ROLSI™ samplers also are used for the sampling of gas and liquid.

The chemical analysis was done by GC, using a PR2100 GC System provided by Alpha Mos, France. The GC is equipped with a RTX1 capillary column (Can be changed to Packed column Shincarbon ST 80/100 or Column RTX-WAX, dependent on the experimental needs), and a thermal conductivity detector (TCD) coupled in series with a flame ionisation detector (FID). For acquiring and analyzing data from the GC, the software Winilab (Supplied by Alpha Mos, France) is used. Figure 3.3 shows the equilibrium cell mounted on a structure specially designed and constructed for this application, inside the liquid bath. The picture also illustrates the stirring mechanism, all the valves and ROLSI™ samplers.

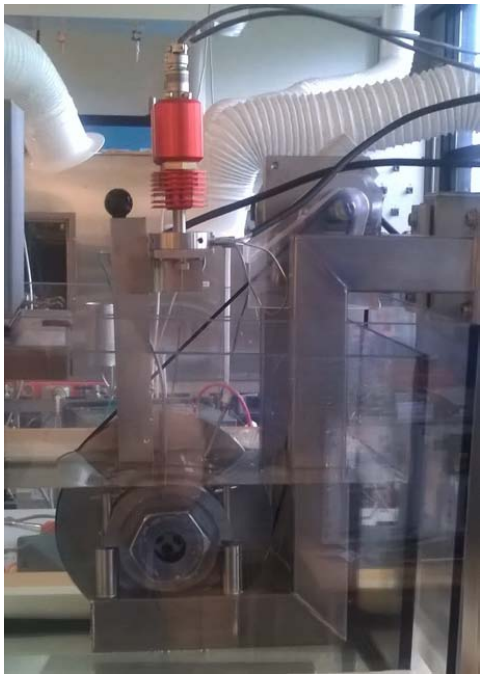

Figure 3.3: Equilibrium Cell in the liquids bath. Picture taken at CERE labs.

3.2.2 The equilibrium cell

The core of this set-up is the high pressure cell, entirely designed and built "in house", in Stainless Steel 316, equipped with sapphire windows, and with an operating volume of approximately 60 cm^3. The cell was planned and designed by the author in collaboration with Professor Dominique Richon, through the use of SolidWorks 3D CAD Design Software, which was used to produce the files that were subsequently handed to the workshop of the department for the building process. A schematic showing the body of the cell can be seen in Figure 3.4.

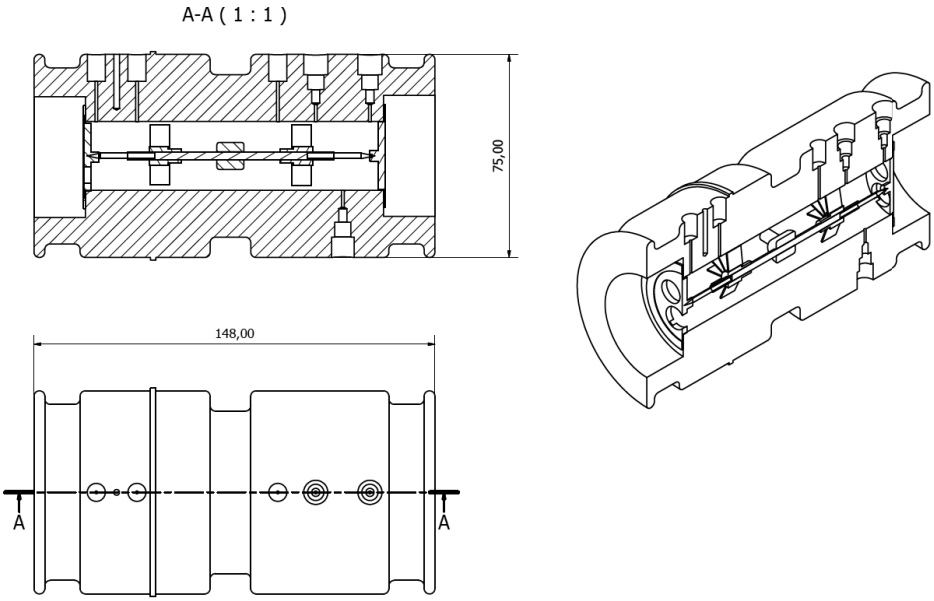

Figure 3.4: Schematic of the equilibrium cell. Print from SolidWorks.

The cell is in stainless steel, which is fitted with sapphire windows in each end. The inner diameter of the cell is 25mm. The sapphire windows have a thickness of 30 mm and it was dimensioned according to the properties of the material provided by the supplier, to cope with pressures of 30 MPa for extended periods of time, but also to pass the safety tests imposed by the internal rules at the department, according to which, the cell had to be tested for a pressure of approximately 140% of the maximum operating pressure (28 MPa). The synthetic sapphire single crystal (Al2O3, 99.9%) was acquired from Encole LLC, USA, with a polishing better than 0.1μm Ra (the average radius of the irregularities or cavities in the surface is inferior 0.1μm).

An important part of the equilibrium cell, is the possibility of proper stirring of the mixture. The stirring should be powerful enough, so that all phases (vapor – liquid – liquid) gets mixed properly and chemical equilibrium is achieved. The stirring is done using powerful magnets from Supermagnete, Germany. A winged axis is placed within the cell, situated in a small sapphire bearing in the center of each sapphire window, which can be seen in figure 3.4 and 3.5. The axis is powered by a magnetic belt, which are fitted on the outside of the cell, similar fitted with high powered magnets. The principal idea is that the magnetic belt turns the axis within the cell, without

any direct contact, since the magnets are powerful enough, to work through the thick stainless steel cell. Drawings showing the Schematic representation of the cell are presented in Figure 3.6.

Figure 3.5: Picture of the axis used for stirring. It is fitted with two sets of wings (each end) and with powerfull magnets in the middle.

From figure 3.6 the individual parts of the cell can be seen; the magnetic stirrer situated within the cell, two ROLSI™ samplers for sampling in liquid and gas phase, two sapphire windows and three valves. The cell is fitted with three valves from TOP INDUSTRIE, France. These are used for loading of liquid, loading of gas and an exhaust valve. It is important to notice, that there is a minimum of dead volume within the cell along with a minimum amount of seals/openings to prevent pressure drops/leaks, which was an important part of the design strategy.

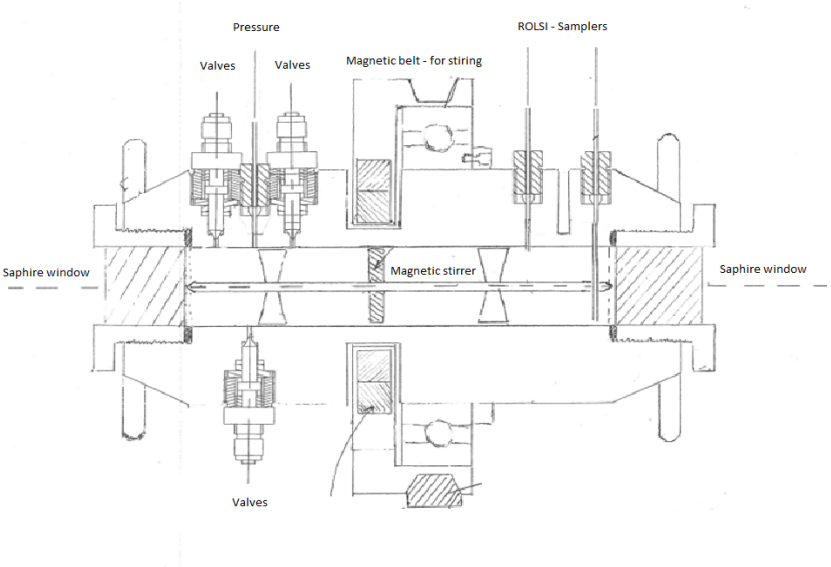

Figure 3.6: Drawing of the equilibrium cell.

A key part when working with phase equilibrium measurements is the thermostation of the equilibrium cell. It should be done in a consistent manor, in the temperature range of operation, securing a high amount of stability. To accomplish this, different solutions are available, most commonly either liquid, or air thermal baths.
For this equipment a liquid thermal bath was chosen, as it provides superior temperature stability, even though the temperature range might be more limited. The temperature ranges can be extended through the use of different liquids, so that it can fit the conditions of interest. The conditions interesting to this work can be done with a simple water bath. The liquid bath was constructed at the Technical University of Denmark, and is fitted with proper isolation, in order to maintain as stable and constant temperature as possible.

3.2.3 Temperature and pressure measurements

Regarding measurement of phase equilibrium, great emphasis is usually placed on the equilibrium cell it-self, sometimes neglecting of forgetting some of the most important parameters in thermodynamic measurements. One of the important parameters in this case is temperature and pressure. In phase equilibria this is evident, regardless of the experimental method used.
The temperature of the cell is monitored with a resolution of 0.01 K and a precision of 0. 1 K, through a four-wire platinum resistance thermometer Pt100 class 1/10 DIN, acquired from Dostmann Electronic GmbH, Germany, placed vertically over at the top of the cell. The thermometer, with a diameter of 1.5 mm, is inserted in a special cavity with thermal paste, in order to improve the thermal contact. The temperature sensor was calibrated according to the International Temperature Scale ITS-90, at the triple point of water, through the careful measurement of their electrical resistance at that temperature, R_0. The thermometer are connected to a data acquisition system Agilent 34970A (Agilent Technologies, Inc., USA) which is in turn connected to a computer via a RS-232 connection, for monitoring and recording of the experimental conditions through the software Agilent BenchLink Data Logger 3 from the same manufacturer.

The pressure inside the cell is monitored by means of a temperature compensated, high precision, pressure transmitter Keller 33X (KELLER AG für Druckmesstechnik, Switzerland), for measurements up to 50 MPa with an accuracy of 0.1% of the full scale (0.05 MPa) over the whole temperature range of operation. This transmitter is equipped with a floating piezoresistive

transducer and an internal microprocessor with an integrated 16-bit A/D converter. The thermal compensation is calculated mathematically by the microprocessor with reference to the calibration data matrix stored in an internal non-volatile memory and determined during calibration in the factory. These calculations are performed approximately every 2 ms, using the temperature readings from the transmitter's internal temperature sensor, yielding a pressure value independent of the operation temperature.
The pressure transmitter is connected to the Agilent 34970A data logger to which the temperature sensor also is connected, which allows the use of a single program for data acquisition. In any case, the collection and recording of temperature and pressure values during the experiments can be set to occur simultaneously, and afterwards, the data from both programs can be exported to data analysis software for a combined evaluation. The zero of the sensor was adjusted against a Crouzet quartz mano 2100, last calibrated in May 2009 by Buhl & Bønsøe A/S, a company accredited by DANAK, The Danish Accreditation and Metrology Fund.

3.2.4 Sampling and analysis

The equilibrium cell is fitted with two automatic electromagnetic capillary ROLSI™ samplers, a product developed by the CENERG-TEP laboratory of the ENSMP (École Nationale Supérieure des Mines de Paris), with a patent registered to Armines and commercialised by Transvalor, France. Developed specifically for the purpose of phase equilibria studies, The ROLSI™ samplers have been establishing themselves as a reference worldwide, being currently used in many universities as well as in industry, in many research groups considered as a reference for phase equilibria and petroleum related studies [6-13]. The ROLSI™ samplers for this equipment have been installed using the same procedure as can be found in Chapter 2.

Another aspect to measurement of accurate phase equilibrium data, which sometimes are neglected, is the importance of analysis. The analysis method adopted should be optimized for the systems of interest, in order to gain the highest amount of accuracy.
There are several methods which can be used with the new set-up, depending on the type of systems under study and on the requirements in terms of detection limits. The gas chromatograph used for the experimental set-up is a PR2100 GC System (Alpha Mos, France). The GC is equipped with a RTX1 capillary column (Can be changed to Packed column Shincarbon ST 80/100 or Column

RTX-WAX, dependent on the experimental needs). It is important to notice, that optimizing the gas chromatograph with regards to components (Column type), pressure and temperature should be considered for every new type of system investigated. Changing the column of a GC can increase the accuracy of phase equilibrium data by orders of magnitude. The GC is fitted with a thermal conductivity detector (TCD) coupled in series with a flame ionisation detector (FID). For acquiring and analyzing data from the GC, the software Winilab (Supplied by Alpha Mos, France) is used.

3.3 Experimental section

3.3.1 Experimental procedure

The cell is fitted with three valves, which are used for loading of liquid, loading of gas and an exhaust valve. The gas valve is also used for putting the cell under vacuum, which is important when exhausting all air for the system.
The cell is initially loaded with the liquids (distributed after the wished feed composition), while the cell is under vacuum. The liquid should, before loaded to the cell, be put under vacuum for degassing. While under vacuum, the gas is introduced to the cell through the gas valve, after weighing in order to obtain the overall correct feed composition (when more than two components are present).

After loading the cell, the equilibration process can take place. The temperature of the liquid bath is set, and when constant temperature is observed, stirring is initiated. The collection and recording of temperature and pressure values over time can be done with any desired frequency. However it should be considered that some studies may last for several days, and that a high frequency in the collection of values may lead to a substantial amount of data, and consequently to files that will be more difficult to handle in a posterior analysis. As mentioned in Chapter 2, proper stirring is an important part, when reaching equilibrium in three phase systems. When proper stirring is present, chemical equilibrium is achieved, when constant pressure is observed within the cell.

When the system is in equilibrium and the phases have settled (two or three clear phase observed through the sapphire window), samples can be withdrawn from each phase and analyzed by gas chromatography. The sampling system consists of two automatic electromagnetic capillary

ROLSI™ samplers. These sampler-injectors are electromagnetic valves that allow samples to be taken from each of the phases without disturbing the phases in equilibrium, and vaporizing them directly to the carrier gas stream of a gas chromatograph, without any manipulation of the samples. Both the ROLSI™ samplers and the GC carrier gas line can be heated up to 523 K, for immediate vaporization of the samples. Besides promoting the immediate vaporization of the samples, the heating has also the purpose of avoiding, or at least minimizing, the possible adsorption of the analytes in the carrier gas line, which would constitute a serious source of errors in the analysis, especially when dealing with samples containing very low amounts of certain compounds. Furthermore the heating of the carrier gas line is optimized, so that no cold spots are present, which is an issue for light components.
In the current configuration, the GC analysis is made using a PR2100 GC System, equipped with a RTX1 capillary column (Also investigated using the Packed column Shincarbon ST 80/100), and a thermal conductivity detector (TCD) coupled in series with a flame ionization detector (FID).

Small amounts of the substances are directly injected into the carrier gas stream using ROLSI™ samplers. The cell is designed so it can turn 45 degrees, so that the cusp of the sampling capillary is immersed in the desired liquid phase. Beside the reason mentioned earlier, this purpose contributes to why the cell is equipped with sapphire windows. Since the samples withdrawn using the ROLSI™ samplers are very small sizes, the equilibrium/pressure inside the cell is not disturbed. In order for the sampling to work optimal, the pressure inside the cell has to be larger than the pressure of the carrier gas stream of the gas chromatograph.

The estimated uncertainty of the developed approach is about 2 to 5 % in composition; when very low solubility is present in a phase (e.g. glycol in gas phase), the experimental uncertainty can become somewhat higher (>10%). For optimal accuracy, several samples are withdrawn (between 5 and 10 samples) at each pressure and temperature condition. This is done to assure reliable sampling by purging capillary tubes, since the components inside the capillary tubes of the ROLSI™ samplers most likely are not representative of phases of equilibrium. Sampling is continued until consistent results are obtained.

Between each experiment, the cell should be carefully cleaned several times with an adequate solvent(s), and placed under vacuum for some hours, in order to evaporate possible traces of solvent before the preparation of a new experiment.

3.3.2 Testing and reference system methane + methanol

After assembling any new equipment, it becomes necessary to perform a series of tests, which will attest the quality of the results to be produced. This can be done by performing measurements on reference systems, or on systems that have been studied frequently and by different authors. Nowadays electronics play a great role in the quality of experimental results. Modern equipment for the measurement of thermodynamic properties are not conceivable without the use of electronic systems in high-quality measurements, for temperature, pressure or any other property. And the output of any common sensor is invariably an electric property, either being resistance, capacitance, current or potential difference, therefore susceptible to be affected by a number of electric and electromagnetic interferences.

The first steps, before beginning measurement on a reference system, were to ensure that the pressure and temperature readings were functioning. At atmospheric pressure, the readings were characterised by short time stability better than ± 0.15 kPa and longtime stability around ± 0.25 kPa. As for the temperature, the thermometer provided readings with a stability better than ± 0.005 K. After this, tests involving the cell started. The air tightness of the cell and the ability of the sapphire crystal to withstand high pressures for prolonged periods were successfully tested, submitting the cell to a pressure of around 30 MPa for 48 hours at 300 K.
A small number of measurements performed of pure methane, confirmed the stability of the pressure and temperature obtained in the first tests and validated the ability of continues sampling with the ROLSI™.
Before moving into measurement of complex mixtures, with multiple phases, it is important to investigate a reference system that have been studied frequently by different authors. This helps validate the experimental equipment and procedures, and works as an important training platform. You should never start with the most difficult part, training and expertise in measurement and analysis of low solubility mixtures are one of the absolut most important parts.

In this work the binary mixture of methane + methanol were selected for the first measurements. This is a complex system, however, experience in these systems have already been acquired. Furthermore, it provides us with the possibility to compare against experimental data produced on the set-up presented in Chapter 2.

3.3.2.1 Gas chromatography

Gas chromatography is a powerful and versatile method, well established in the petroleum industry, which has proven its effectiveness in the study of the type of systems considered in this project. It is important, that development of an appropriate chromatographic method, through the selection of an adequate column and the optimization of a number of experimental parameters are met. When this is achieved, it is then necessary to establish the relations between the area of the chromatographic peaks and the amount of each substance injected on the GC column, in order to create the basis for the desired quantitative analysis.

The systems of interest in this work are hydrocarbons with water and gas hydrate inhibitor (methanol or glycol). These type of systems provide a serious test of the analysis capabilities of the GC (regards to detection and columns), as there is both polar and nonpolar compounds, and usually the columns adequate for the first type of compounds are not suitable for the second. For the detection on the GC, a flame ionization detector (FID) and a thermal conductivity detector (TCD) are used in series. The flame ionisation detector (FID) is the most widely used and presents a very good sensibility to hydrocarbons. The thermal conductivity detector (TCD), in principle, a universal detector based on the difference in the thermal conductivities of the analytes and that of the carrier gas, at the temperature of the detector, is essential in this work for the detection of water. Information of the GC used in this work can be seen in table 3.1.

Table 3.1: Information on the gas chromatograph used for chemical analysis.

Characteristic	PR2100
Column	RTX1 capillary column
Manufacturer	Alpha Mos
Column Length	15 m
Column Internal Diameter	0.320 mm
Column Film Thickness	20 µm
Carrier Gas	Helium
Detector Type	FID/TCD

The development of a chromatographic method consists, among other things, of the development and testing of different experimental conditions such as the inlet temperature, detector temperature, column temperature and temperature program, nature of the carrier gas, carrier gas flow rates, etc., in order to optimize the separation of all the compounds in a typical multi-component system. The aim of this optimization is to obtain well defined, narrow and symmetrical peaks for all the compounds involved. In addition to this, it is desirable to reduce as much as possible the time necessary for each analysis, meaning that the retention times for all the components should be as low as possible, without causing an overlapping of the respective peaks in the chromatogram. The generic chromatographic method used in this work is presented in table 3.2.

Table 3.2: List of parameters used for the generic chromatographic method used for analysis of the mixtures in this work.

Parameters	Setting
Temperature of the injector	220 °C / 493 K
Split ratio	25:1
Total flow	70 mL/min
Carrier gas	He
Temperature of TCD	100 °C / 373 K
Temperature of FID	220 °C / 493 K

The temperature program consisted in a 3 minutes plateau at a temperature of 60 ºC (333 K), followed by an increase in the temperature, at 11 K/min (8.2 minutes), before a new plateau at 150 ºC (423 K) for another 5 minutes, accounting for a total time of approximately 16.2 minutes. The temperature program is presented in figure 3.7.

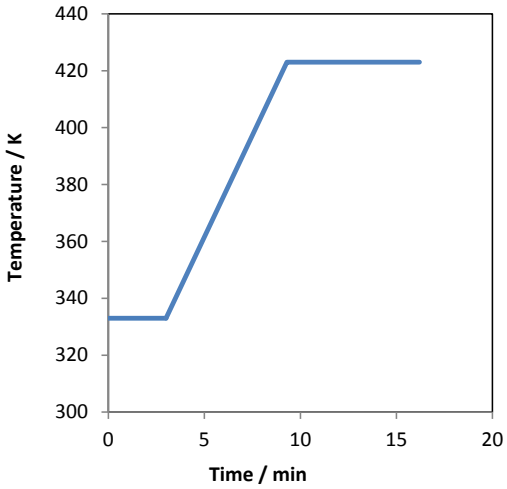

Figure 3.7: Temperature profile used on the gas chromatograph.

3.3.2.2 Calibration of the gas chromatograph

In order to perform quantitative analyses from the phases in equilibrium in the cell, it is necessary to perform calibrations for all the components of interest. In the study of phase equilibrium, the knowledge of the mole fractions in each phase is sufficient to characterize the system. It is possible to obtain this using the GC analysis, by calibrating independently each compound, obtaining a relation between the area of the peak in the chromatogram and the amount of compound injected. This provides the relative sensibility of the detectors to each of the components, and the information of the mole fraction is given by the ratio between the areas of the peaks. During experiments it is important, to investigate that the calibrations are still valid, since the response of a GC can easily change when chemicals are introduced to the column and detectors.

Performing the calibrations, different amounts of a compound are injected, usually using diluted solutions with a precisely known concentration so that smaller amounts of the component of interest can be injected. To increase the quality of the calibration, the volume of each injection is precisely known, and the same exact volume is injected a number of times, in order to increase the accuracy. The system of methane + methanol has been measured various times by different authors [14-16], and which will be used in the validation of the current experimental analytical method.

Methane was initially transferred from the pressurized bottle to a sampling bag, of one liter of capacity and equipped with a valve and a septum containing a syringe port. The film is composed mostly from polyvinyl fluoride, and it is characterized by a high chemical inertia and resistance to gas permeation, assuring the sample integrity. From the sample bag, a number of samples of different volumes, between 50 µL and 400 µL were withdrawn for injection. A minimum of five injections were performed for each volume. Calibration for methanol was done by manual injection, using low volume liquid syringes. A series of injections was performed, using various volumes between 0.5 – 1 µL.

The calibrations are presented in Figure 3.8, where the areas of the chromatographic peaks yielded by the TCD detector are represented as a function of the concentration of methane and methanol injected respectively, and show the corresponding correlations. Similar the FID detector was calibrated with regards to methane.

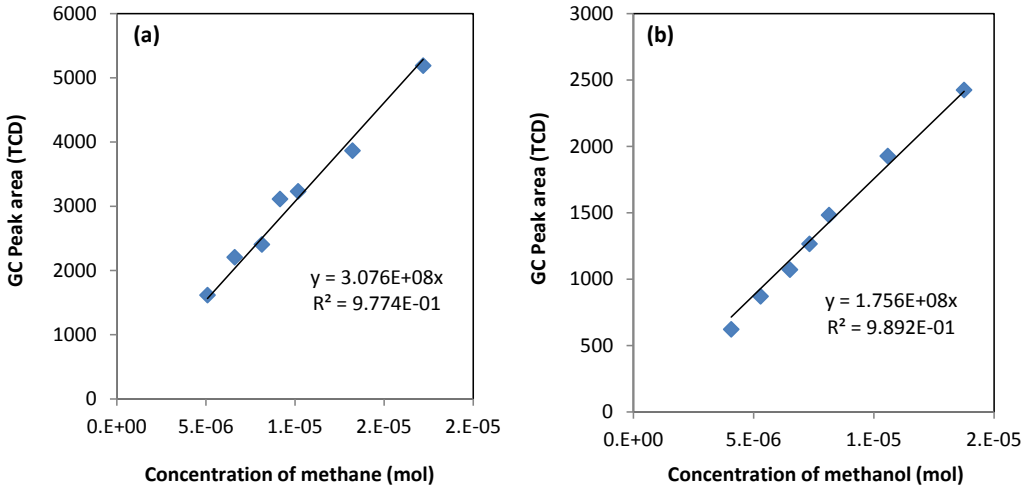

Figure 3.8: Areas of the chromatographic peaks as a function of: (a) the number of moles of methane injected and (b) the number of moles of n-heptane injected.

The lines shown in the graphs are considered as the calibration lines for methane and methanol. A constraint was imposed forcing the equations to intercept zero, therefore yielding a value of zero for the area when no methane or methanol respectively is injected. The resulting equations, relative to

the TCD detector, are given by the following expressions, with a square linear correlation coefficient for equation 3.1 of $r^2 = 0.9774$ and for equation 3.2 of $r^2 = 0.9892$:

$$Area = 3.076 \cdot 10^8 \cdot n_{methane} \quad (3.1)$$

$$Area = 1.756 \cdot 10^8 \cdot n_{methanol} \quad (3.2)$$

Where $n_{methane}$ is the amount of mol methane and $n_{methanol}$ is the amount of methanol in mol.

3.3.2.3 Analytical results for the reference system methane + methanol

After completing the calibrations for the components of the reference system, measurements on the binary system of methane + methanol were performed at temperatures of 298 K, and pressures between 5 MPa and 16 MPa. Firstly, the equilibrium cell was cleaned with toluene, water and ethanol several times, before being placed under vacuum for a period of 24 hours.
Methanol was degassed separately, using a vacuum pump and glass equipment. It was then possible to transfer methanol to the equilibrium cell, while keeping the vacuum, effectively removing gasses from the system. After the successful loading of liquid, methane was added to the cell directly from a high pressure bottle, taking care to rinse the previously evacuated tubing. After equilibration through stirring, samples from the gas and liquid phases were withdrawn and analyzed. A series of 10 measurements were made for each of the experimental conditions studied, in order to evaluate the repeatability of the sampling and of the analysis. For this system, low opening times (0.5s) were used for the ROLSI™ samplers, which provided clear and sharp peaks on the GC. An example of peaks obtained using the Winilab analysis program is shown in figure 3.9 for a two component system (sample and injection done using ROLSI™).

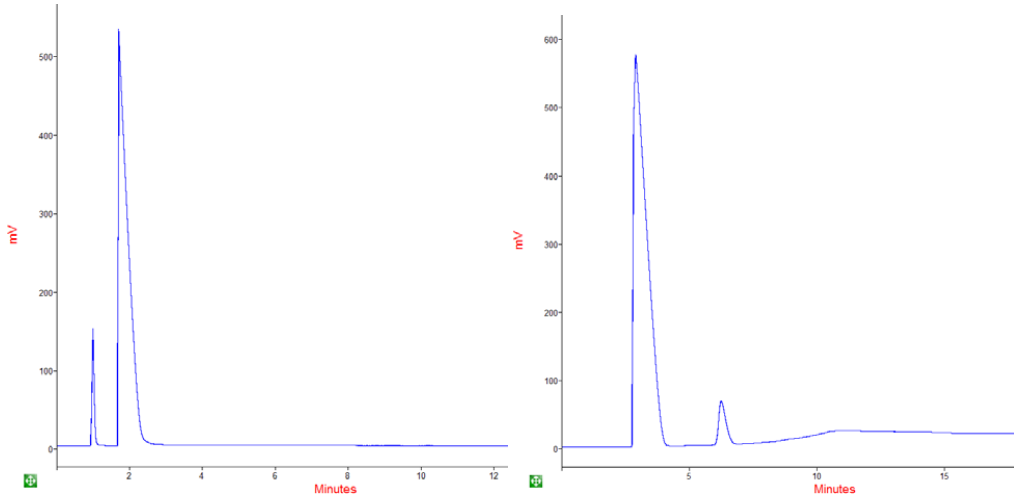

Figure 3.9: Chromatogram (TCD) of the analysis of methane + methanol. Left side is sample from the liquid phase. Right side is from the gas phase.

The results obtained in the analytical study of VLE in the binary system methane + methanol are presented in Table 3.3, where $x_{methane}$ and $y_{methanol}$ correspond to the molar fractions of methane in the liquid phase, and of methanol in the gas phase, respectively.

Table 3.3: Results obtained in the analytical study of the system methane + methanol. $\boldsymbol{x_{methane}}$ and $\boldsymbol{y_{methanol}}$ correspond to the mole fractions of methane in the liquid phase, and of methanol in the gas phase, respectively.

T / K	P / MPa	$x_{methane}$ x 10^3	$y_{methanol}$ x 10^3
298	3.72	29.31	7.00
298	5.52	43.43	5.32
298	9.48	74.64	3.82
298	13.79	108.57	4.41
298	15.51	122.14	4.69

The results obtained in the analysis of the different phases are compared with values found in literature. All values are averaged over at least 10 samples, which are taken for each condition. Figure 3.10 presents the values relative to the solubility of methane in methanol and methanol in the gas phase, making a comparison to literature sources [14-16] and to data obtained in this work using VLE equipment presented in chapter 2.

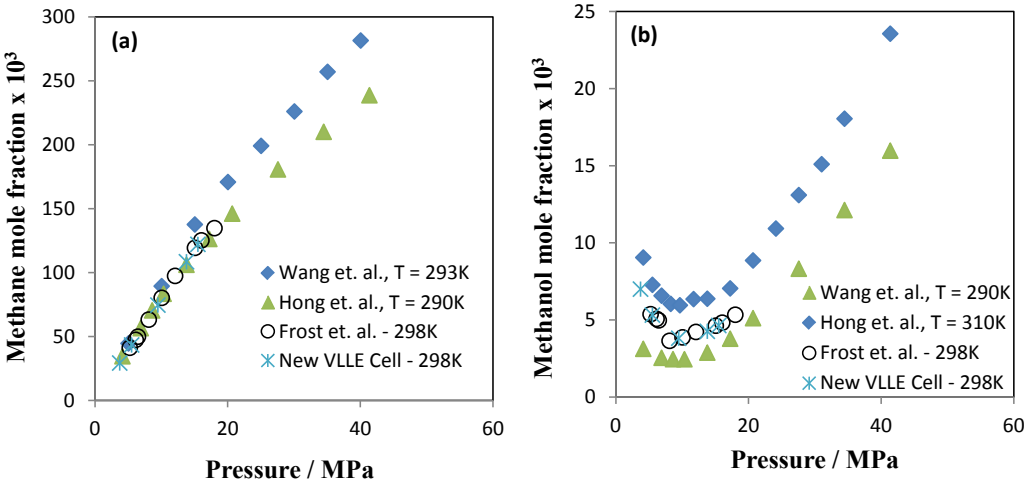

Figure 3.10: Solubility mole fraction of: (a) methane in methanol, (b) methanol in the gas phase, and comparison with literature data [14-16] at 298 K. Each data point presented in this work is the average value obtained at the specific condition.

The results gathered in the analytical study of this binary system confirm the correct performance of the analytical part of the equipment, even in challenging conditions such as these, with the determination of very low concentrations. Good agreement between the results obtained in this work and the literature values can be observed, confirming not only the quality of the set-up developed, but also the validity of the performed calibrations.

3.4 Experimental study of the quaternary system methane + *n*-hexane + methanol + water

After completing the testing of the equipment for measurement of thermodynamic phase equilibrium, a quaternary system containing methane, *n*-hexane, methanol and water, for which no data was found in the literature, was studied at 296.8 K, under pressures between 7 MPa and 10 MPa. The experimental procedures described in this work have been used. The global composition of the prepared mixture is given in Table 3.4.

Table 3.4: Global composition of the quaternary mixture methane + *n*-hexane + methanol + water studied in this work, given in molar fraction of the components.

Component	Mole fraction
methanol	0.19
water	0.45
methane	0.26
n-hexane	0.12

The system is initially investigated at a temperature of 296.8 K and pressures of 6.8 MPa and 9.2 MPa. In preparing this multicomponent mixture, the composition shown in table 3.4 was used. The results obtained in the analysis of the different phases are difficult to compare against literature data, as no data are available for the mixture of methane + n-hexane + methanol + water. There are similar systems [17]; however, they are usually at different temperatures, pressures and feed compositions, which influence the mutual solubility. The experimental results obtained for the VLLE are presented in Tables 3.5 and 3.6, where the shown values are an average of at least 10 samples for each phase. During this study, it was necessary to take many samples from each phase, in order to gain experimental results within acceptable accuracy (<10% on the composition). Modifications of the temperature program was also done, dependent on which phase was analyzed, in order to gain the most optimal peaks for the trace components.

Table 3.5: Results obtained in the study of the quaternary mixture methane + *n*-hexane + methanol + water, at 296.8 K and 9.2 MPa.

Component	Mole Fraction		
	Aqueous phase	Organic phase	Gas phase
methanol	0.3267	$5940 \cdot 10^{-6}$	$1508 \cdot 10^{-6}$
water	0.6663	$414 \cdot 10^{-6}$	$298 \cdot 10^{-6}$
methane	$7340 \cdot 10^{-6}$	0.4481	0.9856
n-hexane	$104 \cdot 10^{-6}$	0.5460	0.0122

Table 3.6: Results obtained in the study of the quaternary mixture methane + *n*-hexane + methanol + water, at 296.8 K and 6.8 MPa.

Component	Mole Fraction		
	Aqueous phase	Organic phase	Gas phase
methanol	0.3123	$6247 \cdot 10^{-6}$	$1649 \cdot 10^{-6}$
water	0.7282	$401 \cdot 10^{-6}$	$376 \cdot 10^{-6}$
methane	$5371 \cdot 10^{-6}$	0.3187	0.9839
n-hexane	$106 \cdot 10^{-6}$	0.6232	0.0111

An initial validation of the experimental results is done, by comparing with literature data for the system of methane + propane + n-heptane + methanol + water. Here data are used at a temperature of 284 K and pressure from 6.9 – 21 MPa. Figures 3.11 and 3.12 presents the experimental results from this work and compare them against data from the literature [17]:

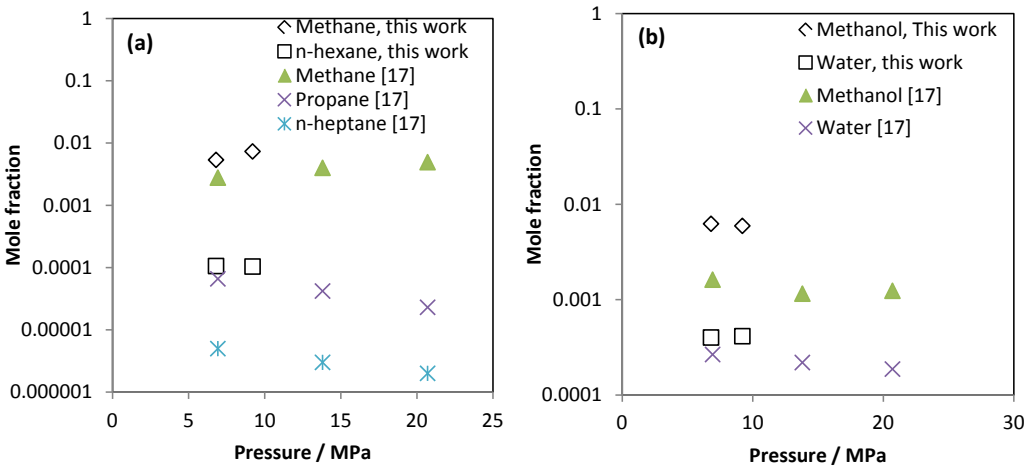

Figure 3.11: Solubility mole fraction of: (a) methane and n-hexane in aqueous phase, (b) methanol and water in the organic phase, and comparison with literature data [17]. Each data point presented in this work is the average value obtained at the specific condition.

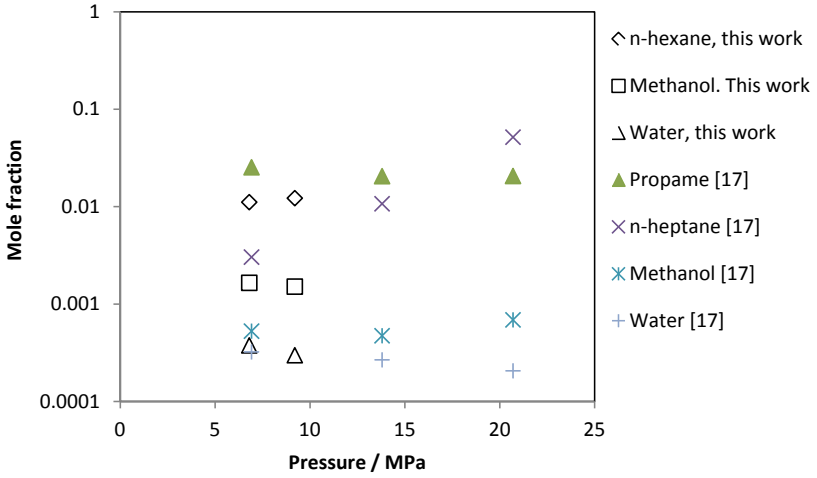

Figure 3.12: Solubility mole fraction of n-hexane, methanol and water in the gas phase and comparison with literature data [17]. Each data point presented in this work is the average value obtained at the specific condition.

This is not a direct comparison, as the literature data are for a five component mixture and are measured at a different temperature, with varying feed composition. However, it can be used to validate, that the new VLLE data are seemingly correct. From figure 3.11 it is seen, that the hydrocarbon solubility in the aqueous phase (methane and n-hexane) are comparable to the literature data. The solubility of water in the organic phase is also comparable to the literature data, especially since the water concentrations in the feed are of the same order. The concentration of methanol varies; however, this can be explained by a large difference of methanol concentration in the feed. Similar, the solubility in the gas phase (figure 3.12) are comparable to the literature data, with the concentration of methanol having the largest difference, due to the feed compositions.

Relative to the experimental results, it is necessary to take into account that this was the first actual measurements performed in a multiphase system, and unfortunately, within a very limited time frame. The issue often related to experimental work, is the break in continuity. Following the popular proverb that practice leads to perfection, is one of the reasons why continuity is so important in experimental work, in order to make use of the experience acquired in the work with a particular set-up. Experimental work is a time consuming discipline, which is not often recognized by the community.

3.5 Conclusions

In this chapter, a new high-quality experimental set-up for the study of phase equilibrium in multi-component systems at high pressures was presented. This relatively complex equipment was completely planned, designed and built for a current project, based on an analytical method with sampling.

Designing and constructing a completely new type of experimental equipment, allowed a high degree of customization, making it more accurate for the immediate needs. A complete description of the set-up was given, presenting a detailed description of all of its main parts and components. The quality of the equipment was confirmed by the extensive testing performed to all the systems involved, from the temperature and pressure measurements to the analytical aspects. These tests revealed the high precision and accuracy of the results which can be achieved with the set-up.

New VLLE experimental results was presented for the system of methane + n-hexane + water + methanol at T = 298.6 K and pressures of 9.2 MPa and 6.8 MPa. This contributes to the high quality of the constructed equipment, which has proven to be able to produce highly accurate results, within a reasonable timeframe.

References

[1] Even Solbraa, Statoil ASA, Research and Development Centre, Trondheim, Norway, Personal Communication, **2013**.

[2] A. J. Rondinone, C. Y. Jones, S. L. Marshall, B. C. Chakoumakos, C. J. Rawn, E. Lara-Curzio, *Canadian Journal of Physics* 81 (**2003**) 381-385.

[3] Y. E. Gorbaty, G. V. Bondarenko, *Review of Scientific Instruments* 66 (**1995**) 4347-4349.

[4] L. Ruffine, A. Barreau, I. Brunella, P. Mougin, J. Jose, *Ind. Eng. Chem. Res.* 44 (**2005**) 8387-8392.

[5] H. Reisig, K. D. Wisotzki, G. M. Schneider, *Fluid Phase Equilib.* 51 (**1989**) 269-283.

[6] H. Madani, A. Valtz, C. Coquelet, A. H. Meniai, D. Richon, *J. Chem. Thermodyn.*

40 (**2008**) 1490-1494.

[7] F. Garcia-Sánchez, G. Eliosa-Jiménez, G. Silva-Oliver, A. Godínez-Silva, *J. Chem. Thermodyn*. 39 (**2007**) 893-905.

[8] M. Grigiante, P. Stringari, G. Scalabrin, E. C. Ihmels, K. Fischer, J. Gmehling, *J. Chem. Thermodyn.* 40 (**2008**) 537-548.

[9] O. Elizalde-Solis, L. A. Galicia-Luna, S. I. Sandler, J. G. Sampayo-Hernández, *Fluid Phase Equilib.* 210 (**2003**) 215-227.

[10] A. Valtz, C. Coquelet, A. Baba-Ahmed, D. Richon, *Fluid Phase Equilib.* 207 (**2003**) 53-67.

[11] S. Mokraoui, C. Coquelet, A. Valtz, P. E. Hegel, D. Richon, *Ind. Eng. Chem. Res.* 46 (**2007**) 9257-9262.

[12] D. Seredynska, G. Ullrich, G. Wiegand, N. Dahmen, E. Dinjus, *J. Chem. Eng. Data* 52 (**2007**) 2284-2287.

[13] D. Richon, *Pure Appl. Chem.* 81 (**2009**) 1769-1782.

[14] L. K. Wang, G. J. Chen, G. H. Han, X. Q. Guo, T. M. Guo, *Fluid Phase Equilib.* 207 (**2003**) 143-154

[15] J. H. Hong, P. V. Malone, M. D. Jett and R. Kobayashi, *Fluid Phase Equilib*. 38 (**1987**) 83-96

[16] M. Frost, E. Karakatsani, N., von Solms, D. Richon, G.M. Kontogeorgis, *Jorunal of chemical engineering data*, 59 (**2014**) 961-969

[17] Chen C.J.; Ng, H.J. *Vapor – liquid and vapor – liquid – liquid for H2S, CO2, selected light hydrocarbons and a gas condensate in aqueous methanol or ethylene glycol solutions.* Gas Processors Association (GPA) report 149; DB Robinson Research Ltd.; Canada, **1995**.

Chapter 4 – Phase equilibrium of North Sea oils with polar chemicals: Experimental work

Today's oil and gas production requires application of various chemicals in large amounts. In order to evaluate the effect of those chemicals on the environment, it is of crucial importance to know how much of the chemicals are discharged via produced water and how much is dissolved in the crude oil. Therefore it is of interest to develop a thermodynamic model to predict the mutual solubility of oil, water and polar chemicals. But for the development and validation of the model, experimental data are required. This chapter presents new experimental liquid-liquid equilibrium (LLE) data for "North Sea Oils + monoethylene glycol (MEG)" and "North Sea Oils + MEG + water" at temperatures from 303 K to 323 K and at atmospheric pressure. The oils used in this work are from offshore fields in the North Sea.

4.1 Introduction

Chemicals are added in almost all the stages in oil and gas production. It is generally accepted that efficient and cost effective oil and gas production is not possible without the use of chemicals [1,2]. Monoethylene glycol (MEG) is one of the most widely used production chemicals. It is used as a gas hydrate inhibitor to ensure reliable production and transportation.

The overall purpose of this project is thermodynamic modeling of distribution of MEG in oil-water system using the CPA EoS. But for the development and validation of a thermodynamic model, experimental data are required. Those data are scarce in general, especially with oils. This has led to a running project with Statoil Research Center, in Norway, where during the past years experimental work has been carried out. This has led to experimental data for five reservoir fluids with MEG and water [3,4,5,6]. The experimental work has been carried out by Muhammad Riaz (Ph.d.), Mustafe Yussuf (Master thesis) and Michael Frost (Master thesis + Ph.d.).

Reservoir fluids are different in nature with regards to physical properties and distribution of hydrocarbons (Paraffinic, naphthenic and aromatic). In this work Liquid-Liquid experiments were carried out for two new Reservoir fluids, in order to investigate the effect of aromatic hydrocarbons and mutual solubility in heavy oils. The reservoir fluids used in this work, are two "heavy" oils which are obtained from offshore fields in the North Sea. In order to distinguish them from each other they are named as Fluid – 1 and Fluid – 2.

This chapter is divided into three sections namely experimental section, results and discussions and conclusions. The experimental section describes the materials and methods used to carry out experiments. Analytical techniques and equipments chosen in this work are discussed in this section. The results obtained from experimental work are described in results and discussion section. The data are analyzed and compared with the literature values of systems of well-defined hydrocarbons. Finally the trends, findings and contribution from this work are concluded.

4.2 Experimental section

4.2.1 Materials

The chemicals used in this work are given in Table 4.1 and no further purification was carried out. The Reservoir fluids were obtained from various fields in the North Sea. Their overall molar mass and density were measured by an external laboratory. The molar mass was measured using a freezing point depression method. The overall density and molar mass of these oils are given in Table 4.5. The composition of Fluid – 1 is given in Table 4.3 and composition of Fluid – 2 is given in Table 4.4.

Table 4. 1: Purity of the Chemicals used in this work.

Chemical	Purity [mole%]	Water content [%]	Supplier
Ethylene glycol	>99.78	<0.119	Acros Organics
Carbon Disulphide	>99.78	<0.119	Acros Organics
1-Dodecane	>99.9	<0.001	MERCK
1-Heptene	>99.99	<0.100	Sigma-Aldrich

4.2.2 Reservoir fluids

The compositional analysis (of pure oil) was carried out by gas chromatograph (SimDist) with specifications given in Table 4.2.

Table 4.2: Specifications of the gas chromatographs used in this work [3].

Characteristic	GC1 (Glycol GC)	GC2 (SimDist)
Type	CP-Wax 52 CB	Varian Capillary Column CP-Sil 5 CB
Column Type	Polar Column	Non-polar Column
Column Length	30 m	25 m
Column Internal Diameter	0.53 mm	0.53 mm
Column Film Thickness	1 µm	2 µm
Injector	0.2 µl	0.1 µl
Carrier Gas	Helium	Helium
Detector Type	FID*	FID

* Flame Ionization Detector

The SimDist used in work was calibrated using a standard containing paraffinic hydrocarbons from $C_1 – C_{40}$. Calibration was performed before every run, and is checked after every 10 runs on the GC. This is done in order to validate that the calibration is still good, and there have not been a shift in retention times. Samples of oil on a GC column will often results in a shift of calibration. The temperature programs for both GCs are shown in Appendices A. 1 and A. 2.

For quantification of components an internal standard 1-heptene was used. The internal standard is usually a component which is not present in an analyte sample and its peak does not overlap with any of other component's peak. A weighed amount of the internal standard (0.014-0.016 mass fraction of condensate) was added in the condensate sample. The sample is injected into a heated zone, vaporized and transported by a carrier gas into a non-polar column. The column partitions the components usually according to their boiling points similar to distillation. The eluted compounds are carried by a carrier gas (helium in this case) into a detector where the component concentration is related to the area under the detector response curve. Each component in the condensate appears as a peak and its amount can be calculated using equation 4.1.

$$w_i = \frac{w_{ISD} \cdot A_i \cdot RRF_i}{A_{ISD}} \tag{4.1}$$

Where w_i is the concentration of the component i (in mass fraction) in oil sample which is required to quantify , w_{ISD} is the mass fraction of internal standard, A_{ISD} is the area of the internal standard peak, A_i is the area of component i and RRF_i is the relative response factor of component i.

The composition reports of Fluid – 1 and Fluid – 2 up to decane plus fraction (C_{10+}) are given in Tables 4.3 and 4.4. Here components in the light end e.g. i-butane, n-butane, i-pentane and n-pentane are presented as individual compounds whereas heavier hydrocarbons are grouped into carbon number fractions (CN). All the components detected by GC between the two neighboring normal paraffin's are grouped together. They are measured and reported as a single carbon number (SCN) fraction, equal to that of the higher normal paraffin. For example all the components eluting between n-hexane and n-heptane in a GC chromatogram are classified as C_7 fraction. The carbon number of a fraction is determined according to the boiling point of the hydrocarbon components. Therefore components may not be classified according to the number of carbon atoms in their molecules. The examples include benzene and toluene. A benzene molecule contains six carbon atoms but because the boiling point of benzene is in the C_7 cut therefore it is classified as a C_7 component. Similarly the toluene molecule has seven carbon atoms but it is classified as C_8 component on the basis of its boiling point.

Table 4.3: Composition ($\boldsymbol{w}$, mass fraction and $\boldsymbol{x}$, mole fraction) density ($\boldsymbol{\rho}$) and Molar Mass ($\boldsymbol{M}$) of Fluid – 1.

Component	$w \cdot 10^2$	$x \cdot 10^2$	$\rho - g/cm^3$	$M - g/mol$
C2, (P)	0.02	0.09	0.3580	30.07
C3, (P)	0.44	1.57	0.5080	44.10
i-C4, (P)	0.33	0.90	0.5630	58.12
n-C4, (P)	1.47	3.98	0.5850	58.12
2,2-DM-C3 (P)	0.01	0.02	0.5970	72.15
Ic5 (P)	1.16	2.54	0.6250	72.15
nC5 (P)	1.88	4.10	0.6310	72.15
Hexanes Total	3.68	6.82	0.6676	85.01
Hexanes - P	3.46	6.32	0.6629	86.18
Hexanes - N	0.22	0.50	0.7500	70.13
Heptanes Total	8.10	14.06	0.7418	90.79
Heptanes - P	3.15	4.96	0.6876	100.20
Heptanes - N	4.25	7.69	0.7663	87.05
Heptanes - A	0.70	1.41	0.8840	78.11
Octanes Total	10.75	16.34	0.7668	103.59
Octanes - P	3.20	4.41	0.7068	114.23
Octanes - N	5.63	8.65	0.7727	102.49
Octanes - A	1.92	3.28	0.8710	92.14
Nonanes Total	6.79	8.99	0.7733	118.86
Nonanes - P	3.43	4.22	0.7214	128.08
Nonanes - N	1.41	1.88	0.7877	117.69
Nonanes - A	1.95	2.89	0.8721	106.17
Decanes Plus	65.38	40.58	0.8528	253.8

Table 4.4: Composition (***w***, mass fraction and ***x***, mole fraction) density (***ρ***) and Molar Mass (***M***) of Fluid – 2.

Component	$w \cdot 10^2$	$x \cdot 10^2$	$\rho - g/cm^3$	$M - g/mol$
C2, (P)	0.00	0.00	0.3580	30.07
C3, (P)	0.00	0.00	0.5080	44.10
i-C4, (P)	0.00	0.01	0.5630	58.12
n-C4, (P)	0.00	0.01	0.5850	58.12
2,2-DM-C3 (P)	0.00	0.00	0.5970	72.15
Ic5 (P)	0.02	0.07	0.6250	72.15
nC5 (P)	0.01	0.03	0.6310	72.15
Hexanes Total	0.10	0.33	0.6704	84.29
Hexanes - P	0.09	0.29	0.6627	86.18
Hexanes - N	0.01	0.04	0.7500	70.13
Heptanes Total	0.50	1.55	0.7485	91.16
Heptanes - P	0.09	0.25	0.6878	100.20
Heptanes - N	0.40	1.27	0.7604	89.73
Heptanes - A	0.01	0.03	0.8840	78.11
Octanes Total	1.26	3.43	0.7698	103.80
Octanes - P	0.30	0.75	0.7088	114.23
Octanes - N	0.75	2.05	0.7720	103.58
Octanes - A	0.21	0.63	0.8710	92.14
Nonanes Total	1.35	3.13	0.7582	122.56
Nonanes - P	0.83	1.85	0.7211	128.07
Nonanes - N	0.26	0.59	0.7850	124.49
Nonanes - A	0.26	0.69	0.8731	106.17
Decanes Plus	96.77	91.44	0.9477	358.0

The components in each carbon fraction can further be divided into paraffinic (P), naphthenic (N) and aromatic (A) contents known as PNA distribution of an oil or condensate. The reservoir fluids investigated are different in terms of PNA distribution and of the heavy end. It is assumed that the PNA distribution of the unknown C_{10+} fraction will be similar to that of the known components. In this way the PNA distribution for Fluid – 1 and Fluid – 2 is calculated using equations 4.2:

$$P = \frac{(wt\%)_P}{100 - (wt\%)_{C10+}}, N = \frac{(wt\%)_N}{100 - (wt\%)_{C10+}} \; and \; A = \frac{(wt\%)_A}{100 - (wt\%)_{C10+}} \tag{4.2}$$

where subscripts P, N and A represent paraffinic, naphthenic and aromatic hydrocarbons respectively and C_{10+} represents decane plus fraction.

Figure 4.1 presents the PNA distribution all systems previously investigated [3,4,5,6], Condensate – 1, Condensate – 2, Condensate – 3, Light Oil – 1, Light Oil – 2 and the hydrocarbon fluids used in this work, Fluid – 1 and Fluid – 2. The investigation of these reservoir fluids is of importance, in order to investigate the effect of aromatic and naphthenic content. Fluid – 1 and Fluid – 2 investigated in this work, are considered as being both aromatic and naphthenic of nature.

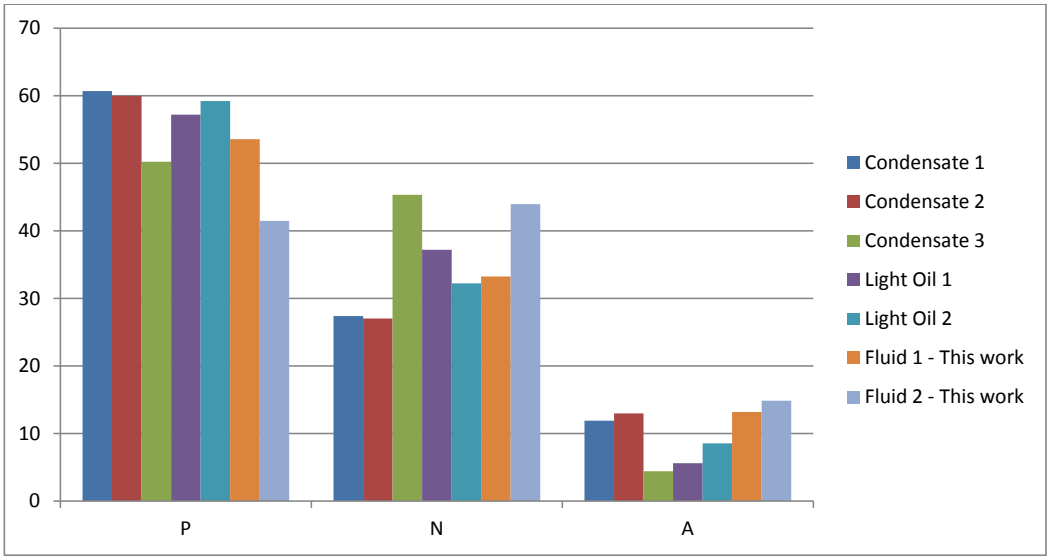

Figure 4.1: PNA distribution of all oil/condensate systems studied (Condensate 1 [4], Condensate 2 [5], Condensate 3 [6], Light Oil 1 [3], Light Oil 2 [3], Fluid – 1, this work and Fluid – 2, this work).

The characterization of reservoir fluids depends on the physical properties such as specific gravity and molecular weight. In order to gain an overview of the oils investigated, a comparison made between the molecular weights, density and plus fractions is shown in Table 4.5. There is great difference, especially with regards to molecular weight and plus fraction, between the fluids analysed. This is an important factor to investigate along with the influence of PNA distribution, as it can have a large impact on the mutual solubility with production chemicals. Especially Fluid – 2 is important in this respect, as it is heavy oil with 91.44 mol% C_{10+} fraction.

Table 4.5: Overall Density, Molar Mass and C10+ Fraction of Condensates and Oils Investigated [3,4,5,6].

Oil/Condensate	Molecular weight g/mol	Density g/cm^3	C_{10+} fraction
Condensate 1[4]	112.7	0.7562	24.25
Condensate 2[5]	106.9	0.7385	5.88
Condensate 3[6]	97.37	0.7205	6.84
Light Oil 1[3]	266	0.9055	76.64
Light Oil 2[3]	135.2	0.7784	31.9
Fluid 1 – This work	157.54	0.8016	40.58
Fluid 2 – This work	336.56	0.9416	91.44

4.2.3 Equipment and experimental procedure

The equipment used in this work for the measurement of mutual solubility is shown in Figure 4.2. The equipment shown in Figure 4.2 consists of:

a. **Air heated oven:** The heating oven consists of two compartments, the lower compartment was used for mixing of fluids (in a mixing machine) and the upper compartment was used for settling of the mixtures (in a glass equilibrium cylinder) to attain equilibrium. The objective of the oven is to carry out mixing and separation at a desired temperature. A required temperature is attained inside the oven by circulation of hot air.

b. **Mixing machine:** The mixing machine was used for the mixing of oil + MEG/water mixtures. MEG and oil are transferred in a 450 ml glass bottle with a cap on it. The bottles are tightened on mixing machine and mixing can be carried out at a desired rpm. The mixing machine was placed in the lower compartment of the heating oven.

c. **Equilibrium cylinder:** The mixture of MEG and hydrocarbons is shown after separation. The upper dark phase is the hydrocarbon rich phase and the lower (colorless) phase is the aqueous phase.

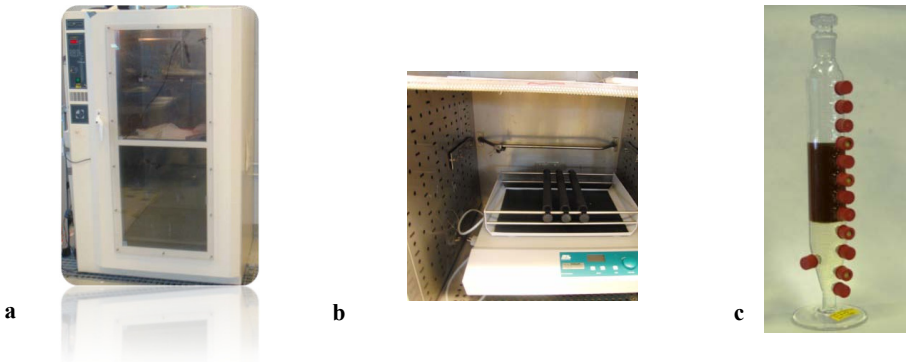

Figure 4.2: Equipments used at various stages of an experiment: (a). Heating oven used for mixing and attaining equilibrium at a fixed temperature (b).Mixing machine placed in lower part of heating oven (c). Equilibrium cylinder showing two phases, the upper phase is hydrocarbon phase and the lower phase is polar phase consisting of MEG and water.

The samples from the two phases in equilibrium cylinder are withdrawn using a special glass syringe. Each syringe is 10 ml in volume and has a nob to lock the fluid inside in order to avoid the spillage of sample.

Analyzing the MEG traces in the hydrocarbon phase and hydrocarbon traces in the polar phase, two different gas chromatographs (GC) are used. The SimDist GC was used to analyze hydrocarbon traces in polar phase and glycol GC was used to analyze MEG traces in hydrocarbon phase. The water content in hydrocarbon phase was analyzed using Karl Fisher coulometer.

The sketch of the experimental setup used in this work is shown in Figure 4.3. A similar setup has been used in the previous work by Folas et al.[7], Derawi et al. [8] and Riaz et al. [4,5] for the experimental study of liquid-liquid equilibria of well-defined hydrocarbons + polar compounds and light gas condensates + polar compounds. In this work modifications were made in the analytical methods, because the hydrocarbon phase is heavier reservoir fluid of higher complexity as compared to well-defined hydrocarbons. [3]

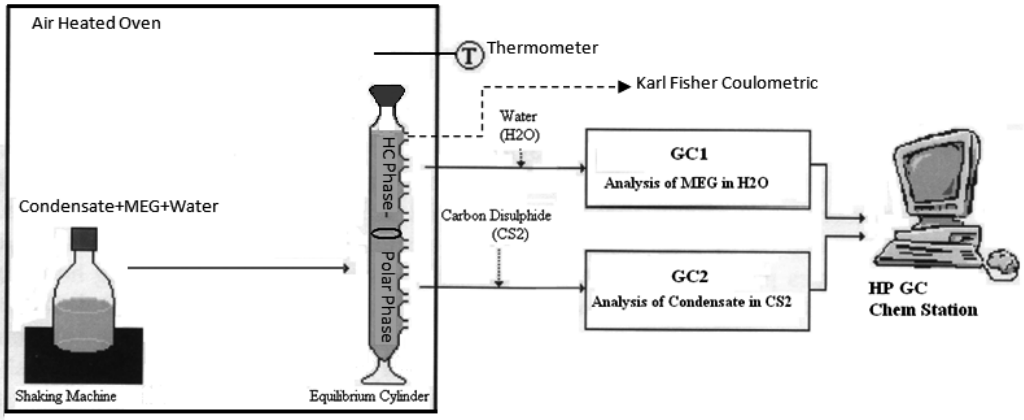

Figure 4.3: Sketch of the experimental setup used in this work.

4.2.3.1 Mixing and equilibrium

MEG, oil and water were mixed at a fixed temperature for up to 24 hours using a mixing machine in an air heated oven. For the MEG + oil systems, approximately equal mass of MEG and oil were added for mixing. In the MEG + oil + water systems the feed mixtures contain oil 0.50 mass fraction and the polar compounds were also 0.50 mass fraction. The polar phase consists of MEG and water where the composition of MEG ranges from 0.40 mass fraction to 0.80 mass fraction which is of interest to the industrial applications in the North Sea.

After mixing the mixture was transferred to two identical glass equilibrium cylinders and it was kept for at least 18-24 hours to attain equilibrium. The equilibrium cylinders contain holes and caps fitted with septa for sampling. Both mixing and separation were carried out in an air heated oven which was used at the temperature range from 275 K to 323 K in this work. A DOSTMANN P500 thermometer (± 0.1 K) was used for temperature measurement.

4.2.3.2 Sampling

After equilibrium, samples from the two phases were withdrawn manually using a syringe and a needle. The needle and the syringe were preheated to avoid phase separation due to temperature gradient. Two Agilent gas chromatographs (GCs) with different column specifications were used for composition analysis: one for the polar phase while another for the hydrocarbon rich phase. The characteristics of gas chromatographs used in this work are given in Table 4.2.

4.2.3.3 Polar phase analysis

For the polar phase analysis, hydrocarbons traces were extracted using the solvent extraction method. The solvent used in this work for the extraction of hydrocarbons from the polar phase is carbon disulphide (CS2) in which hydrocarbons are soluble but MEG has negligible solubility. The amount of CS2 added for extraction was 0.30-0.40 mass fraction in the sample. The CS2 was mixed with the sample from the polar phase for about 900 s and left for separation of the two phases. The extract phase is then analyzed on the SimDist with an internal standard 1-heptene diluted in 1-dodecane. The internal standard was diluted in order to have its concentration in range of the extracted hydrocarbon components. This will result in more accurate response factor and finally more accurate quantification of HC components. The peaks of 1-heptene and 1-dodecane should not overlap with any of the HC components peaks for safe quantification. The concentration of components in the polar phase can be calculated using equation 4.3:

$$w_i = area_i \cdot RF \cdot \left[\frac{m_{ISTD} + m_{Sample}}{m_{Sample}}\right] \cdot \left[\frac{m_{CS_2}}{m_{MEG}}\right] \tag{4.3}$$

where w_i is the mass fraction (in ppm) of hydrocarbon component i in the polar phase, RF the calculated response factor, m_{ISTD} weight of internal standard, m_{Sample} weight of sample run on the GC, m_{MEG} weight of sample taken from MEG phase and m_{CS_2} is weight of carbon disulphide used in extraction. From the GC analysis, the area of 1-heptene is obtained. Using the calculated weight fraction a response factor (RF) can be calculated by equation 4.4:

$$RF = \frac{wt_{1-heptene} \cdot 10^6}{area_{1-heptene}} \tag{4.4}$$

where $wt_{1-heptene}$ is the mass fraction of 1-heptene and $area_{1-heptene}$ is the area of the 1-heptene peak. The mass fraction of 1-heptene in the mixture is calculated using equation 4.5.

$$w_{1-heptene} = \frac{m_{1-heptene}}{m_{sample} + m_{ISTD}} \tag{4.5}$$

4.2.3.4 Hydrocarbon phase analysis

The MEG traces from the hydrocarbon rich phase were extracted using water and analyzed on the glycol GC. The initial column temperature was 353 K and was held for 120 s. The temperature was then increased linearly to 523 K in 1020 s. The temperature 523 K was held for 360 s. The total time for the temperature program is 1500 s. A graphical representation of temperature program is shown in appendix A.

The mass of water added for extraction of MEG was approximately (0.30-0.40) mass fraction of the mass of the sample. Water and the withdrawn sample were mixed for about 900 s in order to accelerate the extraction process. After mixing, some drops of the oil remained trapped in the water phase which makes sampling for GC vial difficult. Therefore the mixture of water and oil was kept in an oven for about 1800 s at temperature about 303.15 K. After separation, the oil will form the upper phase and the water containing extracted MEG will be the lower phase. The samples for GC analysis were taken from the lower phase, using a plastic syringe with a long needle.
The traces of MEG in hydrocarbons were quantified using multiple point external standard method. Several external standards were made covering the expected analyte (i.e. MEG) concentration range. A linear calibration curve was constructed using linear least squares method. In order to construct the calibration curve, the standards were run before and after the actual samples. This was done in order to account for the drift in the signal of the GC's detector if it occurs during the GC analysis.

The MEG is quantified automatically by the HP Chem Station Package using (response factor i.e. mass fraction/area or) linear calibration curve which was constructed using external standard. With a known amount of water used in the extraction, the weight of the MEG can be calculated:

$$m_{MEG} = w_{MEG/H_2O} \cdot m_{H_2O} \tag{4.6}$$

where w_{MEG/H_2O} is the concentration of MEG in water (obtained from the GC), and m_{H_2O} is the mass of added water. With the weight of the sample taken from the hydrocarbon rich phase, the fraction of MEG in oil can be calculated:

$$w_{MEG} = \frac{m_{MEG}}{m_{Sample}} \tag{4.7}$$

where m_{MEG} and $m_{Sample.}$ is the mass of MEG and sample from the hydrocarbon rich phase.

The water content of the hydrocarbon rich phase was analyzed using a Karl Fisher Coulometer which provides very fast and reliable results, especially for systems with low solubilities. In this work the apparatus Mettler Toledo DL37 Coulometric titrator for determining the amount of water in the hydrocarbon rich phase was used. Before the analysis of the sample for water content, external standards were analyzed in order to check the reliability of measurement. Four samples were measured for each temperature and the mean value was reported as the hydrocarbon rich phase water content.
Great care should be taken when analyzing production chemicals solubility in the heavy oils, since in some cases emulsions of water/MEG was observed in the organic phase. This is mainly due to the high density of these fluids.

4.3 Results and discussion

Binary experiments where run with 50 wt% of oil and 50 wt% MEG, where the ternary experiments were run with 50 wt% oil and 50 wt% MEG/water. The amount of water was varied, so experiments were carried out with MEG concentrations of 40 wt%, 60 wt% and 80 wt%. These measurements are carried out at various temperatures and at atmospheric pressure. At each temperature the mutual solubilities were measured for various feed compositions. The reported solubility of hydrocarbons in MEG/water is the sum of solubilities of all hydrocarbon components.

The experimental data for Fluid – 1 with MEG/water, at temperatures from 303.15 K – 323.15 K, are presented in Table 4.6. Experimental data for Fluid – 2 with MEG/water, at temperatures from 303.15 K – 323.15 K, are presented in Table 4.7.

Table 4.6: Experimental Equilibrium data for MEG (1) + Water (2) + Oil (3) at pressure 1 atm, for Fluid – 1.

Feed mole fraction			Polar phase Mole fraction			Hydrocarbon phase Mole fraction		
x_1	x_2	x_3	x_1	x_2	$x_3 \cdot 10^6$	$x_1 \cdot 10^6$	$x_2 \cdot 10^6$	x_3
T = 303.15 K and P = 1 atm								
0.6575	0.0000	0.3425	0.9973	0	2720	354	0	0.9996
0.3952	0.3551	0.2497	0.5264	0.4730	571	239	382	0.9994
0.2356	0.5586	0.2058	0.2965	0.7033	166	124	558	0.9993
0.1345	0.7031	0.1624	0.1605	0.8394	88	44	722	0.9992
T = 313.15 K and P = 1 atm								
0.6630	0.0000	0.3370	0.9972	0.0000	2779	609	0	0.9994
0.3453	0.4140	0.2407	0.4546	0.5450	408	375	523	0.9991
0.2345	0.5682	0.1974	0.2921	0.7077	166	189	713	0.9991
0.1354	0.7053	0.1592	0.1611	0.8388	87	88	936	0.9990
T = 323.15 K and P = 1 atm								
0.6588	0.0000	0.3412	0.9971	0.0000	2921	812	0	0.9992
0.4031	0.3404	0.2565	0.5418	0.4576	573	586	647	0.9988
0.2363	0.5541	0.2096	0.2989	0.7009	186	275	1068	0.9987
0.1417	0.7095	0.1489	0.1665	0.8335	86	164	1575	0.9983

Table 4.7: Experimental Equilibrium data for MEG (1) + Water (2) + Oil (3) at pressure 1 atm, for Fluid – 2.

Feed mole fraction			Polar phase Mole fraction			Hydrocarbon phase Mole fraction		
x_1	x_2	x_3	x_1	x_2	$x_3 \cdot 10^6$	$x_1 \cdot 10^6$	$x_2 \cdot 10^6$	x_3
T = 303.15 K and P = 1 atm								
0.7156	0.0000	0.2844	0.9994	0	1648	541	0	0.9995
0.4109	0.3610	0.2281	0.5322	0.4676	191	223	679	0.9991
0.2435	0.5446	0.2118	0.3090	0.6909	120	98	913	0.9990
0.1339	0.6775	0.1886	0.1650	0.8349	98	40	1076	0.9989
T = 313.15 K and P = 1 atm								
0.7174	0.0000	0.2826	0.9993	0.0000	1665	747	0	0.9993
0.4060	0.3650	0.2290	0.5265	0.4733	209	269	943	0.9988
0.2273	0.5511	0.2216	0.2920	0.7079	117	123	1270	0.9986
0.1245	0.6764	0.1991	0.1554	0.8445	94	55	1359	0.9986
T = 323.15 K and P = 1 atm								
0.7197	0.0000	0.2803	0.9993	0.0000	1677	832	0	0.9992
0.4054	0.3640	0.2306	0.5268	0.4730	243	309	1214	0.9985
0.2372	0.5400	0.2228	0.3052	0.6947	145	154	1390	0.9985
0.1322	0.6670	0.2009	0.1654	0.8345	107	68	1669	0.9983

4.3.1 Reservoir fluids + MEG systems

Reservoir fluids typically consist of paraffinic (P), naphthenic (N) and aromatic (A) compounds. The solubility of MEG in a specific carbon fraction (e.g. C7) will be the highest in the aromatic HC (e.g. benzene) and the lowest in the paraffinic HC (e.g. n-heptane). The same is also true for the solubility of HC in MEG. Since reservoir fluids consist of paraffinic, naphthenic and aromatic hydrocarbons, it is expected that the solubility of MEG in reservoir fluids is between the corresponding solubility of MEG in well-defined hydrocarbons (such as Benzene and n-heptane). In order to validate the mutual solubility data obtained for Fluid – 1 and Fluid – 2, it is compared against results for MEG/Benzene and MEG/n-heptane, as well as previously investigated condensate/oil systems.

Figures 4.4 and 4.5 presents the mutual solubility of the two reservoir fluids with MEG, where it is seen, that the solubility is between the solubility values in the aromatic (benzene) and the paraffinic (n-heptane) hydrocarbon. Comparing against previously investigated condensate/oil systems lets us have a look at the influence of PNA distribution, along with the effect of heavy end (C_{10+} fraction).

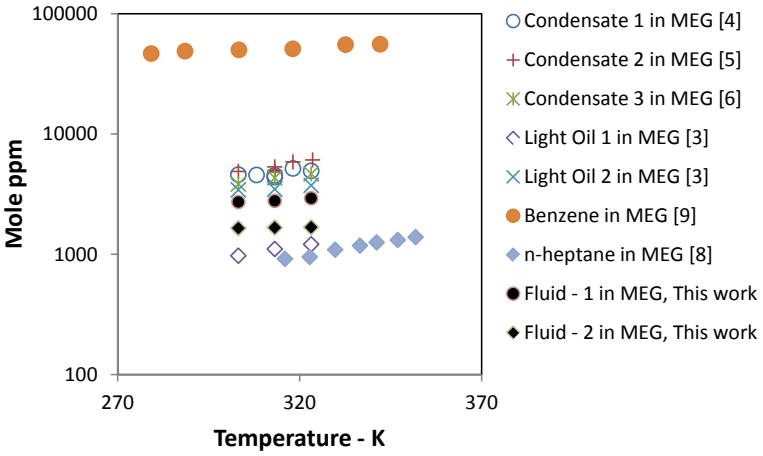

Figure 4.4: Comparison of the solubility (in Mole ppm) of well-defined hydrocarbons (n-heptane [8,10] and benzene [9]) and reservoir-fluids (Condensate 1, Condensate 2, Condensate 3, Light Oil 1, Light Oil 2, Fluid – 1 and Fluid – 2) in MEG as a function of temperature.

The new data are in good agreement with previous measured data, and the solubility is correctly situated between the solubility of MEG/Benzene and MEG/n-heptane. From Figure 4.4 it can be seen that the solubility of Fluid – 1 and Fluid – 2 in MEG is lower than that for previously investigated systems. A decrease in solubility can be seen with increasing average molecular weight of the fluids. Fluid – 2 and Light oil 1 being the two heaviest oils investigated, have the lowest solubility in the polar phase.

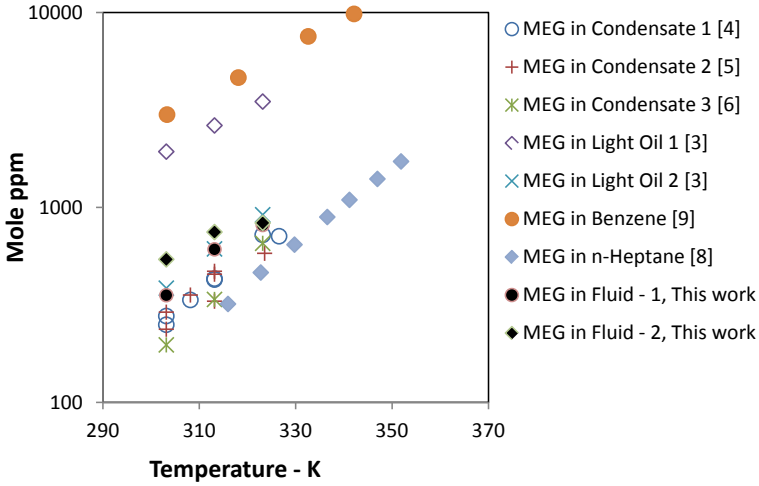

Figure 4.5: Comparison of the solubility (in Mole ppm) of MEG in well-defined hydrocarbons (n-heptane [8] and benzene [9]) and reservoir-fluids (Condensate 1, Condensate 2, Condensate 3, Light Oil 1, Light Oil 2, Fluid – 1 and Fluid – 2) as a function of temperature (K).

Similar trends are observed for the solubility of MEG in the organic phase. The solubility increases for the more heavy oils, with the solubility of MEG in Fluid – 1 being higher than the previous systems. This is disregarding the high solubility of MEG in Light oil – 1. The increased solubility of MEG in organic phase for Fluid – 1 and Fluid – 2, is also caused by the increase of aromatic and naphthenic hydrocarbons in these fluids.

4.3.2 Reservoir fluids + MEG + water systems

Solubility data available for hydrocarbon-MEG-water systems are very scarce, with only very few data being accessible to public view. Razzouk et. al. [11] have presented experimental data for MEG-water-n-hexane system in 2010 and some data are present for MEG-water-benzene, presented by Folas et. al. [9]. These data have been key for verifying the solubility of oil with MEG/water, as the mutual solubility of theses mixtures should be in the area between these two well-defined systems. Figures 4.6 – 4.8 presents the solubility of hydrocarbons in the polar phase, MEG in the organic phase and water in the organic phase at 323.15K and 1 atm, as a function of the MEG concentration in the polar phase. The new results are compared against the data of Razzouk (MEG-Hexane [11]), Folas (MEG-Benzene [9]) and our previously measured condensate/oil systems

(Condensate – 1 [4], Condensate – 2 [5], Condensate – 3 [6], Light Oil – 1 [3] and Light Oil – 2 [3]).

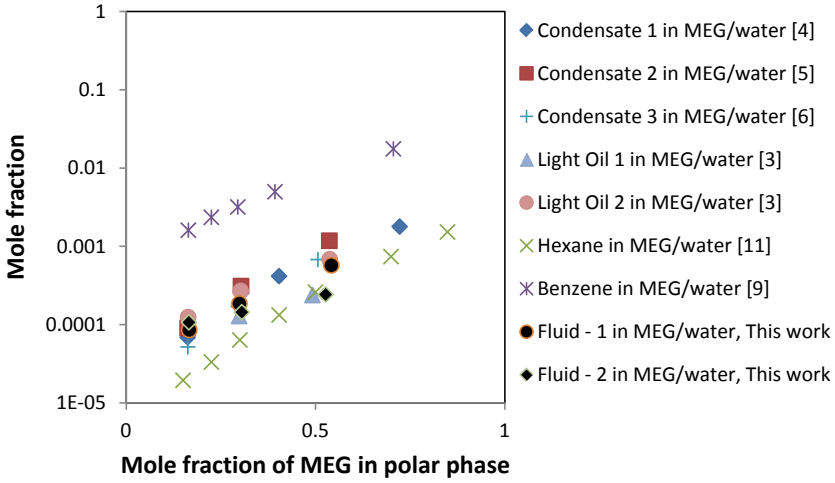

Figure 4.6: Comparison of the solubility (in Mole fraction) of well-defined hydrocarbons (n-hexane [11] and benzene [9]) and reservoir-fluids (Condensate 1, Condensate 2, Condensate 3, Light Oil 1, Light Oil 2, Fluid – 1 and Fluid – 2) in the polar phase as a function of MEG mole fraction in the polar phase at 323.15 K and 1 atm.

Good agreement is observed between the new data and previous work. We can observe an increased solubility of chemicals in the organic phase, as a result of the heavy nature and more aromatic/naphthenic composition of Fluid – 1 and Fluid – 2. The solubility of water in oil seems to be largely unaffected by the difference in fluids. A trend can be seen, where more water have increased solubility in the more heavy and aromatic oils.

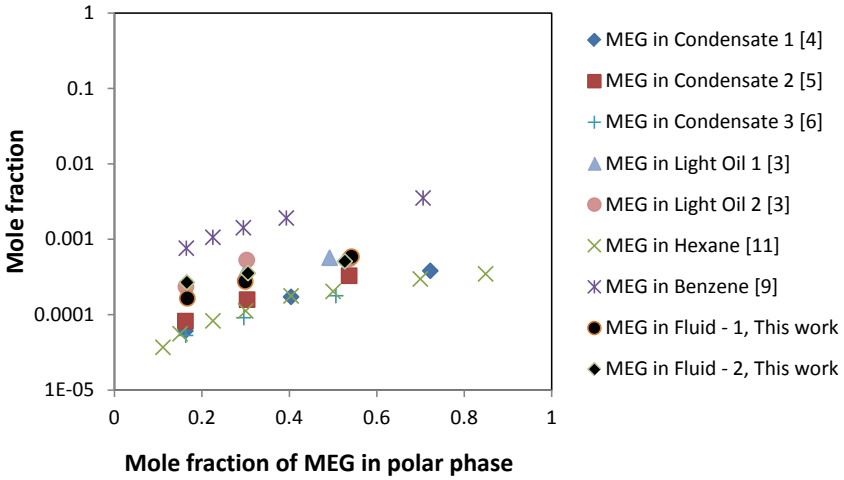

Figure 4.7: Comparison of the solubility (in Mole fraction) of MEG in well-defined hydrocarbons (n-hexane [11] and benzene [9]) and reservoir-fluids (Condensate 1, Condensate 2, Condensate 3, Light Oil 1, Light Oil 2, Fluid – 1 and Fluid – 2) as a function of MEG mole fraction in the polar phase at 323.15 K and 1 atm.

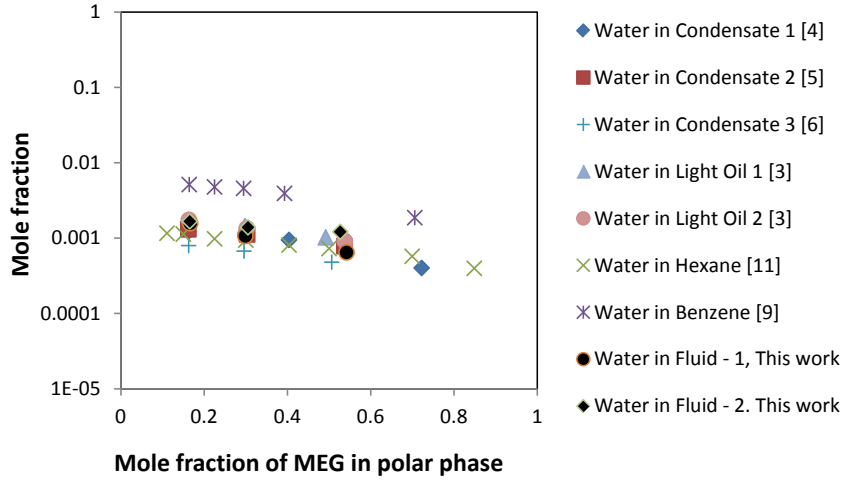

Figure 4.8: Comparison of the solubility (in Mole fraction) of water in well-defined hydrocarbons (n-hexane [11] and benzene [9]) and reservoir-fluids (Condensate 1, Condensate 2, Condensate 3, Light Oil 1, Light Oil 2, Fluid – 1 and Fluid – 2) as a function of MEG mole fraction in the polar phase at 323.15 K and 1 atm.

From analysis on SimDist, a clear distribution of hydrocarbon solubility in the polar phase could be seen. The amount of water present in the mixture has a large influence on the solubility. Figures 4.9 + 4.10 present a detailed analysis of Fluid – 1 and Fluid – 2 with 100%, 80%, 60% and 40% MEG at 303.15 K.

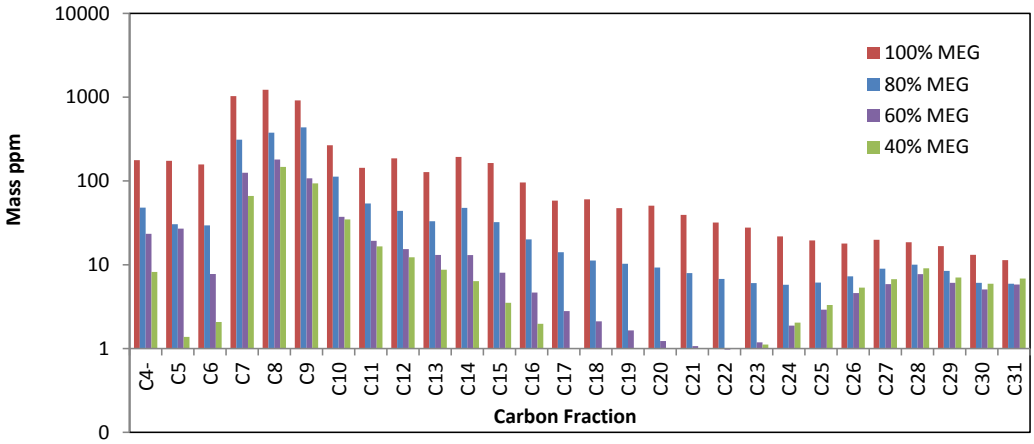

Figure 4.9: Solubility (in mass ppm) of Fluid – 1 in polar phase (MEG + water) at temperature 303.15 K and MEG composition in polar phase.

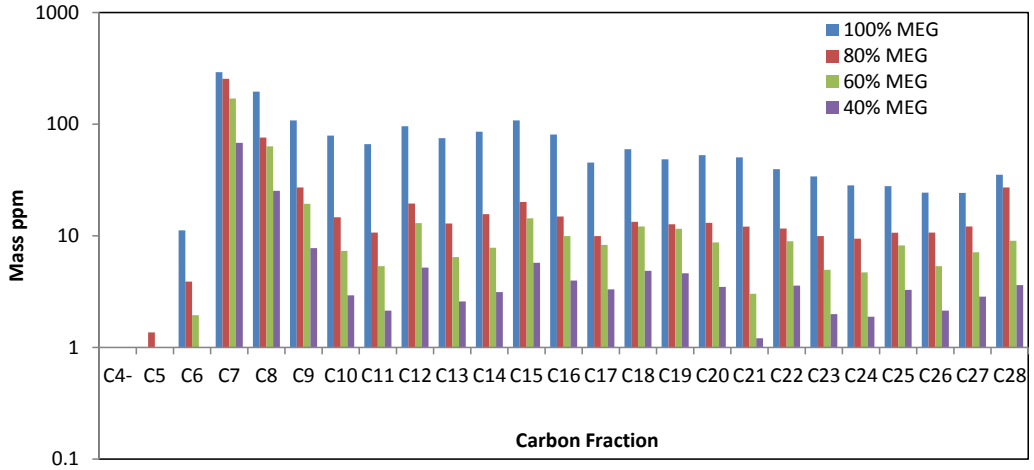

Figure 4.10: Solubility (in mass ppm) of Fluid – 2 in polar phase (MEG + water) at temperature 303.15 K and MEG composition in polar phase.

The detailed analyses of Fluid – 1 show three fractions (C_7-C_9) as the major contributors to the total solubility. The solubility of hydrocarbons in the polar phase is decreasing with increasing carbon number. However, a small increase in hydrocarbon solubility is observed around C_{23}-C_{29}. The solubility of hydrocarbon in the polar phase decreases with increasing concentration of water, as can be seen in figure 4.9, by the low concentration (mass ppm) at 40% MEG.
The detailed analyses of Fluid – 2 in figure 4.10, present two fractions (C_7-C_8) as the major contributors to the total solubility of hydrocarbons in the polar phase. Again we observe that the solubility of hydrocarbons in the phase decrease with increasing water concentration. For both Fluid – 1 and Fluid – 2, the ratio of water and MEG have a large impact on the solubility of oil in the polar phase.
The mutual solubility of MEG, water and oil increases with increasing temperature. It is observed that the solubility of aromatic hydrocarbons (i.e. benzene, toluene etc.) is much higher than that of paraffinic and naphthenic hydrocarbons. The sum of solubilities of benzene and toluene contribute almost half of the total solubility of oil in the polar phase. This is an indication of solvation between polar chemicals and aromatic hydrocarbons.
It is clear, that the PNA distribution has an effect on the mutual solubility of oil with MEG/water. A tendency of increased chemical solubility is observed, and an increased solubility of the aromatic components in the polar phase, as a results of solvation. The PNA distribution is however, not the only factor on the solubility, as the distribution of components (C_{10+} fraction) and overall composition plays a major role as well. This is clear when investigating the detailed solubility; where it is particular low carbon number aromatics, such as benzene and toluene, which have the largest impact on the total solubility hydrocarbons and the solubility of hydrocarbons in the polar phase is clearly decreasing with increasing carbon numbers.

4.4 Conclusions

In this chapter new experimental data for mutual solubility of North Sea oils + MEG systems are presented. To evaluate the effect of water on mutual solubility oils + MEG + water systems are experimentally investigated and the data are presented. The experimental work was carried out for liquid-liquid equilibrium in the temperature range of 303.15 to 323.15 K at atmospheric pressure.
In the reservoir-fluid + MEG systems, the mutual solubility increases with increasing temperature. The solubility of aromatic hydrocarbons is much higher than that of naphthenic and paraffinic

hydrocarbons in each carbon fraction. Benzene and toluene contribute a major part to the solubility of reservoir fluid in MEG. Therefore the more aromatic (in C7-C9 carbon fraction) the oil is the higher will be the solubility and vice versa. In the reservoir-fluid + MEG + water system, the mutual solubility of MEG and oil decreases with increasing water content in the polar phase and the solubility of some of the components become negligible. The mutual solubility increases with increasing temperature. The solubility of aromatic hydrocarbon is higher than that of naphthenic and paraffinic hydrocarbons. The aromatic components like benzene and toluene contribute almost half of the total solubility of oil in MEG.

References

[1] Fink, J. *Oil Field Chemicals*. 1st ed. Gulf Professional Publishing, **2003**.

[2] Nordstad, E. N. Knudsen, B. L. Sæten, J. O. Aas, N. Eilersten, H. B. *Statoil internal report*, **1998**.

[3] Frost, M. Kontogeorgis, G. M. Stenby, E. H. Yan, W. Haugum, T. Christensen, K. O. Solbraa, E. Løkken, T. V. *Fluid Phase Equilibria* (**2013**) 1-6

[4] Riaz, M. Kontogeorgis, G. M. Stenby, E. H. Yussuf, A. M. Haugum, T. Christensen, K. O. Solbraa, E. Løkken, T. V. *Fluid Phase Equilibria* (**2013)**, *340*, 1-6.

[5] Riaz, M. Kontogeorgis, G. M. Stenby, E. H. Yan, W. Haugum, T. Christensen, K. O. Løkken, T. V. Solbraa, E. *Journal of Chemical & Engineering Data 56* (**2011)** 4342-4351

[6] Riaz, M. Yussuf, A. M. Frost, M. Kontogeorgis, G. M. Stenby, E. H. Yan, W. Solbraa, E. *Energy and Fuels 28 (***2014)** 3530-3538.

[7] Folas, G. K. Kontogeorgis, G. M. Michelsen, M. L. Stenby, E. H. *Industrial & Engineering Chemistry Research* 45 (**2006)** 1527-1538.

[8] Derawi, S. O. Kontogeorgis, G. M. Stenby, E. H. Haugum, T. Fredheim, A. O. *Journal of Chemical & Engineering Data* 47 (**2002)** 169-173.

[9] Folas, G. K. Kontogeorgis, G. M. Michelsen, M. L. Stenby, E. H. Solbraa, E. *Journal of Chemical & Engineering Data* 51 **(2006)** 977-983.

[10] Lindboe, M. Haugum, T. Fredheim, A. O. Solbraa, E. Measurement and Modeling of Liquid-Liquid Equilibrium in n-Heptane-MEG Systems **2002**.

[11] Razzouk, A. Naccoul, R. A. Mokbel, I. Duchet-Suchaux, P. Jose, J. Rauzy, E. Berro, C. *Journal of Chemical & Engineering Data* 55 (**2010)** 1468-1472.

Chapter 5 – Modelling approach using the CPA equation of state

Equations of state play an important role in chemical and petroleum engineering design, and they have assumed expanding role in the study of the phase equilibria of fluids and fluid mixtures [1]. The cubic equations of state, such as the Soave-Redlich-Kwong [2] and the Peng-Robinson (PR) [3], are widely used in the oil and gas industry [4] when handling phase equilibrium properties in hydrocarbon mixtures.

Modeling of phase equilibria of complex mixtures containing hydrogen bonding is a challenging issue in the area of thermodynamics. These widely used existing models (SRK, PR), are known to fail to correlate these kind of phase equilibrium, due to the strong hydrogen bonding forces, which cannot be captured by the attractive term of such EoS. Combining the classical cubic EoS with excess Gibbs energy models, the so-called EoS/G^E – models, can provide satisfactory results, however, they are dependent on the accuracy of the activity coefficient model like NRTL [5] and UNIQUAC [6]. Such local composition models often fail to describe well mixtures with associating compounds, especially for multiphase, multicomponent equilibria. Associating components are those which are capable of hydrogen bonding e.g. alcohol, glycol, water and amines etc. Phase equilibria of complex associating systems are important for many applications, for example in the oil industry for studying of gas hydrates, calculation of the amount of hydrate inhibitors and their partitioning between water and oil, azeotropic and extractive separation. Furthermore they have many applications in environmental, polymer and chemical industry.[4]

Over the past 30 years, substantial progress has been made regarding the development of thermodynamic models which can successfully describe complex chemical systems containing associating components and hydrogen bonding. By extending Wertheim's theory [7-10], Chapman et al. [11,12] proposed a general statistical associating fluid theory (SAFT) approach. Huang and

Radosz [13] developed the SAFT equation of state which accounts for hard-sphere repulsive forces, dispersion forces, chain formation and association. In 1996 Kontogeorgis et al. [14] presented the Cubic Plus Association (CPA) equation of state, suitable for describing associating fluids. The equation combines the simplicity of a cubic equation of sate (SRK) and the association theory of Wertheim [7-10]. In the absence of association, the CPA EoS reduces to SRK EoS.
In this thesis the CPA EoS has been applied to a variety of phase equilibria (liquid-liquid, vapor-liquid and vapor-liquid-liquid) of complex polar and associating, non-associating and solvating compounds. These chemicals include alkane/aromatic hydrocarbons, water and polar chemicals (methanol and monoethylene glycol) used as gas-hydrate inhibitors. The CPA EoS has been extended to reservoir fluids by Yan et al. [15] using a characterization procedure similar to that of Pedersen et al. [16] and a set of new correlations for the critical properties. Calculations presented for reservoir-fluids + water and reservoir-fluids + water + methanol/glycols showed promising results [15].

5.1 The Cubic-Plus-Association equation of state

The CPA EoS, proposed by Kontogeorgis et al.[4,15,17] is an extension of the SRK EoS to include also association effect. It can be expressed for mixtures in terms of pressure as a sum of the SRK EoS and the contribution of association term as given by Michelsen and Hendriks [18]:

$$P = \frac{RT}{V_m - b} - \frac{\alpha(T)}{V_m(V_m + b)} - \frac{1}{2}\frac{RT}{V_m}\left(1 + \rho\frac{\partial lng}{\partial \rho}\right)\sum_i x_i \sum_{A_i}\left(1 - X_{A_i}\right) \tag{5.1}$$

where V_m is the molar volume, X_{A_i} is the fraction of A-sites of component *i* that are not bonded with any other component, and x_i is the mole fraction of component i.
The CPA equation of state can be seen as an extension of the cubic SRK EoS. This means, that in the absence of association, the last term of equation 5.1 is eliminated. The key element of the model and of the associating term is X_{A_i}, which is an expression for the fraction of sites A on molecule i, that do not form bonds with other active sites. This is given by equation 5.2:

$$\frac{1}{X_{A_i}} = 1 + \frac{1}{V_m}\sum_j x_j \sum_{B_j} X_{B_j} \Delta^{A_i B_j} \tag{5.2}$$

Where $\Delta^{A_iB_j}$ is the association strength between site A on molecule *i* and site B on molecule *j* and is given by equation 5.3:

$$\Delta^{A_iB_j} = g(\rho)\left[exp\left(\frac{\varepsilon^{A_iB_j}}{RT}\right)-1\right]b_{ij}\beta^{A_iB_j} \tag{5.3}$$

This contains the radial distribution function $g(\rho)$ which is given as:

$$g(\rho) = \frac{1}{1-1.9\eta} \tag{5.4}$$

$$\eta = \frac{1}{4}b\rho \tag{5.5}$$

Where η is the reduced fluid density.

The energy parameter in the SRK part of equation 5.1, is given by a Soave-type temperature dependency, whereas b is considered to be temperature independent.

$$\alpha(T) = a_0\left(1+c_1\left(1-\sqrt{T_r}\right)\right)^2 \tag{5.6}$$

where $T_r = T/T_C$, T_C being the critical temperature.

5.1.1 Pure component parameters

In total the CPA equation contains five pure compound parameters. Three are needed for the SRK term (a_0 , b , c_1) and two for the association part ($\varepsilon^{A_iB_j}$and $\beta^{A_iB_j}$). The parameters for the associating term are the association energy and the association volume, respectively. These parameters are often obtained by fitting experimental vapor pressures and liquid density data. For inert (non self-associating) components, only the SRK parameters need to be determined, which again can be done through fitting experimental vapor pressure and liquid density, or calculated from critical data and acentric factor.

The three pure component parameters a_0 , b and c_1 correspond to a set of "apparent" critical temperature (T_{cm}), critical pressure (P_{cm}) and acentric factor (ω_m). The subscript m means they are

CPA "monomer" parameters, instead of experimental values. From Yan et al. [15] the equations for T_{cm}, P_{cm} and ω_m are given as:

$$m_m = c_1\sqrt{\frac{a_0\Omega_B}{bRT_c\Omega_A}} \tag{5.7}$$

$$T_{cm} = T_c\left(\frac{1+1/c_1}{1+1/m_m}\right)^2 \tag{5.8}$$

$$P_{cm} = \frac{\Omega_B RT_{cm}}{b} \tag{5.9}$$

where $\Omega_A = 0.42748$, $\Omega_B = 0.08664$ and $m_m = 0.480 + 1.574\omega_m - 0.179\omega_m^2$.

5.1.2 Mixing and combining rules

The CPA EoS when applied to mixtures requires mixing rules for the SRK part, while the association part is the same as for pure components.The mixing and combining rules for α and b is the classical van der Waals one-fluid theory:

$$\alpha(T) = \sum_i\sum_j x_i x_j \alpha_{ij} \tag{5.10}$$

$$b = \sum_i\sum_j x_i x_j b_{ij} \tag{5.11}$$

where the combining rules are given as:

$$\alpha_{ij} = \sqrt{\alpha_i\alpha_j}\left(1-k_{ij}\right) \tag{5.12}$$

$$b_{ij} = \frac{b_i + b_j}{2} \tag{5.13}$$

where k_{ij} is referred to as a binary interaction parameter.

For mixtures containing more than one associating compound such as the case of mixtures of glycols and water, combining rules are needed for the association parameters. Different combining rules have been suggested [19]. Two types of combining rules have been shown to perform best, the

CR-1 combing rule proposed by Derawi et al. [20] and the Elliott combining rule (ECR) proposed by Suresh and Elliott [21].

The expressions for the cross-association energy and cross-association volume parameters with CR-1 combining rule are given by the equations below:

$$\varepsilon^{A_iB_j} = \frac{\varepsilon^{A_iB_i} + \varepsilon^{A_jB_j}}{2} \tag{5.14}$$

$$\beta^{A_iB_j} = \sqrt{\beta^{A_iB_i}\beta^{A_jB_j}}\left(\frac{b_i+b_j}{2}\right) \tag{5.15}$$

The expression for the cross-association strength with the Elliott Combining Rule (ECR) is given by equation 5.16:

$$\Delta^{A_iB_j} = \sqrt{\Delta^{A_iB_i}\Delta^{A_jB_j}} \tag{5.16}$$

The CR-1 and ECR rules are functionally similar; the only difference is the function of *b* in the expression for the cross – association volume (which is important for size-asymmetric systems e.g. water with heavy alcohols or glycols).

In the case of mixtures containing self-associating (water, glycols, alcohols) and inert compounds (e.g. aromatic hydrocarbons), where there is the possibility of cross-association (solvation), the modified CR-1 combining rule proposed by Folas et al. [22] is used. Using the modified CR-1 combining rule, allows for the cross association volume $\beta^{A_iB_j}$ to be determined from experimental data, and the cross association energy parameter becomes equal to the half of the association energy of the associating compound:

$$\varepsilon^{A_iB_j} = \frac{\varepsilon_{Associating}}{2} \tag{5.17}$$

$$\beta^{A_iB_j} = \beta^{cross}\left(Fitted\right) \tag{5.18}$$

5.1.3 Association schemes

The association term in the CPA EoS depends on the number and type of association sites for the given associating compounds, i.e. the association scheme. Huang and Radosz [13] have classified eight different association schemes and Table 5.1 provides a schematic explanation of the different types of association schemes used in this thesis. In this work methanol is described as 2B where the two lone-pairs on oxygen are considered to be a single site. The four-site (4C) association scheme is used in this work for MEG, in accordance to Derawi et al. [20,23]. Although glycols have at least 6 sites based on their chemical structure, the choice of the 4C scheme is consistent with the 2B scheme for alcohol where the two lone pairs of oxygen are considered to be a single site. The four site (4C) association scheme is traditionally used for water within the CPA framework [14,20,24-25].

Table 5.1: Association schemes based on the terminology of Huang and Radosz [13]

Species	Formula	Association Scheme	Site fractions (X)
Water	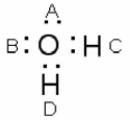	4C	$X^A = X^B = X^C = X^D$ $X_1 = X^A X^B X^C X^D$
Alcohol	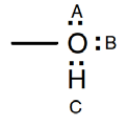	3B	$X^A = X^B; X^C = 2X^A - 1$ $X_1 = X^A X^B X^C$
	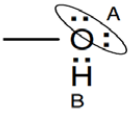	2B	$X^A = X^B$ $X_1 = X^A X^B$
Glycol	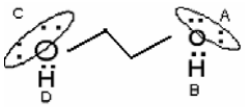	4C	$X^A = X^B = X^C = X^D$ $X_1 = X^A X^B X^C X^D$

5.2 C_{7+} Characterization

Reservoir fluids are often divided into two categories, the well-defined petroleum fractions and the undefined petroleum fractions. The undefined fraction consists of heavy components that are lumped together as the plus-fraction (C_{7+} fraction), and will be present in almost every naturally occurring hydrocarbon system. The well-defined components usually include:

- Non hydrocarbon fractions, CO_2, N_2, H_2S
- Methane to normal pentane (C_1 to n-C_5), where butane and pentane are present as isomers as well
- Hexane C_6 and heavier, where the number of isomers increase exponentially

In order to perform any reliable phase behaviour calculations, the physical properties of the undefined fractions need to be identified. This is often done through true boiling point distillation or by gas chromatography. This will result in a number of cuts, which are defined by the boiling point T_b. The analysis provides key data, such as boiling point, the specific gravity (SG) and molecular weight (MW) for each distillation cut. The individual true boiling point (TBP) can often be treated as a component, with the properties associated with pure components such as molecular weight, density and other physical properties. In the absence of analytical TBP or chromatography analysis data for the plus fraction, the plus fraction must be characterized otherwise. Through splitting schemes/molar distribution it is possible to divide the plus fraction into hydrocarbon groups with a single carbon number (SCN). To be able to use equations of state (EoS) for complex hydrocarbon mixtures, the acentric factor, critical pressure and critical temperature must be provided for all components in the mixture. It is therefore of great importance, that the undefined heavy fraction is adequately characterized in terms of an appropriate number of pseudo components, with the associated EoS model parameters.

There have been reported many reservoir fluid characterization methods, which can be found in the literature [26]. Naturally occurring oil or condensate mixtures may contain thousands of different components. Such high numbers are impractical to handle in phase equilibrium calculations. Some components therefore must be lumped together and the are represented as pseudocomponents. C_{7+} characterization consists of representing the hydrocarbons with seven and more carbon atoms (C_{7+} fraction) as a convenient number of pseudo components and finding the necessary EoS parameters for each of the pseudo components [4].

To characterize the C_{7+} fraction in reservoir fluids, two methods are often used: the method proposed by Pedersen et al. [16,27] and that by Whitson et al. [28]. The methods presented by Pedersen et al. [16] and by Whitson et al. [28] can both be applied directly to the CPA EoS.

Yan et al. proposed modified correlations using a two step perturbation method, for calculating the CPA "monomer" critical temperature T_{cm}, critical pressure P_{cm} and acentric factor ω_m [4,15]. Perturbation expansion correlations were developed by Twu [29], which initially correlate the properties of normal paraffins as the reference, and then extend these correlations to petroleum fractions:

$$T_{cm0} = \frac{\left(1885.45947 + 0.222337924T_b\right)T_b}{950.853406 + T_b} \tag{5.19}$$

$$lnP_{cm0} = -4.05282558 \cdot 10^{-1}\ T_b^{24} + 8.76125776 \cdot 10^{-9} T_b^3 - 7.4578304 \cdot 10^{-6} T_b^2 \tag{5.20}$$

$$-1.09972989 \cdot 10^{-4} T_b + 4.16059295$$

$$\omega_{m0} = exp\left(\frac{-2553.0653 + 3.68418T_b}{608.7226 + T_b}\right) \tag{5.21}$$

where T_b is the true boiling point in K. In these equations the temperatures are in Kelvin and pressure in bar. The subscript 0 refers to the properties of n-alkanes. Soave's correlation [31] is used for the specific gravity (SG):

$$SG_0 = \left(1.8T_b\right)^{1/3}\left(11.7372 + 3.336 \cdot 10^{-3} T_b - 976.3T_b^{-1} + 3.257 \cdot 10^5 T_b^{-2}\right)^{-1} \tag{5.22}$$

A perturbation step is needed, where the specific gravity difference is used as the perturbation parameter:

$$\Delta SG = SG - SG_0 \tag{5.23}$$

This leads to the following equations:

$$\frac{T_{cm}}{T_{cm0}} = \frac{1 - 12.0690795\Delta SG + 22.8626562\Delta SG^2 + 89.7115818\Delta SG^3}{1 - 12.6311386\Delta SG + 30.6779472\Delta SG^2 + 62.4698965\Delta SG^3} \tag{5.24}$$

$$ln\left(\frac{P_{cm}}{P_{cm0}}\right) = \frac{\Delta SG\left[-677.989269 + \left(76624.406 - 29811.8749 / SG\right)\Delta SG\right]}{\left(1 + 10949.2202\Delta SG + 28099.1573\Delta SG^2\right)} \tag{5.25}$$

The CPA acentric factor ω_m is not treated as a free parameter. Instead, it is back calculated by matching the T_b of the fraction. The direct vapor pressure calculation procedure proposed by Soave [27] can be used, which does not need any iteration. Equation 5.21 is used only if T_b exceeds T_c for extremely heavy compounds.

References

[1] Wei, Y. S. Sadus, R. J. *AIChE Journal* **2000**, *46*, 169-196.

[2] G Soave. *Chemical Engineering Science*, **1972**, 27(6):1197–1203

[3] DY Peng and DB Robinson. *Industrial & Engineering Chemistry Fundamentals*, **1976,** 15(1):59–64

[4] G. M Kontogeorgis and G. K Folas. *Thermodynamic Models for Industrial Applications: From Classical and Advanced Mixing Rules to Association Theories*. Wiley, **2010**.

[5] Renon, H. Prausnitz, J. M. *AIChE Journal* **1968**, 14, 135-144.

[6] Abrams, D. S. Prausnitz, J. M. *AIChE Journal* **1975**, 21, 116.

[7] Wertheim, M. S. *J Stat Phys* **1984**, 35, 19-34.

[8] Wertheim, M. S. *J Stat Phys* **1984**, 35, 35-47.

[9] Wertheim, M. S. *J Stat Phys* **1986**, 42, 459-476

[10] Wertheim, M. S. *J Stat Phys* **1986**, 42, 477-492

[11] Chapman, W. G. Gubbins, K. E. Jackson, G. Radosz, M. *Industrial & Engineering Chemistry Research* **1990**, 29, 1709-1721

[12] S Chapman, W. Jackson, G. Gubbins, K. *Molecular Physics* **1988**, 65, 1057-1079

[13] Huang, S. H. Radosz, M. *Industrial & Engineering Chemistry Research* **1990**, 29, 2284-2294

[14] Kontogeorgis, G. M. Voutsas, E. C. Yakoumis, I. V. Tassios, D. P. *Industrial & Engineering Chemistry Research* **1996**, 35, 4310-4318.

[15] Yan, W. Kontogeorgis, G. M. Stenby, E. H. *Fluid Phase Equilibria* **2009**, 276, 75-85

[16] Pedersen, K. S. Thomassen, P. Fredenslund, A. *Advances in Thermodynamics, C7+ Fraction Characterization*, Taylor & Francis: New York, **1989**, Vol. 1

[17] Kontogeorgis, G. M. V. Yakoumis, I. Meijer, H. Hendriks, E. Moorwood, T. *Fluid Phase Equilibria* **1999**, 158-160, 201-209

[18] Michelsen, M. L. Hendriks, E. M. *Fluid Phase Equilibria* **2001**, 180, 165-174

[19] Folas, G. K. *Modeling of Complex Mixtures Containing Hydrogen Bonding Molecules*, DTU: 2800 Kgs Lyngby, Denmark, **2006**

[20] Derawi, S. O. Kontogeorgis, G. M. Michelsen, M. L. Stenby, E. H. *Industrial & Engineering Chemistry Research* **2003**, 42, 1470-1477

[21] Suresh, S. J. Elliott, J. R. *Industrial & Engineering Chemistry Research* **1992**, 31, 2783-2794

[22] Folas, G. K. Kontogeorgis, G. M. Michelsen, M. L. Stenby, E. H. *Industrial & Engineering Chemistry Research* **2006**, 45, 1527-1538

[23] Derawi, S. O. Michelsen, M. L. Kontogeorgis, G. M. Stenby, E. H. *Fluid Phase Equilibria* **2003**, 209, 163-184

[24] Voutsas, E.C.; Yakoumis, I.V.; Tassios, D.P., *Fluid Phase Equilib.* **1999,** 158 – 160*,* 151.

[25] Voutsas, E.C.; Boulougouris, G.C.; Economou, I.G.; Tassios, D.P., *Ind. Eng. Chem. Res.* **2000,** 39*,* 797

[26] C. Whitson, M. Brule, Phase Behavior, *Monograph series, vol. 20*, SPE, Richardson, TX, **2000**

[27] Soave, G. *Fluid Phase Equilibria* **1986**, 31, 203-207

[28] Whitson, C. H. Søreide, I. Chorn, L. G. Mansoori, G. A. *Advances in Thermodynamics, C7+ Fraction Characterization*, Taylor & Francis: New York, **1989**, Vol. 1

[29] Twu, C. H. *Fluid Phase Equilibria* **1984**, 16, 137-150

[30] Soave, G. S. *Fluid Phase Equilibria* **1998**, 143, 29-39.

Chapter 6 – Modelling of well-defined complex systems

Injection of chemicals such as methanol and ethylene glycol is an important and widely used technique for inhibiting gas hydrate formation. It makes hydrate formation thermodynamically impossible under certain conditions (pressure and temperature). However, they are often injected at higher rate than is actually necessary due to uncertainties in determining the actual requirement. Mixtures of associating components, and particular mixtures of water and alcohols or glycols with hydrocarbons, are of great interest to the oil and gas industry. The accurate description of such systems is a challenging problem of high technological importance for several petrochemical processes.

Notwithstanding the considerable progresses attained over the last years, present thermodynamic models for prediction of phase equilibrium still face a number of challenges, specifically concerning equilibrium at very high pressures, in multi-component systems or in systems containing associating compounds. The typical systems considered in this work, consisting of hydrocarbons, water and a hydrate inhibitor, include associating compounds, making them of great interest from a theoretical point of view. They help evaluate the extent of the association and the ability of these models to correctly describe the phase equilibria, as these associating species forming hydrogen bonds often exhibit a highly non-ideal thermodynamic behavior.

In pure fluids, strong attractive interactions between similar molecules, such as hydrogen bonds or Lewis acid-base interactions result in the formation of molecular clusters that considerably affect their thermodynamic properties. When mixtures are considered, such interactions can occur not only between molecules of the same species (self-association), but also between molecules of different species (cross-association). Traditional thermodynamic models such as cubic equations of state (ex. PR and SRK) perform well for vapor-liquid equilibria but are less satisfactory for liquid-liquid equilibria (LLE) and vapor-liquid-liquid equilibria (VLLE), especially for multicomponent mixtures. The same is true for activity coefficient models such as UNIFAC which can often be used for preliminary design purposes. It is, therefore, desirable for thermodynamic models to account

correctly for association. Examples of applicable equations of state (EoS) are the Cubic Plus Association EoS (CPA) [1,2], or the various variations of the Statistical Associating Fluid Theory EoS (SAFT) [3-8], some of them are compared in a number of publications [9,10].
In the present chapter, the CPA EoS, proposed by Kontogeorgis et al. [11], was used in the modelling of binary and ternary mixtures containing water, hydrocarbons and methanol/MEG as a thermodynamic hydrate inhibitor.

6.1 Results

It has been shown in a previous work [12] that the CPA EoS can satisfactorily correlate the glycol/alcohol-alkane LLE and VLLE using a single temperature independent interaction parameter [13]. The experimental data show that the solubility of glycol/alcohol in the organic phase is an order of magnitude lower than that of the solubility of hydrocarbons in the polar phase [14]. The classical cubic equations of state fail to describe these solubilities [12]. The modeling results presented next, refer to representative binary and ternary systems. Investigation is done for binary systems containing non-associating alkanes in a mixture with an associating compound, consisting of n-nonane + MEG, methane + methanol, methane + water and methane + MEG, and finally a binary mixture of aromatic hydrocarbon, ethylbenzene + MEG. The ternary mixtures in this work consist of two non-associating alkanes (methane and n-nonane) and an aromatic hydrocarbon (ethylbenzene) in mixtures of gas hydrate inhibitor (MEG or methanol) and water. Finally modeling of the VLLE data of methane + n-hexane + methanol + water measured in this work is done. The parameters relative to the components used in the calculations were taken from previous works [15-17]. All the parameters are presented and summarized in table 6.1.

Table 6.1: CPA Parameters for Components Considered in This Work. The 2B Association Scheme is used for Methanol and 4C is used for Both Water and MEG.

Compound	Reference	T_c (K)	Association Scheme	a_0 (L^2bar/mol^2)	b (L/mol)	c_1	ε (barL/mol)	$\beta \cdot 10^3$
MEG	[15]	720.00	4C	10.8190	0.051400	0.67440	197.53	14.1
Water	[16]	647.29	4C	1.22770	0.014515	0.67359	166.55	69.2
Methanol	[16]	512.64	2B	4.05310	0.030978	0.43102	245.91	16.1
ethylbenzene	[13]	617.10	n.a.	28.86164	0.108720	0.85390	---	---
n-nonane	[17]	594.60	n.a.	41.25395	0.160350	1.04628	---	---
methane	[17]	190.60	n.a.	2.334093	0.029853	0.49886	---	---
n-hexane	[17]	507.60	n.a.	23.6810	0.107890	0.83130	---	---

6.1.1 Binary system n-nonane + MEG

The binary system of n-nonane and MEG, have been modeled using the CPA equation of state at three different temperatures (303.15, 313.15 and 323.15 K). As no existing binary interaction parameter is available for this system, an investigation using three different k_{ij} (k_{ij} = 0, k_{ij} = 0.0146 (fitted by regression) and k_{ij} =0.01 (fitted manually)) is made. Tables 6.2 and 6.3 presents two different sets of calculations (k_{ij} = 0, k_{ij} = 0.0146 (fitted by regression) and k_{ij} =0.01 (fitted manually)) made with the CPA equation of state. Experimental data have been measured at Statoil, Trondheim, as part of the master thesis by Mustafe Yussuf [18]. The figures present the experimental data, and the AAD% between experimental and calculated solubility.

Table 6.2: % AAD between experimental and calculated solubilities for n-nonane in MEG using different binary interaction parameters.

Temperature	Experimental	AAD%		
	$\boldsymbol{x_1 \cdot 10^6}$	k_{ij} = 0	k_{ij} = 0.01	k_{ij} = 0.0146
303.15	185	51.4	35.1	29.7
313.15	280	67.9	50.0	42.9
323.15	428	77.6	61.2	54.2
	Average	65.6	48.8	42.3

Table 6.3: % AAD between experimental and calculated solubilities for MEG in hydrocarbon rich phase using different binary interaction parameters.

Temperature	Experimental	AAD%		
	$\boldsymbol{x_2 \cdot 10^6}$	k_{ij} = 0	k_{ij} = 0.01	k_{ij} = 0.0146
303.15	338	39.1	0.6	14.2
313.15	349	60.5	14.6	0.3
323.15	462	42.9	6.1	9.1
	Average	47.5	7.1	7.9

It can be seen, that using a binary interaction parameter of k_{ij} = 0, the CPA EoS has poor description of the solubility for both liquid phases. Using a small binary interaction parameter, it is possible to

accurately predict the solubility of hydrocarbon in the polar phase; however the MEG in hydrocarbon phase is over predicted in all cases. Figure 6.1 show experimental data for the binary mixture (points) along with calculations using the CPA EoS (lines) with k_{ij} = 0, k_{ij} = 0.0146 (fitted by regression) and k_{ij} =0.01 (fitted manually).

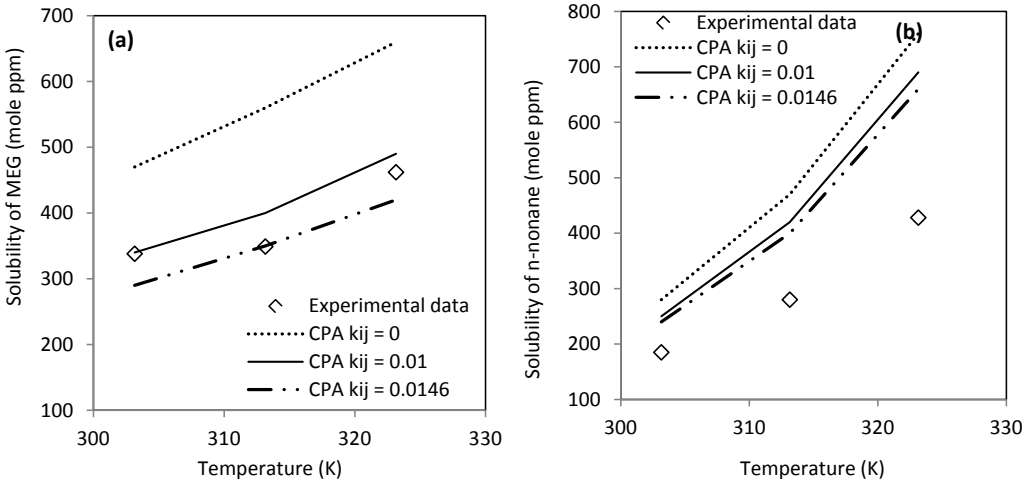

Figure 6.1: Experimental [18] and calculated solubility of: (a) MEG in the hydrocarbon rich phase (b) n-nonane in the polar phase and, using the CPA equation of state. The experimental data are indicated as points and the CPA calculations as lines.

6.1.2 Binary system ethylbenzene + MEG

Traditional thermodynamic models like cubic Equations of State (often even with advanced mixing rules) exhibit problems for multicomponent VLLE of water-alcohol/glycol-hydrocarbons [19], while it is often stated that cubic EoS cannot be used for simultaneous VLE and LLE e.g. of alcohol-hydrocarbons with the same interaction parameters [20]. Relatively few investigations have been reported for multicomponent LLE of this type of mixtures [21-23]. Previously, CPA has been successfully applied to mixtures containing various associating compounds (alcohols, glycols, water) and aliphatic hydrocarbons. In this section the importance of accounting for the solvation between aromatics/olefinics and a polar compound is evaluated, both for binary as well as for multicomponent systems. The binary interaction parameter between MEG and ethylbenzene (k_{ij} = 0.0125) has been fitted by regression to LLE data [18]. A comparison is made of the effect of

solvation, where calculations are made using the CPA EoS, with and without adding a cross-association parameter (β_{cross}).

In table 6.4 the experimental data are presented, along with calculations made with the CPA EoS and the %AAD. The calculations are made using a $k_{ij} = 0.0125$ and $\beta_{cross} = 0$. In table 6.5 the experimental data are presented, along with calculations made with the CPA EoS and the %AAD. The calculations are made using a $k_{ij} = 0.0254$ and $\beta_{cross} = 0.02$. The cross-association volume was fitted to the experimental LLE data [18].

Table 6.4: % AAD Between Experimental and Calculated mutual Solubility of MEG and ethylbenzene using a binary interaction parameter $k_{ij} = 0.0125$ and $\beta_{cross} = 0$.

Temperature K	MEG in Ethtlbenzene $x_1 \cdot 10^6$	CPA predictions	AAD%	Ethylbenzene in MEG $x_2 \cdot 10^6$	CPA predictions	AAD%
303.15	2195	340	84.5	12095	11050	8.6
313.15	3030	570	81.2	12209	12220	0.1
323.15	3386	930	72.5	12696	13520	6.5
Average			79.4			5.1

Table 6.5: % AAD between Experimental and Calculated mutual Solubility of MEG and ethylbenzene using a binary interaction parameter $k_{ij} = 0.0254$ and $\beta_{cross} = 0.02$.

Temperature K	MEG in Ethtlbenzene $x_1 \cdot 10^6$	CPA predictions	AAD%	Ethylbenzene in MEG $x_2 \cdot 10^6$	CPA predictions	AAD%
303.15	2195	1330	39.4	12095	11260	6.9
313.15	3030	1960	35.3	12209	12640	3.5
323.15	3386	2820	16.7	12696	14180	11.7
Average			30.5			7.4

It can be seen from tables 6.4-6.5, that accounting for solvation (including the cross association volume), greatly increases the accuracy of the calculations made with the CPA EoS with regards to the solubility of glycol in the hydrocarbon rich phase. Furthermore it should be noticed, that a small binary interaction parameter is needed, in order to accurately predict the solubility in both phases. The binary interaction parameter was fitted by regression to LLE data [18]. Figure 6.2 shows experimental data for the binary mixture of ethylbenzene + MEG and the calculations made with

the CPA EoS. The dotted lines represent CPA calculations where solvation is not taken into account ($\beta_{cross} = 0$), and the black lines represent the calculations accounting for solvation ($\beta_{cross} = 0.02$).

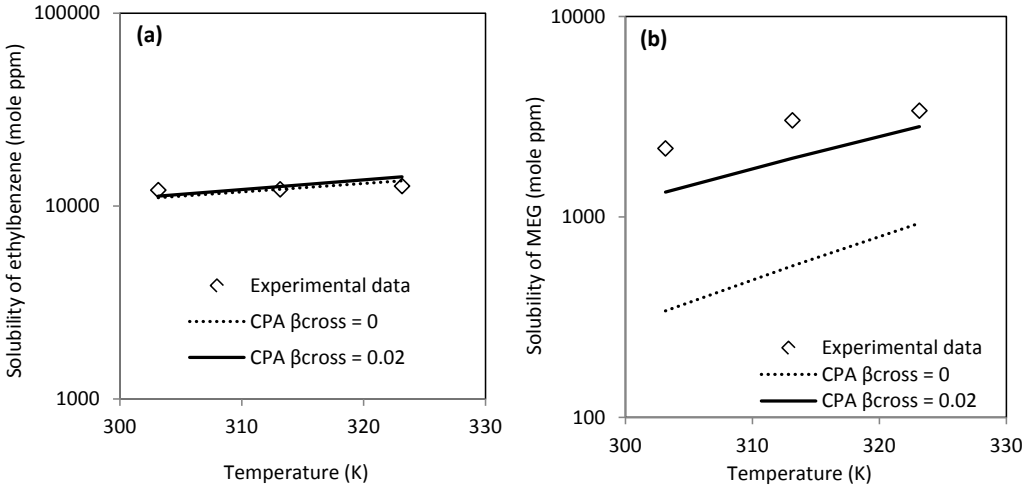

Figure 6.2: Experimental and calculated solubility of: (a) ethylbenzene in MEG phase and (b) MEG in the HC rich phase, using the CPA equation of state. The experimental data [18] are indicated as points and the CPA calculations as lines, using a $k_{ij} = 0.0125$ between MEG-ethylbenzene.

6.1.3 Binary system methane + methanol

The binary system methane + methanol were also modelled at 298 K. The correlation of the experimental data measured in this work [24] is presented in Figure 6.3.

It can be observed that the correct modeling of the gas phase is achieved using a k_{ij} of 0.01 [25]. However, this value seems inadequate for the representation of the liquid phase. CPA can capture the minimum solubility of methanol in methane with T-independent k_{ij}, as seen in Figure 6.3. Improvement of calculated methane content in the liquid phase can be obtained using a different binary interaction parameter; however, this would provide larger deviations in the prediction of the gas phase.

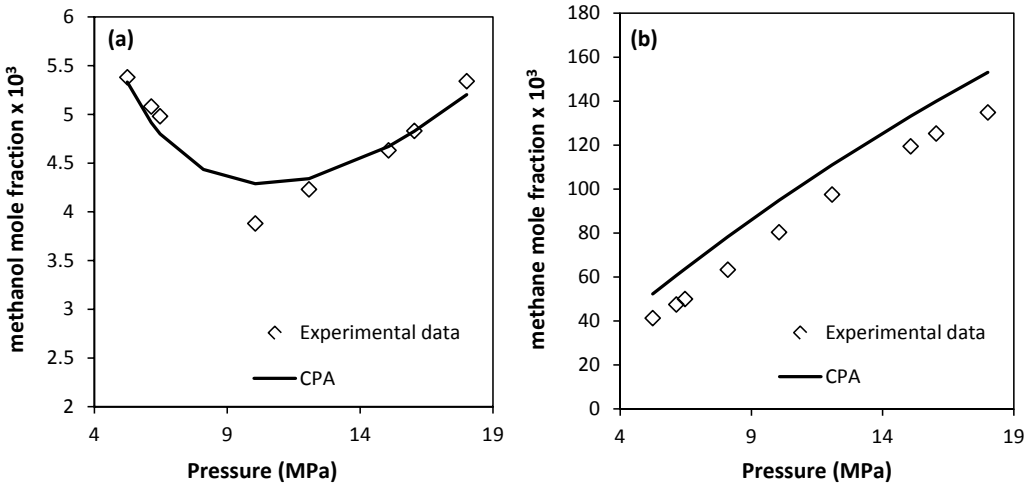

Figure 6.3: Experimental [24] and calculated solubility of: (a) methanol in the gas phase and (b) methane in the liquid phase, using the CPA equation of state with k_{ij} = 0.01 [25]. The experimental data are indicated as points and the CPA calculations as lines.

In table 6.6 the experimental data are presented, along with calculations made with the CPA EoS and the %AAD. The calculations are made using a k_{ij} = 0.01.

Table 6.6: % AAD between Experimental [24] and Calculated mutual Solubility of methanol and methane at 298 K, using a binary interaction parameter k_{ij} = 0.01.

Pressure MPa	Methanol in methane $x_1 \cdot 10^3$	CPA Calculations	AAD%	Methane in methanol $x_2 \cdot 10^3$	CPA Calculations	AAD%
5.24	5.38	5.33	0.9	41.26	52.28	26.7
6.14	5.08	4.91	3.3	47.47	60.67	27.8
6.47	4.98	4.80	3.6	49.95	63.70	27.5
10.05	3.88	4.29	10.5	80.32	94.85	18.1
12.08	4.23	4.34	2.6	97.49	110.99	13.8
15.07	4.63	4.67	0.9	119.41	133.15	11.5
16.04	4.83	4.83	0.1	125.25	139.93	11.7
18.01	5.34	5.20	2.6	134.83	153.13	13.6
Average			5.1			19.4

6.1.4 Binary system methane + water

The binary system methane + water was modelled at four temperatures, between 283 K and 323 K. Predictions using CPA was performed using a single temperature independent binary interaction parameter (k_{ij} = 0.0098 [26]) based on VLE data. Figure 6.4 presents the results of the modelling for the liquid phase, and a comparison with the values obtained in this work by the synthetic method. As for the gas phase, the results are shown in Figure 6.5.

It should be underlined that although two separate graphs are presented, the modeling of the system was performed considering simultaneously the data relative to both phases. The representation is made using different plots for different phases in order to allow for a better observation of the performance of the model, due to the very low mutual solubility of these compounds.

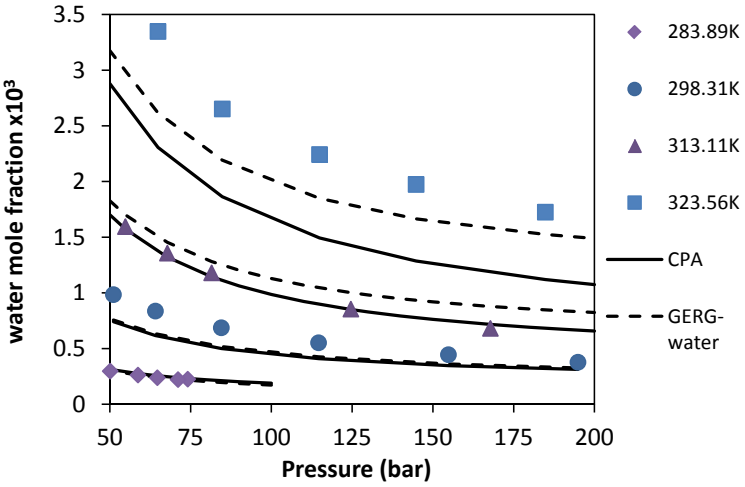

Figure 6.4: Experimental [24] and calculated solubility of water in the gas phase, using the CPA equation of state with k_{ij} = 0.0098. The experimental data are indicated as points, the CPA calculations as solid lines and GERG-Water correlations as dotted lines.

For the specific compositions, it was of interest to compare CPA to the GERG-water calculation method. GERG-water is currently an ISO standard when it comes to water content and water dew point in natural gas. The semiempirical GERG-water method is based on the Peng−Robinson equation of state with a modified energy parameter. It should be stressed that GERG-water used temperature-dependent interaction parameters for describing the water−methane system and it has a limited applicability range in terms of temperature, pressure, and compositions. It is validated for

temperatures ranging from 258.15 K to 278.15 K and can be extended to temperatures of 223.15 K to 313.15 K with unknown uncertainties. As can be seen from Figure 6.4, the two models have similar %AAD (14.5 % for GERG-water and 17.4 % for CPA).

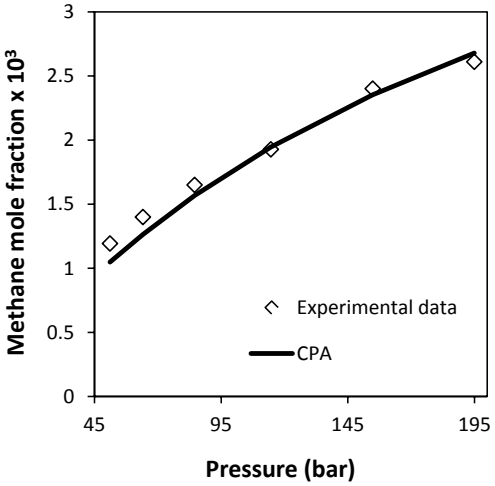

Figure 6.5: Experimental [24] and calculated solubility of methane in the liquid phase at 298 K, using the CPA equation of state with $k_{ij} = 0.0098$. The experimental data are indicated as points and the CPA calculations as lines.

6.1.5 Ternary system n-nonane + MEG + water

The ternary system of n-nonane + MEG + water, have been modeled using CPA at 313.15 K and three different feed compositions. The binary interaction parameter between n-nonane and MEG is adopted from the binary system ($k_{ij} = 0.0146$). Experimental data have been measured at Statoil, Trondheim, as part of the master thesis by Mustafe Yussuf [18].

Binary interaction parameters and cross-association volume are adopted from the corresponding binary system. The parameters used for this system can be seen in table 6.7.

Table 6.7: Binary interaction parameters and cross-association volumes used for modeling of LLE of n-nonane + MEG + water.

System	Reference	k_{ij}	β_{cross}
MEG-water	[27]	-0.1150[a]	---
MEG-nonane	This work	0.0146	---
Water-nonane	[25]	-0.003	---

[a] Elliot combining rule,

The modeling results are presented in table 6.9 and in figure 6.6 as a function of MEG composition. It can be seen that CPA accurately predicts the water and glycol content in the gas phase. These results are pure predictions as no binary interaction parameter are fitted to the experimental data, and is instead adopted from binary system. Predictions of hydrocarbon in the polar phase are in good agreement with the experimental data at higher MEG concentrations, however, it under-predicts the solubility at decreasing MEG concentration. Overall satisfactory results are obtained. The average deviations are shown in table 6.8.

Table 6.8: Average Deviation of CPA predictions from experimental data for the n-nonane + MEG + water system at T = 313.15 K and 1 atm.

	Polar Phase	Hydrocarbon phase	
	HC	MEG	Water
Average	45	12	28

Table 6.9: % AAD between experimental [18] and calculated mutual solubility of n-nonane, MEG and water using parameters presented in table 6.6.

Component	Feed	Polar Phase (mole ppm)			Hydrocarbon Phase (mole ppm)		
	(mole fraction)	Exp.	Cal.	% AAD	Exp.	Cal.	% AAD
MEG	0.4042	---	---	---	183	221	21
Water	0.3517	---	---	---	457	297	35
Nonane	0.2806	22	23	4.3	---	---	---
MEG	0.2434	---	---	---	101	103	1.5
Water	0.5596	---	---	---	704	514	27
Nonane	0.2286	3	1.7	41	---	---	---
MEG	0.1382	---	---	---	35	40	14
Water	0.6976	---	---	---	858	660	23
Nonane	0.1918	2	0.21	89	---	---	---

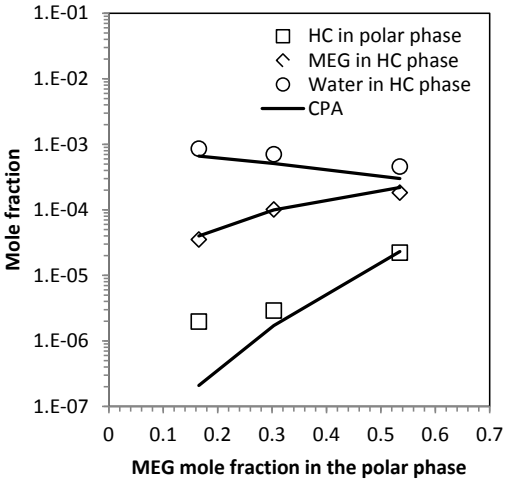

Figure 6.6: Experimental [18] and calculated solubility of n-nonane + MEG + water, using the CPA equation of state with parameters from table 6.6. The experimental data are indicated as points and the CPA calculations as lines.

6.1.6 Ternary system ethylbenzene + MEG + water

The CPA EoS has been used to predict the mutual solubility of ethylbenzene + MEG + water. Again the experimental data have been measured at Statoil, Trondheim, as part of the master thesis by Mustafe Yussuf [18]. The aromatic hydrocarbons are non-self-associating but there is a possibility of cross-association (solvation). For modeling of such mixtures using the CPA EoS, a solvation scheme is employed involving combining rules for the cross-associating energy and volume parameters. Using this approach the cross-association volume and the binary interaction parameters are fitted to the binary experimental data.

Binary interaction parameters and cross-association volume are adopted from the corresponding binary systems. The parameters used for this system can be seen in table 6.10.

Table 6.10: Binary interaction parameters and cross-association volumes used for modeling of LLE of ethylbenzene + MEG + water.

System	Reference	k_{ij}	β_{cross}
MEG-water	[27]	-0.1150[a]	---
MEG-ethylbenzene	This work	0.0254	0.020
	This work	0.0125	0
Water-ethylbenzene	[13]	-0.0165	0.051

[a] Elliot combining rule,

Modeling results for the mutual solubility of ethylbenzene, MEG and water are shown in tables 6.12 and 6.13. In these tables are presented predictions with the CPA EoS, using the pure component parameters given in table 6.1 and the binary interaction parameters given in table 6.10. The calculations presented in table 6.11 are made with a $\beta_{cross} = 0$, not accounting for the solvation effect of the ethylbenzene, where the calculations presented in table 6.12 are made with a $\beta_{cross} = 0.02$. Table 6.11 shows the average deviation of the predictions from experimental data, based on the results in tables 6.12 and 6.13.

Table 6.11: Average Deviation of CPA predictions from experimental data for the ethylbenzene + MEG + water system.

β_{cross}	Ethylbenzene in polar phase	MEG in HC phase	Water in HC phase
0	18	87	26
0.02	31	31	24

Table 6.12: % AAD between Experimental [18] and Calculated mutual Solubility of ethylbenzene, MEG and water using binary interaction parameter*s* presented in table 6.7. The cross-association volume β_{cross} is 0 between MEG-ethylbenzene (not accounting for solvation in the system).

Component	Feed	Polar Phase (mole ppm)			Hydrocarbon Phase (mole ppm)		
	(mole fraction)	Exp.	Cal.	% Dev.	Exp.	Cal.	% Dev.
MEG	0.3403	---	---	---	1512	240	84
Water	0.4279	---	---	---	2284	1560	32
Ethylbenzene	0.2376	1360	1300	4	---	---	---
MEG	0.2405	---	---	---	1144	150	87
Water	0.5316	---	---	---	2838	2100	26
Ethylbenzene	0.2278	459	550	20	---	---	---
MEG	0.1285	---	---	---	650	60	91
Water	0.6842	---	---	---	3525	2810	20
Ethylbenzene	0.1872	115	150	30	---	---	---

Table 6.13: % AAD between Experimental [18] and Calculated mutual Solubility of ethylbenzene, MEG and water using binary interaction parameter*s* presented in table 6.7. The cross-association volume $\beta_{cross} = 0.02$ is used for MEG-ethylbenzene.

Component	Feed	Polar Phase (mole ppm)			Hydrocarbon Phase (mole ppm)		
	(mole fraction)	Exp.	Cal.	% Dev.	Exp.	Cal.	% Dev.
MEG	0.3403	---	---	---	1512	1300	14
Water	0.4279	---	---	---	2284	1640	28
Ethylbenzene	0.2376	1360	1610	18	---	---	---
MEG	0.2405	---	---	---	1144	810	29
Water	0.5316	---	---	---	2838	2160	24
Ethylbenzene	0.2278	459	630	37	---	---	---
MEG	0.1285	---	---	---	650	320	51
Water	0.6842	---	---	---	3525	2840	19
Ethylbenzene	0.1872	115	160	39	---	---	---

The mutual solubility of ethylbenzene, MEG and water is presented in figures 6.7. Calculations with the CPA EoS greatly under-predict the solubility of water and MEG in the organic phase, when the cross association between ethylbenzene and MEG is not accounted for. Using a $\beta_{cross} = 0.02$ improves the result, and accurately predicts the solubilities.

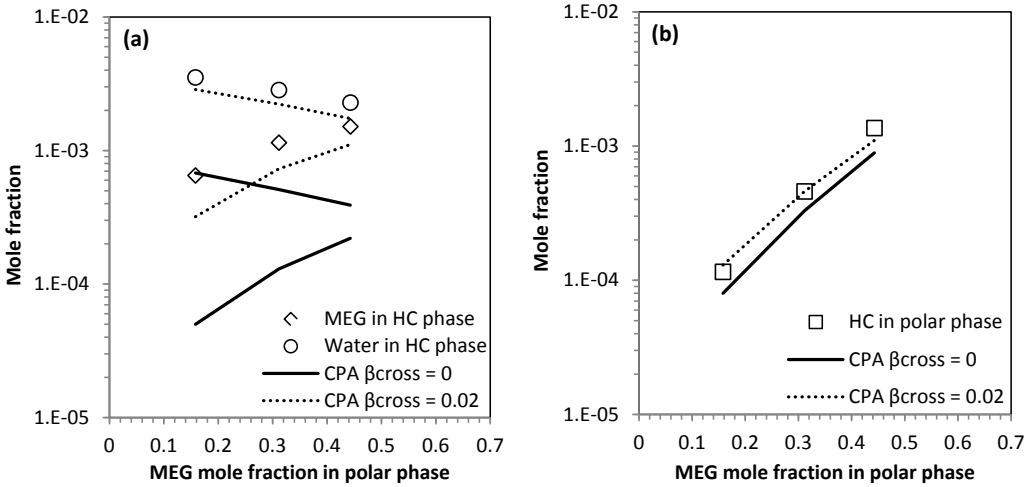

Figure 6.7: Experimental [18] and calculated solubility of: (a) MEG and water in the HC rich phase, (b) ethylbenzene in the polar phase, using the CPA equation of state with k_{ij} from table 6.7. The experimental data are indicated as points and the CPA calculations as lines.

6.1.7 Ternary system methane + methanol + water

With regards to the ternary system in Figure 6.8, CPA yields acceptable results, and when the two different k_{ij}'s for the water + methanol system (k_{ij} = -0.09 [28] and k_{ij} = -0.153 [29]) are compared, it becomes evident that the k_{ij} fitted to VLE data performs better when it comes to water content correlations, while the k_{ij} fitted to SLE data performs better for the methanol gas content and the methane solubility calculations. Overall, the lowest deviations were found when the methanol solubility in the gas phase was calculated, while the model generally overestimates the methane solubility in the liquid phase and underestimates the water vapor content.

The binary interaction parameters for methane + methanol and methane + water set as done for the binary systems respectively (k_{ij} = 0.01 and k_{ij} = 0.0098).

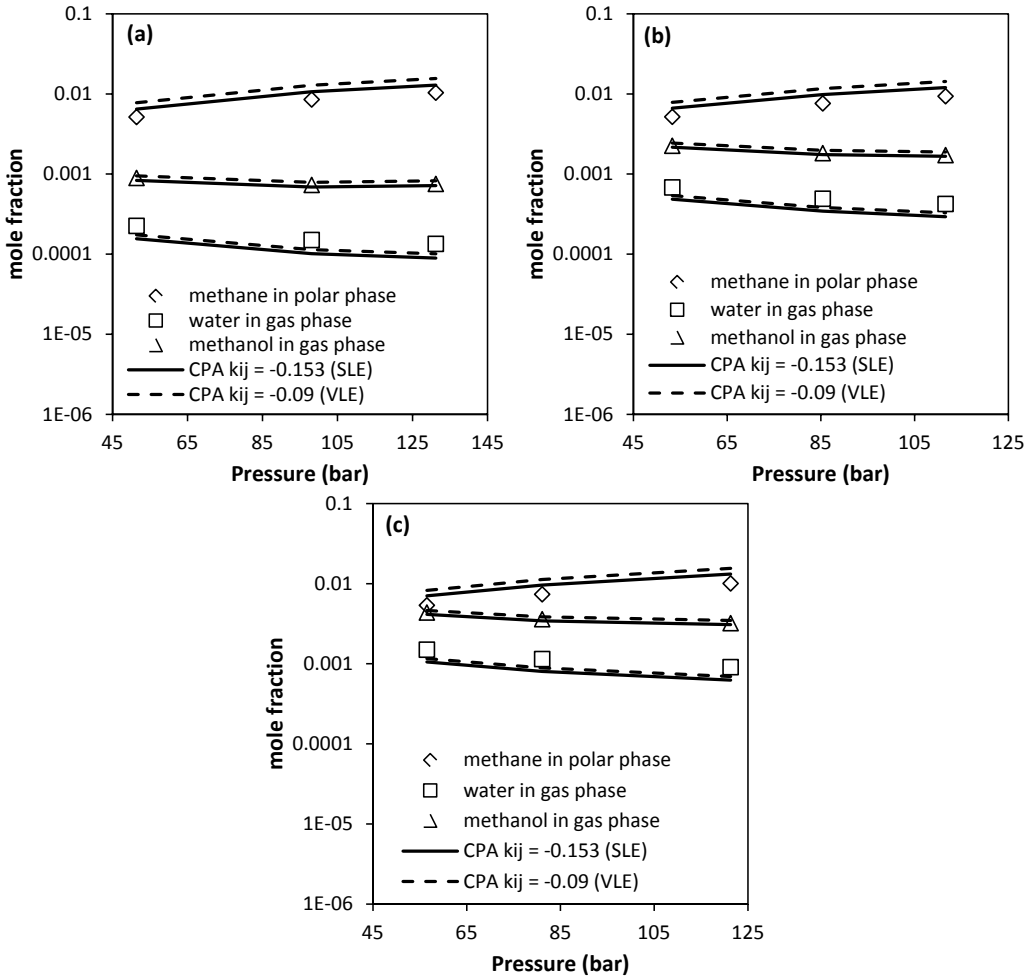

Figure 6.8: Prediction with CPA of methanol solubility in the vapor phase, methane solubility in the liquid phase and gas phase water content for methanol-methane-water at (a) 280.25K, (b) 298.77K and (c) 323.45K. Points are experimental data from this work, solid lines are correlations with water-methanol k_{ij} equal to -0.153 (fitted to SLE data) and dotted lines are correlations with water-methanol k_{ij} equal to -0.09 (fitted to VLE data.

6.1.8 Quaternary system methane + n-hexane + methanol + water

The quaternary system constituted by methane + *n*-hexane + methanol + water was modeled at conditions similar to the observed in the experimental measurements. The binary interaction parameters used in these predictions are summarized in Table 6.14.

Table 6.14: Values of k_{ij} found in the modeling of the quaternary system methane + *n*-hexane + methanol + water.

Compounds	k_{ij}
methane + methanol	0.0134
methane + water	0.0098
n-hexane + methanol	0.01
n-hexane + water	0.0355
methanol + water	-0.09

The results for the system at 298 K and pressures of 6.8 MPa and 9.2 MPa are presented in Tables 6.15 and 6.16, where a comparison with the experimental values obtained in this work is also given.

For the first set of results, at 9.8 MPa, the agreement of the calculations with the experimental values is remarkable, considering the predictive character of the calculation and the complexity of the system. The success of the model is evident even in the prediction of extremely small amounts, such as the mole fraction of *n*-hexane in the aqueous phase. For the aqueous phase, the mole fraction of water and methanol are predicted with accuracy better than 10%, however, the methane content is slightly over-estimated.

For the organic phase, the model accurately predicts the molar fraction of methane and hexane. The predicted solubility of methanol and water do not differ greatly from the experimental values, again considering that these are very low values.
As for the composition of the gas phase, the agreement between the predictions of the model and the experimental values is again very good, demonstrating that the CPA EoS shows a great potential for the prediction of equilibrium in these type of systems.

Table 6.15: Results obtained using the CPA EoS, for the mixture methane + *n*-hexane + methanol + water, at 296.2 K and 9.2 MPa, and comparison with experimental values [this work]. All binary parameters are presented in table 6.14.

Phase	Component	Mole Fraction		
		Experimental	CPA	%AAD
Aqueous Phase	methane	$7340 \cdot 10^{-6}$	$8523 \cdot 10^{-6}$	16.1
	n-hexane	$104 \cdot 10^{-6}$	$75 \cdot 10^{-6}$	27.9
	methanol	0.3267	0.3018	7.6
	water	0.6663	0.6896	3.5
Organic Phase	methane	0.4481	0.4017	10.4
	n-hexane	0.5460	0.5897	8.0
	methanol	$5940 \cdot 10^{-6}$	$8100 \cdot 10^{-6}$	36.4
	water	$414 \cdot 10^{-6}$	$571 \cdot 10^{-6}$	37.9
Gas Phase	methane	0.9856	0.9845	0.1
	n-hexane	0.0122	0.0135	10.7
	methanol	$1508 \cdot 10^{-6}$	$1628 \cdot 10^{-6}$	8.0
	water	$298 \cdot 10^{-6}$	$378 \cdot 10^{-6}$	26.8

Table 6.16: Results obtained using the CPA EoS, for the mixture methane + *n*-hexane + methanol + water, at 296.2 K and 6.8 MPa, and comparison with experimental values [this work]. All binary parameters are presented in table 6.14.

Phase	Component	Mole Fraction		
		Experimental	CPA	%AAD
Aqueous Phase	methane	$5371 \cdot 10^{-6}$	$6740 \cdot 10^{-6}$	25.5
	n-hexane	$106 \cdot 10^{-6}$	$81 \cdot 10^{-6}$	23.1
	methanol	0.3123	0.3025	3.1
	water	0.7282	0.6907	5.2
Organic Phase	methane	0.3187	0.3109	2.5
	n-hexane	0.6232	0.6804	9.2
	methanol	$6247 \cdot 10^{-6}$	$8122 \cdot 10^{-6}$	30.0
	water	$401 \cdot 10^{-6}$	$564 \cdot 10^{-6}$	40.7
Gas Phase	methane	0.9839	0.9866	0.3
	n-hexane	0.0111	0.0112	0.6
	methanol	$1649 \cdot 10^{-6}$	$1784 \cdot 10^{-6}$	8.2
	water	$376 \cdot 10^{-6}$	$463 \cdot 10^{-6}$	23.0

Quite similar results are obtained at lower pressure (6.8 MPa). The CPA EoS can accurately predict the solubility in the different phases, within orders of magnitude.

Experimental data should always be used to back up models and theory. In this case, the well-established EoS can help validate, along with the comparisons made to literature data, that the experimental data measured in this work, is seemingly correct.

Figure 6.9 shows the experimental data (points) together with the CPA predictions (lines).

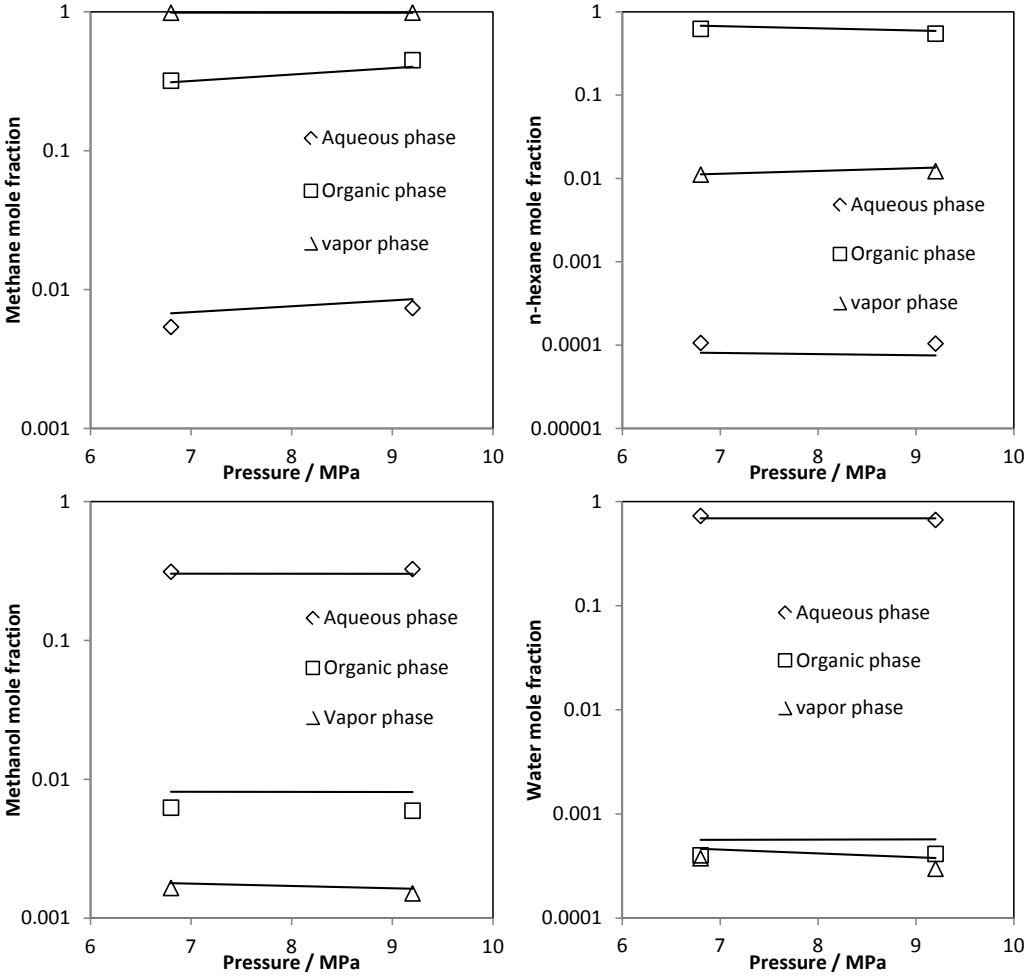

Figure 6.9: VLLE predictions for the system of methane + n-hexane + methanol + water at 296.2 K. Points are experimental data from this work. Solid lines are predictions with the CPA EoS using parameters from table 6.14.

6.2 Conclusions

In this chapter, the applicability of the CPA EoS proposed by Kontogeorgis et al. [11] was further validated for modeling of a number of binary and ternary mixtures (liquid-liquid and vapor-liquid) containing a variety of complex polar and associating, non-associating and solvating compounds, such as water, alkane/aromatic hydrocarbons and MEG/methanol (thermodynamic gashydrate

inhibitor). The model was successfully applied to different types of equilibrium, in a relatively wide range of both pressures and temperatures, with the need for only small corrections, as indicated by the low values for the binary interaction parameter, k_{ij}, used in most cases.

Satisfactory modeling results are obtained for the mutual solubility of methane + water and methane + methanol by using a single temperature independent binary interaction parameter. Prediction of the water content in the gas phase is comparable to other models, such as the semiempirical GERG-water method, which is based on the Peng−Robinson equation of state with a modified energy parameter. Better predictions might be obtained, if a temperature dependent k_{ij} is adopted for CPA in modeling of the system. The CPA EoS can satisfactory predict the mutual solubility of aromatic hydrocarbons (ethylbenzene) with MEG and MEG/water, when the cross association is taken into account, using a single temperature independent $k_{ij} = 0.0254$ and $\beta_{cross} = 0.02$.

For the ternary system of methane + water + methanol, overall, the lowest deviations were found for the methanol solubility in the gas phase, while the model generally overestimates the methane solubility in the liquid phase and underestimates the water vapor content. Overall CPA is a powerful tool for predictions of mutual solubility in hydrocarbon systems containing water and gas hydrate inhibitors (MEG/methanol).

Accurate predictions are made for VLLE of a quaternary system of methane + n-hexane + methanol + water, using the CPA EoS with binary interaction parameters taken from binary systems. Predictions are in good agreement with the experimental data, even for very low solubility, such as n-hexane in aqueous phase. In conclusion, the CPA EoS predicts satisfactorily the multiphase equilibrium of multicomponent water – alcohol – aliphatic hydrocarbon systems, based solely on the binary interaction parameters taken from binary systems, using the 2B association scheme for methanol and the 4C association scheme for water.

References

[1] G. M. Kontogeorgis, M. L. Michelsen, G. K. Folas, S. Derawi, N. von Solms, E. H.

Stenby, *Ind. Eng. Chem. Res.* 45 (**2006**) 4855-4868.

[2] G. M. Kontogeorgis, M. L. Michelsen, G. K. Folas, S. Derawi, N. von Solms, E. H.

Stenby, *Ind. Eng. Chem. Res.* 45 (**2006**) 4869-4878.

[3] A. M. A. Dias, F. Llovell, J. A. P. Coutinho, I. M. Marrucho, L. F. Vega, *Fluid Phase Equilib.* 286 (**2009**) 134-143.

[4] J. Gross, *J. Chem. Phys.* 131 (**2009**).

[5] R. E. Martini, M. Cismondi, S. Barbosa, E. Brignole, *Sep. Sci. Technol.* 44 (**2009**) 2661-2680.

[6] A. Tihic, N. von Solms, M. L. Michelsen, G. M. Kontogeorgis, L. Constantinou, *Fluid Phase Equilib.* 281 (**2009**) 60-69.

[7] I. Tsivintzelis, A. Grenner, I. G. Economou, G. M. Kontogeorgis, *Ind. Eng. Chem. Res.* 48 (**2009**) 7860.

[8] N. von Solms, M. L. Michelsen, G. M. Kontogeorgis, *Ind. Eng. Chem. Res.* 42 (**2003**) 1098-1105

[9] I. G. Economou, *Ind. Eng. Chem. Res.* 41 (**2002**) 953-962.

[10] E. A. Muller, K. E. Gubbins, *Ind. Eng. Chem. Res.* 40 (**2001**) 2193-2211.

[11] Kontogeorgis, G. M. Voutsas, E. C. Yakoumis, I. V. Tassios, D. P. *Industrial & Engineering Chemistry Research* 35 (**1996)** 4310-4318

[12] Kontogeorgis, G. M. Folas, G. K. *Thermodynamic Models for Industrial Applications: From Classical and Advanced Mixing Rules to Association Theories*, 1st ed. Wiley, **2010**.

[13] Folas, G. K. Kontogeorgis, G. M. Michelsen, M. L. Stenby, E. H. *Industrial & Engineering Chemistry Research* 45(**2006)** 1527-1538.

[14] Maczynski, A. Wiśniewska-Goclowska, B. Goral, M. *J. Phys. Chem. Ref. Data* 33 (**2004)** 549-577.

[15] S.O. Derawi, G.M. Kontogeorgis, M.L. Michelsen, E.H. Stenby, *Ind. Eng. Chem. Res.* 42 (**2003**) 1470-1477

[16] G.M. Kontogeorgis, I.V. Yakoumis, H. Meijer, E. Hendriks, T. Moorwood, *Fluid Phase Equilibr.* 201 (**1999**) 158-160

[17] Folas, G. K. *Modeling of Complex Mixtures Containing Hydrogen Bonding Molecules*, DTU: 2800 Kgs Lyngby, Denmark, **2006**.

[18] Yussuf, M. *Measurement of Phase Equilibria for Oil-Water-MEG Mixtures. MSc Thesis*, DTU: 2800 Kgs Lyngby, Denmark, **2011**.

[19] Mathias, P.M.; Klotz, H.C. *Chem. Eng. Progress.* **1994,** *90,* 63.

[20] Gupta, S.; Olson, D. Industrial needs in physical properties. *Ind. Eng. Chem. Res.* 42 **(2003)** 6359.

[21] Wong, D.S.H.; Sandler, S.I. *AIChE Journal* .38 *(***1992)** 671.

[22] Orbey, H.; Sandler, S.I.; Wong, D.S.H. *Fluid Phase Equilib.* 85 (**1993)** 41.

[23] Suresh, J.; Beckman, E.J. *Fluid Phase Equilib.*99 (**1994)** 219.

[24] Frost, M., Karakatsani, E., von Solms, N., Richon, D., Kontogeorgis, G. M., *Jorunal of chemical engineering data*, 59 (**2014**) 961-969

[25] Riaz, M. *Distribution of complex chemicals in oil−water systems. Ph.D. Thesis*, Technical Univeristy of Denmark, September **2011**

[26] Tsivintzelis, I., Maribo-Mogensen, B., *The Cubic-Plus-Association EoS Parameters for pure compounds and interaction parameters, CPA Technical Report*, DTU, **2013**

[27] S.O. Derawi, G.M. Kontogeorgis, M.L. Michelsen, E.H. Stenby, *Fluid Phase Equlibr*. 209 (**2003**) 163-184

[28] Folas, G. K.; Gabrielsen, J.; Michelsen, M. L.; Stenby, E. H.; Kontogeorgis, G. M. *Ind. Eng. Chem. Res.* 44 (**2005**) 3823

[29] Folas, G. K.; Derawi, S. O.; Michelsen, M. L.; Stenby, E. H.; Kontogeorgis, G. M. *Fluid Phase Equilib.* 228-229 (**2005**) 121−126

Chapter 7 – Modeling of reservoir fluids

As the exploitable oil resources decrease, more sophisticated recovery methods are employed in the oil industry to produce the remaining resources. One result of using more sophisticated recovery methods is that oil field chemicals are more widely used, especially in the offshore oil production. These chemicals belong to different families like alcohols, glycols, alkanolamines, surfactants and polymers. They have various functions, e.g., methanol and MEG are used as gas hydrate inhibitors, surfactants are used to lower interfacial tension between crude oil and microemulsion and polymers in a polymer-waterflooding process act primarily as thickeners [1,2]

The knowledge of the phase equilibria of aqueous mixtures with hydrocarbons and chemicals is important for environmental purposes since hydrocarbons must be removed from gas processing, refinery and petrochemical plant wastewater streams and from sea or fresh water when oil spills occurs. For this purpose, the solubility and volatility of hydrocarbons is required to describe their phase distribution through the removal process. Such information is also important in the design and operation of separation equipments. In addition, it is also useful in predicting the water and the chemical contents of the fuels [3]. Most phase equilibrium calculations on oil and gas mixtures are performed using a cubic equation of state, for example, the Soave-Redlich-Kwong (SRK) or Peng-Robinson (PR) EoS [4]. However, systems containing reservoir fluids and polar/associating compounds (e.g. water, glycols and methanol etc.) are hard to describe using the conventional EoS especially at high temperature and pressure conditions [5].

The CPA equation of state (EoS), proposed by Kontogeorgis et al. [6], is an extension of the conventional SRK EoS. The equation combines the simplicity of a cubic equation of state and Wertheim's theory for the association part [7]. It gives a better description of systems containing associating compounds compared with the empirical or semi-empirical modifications of cubic EoS, and reduces to the SRK EoS for non-associating compounds [5]. In previous studies the CPA EoS has been extensively tested for well-defined systems containing associating compounds, most of which have already been summarized by Kontogeorgis et al. [8,9,10]

The CPA EoS has been extended to reservoir fluids by Yan et al.[5] using a characterization procedure similar to that of Pedersen et al.[11] and a set of new correlations for the critical properties for CPA. An issue is that experimental data are available only for very few systems, and more data are required for an extensive investigation and full validation of the model [8]. Therefore an experimental work has been carried out at Statoil research center in order to aquire more data. The details of experimental work are given in chapter 5. Initially two North Sea condensates were investigated in the work by Riaz et. al. [12] and LLE data was produced for condensate - 1/condensate - 2 + MEG and condensate - 1/condensate - 2 + MEG + water systems. Based on the experimental method established, the experimental work was extended to a third condensate (condensate - 3) and two light-oils (light oil - 1 and light oil - 2) as a part of master thesis projects [13,14], and has been continued in this work by measuring data for two heavy reservoir fluids with MEG and water. This has led to experimental data for 7 unique hydrocarbon fluids with MEG and MEG/water at various temperatures and atmospheric pressure.

In this chapter thermodynamic modeling of mutual solubility of the above systems is carried out using the CPA EoS and the oil characterization method of Yan et al.[5].

7.1 Oil systems – Overview

During the last 6 years liquid-liquid equilibrium data have been measured for 7 different oil systems with MEG and water. This work has all been done in close collaboration with Statoil research Center in Trondheim, Norway. The investigated oils are different in terms of PNA distribution, composition and overall physical properties. The characterization of reservoir fluids depends on the physical properties such as specific gravity and molecular weight, making it important to investigate modelling of different oil systems. In order to gain an overview of the oil's investigated, a comparison are made between the molecular weights, density and carbon plus fractions (C_{10+}). Composition analysis has been performed on the oils used in this project, which gives the composition and PNA distribution up to C_{10+} fraction.

Table 7.1 present the molecular weights, density and C_{10+} fraction of the oils investigated. It can be seen, that the hydrocarbon fluids are different, especially with regards to molecular weight and C_{10+} fraction. It is important when modelling these oil systems with MEG and water, to investigate the

influence of PNA distribution among the hydrocarbons, along with the influence of physical properties and hydrocarbon distribution (molecular weight and C_{10+} fraction)

Table 7.1: Molecular weight, density and plus fraction of all oil systems investigated [15-18 + this work]

Oil/Condensate	Reference	Molecular weight (g/mol)	Density (g/cm^3)	C_{10+} fraction (mole%)
Condensate – 1	[15,16]	112.7	0.7562	24.25
Condensate – 2	[16]	106.9	0.7385	5.88
Condensate – 3	[17]	97.37	0.7205	6.84
Light Oil – 1	[18]	266	0.9055	76.64
Light Oil – 2	[18]	135.2	0.7784	31.9
Fluid – 1	This work	157.54	0.8016	40.58
Fluid – 2	This work	336.56	0.9416	91.44

Analysis has been performed for the condensed composition of all the oil fluids by Intertek West Lab (external laboratory). This analysis provides the composition and PNA distribution up to C_{10+} fraction. From the analysis of the pure oils/condensates we can see the differences in PNA distribution (of the light end), which are presented in figure 7.1:

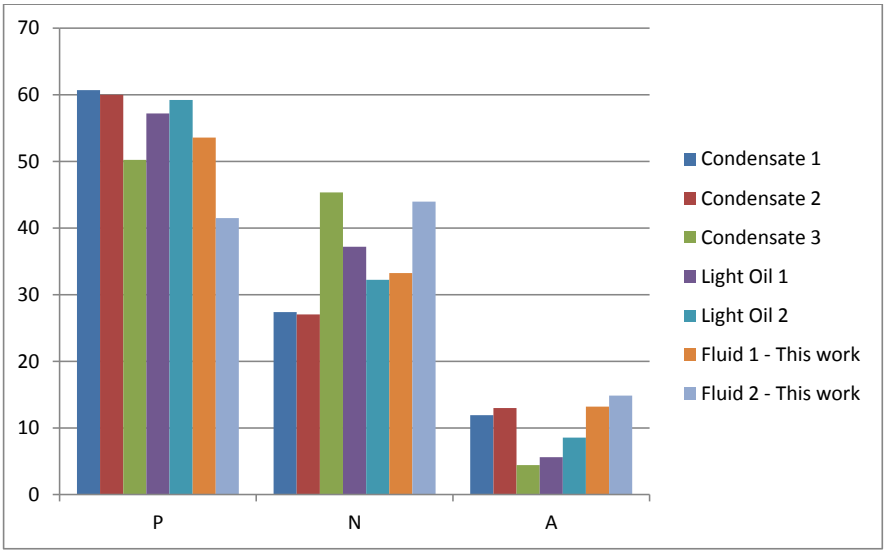

Figure 7.1: PNA distribution (Based on the analysis of light ends) of the oil's investigated in this work and recent literature [15-18]

The experimental work has been ongoing for several years, and covers two PhD projects and two master theses. All experimental data modeled in this work, are measured at Statoil Research facility in Trondheim, Norway. The experimental work has been carried out by Muhammad Riaz (Ph.d.), Mustafe Yussuf (Master thesis) and Michael Frost (Master thesis + Ph.d.). The experimental data obtained through these works, are LLE solubility data for oil systems with MEG and oil systems with MEG + Water.

Experimental data are available over a range of temperatures and at atmospheric pressure for all the systems presented in Table 7.1 and Figure 7.1. Table 7.2 presents the amount of available data points for the LLE of oil's with MEG + Water. In table 7.2, the solubility points are a single experimental measured value of solubility of either MEG in HC phase, water in HC phase or HC in polar phase.

Table 7.2: Experimental data sets available for oil systems with MEG + Water. All experimental data can be found in appendix B.

System	Temperatures	Experimental solubility points
Condensate – 1	303.15 K and 323.15 K	18
Condensate – 2	303.15 K and 323.15 K	18
Condensate – 3	313.15 K	9
Light Oil – 1	313.15 K and 323.15 K	12
Light Oil – 2	313.15 K and 323.15 K	12
Fluid – 1	303.15 K, 313.15 K and 323.15 K	27
Fluid – 2	303.15 K, 313.15 K and 323.15 K	27
Total		123

All the data available are modeled using the CPA EoS, with our current oil characterization procedures. This provides a total of 123 experimental points of the mutual solubility of oil + MEG + Water, which varies over different temperatures and feed compositions.

7.2 Modeling and oil characterization procedures

The hydrocarbon fractions that constitute reservoir fluids covers a wide range from light to heavy carbon fractions and therefore different binary interaction parameters, $k_{ij,}$ for each pair (MEG-HC and water-HC) should be used. The k_{ij} are usually obtained from well-defined binary systems (e.g. n-hexane-MEG, n-heptane-MEG, etc.). Experimental data are, however, only available for few hydrocarbon (paraffinic and naphthenic) components and MEG, possible due to the difficulty involved in measurement of such low solubility's present in these systems. In the work by Riaz et. al. [12] a simple strategy was adopted i.e. to use a single average temperature independent k_{ij} for all MEG-HC pairs. The binary interaction parameters between water and hydrocarbons where obtained from a generalized expression, where N_C is the carbon number.

$$k_{ij} = -0.026 \cdot N_C + 0.1915 \tag{7.1}$$

In this work new correlations have been suggested for binary interaction parameters *(k_{ij})* between MEG-HC and water-HC. All experimental data available for oil systems with MEG and MEG/water are modelled using both the approach of Riaz et. al. [12] and the approach developed in this work. Modeling of previous systems has been presented in literature by Riaz et. al. [15-17] and Frost et. al. [18].

7.2.1 New correlations for binary interaction parameters (k_{ij})

7.2.1.1 Water – hydrocarbons k_{ij}

Previously a simple correlation was created for interaction parameters between water and hydrocarbons, as a function of carbon number up to C_{10}. In previously modeling work, all plus fraction interaction parameters was assumed identical to the value of C_{10} (See table 7.3), in order to not gain large negative values between high carbon number hydrocarbons and water.

Table 7.3: Binary interaction parameters for LLE of water-hydrocarbon systems, based on the generalized expression which is derived based on data from propane up to n-decane (equation 7.1)

System	k_{ij}	%AAD in x_w	%AAD in x_{HC}
propane – water	0.1135	3.4	35.9
butane – water	0.0875	11.7	26.5
n-pentane – water	0.0615	13.4	28.4
hexane – water	0.0355	11.9	31.1
heptane – water	0.0095	11.5	63.3
octane – water	-0.0165	9.7	44.1
decane – water	-0.0685	8.2	264
C_{10+}	-0.0685[a]		

[a] k_{ij} is set to the value of water-decane for all HC-water fraction

Using references with experimental data [19-31] for water in heavy hydrocarbons, it has been possible to extend this correlation to the heavy end of oils. This shows a different picture, than what has been assumed until now. Figure 7.2 shows the relationship between the k_{ij}'s and molecular weight of alkanes for the binary pair of water and alkanes. From such correlations, it is possible to interpolate or extrapolate and thus obtain the k_{ij}*'s* when these are not available. Having it as a function of molecular weight is ideal when working with oil characterization, as molecular weight is obtained for all carbon fractions during the characterization.

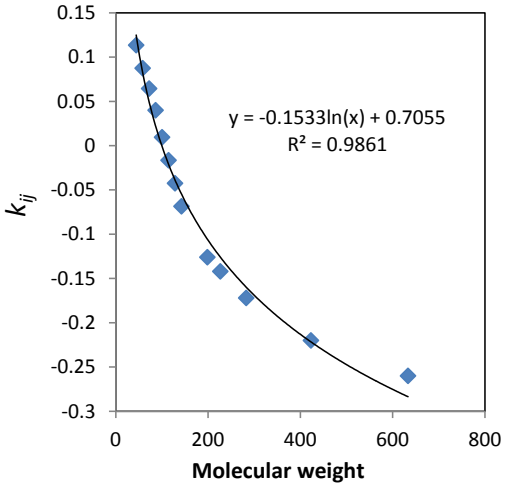

Figure 7.2: Correlation for binary interaction parameters (k_{ij}) for water – HC.

Fitting binary interaction parameters to the binary systems available for water-HC, results in a logarithmic correlation for the binary interaction parameters, where M_C is the molecular weight of the carbon fraction:

$$k_{ij} = -0.1533 \cdot \ln(M_C) + 0.7055 \quad (7.2)$$

This correlation has been used in this work for modeling of oil systems with MEG and water, and has shown to improve the predictions of water content in the hydrocarbon rich phase. Table 7.4 shows % AAD (percentage average absolute deviation) in the solubility of water in the hydrocarbon as well as the solubility of HC in the water for various water-alkane systems, using the correlation for estimating binary interaction parameters.

Table 7.4: Percentage Average Absolute Deviation (%AAD) between experimental and calculated water solubilities in the hydrocarbon phase (x_w) and the hydrocarbon solubilities in the aqueous phase (x_{HC}) using the developed correlation given in equation 7.2 for binary interaction parameters.

System	Reference	k_{ij}	%AAD in x_w	%AAD in x_{HC}
water-propane	[19,20]	0.1251	11.4	24.1
water-butane	[21-24]	0.0827	11.3	28.1
water-n-pentane	[25]	0.0496	9.9	30.1
water-n-hexane	[26]	0.0223	8.7	34.0
water-n-heptane	[27]	-0.0008	12.2	60.2
water-n-octane	[27]	-0.0209	11.1	38.2
water-n-decane	[28]	-0.0545	9.6	244
water-C14	[29]	-0.1055	6.5	-
water-C16	[29]	-0.1258	6.1	-
water-C20	[30]	-0.1597	3.6	-
water-C30	[31][a]	-0.2215	1.3	-
water-C45	[31][a]	-0.2834	10.3	-

[a] Based on the correlations of Tsonopoulos et al.

7.2.1.2 MEG – hydrocarbons k_{ij}

In the previous work of Yan et al. [5], Riaz et. al. and Frost et. al., an average k_{ij} has been used for all MEG - hydrocarbon pairs for modeling of the reservoir fluid, MEG and water systems. The average binary interaction parameter was fitted to binary data for the specific oil system, having various values ranging from pure predictions $k_{ij} = 0$ to $k_{ij} = 0.05$. The well-defined hydrocarbons + MEG systems previously studied with the CPA EoS are given in Table 7.5 along with the interaction parameter.

Table 7.5: Binary Interaction Parameters for LLE of MEG-HC Systems.

System	Reference	k_{ij}
MEG-methane	[32]	0.134
MEG-hexane	[33]	0.059
MEG-heptane	[33]	0.047
MEG-methylcyclohexane	[33]	0.061
MEG-ethylbenzene	[34]	0.013
MEG-nonane	[34]	0.015

It can be seen from Table 7.5 that binary interaction parameters are available only for few hydrocarbon (paraffinic and naphthenic) components and MEG due to scarcity of experimental data. Previously an avereage k_{ij} was used for all MEG-HC pairs, most commonly MEG-HC $k_{ij} = 0$ or $k_{ij} = 0.02$. In this work we will model all oil systems using the previous approach, and using new correlation for estimating k_{ij} for MEG-HC as a function of molecular weight.

Investigation of hydrocarbon solubility in MEG shows the same trend for k_{ij} as seen for water-HC, however, the correlation are until now based on the oil characterization procedure used. For further optimization of the correlation, a few systems of MEG with heavy hydrocarbons (C_{10+}) should be investigated. Equation 7.3 shows the correlation for k_{ij} between MEG and hydrocarbons as a function of molecular weight (M_C):

$$k_{ij} = -0.0701 \cdot \ln(M_C) + 0.3521 \qquad 7.3$$

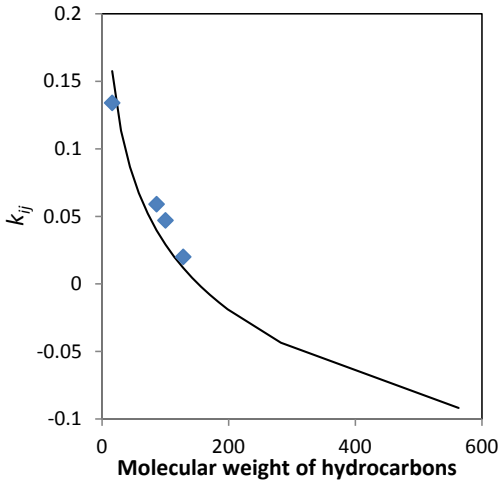

Figure 7.3: Correlation for binary interaction parameters (k_{ij}) for MEG – HC

7.3 Results and discussions

In this work modeling has been done for the 7 different oil systems [15-18] presented with MEG and MEG + water. The systems are modeled using the different approaches explained previously, where different methods of using k_{ij}'s between MEG-HC are investigated by modeling with an average temperature independent $k_{ij} = 0$, $k_{ij} = 0.02$ and estimating the k_{ij}'s using the correlation given in equation 7.3. All detailed results (experimental data and values from the CPA EoS), are placed in appendix B.

7.3.1 Condensate – 1

The composition of condensate - 1 is given in Table 7.6 with density, molar mass and PNA distribution of carbon fractions (C_6 to C_9). The following sections will focus on the characterization and the modeling using the CPA equation of state.

Table 7.6: Condensed composition of Condensate – 1 [15] (Mole %, Weight %, Molecular weight and Density)

Component	Mole %	Weight %	Molecular weight	Density kg/m^3
Methane	0	0	16.04	300
Ethane	0.004	0.001	30.07	356.7
Propane	0.896	0.351	44.09	506.7
iso-Butane	2.382	1.229	58.12	562.1
n-Butane	7.813	4.031	58.12	583.1
Neopentane	0.046	0.03	72.15	597
iso-Pentane	5.456	3.494	72.15	623.3
n-Pentane	7.275	4.659	72.15	629.9
Hexanes, C6 total	**10.292**	**7.77**	**85**	**666.2**
n-Hexane	*4.705*	*3.599*	*86.2*	*662.7*
iso-Paraffins (C6)	*4.867*	*3.722*	*86.2*	*660.8*
Naphtenes (C6)	*0.72*	*0.448*	*70.1*	*748.1*
Heptanes, C7 total	**16.046**	**13.016**	**91.4**	**736.2**
n-Heptane	*3.273*	*2.911*	*100.2*	*686.9*
iso-Paraffins (C7)	*3.612*	*3.213*	*100.2*	*690.5*
Naphtenes (C7)	*7.601*	*5.811*	*86.1*	*768.1*
Aromatics (C7)	*1.559*	*1.081*	*78.1*	*883.1*
Octanes, C8 total	16.632	15.293	103.6	768.6
n-Octane	*2.167*	*2.197*	*114.2*	*707*
iso-Paraffins (C8)	*2.104*	*2.146*	*114.9*	*706.8*
Naphtenes (C8)	*8.715*	*7.968*	*103*	*771.1*
Aromatics (C8)	*3.646*	*2.982*	*92.1*	*872*
Nonanes, C9 total	**8.903**	**9.363**	**118.5**	**780.6**
n-Nonane	*1.664*	*1.894*	*128.3*	*723*
iso-Paraffins (C9)	*2.176*	*2.479*	*128.3*	*722.9*
Naphtenes (C9)	*1.889*	*1.999*	*119.2*	*794.4*
Aromatics (C9)	*3.174*	*2.991*	*106.2*	*872.1*
Decanes plus, C10+	**24.254**	**40.766**	**189.4**	**846.4**
Sum	100	100		
Mean molecular weight:			112.7	
Gas gravity:				756.2

7.3.1.1 Reservoir fluid characterization

Using information from Table 7.6 and the Pedersen et al. [11] method of characterization with the modified correlation of Yan et al. [5] for critical temperature, critical pressure and acentric factor, the hydrocarbon fluid has been characterized. The results obtained after lumping are given in Table 7.7.

Table 7.7: Characterization of Condensate – 1

Component	Mole%	$T_{cm}(K)$	$P_{cm}(bar)$	ω_m	MW (g/mol)
Ethane	0.004	305.4	48.8	0.098	30.07
Propane	0.896	378.6	47.2	0.105	44.10
i-Butane	2.382	415.8	40.1	0.151	58.12
n-Butane	7.813	436.3	43.6	0.158	58.12
i-Pentane	5.502	460.4	33.8	0.227	72.15
n-Pentane	7.275	479.4	38.0	0.217	72.15
C_6	10.292	522.3	34.9	0.244	86.18
C_7	16.046	560.8	35.9	0.230	91.40
C_8	16.632	593.5	35.0	0.254	103.60
C_9	8.903	621.2	32.3	0.293	118.50
C_{10}	5.038	647.8	30.4	0.325	136.00
C_{11}	3.992	671.7	28.9	0.354	150.00
C_{12}	3.162	694.8	27.4	0.383	164.00
C_{13}	2.506	715.4	26.3	0.409	178.00
C_{14}	1.985	735.9	25.1	0.436	192.00
$C_{15} - C_{16}$	2.819	764.6	23.5	0.476	212.19
$C_{17} - C_{18}$	1.769	798.1	21.9	0.522	240.19
$C_{19} - C_{22}$	1.808	835.3	20.3	0.570	278.99
C_{23+}	1.176	911.3	17.2	0.698	371.40

7.3.1.2 Mutual solubility of Condensate – 1 + MEG

In the system of condensate - 1 + MEG, MEG is a self-associating compound whereas hydrocarbons are inert or non-associating. The only binary interaction parameter therefore required is that between MEG and each hydrocarbon (fraction from C_3 to C_{23}) whereas no combining rules are required.

The CPA correlations for the mutual solubility of condensate - 1 and MEG along with the experimental data are shown in Figure 7.4. The mutual solubility of MEG and condensate - 1 is estimated satisfactorily even with zero binary interaction parameters (pure prediction). In the previous work of Yan et al. [5], Riaz et. al. [12] and Frost et. al. [18], an average k_{ij} has been used for all MEG - hydrocarbon pairs for modeling of the reservoir fluid, MEG and water systems. Modeling has been done for the mutual solubility of condensate – 1 and MEG using $k_{ij} = 0$, $k_{ij} = 0.02$ and k_{ij} obtained from the developed correlations given in equation 7.3.

The modeling results show that the solubility of MEG in condensate – 1 is in good agreement with experimental data, whereas the solubility of hydrocarbons in MEG phase is over-predicted using a $k_{ij} = 0$. The correlation of solubility of hydrocarbons in MEG is improved using an average $k_{ij} = 0.02$ or using the developed correlation for estimating the k_{ij}'s. It has also been observed that the use of non-zero binary interaction parameter is required for obtaining simultaneous good fitting of the solubility of HC in the polar phase and MEG in hydrocarbon phase. Improved results might be obtained by taking in to account the cross-association volume and the energy for MEG and aromatic hydrocarbons (i.e. benzene, toluene and xylene) present in the condensate, however, satisfactory modeling results are obtained using existing characterization method (of Yan et al.) without explicitly taking aromaticity into account and using correlations for predicting binary interaction parameters (k_{ij}) for all MEG-HC pairs.

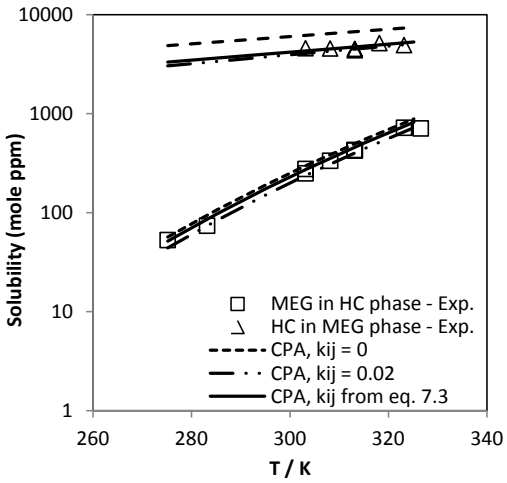

Figure 7.4: Mutual solubility (in mole ppm, x*10^6) of condensate - 1 and MEG as a function of temperature (K). The experimental data [15] are indicated as points and the CPA calculations as lines using a $k_{ij} = 0$, $k_{ij} = 0.02$ and k_{ij} from correlation given in eq. 7.3 for MEG-HC.

7.3.1.3 Mutual solubility of Condensate – 1 + MEG + water

In the system of condensate - 1 + MEG + water, there are in addition to self-association, two compounds (MEG, water) which cross-associate. The Elliott combining rule is used for MEG and water with a k_{ij} = -0.115 taken from previous work [34]. The modeling results are performed using an average binary interaction parameter k_{ij} = 0, k_{ij} = 0.02 and k_{ij} from developed correlations for all MEG-HC pairs (equation 7.3). All k_{ij}'s for water-HC are estimated using the correlation given in equation 7.2. The modeling results are correct in order of magnitude. Improvements in the predictions of MEG solubility in the hydrocarbon phase is obtained using the developed correlations for k_{ij} between all MEG-HC pairs or an average k_{ij} = 0.02. All detailed modeling results are presented in appendix B. The deviations between experimental data and calculations are summarized in Table 7.8.

The solubility of water in hydrocarbon phase decreases with increasing MEG mole fraction, the solubility of MEG in hydrocarbon rich phase and hydrocarbons in the polar phase increases with increasing MEG content in the polar phase as shown in Figures 7.5 and 7.6. These experimental trends are well captured using the CPA EoS even for this complex mixture containing associating and non-associating components. The hydrocarbon phase is also a complex North Sea fluid with numerous well-defined and ill-defined components with paraffinic, naphthenic and aromatic nature.

Table 7.8: Average Deviation (%) of CPA Predictions from Experimental Data for Investigated Condensate - 1 + MEG + Water System at T=303.15 K, T=323.15 K and P=1 atm.

k_{ij}		%AAD			
		Polar Phase	Hydrocarbon phase		Average
Water – HC	MEG – HC	HC	MEG	Water	
From eq. 7.2	0.00	27	93	12	44
From eq. 7.2	0.02	24	52	13	30
From eq. 7.2	From eq. 7.3	21	55	12	29

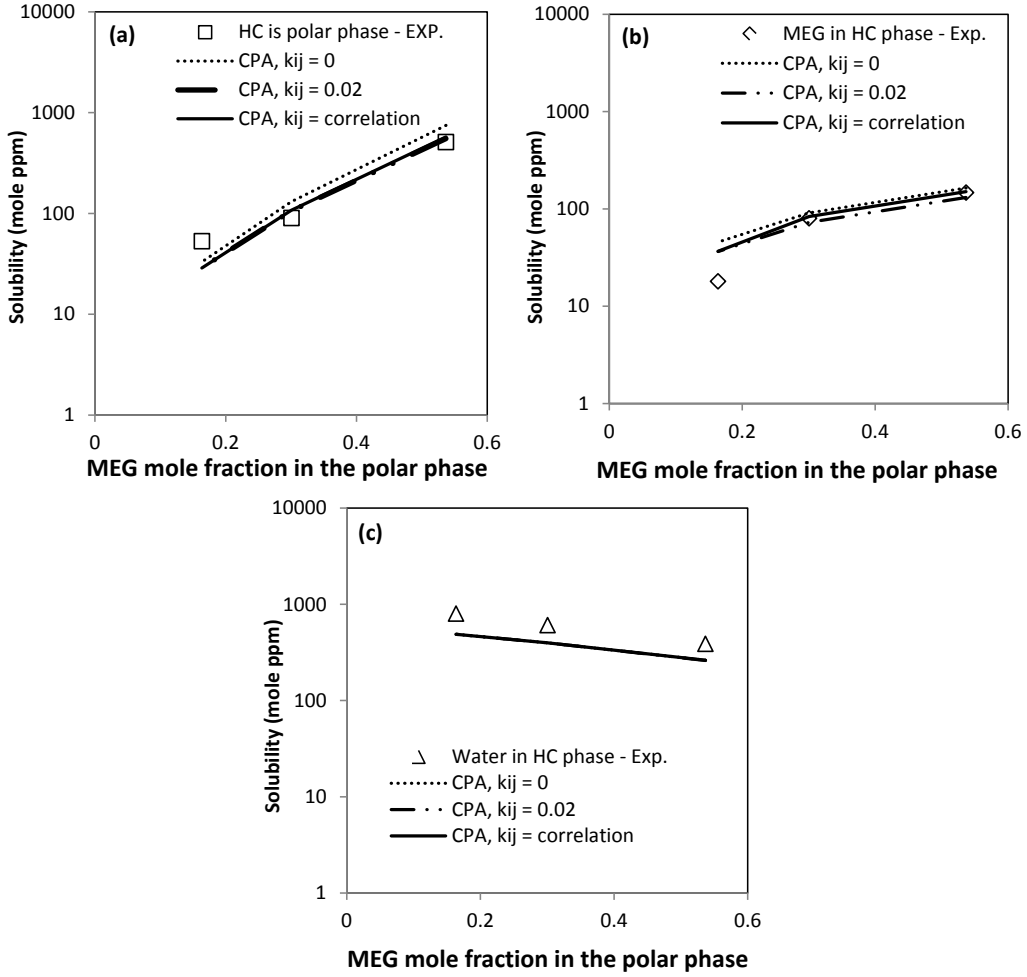

Figure 7.5: Modeling of the mutual solubility (in mole ppm, $x \cdot 10^6$) of Condensate - 1, MEG and water at temperature 303.15 K and pressure 1 atm.: (a) Hydrocarbons in polar phase (b) MEG in organic phase (c) water in organic phase. The points are experimental data and the lines are modeling results with the CPA EoS using k_{ij} for MEG-water=-0.115 and HC-water from correlation given in Eq. 7.2. For MEG-HC there are used a $k_{ij} = 0$, $k_{ij} = 0.02$ and k_{ij} from correlation given in eq. 7.3.

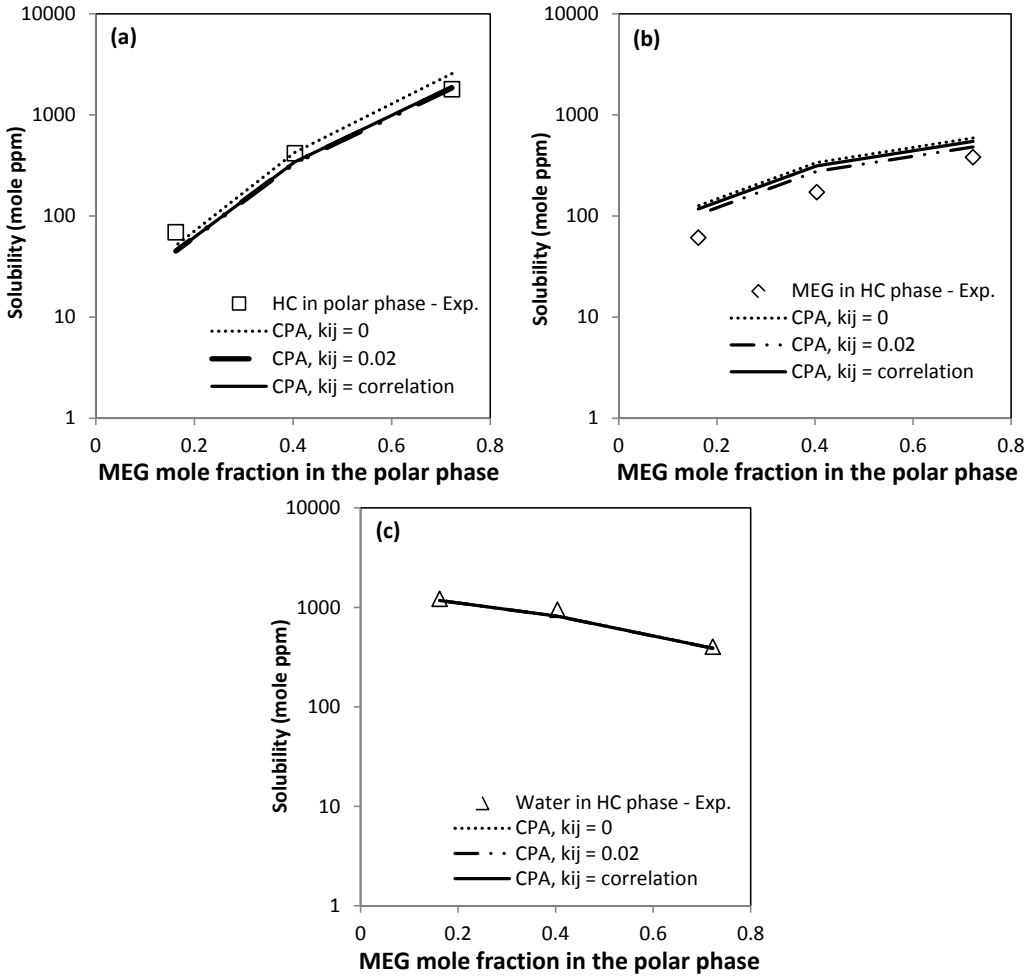

Figure 7.6: Modeling of the mutual solubility (in mole ppm, $x \cdot 10^6$) of Condensate - 1, MEG and water at temperature 323.15 K and pressure 1 atm.: (a) Hydrocarbons in polar phase (b) MEG in organic phase (c) water in organic phase. The points are experimental data and the lines are modeling results with the CPA EoS using k_{ij} for MEG-water=-0.115 and HC-water from correlation given in Eq. 7.2. For MEG-HC there are used a $k_{ij} = 0$, $k_{ij} = 0.02$ and k_{ij} from correlation given in eq. 7.3.

7.3.2 Condensate – 2

The composition of condensate - 2 is given in Table 7.9 with density, molar mass and PNA distribution of carbon fractions (C_6 to C_9).

Table 7.9: Condensed composition of Condensate – 2 [16] (Mole %, Weight %, Molecular weight and Density)

Component	Mole %	Weight %	Molecular weight	Density kg/L
Methane	0	0	16.04	0.3
Ethane	0	0	30.07	0.358
Propane	0	0	44.1	0.508
iso-Butane	0.02	0.01	58.12	0.563
n-Butane	0.55	0.34	58.12	0.585
Neopentane	0.04	0.03	72.15	0.597
iso-Pentane	10.69	8.06	72.15	0.625
n-Pentane	12.97	9.78	72.15	0.631
Hexanes, C6 total	**16.12**	**14.31**	**84.92**	**0.6676**
n-Hexane	14.85	13.38	86.18	0.6625
Naphtenes (C6)	1.27	0.93	70.13	0.75
Heptanes, C7 total	**22.29**	**21.17**	**90.9**	**0.7427**
n-Heptane	8.35	8.74	100.2	0.6874
Naphtenes (C7)	10.24	9.41	87.93	0.7605
Aromatics (C7)	3.7	3.02	78.11	0.884
Octanes, C8 total	**20.67**	**22.46**	**103.93**	**0.7658**
n-Octane	6.27	7.48	114.23	0.7063
Naphtenes (C8)	9.7	10.45	102.99	0.772
Aromatics (C8)	4.7	4.53	92.14	0.871
Nonanes, C9 total	**10.77**	**13.37**	**118.73**	**0.7787**
n-Nonane	4.41	5.89	127.86	0.7213
Naphtenes (C9)	2.69	3.41	120.88	0.7867
Aromatics (C9)	3.67	4.07	106.17	0.8717
Decanes plus, C10+	**5.88**	**10.47**	**170.2**	**0.8218**
Sum	100	100		

7.3.2.1 Reservoir fluid characterization

Using information from Table 7.9 and the Pedersen et al. [11] method of characterization with the modified correlation of Yan et al. [5] for critical temperature, critical pressure and acentric factor, the hydrocarbon fluid has been characterized. The results obtained after lumping are given in Table 7.10.

Table 7.10: Characterization of Condensate – 2

Component	Mole%	$T_{cm}(K)$	$P_{cm}(bar)$	ω_m	MW (g/mol)
i-Butane	0.02	415.8	40.1	0.151	58.12
n-Butane	0.55	436.3	43.6	0.158	58.12
i-Pentane	10.73	460.4	33.8	0.227	72.15
n-Pentane	12.97	479.4	38.0	0.217	72.15
C_6	16.12	522.3	34.9	0.244	86.18
C_7	22.29	562.5	36.6	0.225	90.90
C_8	20.67	592.8	34.7	0.256	103.90
C_9	10.77	620.7	32.1	0.294	118.70
C_{10}	1.708	646.6	30.1	0.328	136.00
C_{11}	1.212	670.0	28.4	0.359	150.00
C_{12}	0.86	692.5	26.9	0.390	164.00
C_{13}	0.61	712.7	25.6	0.417	178.00
C_{14}	0.433	732.7	24.4	0.446	192.00
C_{15}	0.307	752.7	23.2	0.476	206.00
C_{16}	0.218	770.1	22.2	0.502	220.00
C_{17}	0.155	787.2	21.3	0.528	234.00
C_{18+}	0.378	835.0	19.2	0.599	282.20

7.3.2.2 Mutual solubility of Condensate – 2 + MEG

The modeling results for the mutual solubility of condensate - 2 and MEG are shown in Figure 7.7 along with the experimental data, as a function of temperature. The results presented are in very good agreement with the experimental data. Different binary interaction parameters have been used between hydrocarbons and MEG, $k_{ij} = 0$, $k_{ij} = 0.02$ and k_{ij} obtained from the developed correlations given in equation 7.3. The modeling results show that the solubility of hydrocarbons in MEG is in good agreement with experimental data using zero binary interaction parameter, whereas the solubility of MEG in the hydrocarbon phase is under-predicted using a $k_{ij} = 0$. The correlation of solubility of MEG in hydrocarbon phase is improved using the developed correlation for estimating the k_{ij}'s between MEG and hydrocarbons, however, this comes at the cost of accuracy in calculated hydrocarbon content in the MEG phase.

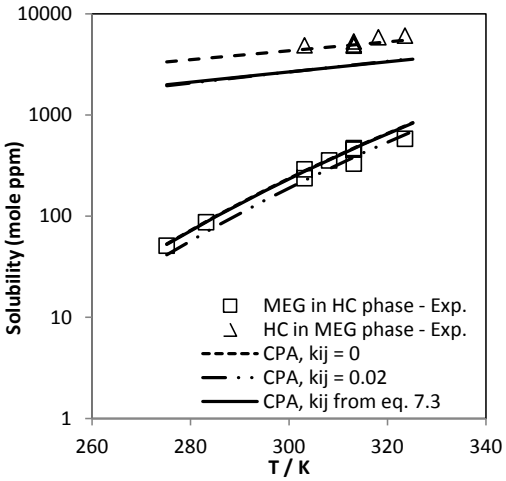

Figure 7.7: Mutual solubility (in mole ppm, $x \cdot 10^6$) of condensate - 2 and MEG as a function of temperature (K). The experimental data [16] are indicated as points and the CPA calculations as lines using a $k_{ij} = 0$, $k_{ij} = 0.02$ and k_{ij} from correlation given in eq. 7.3 for MEG-HC.

7.3.2.3 Mutual solubility of Condensate – 2 + MEG + water

The modeling results for the condensate - 2 + MEG + water system at temperatures 303.15 and 323.15 K are given in detail in appendix B. At each temperature three feed compositions are used to investigate the effect of MEG mole faction in polar phase on mutual solubility. This complex mixture of associating (MEG, water) and non-associating compounds (hydrocarbon components) is modeled with the CPA EoS using temperature independent k_{ij} for water-HC obtained from the correlation of equation 7.2 and $k_{ij} = 0$, $k_{ij} = 0.02$ and k_{ij} from equation 7.3 between MEG and hydrocarbons.

The CPA EoS can satisfactory predict mutual solubilities, where in most cases the results are in the correct order of magnitude. The solubility of water in hydrocarbon rich phase decreases, the solubility of MEG in hydrocarbon rich phase increases and the solubility of hydrocarbons in the polar phase increases with increasing MEG mole fraction in the polar phase. The model satisfactorily describes these data trends as shown in Figures 7.8 and 7.9 at temperatures 303.15 and 323.15 K respectively. A better prediction of the solubility of water in hydrocarbons phase is obtained at 323.15 K as compared to 303.15 K. This may be due to the limitations of CPA for

describing the solubility of water in hydrocarbons at lower temperatures [8]. But overall promising modeling results are obtained for the complex system of condensate - 2 + MEG + Water. Table 7.11 summarizes the deviations between experimental data and calculations made with the CPA EoS.

Table 7.11: Average Deviation (%) of CPA Predictions from Experimental Data for Investigated Condensate - 2 + MEG + Water System at T=303.15 K, T=323.15 K and P=1 atm.

k_{ij}		%AAD			
		Polar Phase	Hydrocarbon phase		Average
Water – HC	MEG – HC	HC	MEG	Water	
From eq. 7.2	0.00	56	38	28	41
From eq. 7.2	0.02	67	14	28	36
From eq. 7.2	From eq. 7.3	66	21	28	38

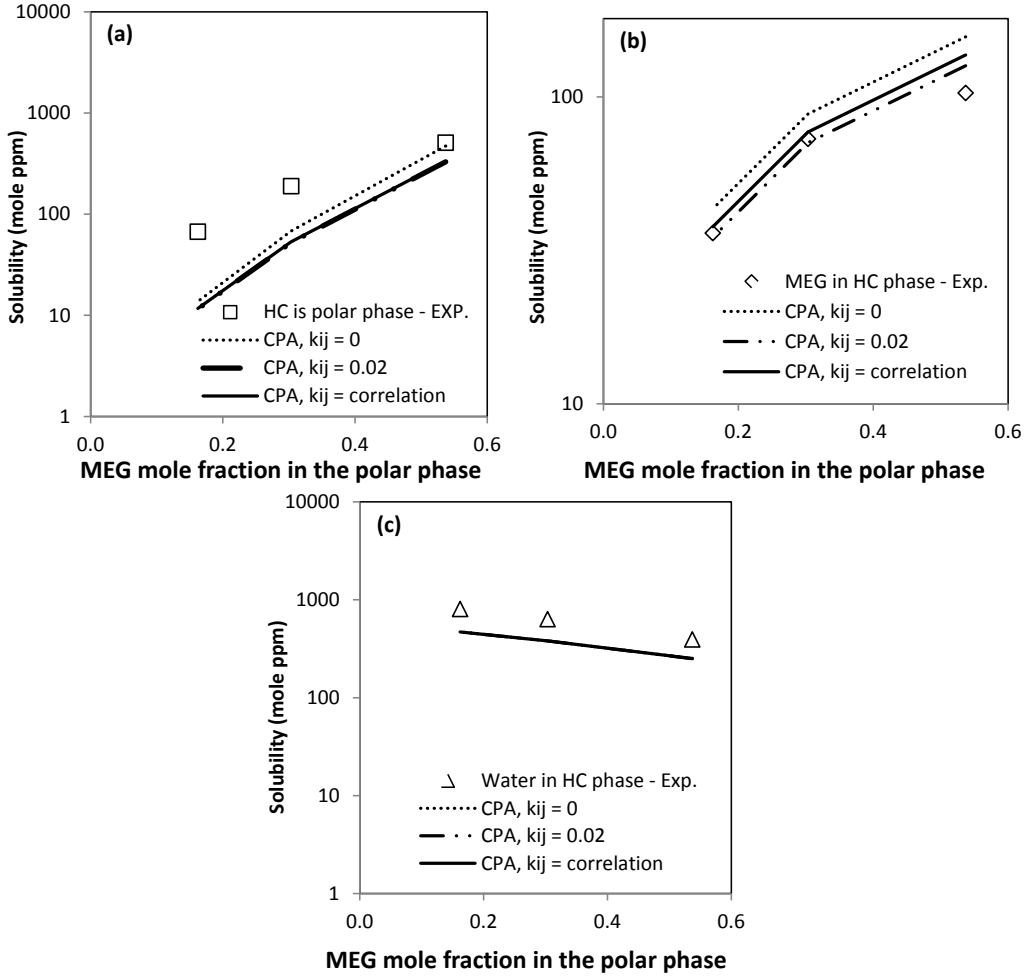

Figure 7.8: Modeling of the mutual solubility (in mole ppm, $x \cdot 10^6$) of Condensate - 2, MEG and water at temperature 303.15 K and pressure 1 atm.: (a) Hydrocarbons in polar phase (b) MEG in organic phase (c) water in organic phase. The points are experimental data and the lines are modeling results with the CPA EoS using k_{ij} for MEG-water=-0.115 and HC-water from correlation given in Eq. 7.2. For MEG-HC there are used a $k_{ij} = 0$, $k_{ij} = 0.02$ and k_{ij} from correlation given in eq. 7.3.

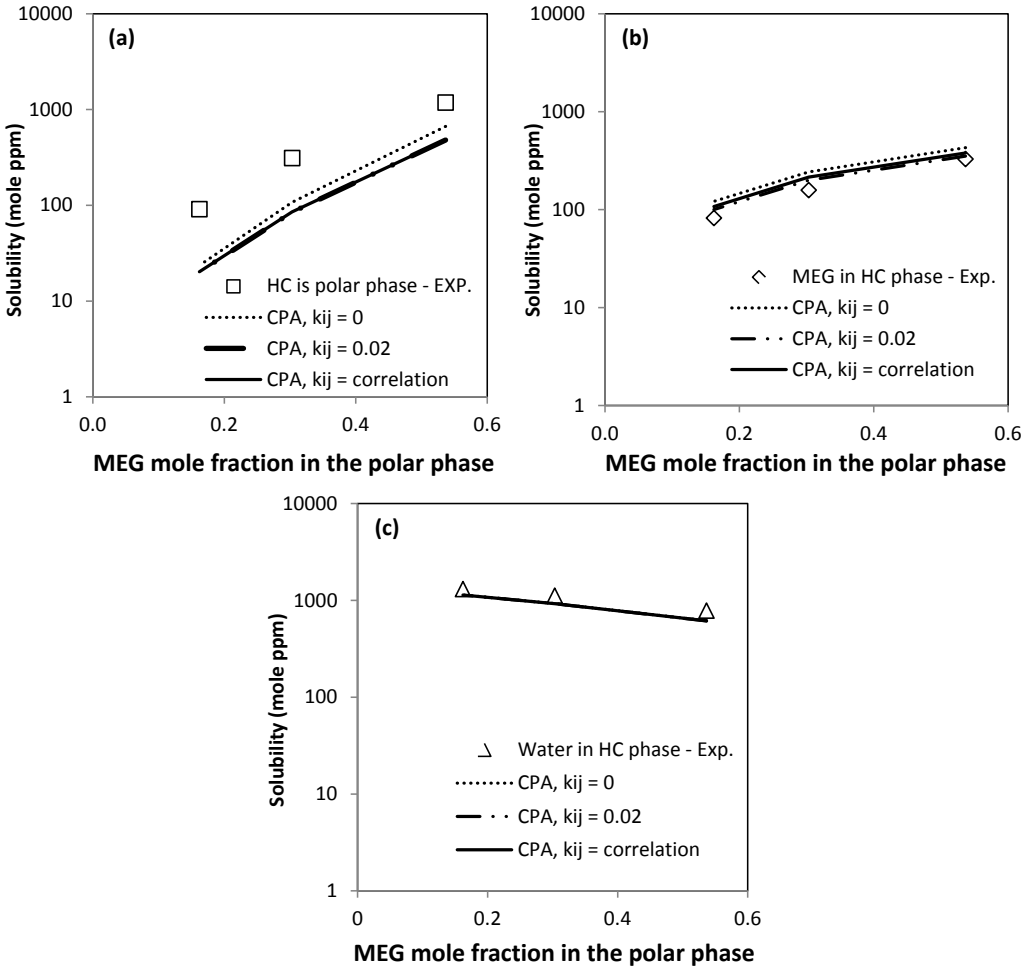

Figure 7.9: Modeling of the mutual solubility (in mole ppm, $x \cdot 10^6$) of Condensate - 2, MEG and water at temperature 323.15 K and pressure 1 atm.: (a) Hydrocarbons in polar phase (b) MEG in organic phase (c) water in organic phase. The points are experimental data and the lines are modeling results with the CPA EoS using k_{ij} for MEG-water=-0.115 and HC-water from correlation given in Eq. 7.2. For MEG-HC there are used a $k_{ij} = 0$, $k_{ij} = 0.02$ and k_{ij} from correlation given in eq. 7.3.

7.3.3 Condensate – 3

The composition of condensate - 3 is given in Table 7.12, which shows that it is a lighter hydrocarbon fluid compared to condensate - 1 and condensate – 2. It has a lower overall molar mass and overall density as compared to the other condensates, as shown in Table 7.1. The PNA distribution of the hydrocarbon fluid is given in Figure 7.1 in comparison to the other fluids, which shows that it is more naphthenic and has lower aromatic content than that of the condensate - 1 and the condensate - 2.

Table 7.12: Condensed composition of Condensate – 3 [17] (Mole %, Weight %, Molecular weight and Density)

Component	Mole %	Weight %	Molecular weight	Density kg/L
Propane (P)	1.069	0.509	44.1	0.5080
2-methylpropane (P)	5.919	3.718	58.12	0.5630
butane (P)	7.165	4.500	58.124	0.5850
2,2-DM-Propane(P)	0.1507	0.117	72.15	0.5970
2-methylbutane (P)	6.616	5.159	72.151	0.6250
pentane (P)	6.616	4.488	72.151	0.6310
Hexane total	**14.074**	**12.841**	**84.429**	**0.6642**
Hexanes – (P)	12.914	11.761	84.272	0.6640
Hexanes – (N)	1.160	1.080	86.178	0.6662
Heptane total	**25.547**	**24.912**	**90.238**	**0.7429**
Heptanes (P)	6.610	7.158	100.205	0.6896
Heptanes (N)	17.501	16.543	87.468	0.7594
Heptanes (A)	1.435	1.211	78.114	0.8842
Octane total	**20.4272**	**22.943**	**103.933**	**0.7680**
Octanes (P)	3.003	3.699	113.965	0.7134
Octanes (N)	15.282	17.111	103.614	0.7694
Octanes (A)	2.141	2.132	92.143	0.8714
Nonane total	**6.4376**	**8.327**	**119.701**	**0.7809**
Nonanes (P)	2.195	2.856	120.387	0.7688
Nonanes (N)	3.810	4.948	120.144	0.7836
Nonanes (A)	0.4310	0.524	112.297	0.8240
Decane Plus ($C10^{+}$)	**6.836**	**12.484**	**169.9**	**0.8120**
Sum	100	100		

7.3.3.1 Reservoir fluid characterization

Using information from Table 7.12 and the Pedersen et al. [11] method of characterization with the modified correlation of Yan et al. [5] for critical temperature, critical pressure and acentric factor,

the hydrocarbon fluid has been characterized. The results obtained after lumping are given in Table 7.13.

Table 7.13: Characterization of Condensate – 3

Component	Mole%	$T_{cm}(K)$	$P_{cm}(bar)$	ω_m	MW (g/mol)
Ethane	0	305.4	48.8	0.098	30.07
Propane	1.041	378.6	47.2	0.105	44.10
i-Butane	5.237	415.8	40.1	0.151	58.12
n-Butane	6.339	436.3	43.6	0.158	58.12
i-Pentane	5.728	460.4	33.8	0.227	72.15
n-Pentane	5.558	479.4	38.0	0.217	72.15
C_6	14	522.3	34.9	0.244	86.18
C_7	26.687	563.5	36.9	0.223	90.20
C_8	21.841	591.6	34.3	0.259	103.80
C_9	6.699	622.7	32.8	0.289	117.20
C_{10}	2.008	647.2	30.2	0.327	136.00
C_{11}	1.421	669.1	28.2	0.362	150.00
C_{12}	1.006	690.2	26.3	0.397	164.00
C_{13}	0.712	709.0	24.8	0.428	178.00
C_{14}	0.504	727.6	23.3	0.462	192.00
C_{15}	0.356	746.3	21.9	0.497	206.00
C_{16}	0.252	762.5	20.8	0.527	220.00
C_{17}	0.179	778.3	19.7	0.559	234.00
C_{18+}	0.432	821.9	17.3	0.648	281.90

7.3.3.2 Mutual solubility of Condensate – 3 + MEG

The modeling result for the mutual solubility of condensate - 3 and MEG are shown in Figure 7.10 in comparison to the experimental data as a function of temperature [17]. Different binary interaction parameters have been used between hydrocarbons and MEG, k_{ij} = 0, k_{ij} = 0.02 and k_{ij} obtained from the developed correlations given in equation 7.3. The CPA EoS correlates very satisfactorily the solubilities in both phases using the correlation given in equation 7.3 for estimating, temperature independent k_{ij} between all MEG-HC pairs. With zero binary interactions parameter (prediction) CPA satisfactorily describes the trend of mutual solubility as a function of temperature but the solubilities in both phases are over predicted.

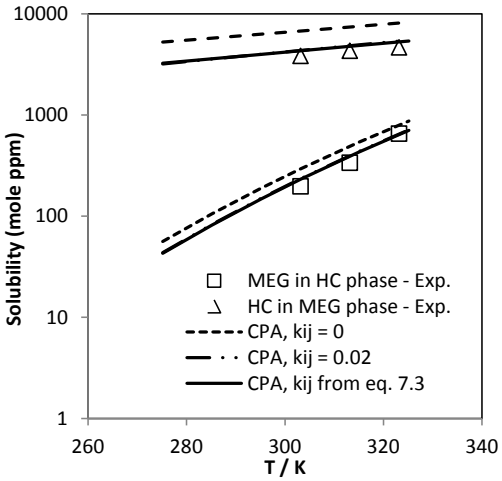

Figure 7.10: Mutual solubility (in mole ppm, $x \cdot 10^6$) of condensate - 3 and MEG as a function of temperature (K). The experimental data [17] are indicated as points and the CPA calculations as lines using a $k_{ij} = 0$, $k_{ij} = 0.02$ and k_{ij} from correlation given in eq. 7.3 for MEG-HC.

7.3.3.3 Mutual solubility of Condensate – 3 + MEG + water

For the condensate - 3 + MEG + water system the detailed modeling results are given in appendix B Once again using temperature independent $k_{ij} = 0$, $k_{ij} = 0.02$ and k_{ij} obtained from correlations in equation 7.3 and water-HC k_{ij} from the correlation in equation 7.2, excellent modeling results are obtained. Table 7.14 summarizes the deviations between experimental data and calculations made with the CPA EoS.

Table 7.14: Average Deviation (%) of CPA Predictions from Experimental Data for Investigated Condensate - 2 + MEG + Water System at T=313.15 K and P=1 atm.

k_{ij}		%AAD			
		Polar Phase	Hydrocarbon phase		Average
Water – HC	MEG – HC	HC	MEG	Water	
From eq. 7.2	0.00	11	48	17	25
From eq. 7.2	0.02	18	21	17	19
From eq. 7.2	From eq. 7.3	23	18	17	19

Similar to the condensate - 1 and the condensate - 2, the experimental trends for the solubility as a function of MEG mole fraction in the polar phase are satisfactorily captured with very good accuracy as shown in Figure 7.11.

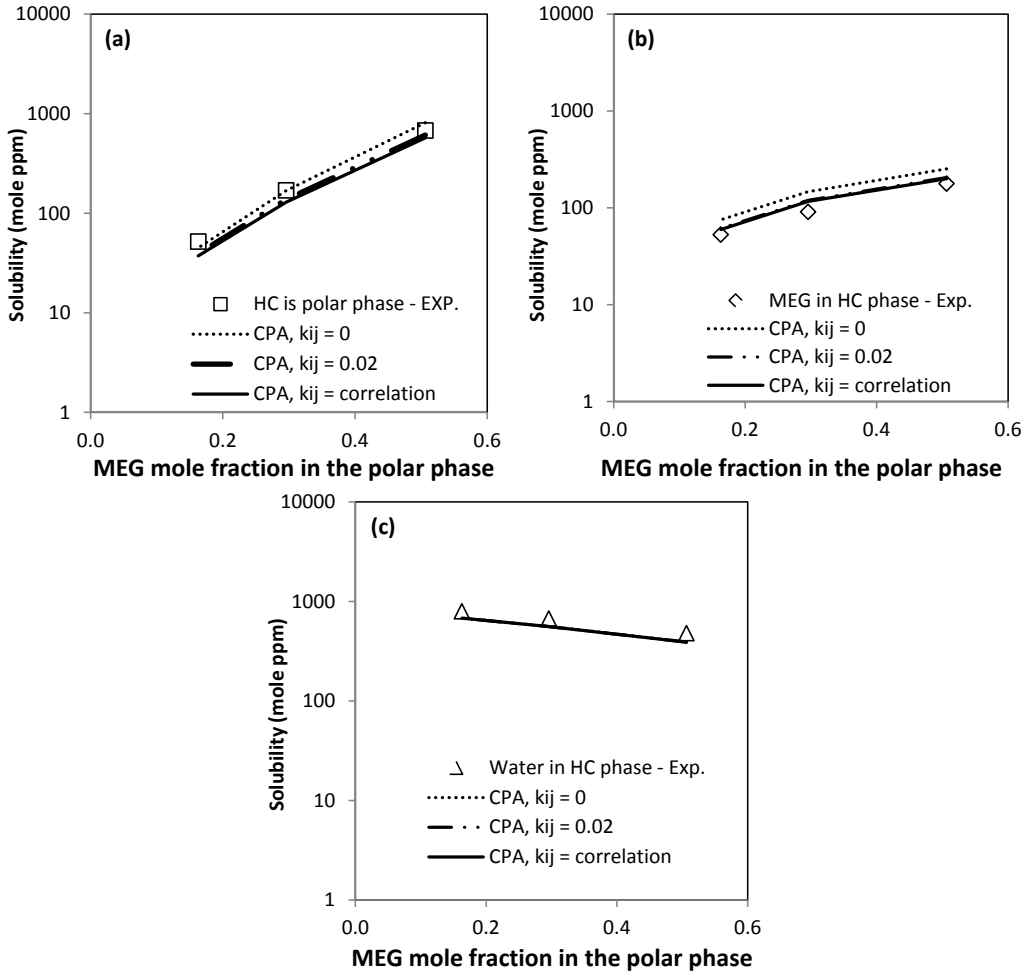

Figure 7.11: Modeling of the mutual solubility (in mole ppm, $x \cdot 10^6$) of Condensate - 3, MEG and water at temperature 313.15 K and pressure 1 atm.: (a) Hydrocarbons in polar phase (b) MEG in organic phase (c) water in organic phase. The points are experimental data and the lines are modeling results with the CPA EoS using k_{ij} for MEG-water=-0.115 and HC-water from correlation given in Eq. 7.2. For MEG-HC there are used a $k_{ij} = 0$, $k_{ij} = 0.02$ and k_{ij} from correlation given in eq. 7.3.

7.3.4 Light Oil – 1

During this work, experimental LLE was measured for two heavy oil fluids which was considered "heavier" (high C_{10+} fractions) than the condensates investigated. These are labeled Light Oil – 1 and Light Oil – 2. The composition of light oil - 1 is given in Table 7.15 which shows that it has 91.45 mass % decane plus fraction. This means that we have a PNA distribution of only 9.55 mass % of the oil and the details of many components are unknown.

Table 7.15: Condensed composition of Light Oil – 1 [18] (Mole %, Weight %, Molecular weight and Density)

Component	Mole %	Weight %	Molecular weight	Density kg/L
Methane	0.04	0	16.04	0.3
Ethane	0.3	0.03	30.07	0.358
Propane	0.81	0.13	44.1	0.508
iso-Butane	0.41	0.09	58.12	0.563
n-Butane	1.02	0.22	58.12	0.585
Neopentane	0.02	0	72.15	0.597
iso-Pentane	0.72	0.2	72.15	0.625
n-Pentane	0.9	0.25	72.15	0.631
Hexanes, C6 total	**1.92**	**0.61**	**84.9**	**0.6679**
n-Hexane	1.77	0.57	86.18	0.6628
Naphtenes (C6)	0.15	0.04	70.13	0.75
Heptanes, C7 total	**4.92**	**1.71**	**92.14**	**0.7371**
n-Heptane	1.45	0.55	100.2	0.6875
Naphtenes (C7)	3.35	1.12	89.16	0.7598
Aromatics (C7)	0.12	0.04	78.11	0.884
Octanes, C8 total	**6.21**	**2.5**	**107.14**	**0.7482**
n-Octane	2.39	1.03	114.23	0.7073
Naphtenes (C8)	3.46	1.35	103.79	0.7723
Aromatics (C8)	0.36	0.12	92.14	0.871
Nonanes, C9 total	**6.09**	**2.81**	**123.24**	**0.7513**
n-Nonane	3.79	1.82	128.11	0.7212
Naphtenes (C9)	1.49	0.67	120.16	0.7875
Aromatics (C9)	0.81	0.32	106.17	0.873
Decanes plus, C10+	**76.64**	**91.45**	**317.3**	**0.9283**
Sum	100	100		

7.3.4.1 Reservoir fluid characterization

Using information from Table 7.15 and the Pedersen et al. [11] method of characterization with the modified correlation of Yan et al. [5] for critical temperature, critical pressure and acentric factor,

the hydrocarbon fluid has been characterized. The results obtained after lumping are given in Table 7.16. It can be seen from the characterization, that it goes to much higher carbon fractions (C_{53+}).

Table 7.16: Characterization of Light Oil – 1

Component	Mole%	$T_{cm}(K)$	$P_{cm}(bar)$	ω_m	MW (g/mol)
Methane	0.04	190.6	46.0	0.008	16.04
Ethane	0.3	305.4	48.8	0.098	30.07
Propane	0.81	378.6	47.2	0.105	44.10
i-Butane	0.41	415.8	40.1	0.151	58.12
n-Butane	1.02	436.3	43.6	0.158	58.12
i-Pentane	0.72	460.4	33.8	0.227	72.15
n-Pentane	0.9	479.4	38.0	0.217	72.15
C_6	1.92	522.3	34.9	0.244	86.18
C_7	4.921	561.0	36.0	0.229	92.14
C_8	6.211	587.8	33.0	0.269	107.14
C_9	6.091	612.4	29.5	0.317	123.24
$C_{10} - C_{13}$	19.318	675.8	26.4	0.389	155.74
$C_{14} - C_{17}$	14.479	759.9	22.6	0.490	211.74
$C_{18} - C_{20}$	8.425	815.9	20.6	0.556	261.33
$C_{21} - C_{24}$	8.741	861.8	19.0	0.612	309.74
$C_{25} - C_{29}$	7.915	909.7	17.3	0.702	371.99
$C_{30} - C_{34}$	5.52	953.3	15.9	0.775	441.99
$C_{35} - C_{41}$	5.04	1001.1	14.5	0.796	523.98
$C_{42} - C_{52}$	4.204	1056.1	12.8	0.848	644.01
C_{53+}	3.013	1145.8	9.5	0.912	865.23

7.3.4.2 Mutual solubility of Light Oil - 1 + MEG

The modeling results and the experimental data for mutual solubility of light oil – 1 + MEG are shown in Figure 7.12, as a function of temperature. As mentioned earlier light oil – 1 has much higher overall molar mass as compared the condensates investigated as shown in Table 7.1. The mutual solubility trend is reversed for light oil – 1, meaning that the solubility of MEG in hydrocarbon phase is higher than that of the solubility of hydrocarbons in MEG phase.

It can be seen that the solubility of hydrocarbons in MEG phase is satisfactorily correlated using the correlation given by equation 7.3 to estimate k_{ij} for all MEG-HC pairs. The experimental trends are captured; even the shift in solubility at temperature above 320 K, however, the solubility of MEG in

hydrocarbon phase is under-correlated. More experimental data is required for oil with higher decane plus fraction and reliable measurement of PNA distribution in decane plus fraction is necessary. If the analysis shows that the heavy end has considerably higher aromatic content, solvation should be added to account for the increased solubility of MEG in hydrocarbon phase.

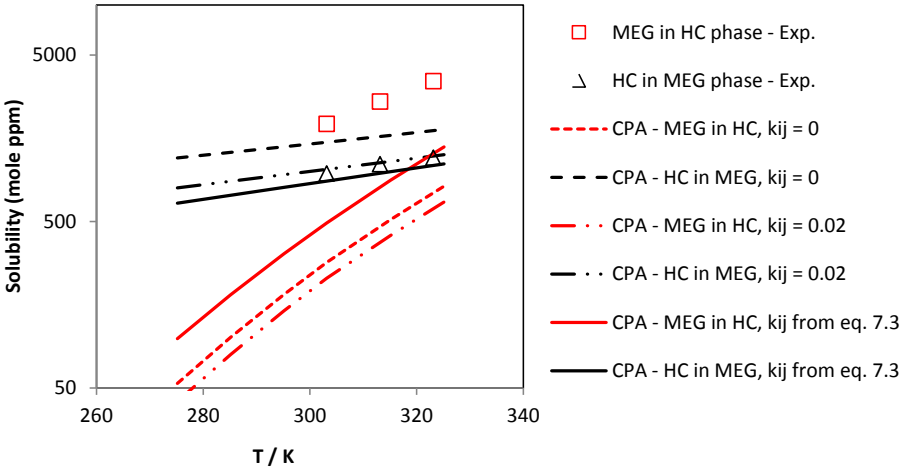

Figure 7.12: Mutual solubility (in mole ppm, $x \cdot 10^6$) of light oil – 1 and MEG as a function of temperature (K). The experimental data [18] are indicated as points and the CPA calculations as lines using a $k_{ij} = 0$, $k_{ij} = 0.02$ and k_{ij} from correlation given in eq. 7.3 for MEG-HC.

7.3.4.3 Mutual solubility of Light Oil - 1 + MEG + water

In the previous section the modeling results for light oil - 1 + MEG are presented showing higher deviations for the solubility of MEG in hydrocarbon phase. In this section modeling results for light oil - 1 + MEG + water are presented using temperature independent $k_{ij} = 0$, $k_{ij} = 0.02$ and k_{ij} obtained from correlations in equation 7.3 and water-HC k_{ij} from the correlation in equation 7.2. Here the modeling results are in very good agreement with the experimental data and in contrast to the light oil - 1 + MEG system deviations are lower for the prediction of solubility of MEG in oil and water in oil. This further highlights a need of more experimental data for oils with high carbon plus fractions. Table 7.17 summarizes the deviations between experimental data and calculations made with the CPA EoS.

Table 7.17: Average Deviation (%) of CPA Predictions from Experimental Data for Investigated Light Oil – 1 + MEG + Water System at T=313.15 K, T=323.15 K and P=1 atm.

k_{ij}		%AAD			
		Polar Phase	Hydrocarbon phase		Average
Water – HC	MEG – HC	HC	MEG	Water	
From eq. 7.2	0.00	30	47	14	30
From eq. 7.2	0.02	41	57	14	37
From eq. 7.2	From eq. 7.3	54	19	14	29

For light oil - 1 + MEG + water systems CPA can satisfactorily predict the experimental trends and describe solubilities in both phases with reasonable accuracy as shown in Figures 7.13 and 7.14. These results are as good as for the investigated systems of condensates in the preceding sections. Using the developed correlations to estimate all binary interaction parameters (for MEG-HC and water-HC using eq. 7.2 + 7.3) with the CPA EoS, the predictions of solubility of MEG in hydrocarbon phase is greatly improved. This increase in accuracy is achieved on the behalf of lost accuracy in prediction of hydrocarbon content in the polar phase. This trend is observed at both 313.15 K and 323.15 K.

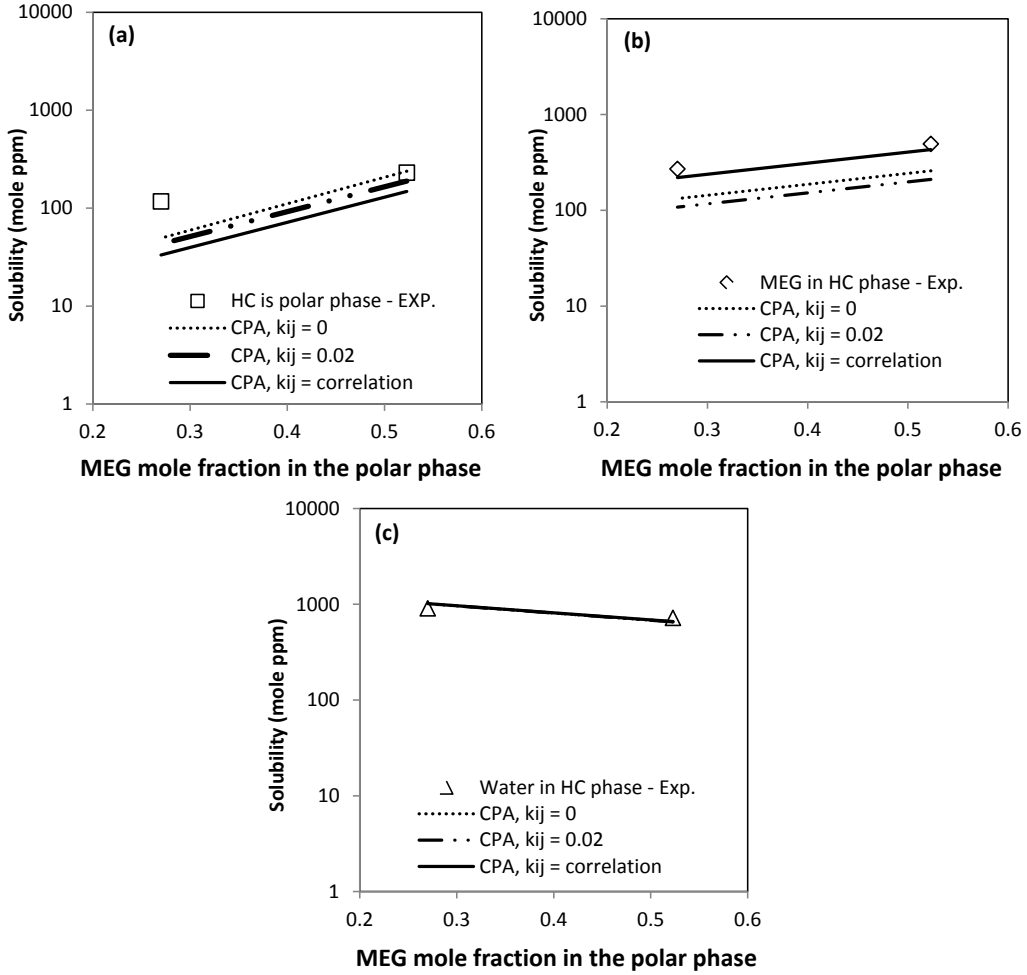

Figure 7.13: Modeling of the mutual solubility (in mole ppm, $x \cdot 10^6$) of Light Oil - 1, MEG and water at temperature 313.15 K and pressure 1 atm.: (a) Hydrocarbons in polar phase (b) MEG in organic phase (c) water in organic phase. The points are experimental data and the lines are modeling results with the CPA EoS using k_{ij} for MEG-water=-0.115 and HC-water from correlation given in Eq. 7.2. For MEG-HC there are used a $k_{ij} = 0$, $k_{ij} = 0.02$ and k_{ij} from correlation given in eq. 7.3.

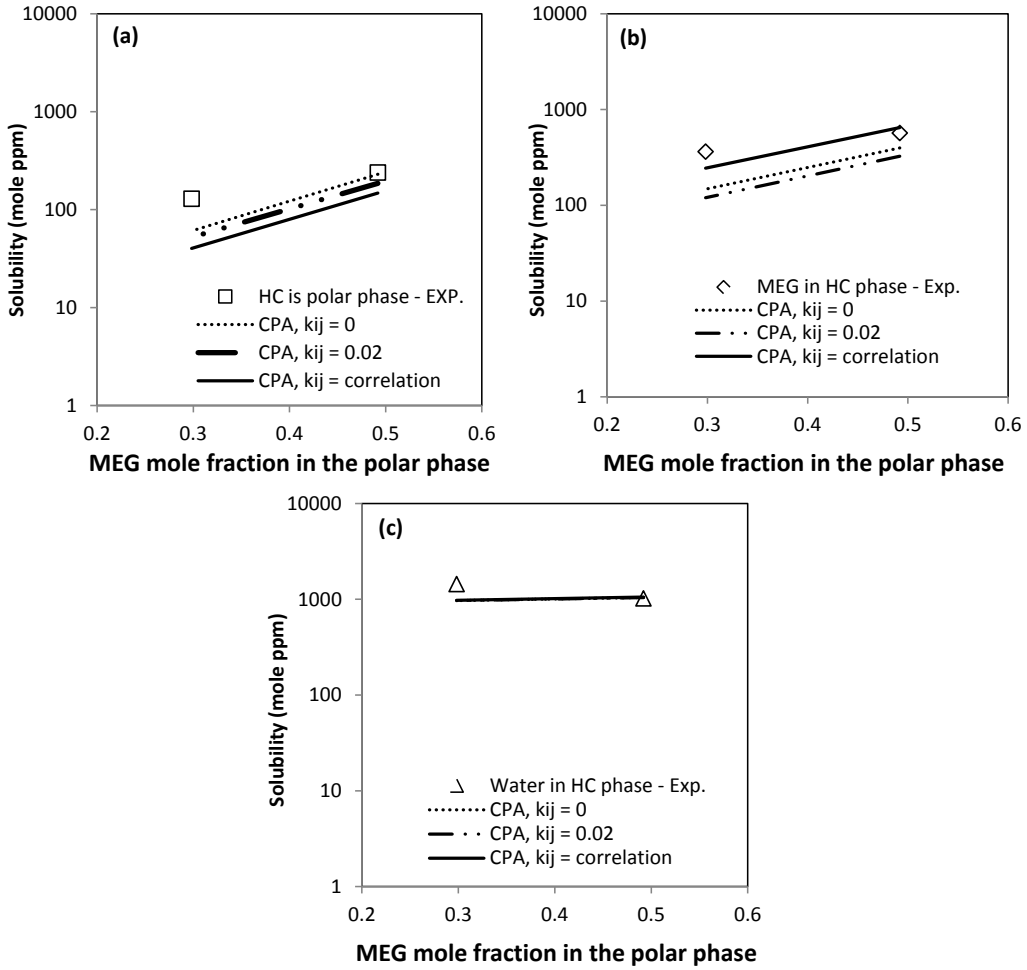

Figure 7.14: Modeling of the mutual solubility (in mole ppm, $x \cdot 10^6$) of Light Oil - 1, MEG and water at temperature 323.15 K and pressure 1 atm.: (a) Hydrocarbons in polar phase (b) MEG in organic phase (c) water in organic phase. The points are experimental data and the lines are modeling results with the CPA EoS using k_{ij} for MEG-water=-0.115 and HC-water from correlation given in Eq. 7.2. For MEG-HC there are used a $k_{ij} = 0$, $k_{ij} = 0.02$ and k_{ij} from correlation given in eq. 7.3.

7.3.5 Light Oil – 2

The composition of light oil - 2 is given in Table 7.18. The fluid is lighter than light oil - 1 and heavier than the condensates investigated in this work, as shown in Table 7.1.

Table 7.18: Condensed composition of Light Oil – 2 [18] (Mole %, Weight %, Molecular weight and Density)

Component	Mole %	Weight %	Molecular weight	Density kg/L
Ethane (P)	0.0800	0.019	30.070	0.3580
Propane(P)	1.972	0.681	44.100	0.5080
2-methylpropane (P)	1.881	0.856	58.124	0.5630
butane (P)	6.672	3.037	58.124	0.5850
2,2-DM-Propane(P)	0.0268	0.015	72.151	0.5970
2-methylbutane (P)	4.420	2.498	72.151	0.6250
pentane (P)	5.562	3.143	72.151	0.6310
Hexane total	**8.009**	**5.344**	**85.181**	**0.6680**
Hexanes – (P)	7.722	5.149	87.517	0.6687
Hexanes – N	0.288	0.195	86.178	0.6500
Heptane total	**12.682**	**9.108**	**91.698**	**0.7160**
Heptanes P	5.189	4.073	100.205	0.7506
Heptanes N	6.196	4.242	87.415	0.6897
Heptanes A	1.296	0.793	78.114	0.6936
Octane total	**13.172**	**10.778**	**104.473**	**0.7518**
Octanes P	3.628	3.288	115.720	0.7601
Octanes N	6.692	5.431	103.630	0.7416
Octanes A	2.852	2.058	92.143	0.7660
Nonane total	**8.063**	**7.553**	**119.594**	**0.7880**
Nonane P	2.829	2.722	122.792	0.7694
Nonanes N	4.307	4.004	118.681	0.7939
Nonanes A	0.926	0.827	114.068	0.8239
Decane Plus ($C10^{+}$)	**31.896**	**56.968**	**228.043**	**0.8486**
Sum	100	**100**		

7.3.5.1 Reservoir fluid characterization

The results obtained after characterization and lumping are given in Table 7.19.

Table 7.19: Characterization of Light Oil – 2

Component	Mole%	$T_{cm}(K)$	$P_{cm}(bar)$	ω_m	MW (g/mol)
Ethane	0.17	305.4	48.8	0.098	30.07
Propane	2.351	378.6	47.2	0.105	44.10
i-Butane	1.831	415.8	40.1	0.151	58.12
n-Butane	6.472	436.3	43.6	0.158	58.12
i-Pentane	4.101	460.4	33.8	0.227	72.15
n-Pentane	5.732	479.4	38.0	0.217	72.15
C_6	8.413	522.3	34.9	0.244	86.18
C_7	13.694	560.8	35.9	0.230	91.82
C_8	14.274	591.0	34.1	0.261	104.45
C_9	8.383	621.4	32.3	0.292	118.10
$C_{10} – C_{11}$	8.783	657.5	29.1	0.345	142.49
C_{12}	3.516	690.8	26.4	0.395	164.00
$C_{13} – C_{14}$	5.659	719.5	24.4	0.440	184.49
$C_{15} – C_{16}$	4.222	756.8	21.9	0.502	212.49
$C_{17} – C_{18}$	3.15	788.1	20.0	0.556	240.49
$C_{19} – C_{21}$	3.29	818.4	18.5	0.608	274.64
$C_{22} – C_{24}$	2.12	853.3	16.8	0.672	316.64
$C_{25} – C_{30}$	2.246	895.8	14.9	0.756	375.10
C_{31+}	1.594	975.3	11.9	0.919	518.27

7.3.5.2 Mutual solubility of Light Oil - 2 + MEG

Correlation and prediction of the mutual solubility of light oil – 2 and MEG are shown in Figure 7.15 in comparison to the experimental data, as a function of temperature. It can be seen that the modeling results are in good agreement with the experimental data using the correlation given in equation 7.3 for all MEG-HC binaries. Improved results are observed when using the correlation for binary interaction parameters, compared to using a single average k_{ij} between MEG-HC and pure predictions ($k_{ij} = 0$).

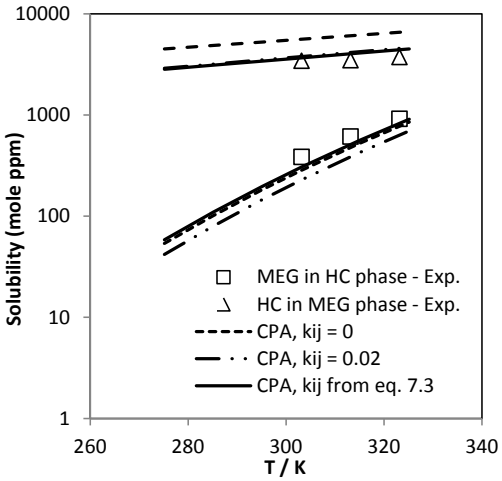

Figure 7.15: Mutual solubility (in mole ppm, $x \cdot 10^6$) of light oil – 2 and MEG as a function of temperature (K). The experimental data [18] are indicated as points and the CPA calculations as lines using a $k_{ij} = 0$, $k_{ij} = 0.02$ and k_{ij} from correlation given in eq. 7.3 for MEG-HC.

7.3.5.3 Mutual solubility of Light Oil - 2 + MEG + water

The CPA predictions for the mutual solubilities for the light oil - 2 + MEG + water systems are given in appendix B, showing that the results are correct in order of magnitude in most cases. Furthermore trends in solubilities as a function of MEG mole fraction in the polar phase are very well described as shown in Figure 7.16. Table 7.20 summarizes the deviations between experimental data and calculations made with the CPA EoS.

Table 7.20: Average Deviation (%) of CPA Predictions from Experimental Data for Investigated Light Oil – 2 + MEG + Water System at T=323.15 K and P=1 atm.

k_{ij}		%AAD			
		Polar Phase	Hydrocarbon phase		Average
Water – HC	MEG – HC	HC	MEG	Water	
From eq. 7.2	0.00	38	38	27	34
From eq. 7.2	0.02	26	40	27	31
From eq. 7.2	From eq. 7.3	28	37	27	31

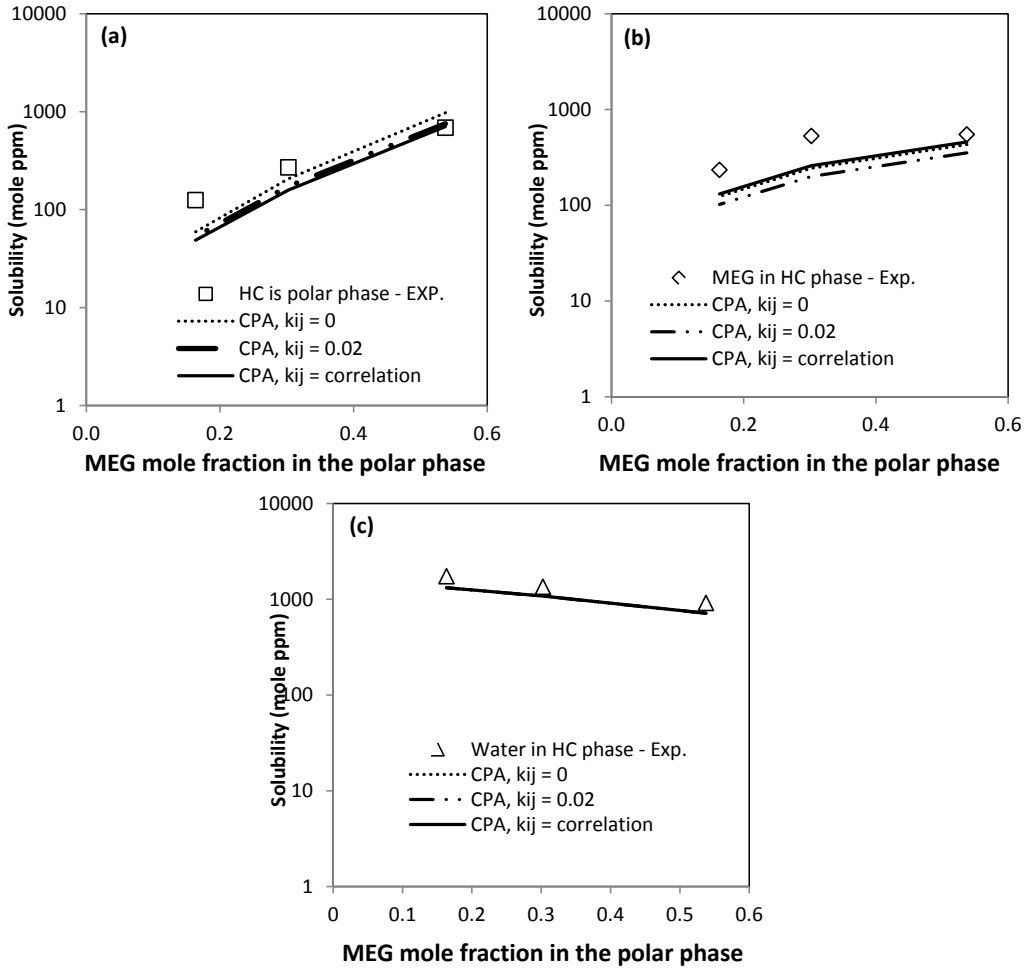

Figure 7.16: Modeling of the mutual solubility (in mole ppm, $x \cdot 10^6$) of Light Oil - 2, MEG and water at temperature 323.15 K and pressure 1 atm.: (a) Hydrocarbons in polar phase (b) MEG in organic phase (c) water in organic phase. The points are experimental data and the lines are modeling results with the CPA EoS using k_{ij} for MEG-water=-0.115 and HC-water from correlation given in Eq. 7.2. For MEG-HC there are used a $k_{ij} = 0$, $k_{ij} = 0.02$ and k_{ij} from correlation given in eq. 7.3.

7.3.6 Fluid – 1

During this work, experimental LLE was measured for two heavy oil fluids (C_{10+} fraction of 40.58 and 91.44 mole%). These are labeled Fluid – 1 and Fluid – 2. Especially Fluid – 2 is providing a serious test of the oil characterization and modeling using the CPA EoS, have above 90% unknown components and being quite napthenic/aromatic of nature. The composition of Fluid – 1 is given in Table 7.21 which shows that it has 40.58 mole % decane plus fraction.

Table 7.21: Condensed composition of Fluid – 1, this work (Mole %, Weight %, Molecular weight and Density)

Component	Weight %	Mole %	Density kg/L	Molecular Weight
C2, (P)	0.02	0.09	0.3580	30.07
C3, (P)	0.44	1.57	0.5080	44.10
i-C4, (P)	0.33	0.90	0.5630	58.12
n-C4, (P)	1.47	3.98	0.5850	58.12
2,2-DM-C3 (P)	0.01	0.02	0.5970	72.15
Ic5 (P)	1.16	2.54	0.6250	72.15
nC5 (P)	1.88	4.10	0.6310	72.15
Hexanes Total	3.68	6.82	0.6676	85.01
Hexanes - P	3.46	6.32	0.6629	86.18
Hexanes - N	0.22	0.50	0.7500	70.13
Heptanes Total	8.10	14.06	0.7418	90.79
Heptanes - P	3.15	4.96	0.6876	100.20
Heptanes - N	4.25	7.69	0.7663	87.05
Heptanes - A	0.70	1.41	0.8840	78.11
Octanes Total	10.75	16.34	0.7668	103.59
Octanes - P	3.20	4.41	0.7068	114.23
Octanes - N	5.63	8.65	0.7727	102.49
Octanes - A	1.92	3.28	0.8710	92.14
Nonanes Total	6.79	8.99	0.7733	118.86
Nonanes - P	3.43	4.22	0.7214	128.08
Nonanes - N	1.41	1.88	0.7877	117.69
Nonanes - A	1.95	2.89	0.8721	106.17
Decanes Plus	65.38	40.58	0.8528	253.8
Totals	**100.01**	**99.99**	-	-

7.3.6.1 Reservoir fluid characterization

The results obtained after characterization and lumping are given in Table 7.22.

Table 7.22: Characterization of Fluid – 1

Component	Mole%	$T_{cm}(K)$	$P_{cm}(bar)$	ω_m	MW (g/mol)
Ethane	0.009	305.4	48.8	0.098	30.07
Propane	1.572	378.6	47.2	0.105	44.10
i-Butane	0.901	415.8	40.1	0.151	58.12
n-Butane	3.984	436.3	43.6	0.158	58.12
i-Pentane	2.543	460.4	33.8	0.227	72.15
n-Pentane	4.105	479.4	38.0	0.217	72.15
C_6	6.828	522.3	34.9	0.244	86.18
C_7	14.076	562.3	36.5	0.226	90.80
C_8	16.358	593.0	34.8	0.255	103.60
C_9	9.000	619.1	31.6	0.298	118.90
$C_{10} - C_{11}$	8.155	655.3	28.4	0.352	142.61
$C_{12} - C_{14}$	9.269	707.2	24.5	0.432	176.96
$C_{15} - C_{16}$	4.658	754.3	21.4	0.511	212.61
$C_{17} - C_{18}$	3.724	785.6	19.6	0.566	240.61
$C_{19} - C_{21}$	4.233	816.0	18.1	0.619	274.96
$C_{22} - C_{25}$	3.828	855.7	16.2	0.693	323.05
$C_{26} - C_{30}$	2.904	899.4	14.4	0.781	384.88
$C_{31} - C_{37}$	2.103	944.2	12.7	0.872	465.79
C_{38+}	1.753	1023.8	9.9	1.042	641.23

7.3.6.2 Mutual solubility of Fluid - 1 + MEG

The CPA correlations for the mutual solubility of Fluid – 1 and MEG along with the experimental data are shown in Figure 7.17. Modeling has been done for the mutual solubility of Fluid – 1 and MEG using $k_{ij} = 0$, $k_{ij} = 0.02$ and k_{ij} obtained from the developed correlations given in equation 7.2.

The modeling results show that the solubility of MEG in hydrocarbon phase is under-predicted and the solubility of hydrocarbons in MEG is over-predicted using a $k_{ij} = 0$. The calculated mutual solubility is improved using the developed correlation for estimating the k_{ij}'s, providing accurate predictions of both MEG content in hydrocarbon phase and hydrocarbon content in the polar phase over the entire temperature range.

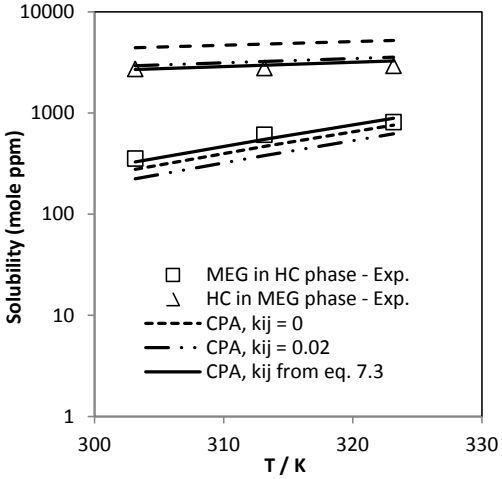

Figure 7.17: Mutual solubility (in mole ppm, $x \cdot 10^6$) of Fluid – 1 and MEG as a function of temperature (K). The experimental data [this work] are indicated as points and the CPA calculations as lines using a $k_{ij} = 0$, $k_{ij} = 0.02$ and k_{ij} from correlation given in eq. 7.3 for MEG-HC.

7.3.6.3 Mutual solubility of Fluid - 1 + MEG + water

In the system of Fluid – 1 + MEG + water, the Elliott combining rule is used for MEG and water with a $k_{ij} = -0.115$ [22]. The modeling results are performed using an average binary interaction parameter $k_{ij} = 0$, $k_{ij} = 0.02$ and k_{ij} from developed correlations for all MEG-HC pairs (eq. 7.3). All k_{ij}'s for water-HC are estimated using the correlation given in equation 7.2.

Similar to the previous systems, the modeling results are correct in order of magnitude, where clear improvements in the predictions of MEG solubility in hydrocarbon phase is obtained using the developed correlations for k_{ij} between all MEG-HC pairs. All detailed modeling results are presented in appendix B. The deviations between experimental data and calculations are summarized in Table 7.23.

The experimental trends are well captured using the CPA EoS at all temperatures (303.15 K, 313.15 K and 323.15 K) as shown in Figures 7.18 – 7.20, even for this complex mixture containing associating and non-associating components.

It can be seen, that using the new developed correlation (eq. 7.3) for estimating all binary interaction parameters between MEG-HC, greatly increases the accuracy in predictions of MEG

content in the hydrocarbon phase. This is achieved at the cost of some accuracy of predicted hydrocarbon content in the polar phase. The hydrocarbon content in the polar phase is, however, expected to be under-predicted, as we do not account of the aromaticity of the mixture. In order to enhance the predictions, effort should be done to account for the cross-association volume and energy for MEG and aromatic hydrocarbons (i.e. benzene, toluene and xylene) present in the oil.

Table 7.23: Average Deviation (%) of CPA Predictions from Experimental Data for Investigated Fluid – 1 + MEG + Water System at T=303.15 K, T=313.15 K, T=323.15 K and P=1 atm.

k_{ij}		%AAD			
		Polar Phase	Hydrocarbon phase		Average
Water – HC	MEG – HC	HC	MEG	Water	
From eq. 7.2	0.00	38	25	11	25
From eq. 7.2	0.02	46	39	11	32
From eq. 7.2	From eq. 7.3	50	15	12	26

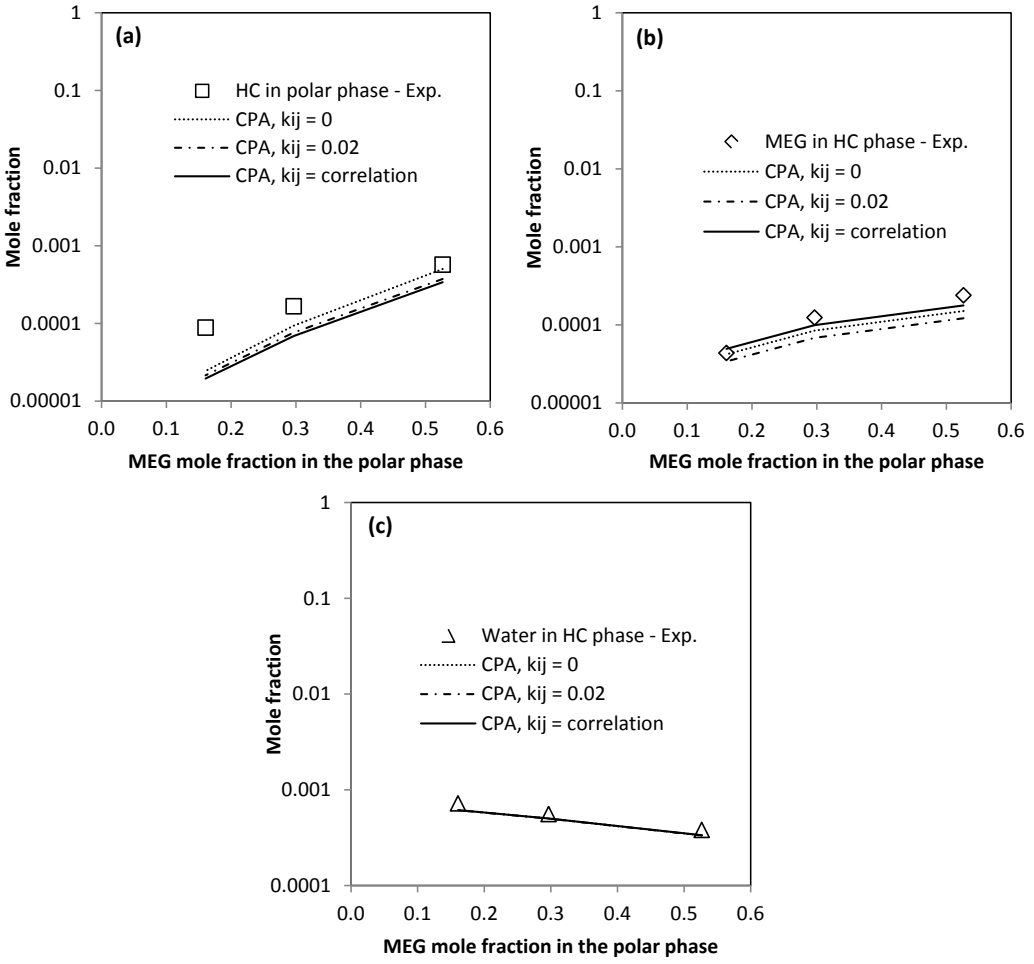

Figure 7.18: Modeling of the mutual solubility (in mole fraction, x) of Fluid – 1, MEG and water at temperature 303.15 K and pressure 1 atm.: (a) Hydrocarbons in polar phase (b) MEG in organic phase (c) water in organic phase. The points are experimental data and the lines are modeling results with the CPA EoS using k_{ij} for MEG-water=-0.115 and HC-water from correlation given in Eq. 7.2. For MEG-HC there are used a $k_{ij} = 0$, $k_{ij} = 0.02$ and k_{ij} from correlation given in eq. 7.3.

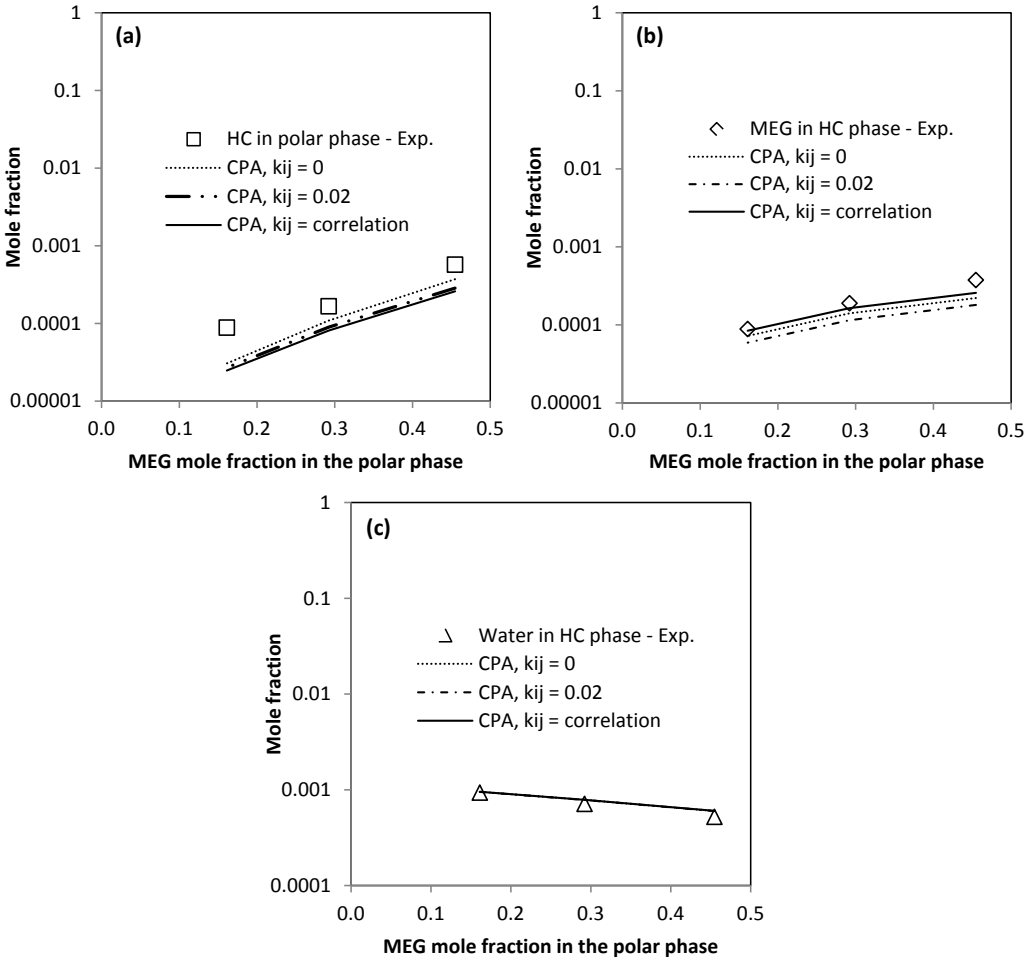

Figure 7.19: Modeling of the mutual solubility (in mole fraction, x) of Fluid – 1, MEG and water at temperature 313.15 K and pressure 1 atm.: (a) Hydrocarbons in polar phase (b) MEG in organic phase (c) water in organic phase. The points are experimental data and the lines are modeling results with the CPA EoS using k_{ij} for MEG-water=-0.115 and HC-water from correlation given in Eq. 7.2. For MEG-HC there are used a k_{ij} = 0, k_{ij} = 0.02 and k_{ij} from correlation given in eq. 7.3.

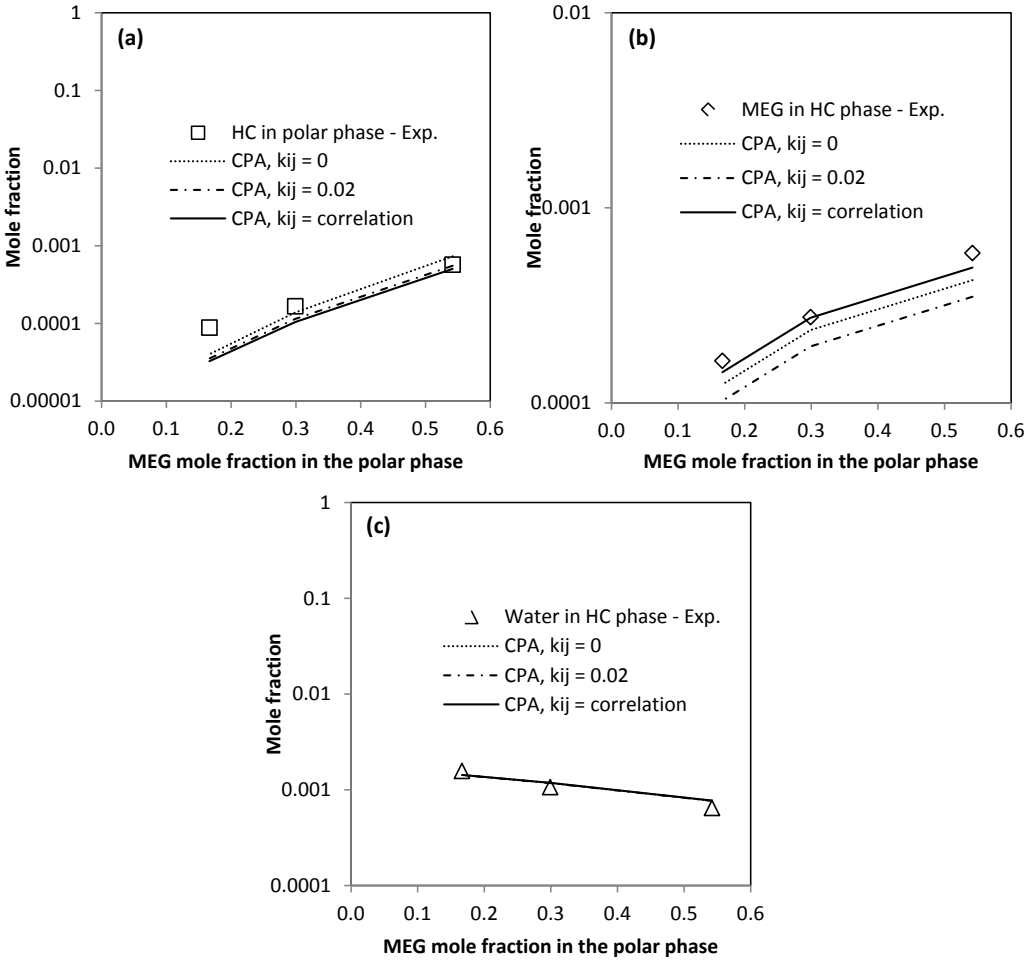

Figure 7.20: Modeling of the mutual solubility (in mole fraction, x) of Fluid – 1, MEG and water at temperature 323.15 K and pressure 1 atm.: (a) Hydrocarbons in polar phase (b) MEG in organic phase (c) water in organic phase. The points are experimental data and the lines are modeling results with the CPA EoS using k_{ij} for MEG-water=-0.115 and HC-water from correlation given in Eq. 7.2. For MEG-HC there are used a k_{ij} = 0, k_{ij} = 0.02 and k_{ij} from correlation given in eq. 7.3.

7.3.7 Fluid – 2

Fluid – 2 is providing a serious test of the oil characterization and modeling using the CPA EoS, as it has above 90% of unknown components and being napthenic/aromatic of nature. The composition of Fluid – 2 is given in Table 7.24 which shows that it has 91.44 mole % decane plus fraction.

Table 7.24: Condensed composition of Fluid – 2, this work (Mole %, Weight %, Molecular weight and Density)

Component	Weight %	Mole %	Density kg/L	Molecular Weight
C2, (P)	0.00	0.00	0.3580	30.07
C3, (P)	0.00	0.00	0.5080	44.10
i-C4, (P)	0.00	0.01	0.5630	58.12
n-C4, (P)	0.00	0.01	0.5850	58.12
2,2-DM-C3 (P)	0.00	0.00	0.5970	72.15
Ic5 (P)	0.02	0.07	0.6250	72.15
nC5 (P)	0.01	0.03	0.6310	72.15
Hexanes Total	0.10	0.33	0.6704	84.29
Hexanes - P	0.09	0.29	0.6627	86.18
Hexanes - N	0.01	0.04	0.7500	70.13
Heptanes Total	0.50	1.55	0.7485	91.16
Heptanes - P	0.09	0.25	0.6878	100.20
Heptanes - N	0.40	1.27	0.7604	89.73
Heptanes - A	0.01	0.03	0.8840	78.11
Octanes Total	1.26	3.43	0.7698	103.80
Octanes - P	0.30	0.75	0.7088	114.23
Octanes - N	0.75	2.05	0.7720	103.58
Octanes - A	0.21	0.63	0.8710	92.14
Nonanes Total	1.35	3.13	0.7582	122.56
Nonanes - P	0.83	1.85	0.7211	128.07
Nonanes - N	0.26	0.59	0.7850	124.49
Nonanes - A	0.26	0.69	0.8731	106.17
Decanes Plus	96.77	91.44	0.9477	358.0
Totals	**100.01**	**100.00**	-	-

7.3.7.1 Reservoir fluid characterization

The results obtained after characterization and lumping are given in Table 7.25. It can be seen from the characterization, that it goes to much higher carbon fractions (C_{60+}) than previously observed.

Table 7.25: Characterization of Fluid – 2

Component	Mole%	$T_{cm}(K)$	$P_{cm}(bar)$	ω_m	MW (g/mol)
i-Butane	0.01	415.8	40.1	0.151	58.12
n-Butane	0.01	436.3	43.6	0.158	58.12
i-Pentane	0.07	460.4	33.8	0.227	72.15
n-Pentane	0.03	479.4	38.0	0.217	72.15
C_6	0.33	522.3	34.9	0.244	86.18
C_7	1.55	564.1	37.2	0.221	91.20
C_8	3.43	593.9	35.1	0.253	103.80
C_9	3.13	614.6	30.2	0.311	122.60
$C_{10} – C_{14}$	22.974	689.1	26.2	0.399	162.42
$C_{15} – C_{19}$	17.305	786.2	21.7	0.519	232.42
$C_{20} – C_{23}$	10.715	849.2	19.4	0.597	296.01
$C_{24} – C_{28}$	10.391	900.6	17.6	0.673	358.42
$C_{29} – C_{34}$	9.144	946.6	15.9	0.786	434.69
$C_{35} – C_{40}$	6.508	996.0	14.4	0.805	518.69
$C_{41} – C_{48}$	5.858	1040.8	13.0	0.848	614.85
$C_{49} – C_{59}$	4.737	1093.4	11.2	0.900	744.12
C_{60+}	3.809	1170.7	8.3	0.942	947.57

7.3.7.2 Mutual solubility of Fluid - 2 + MEG

The CPA correlations for the mutual solubility of Fluid – 2 and MEG along with the experimental data are shown in Figure 7.21 Modeling has been done for the mutual solubility of Fluid – 2 and MEG using $k_{ij} = 0$, $k_{ij} = 0.02$ and k_{ij} obtained from the developed correlations given in equation 7.2.

The solubility of MEG in hydrocarbon phase is captured accurately using the correlation given in equation 7.3 for all MEG-HC k_{ij}. The solubility of hydrocarbons in MEG phase is under-predicted for all methods of using k_{ij}, and is very difficult to describe for Fluid – 2, as it is contains high amount of unknown components.

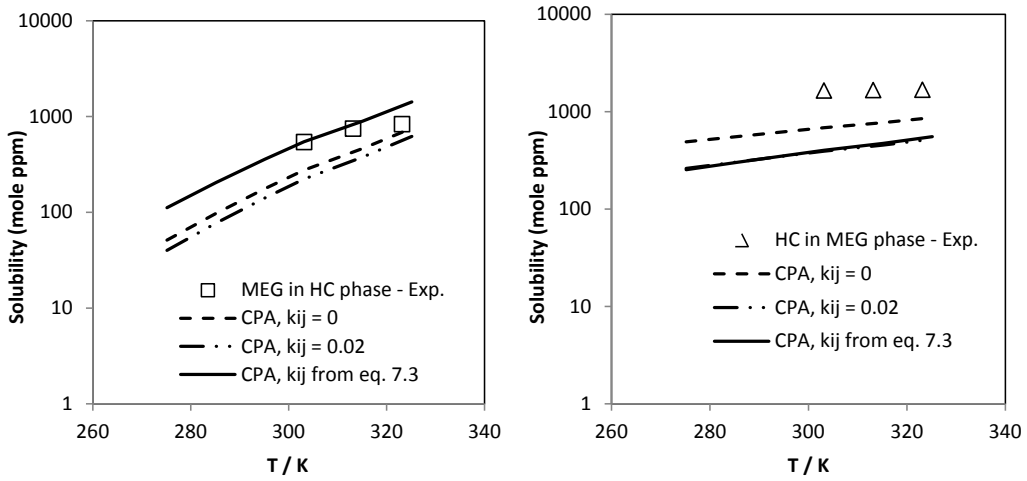

Figure 7.21: Mutual solubility (in mole ppm, $x \cdot 10^6$) of Fluid – 2 and MEG as a function of temperature (K). The experimental data [this work] are indicated as points and the CPA calculations as lines using a $k_{ij} = 0$, $k_{ij} = 0.02$ and k_{ij} from correlation given in eq. 7.3 for MEG-HC.

7.3.7.3 Mutual solubility of Fluid - 2 + MEG + water

In the system of Fluid – 2 + MEG + water, the Elliott combining rule is used for MEG and water with a $k_{ij} = -0.115$ [22]. The modeling results are performed using an average binary interaction parameter $k_{ij} = 0$, $k_{ij} = 0.02$ and k_{ij} from developed correlations for all MEG-HC pairs. All k_{ij}'s for water-HC are estimated using the correlation given in equation 7.3.

The modeling results are correct in order of magnitude for MEG and water in the hydrocarbon phase. The solubility of hydrocarbons in the polar phase is greatly under-predicted, most likely as a result of the oil containing a high amount of unknown components and having a high amount of aromatic and naphthenic hydrocarbons. Similar to previous results, clear improvements in the predictions of MEG solubility in hydrocarbon phase is obtained using the developed correlations for k_{ij} between all MEG-HC pairs. In order to enhance the predictions, effort should be done to account for the cross-association volume and energy for MEG and aromatic hydrocarbons (i.e. benzene, toluene and xylene) present in the oil.

Experimental data and predictions made with the CPA EoS are shown in Figures 7.22 – 7.24. Here the experimental trends are captured well at all temepratures (303.15 K, 313. 15 K and 323.15 K).

All detailed modeling results are presented in appendix B. The deviations between experimental data and calculations are summarized in Table 7.26.

Table 7.26: Average Deviation (%) of CPA Predictions from Experimental Data for Investigated Fluid – 2 + MEG + Water System at T=303.15 K, T=313.15 K, T=323.15 K and P=1 atm.

k_{ij}		%AAD			
		Polar Phase	Hydrocarbon phase		Average
Water – HC	MEG – HC	HC	MEG	Water	
From eq. 7.2	0.00	93	41	19	51
From eq. 7.2	0.02	95	52	19	55
From eq. 7.2	From eq. 7.3	96	25	18	46

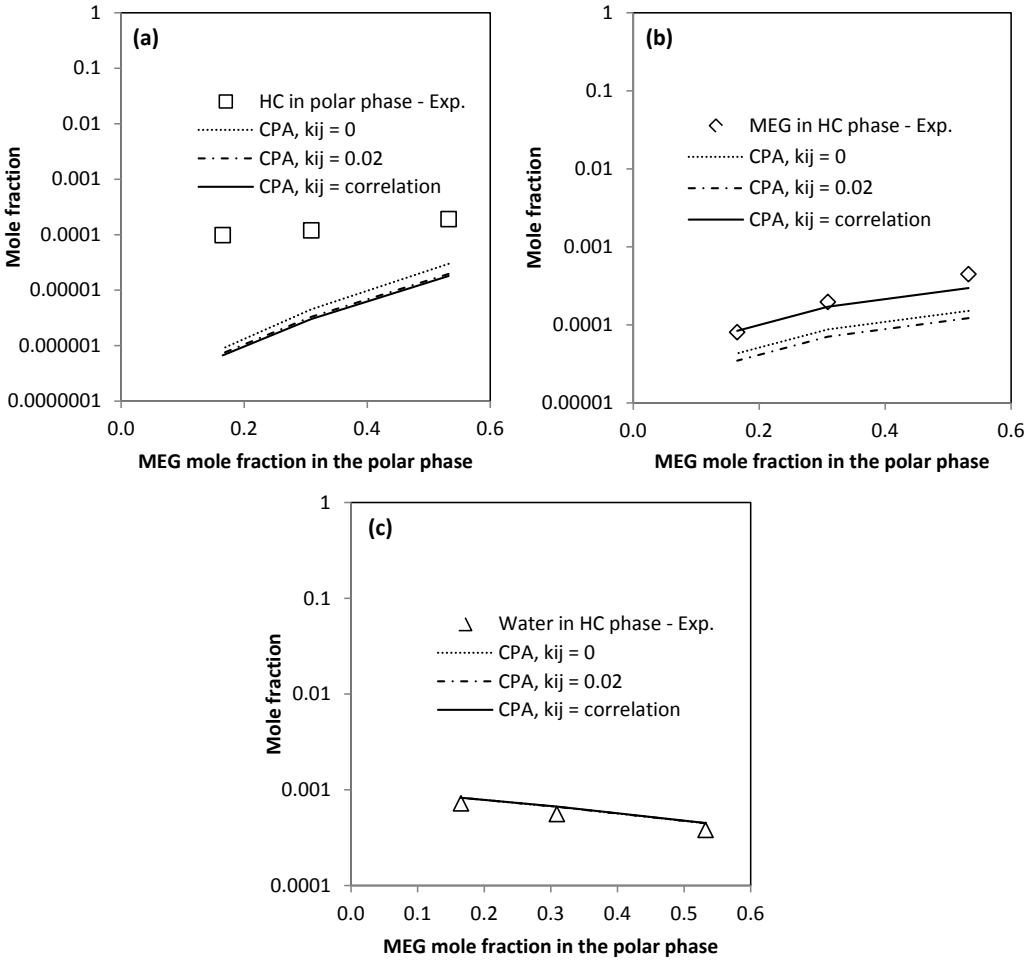

Figure 7.22: Modeling of the mutual solubility (in mole fraction, x) of Fluid – 2, MEG and water at temperature 303.15 K and pressure 1 atm.: (a) Hydrocarbons in polar phase (b) MEG in organic phase (c) water in organic phase. The points are experimental data and the lines are modeling results with the CPA EoS using k_{ij} for MEG-water=-0.115 and HC-water from correlation given in Eq. 7.2. For MEG-HC there are used a $k_{ij} = 0$, $k_{ij} = 0.02$ and k_{ij} from correlation given in eq. 7.3.

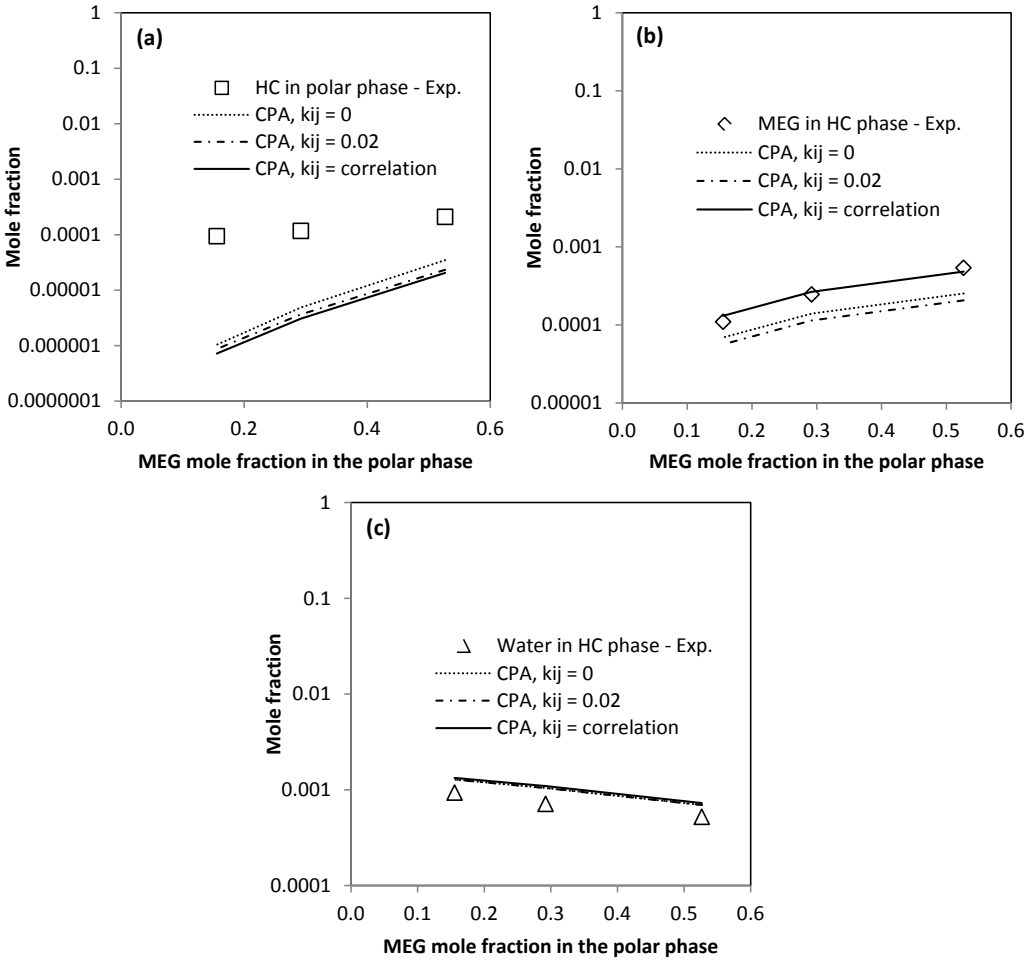

Figure 7.23: Modeling of the mutual solubility (in mole fraction, x) of Fluid – 2, MEG and water at temperature 303.15 K and pressure 1 atm.: (a) Hydrocarbons in polar phase (b) MEG in organic phase (c) water in organic phase. The points are experimental data and the lines are modeling results with the CPA EoS using k_{ij} for MEG-water=-0.115 and HC-water from correlation given in Eq. 7.2. For MEG-HC there are used a k_{ij} = 0, k_{ij} = 0.02 and k_{ij} from correlation given in eq. 7.3.

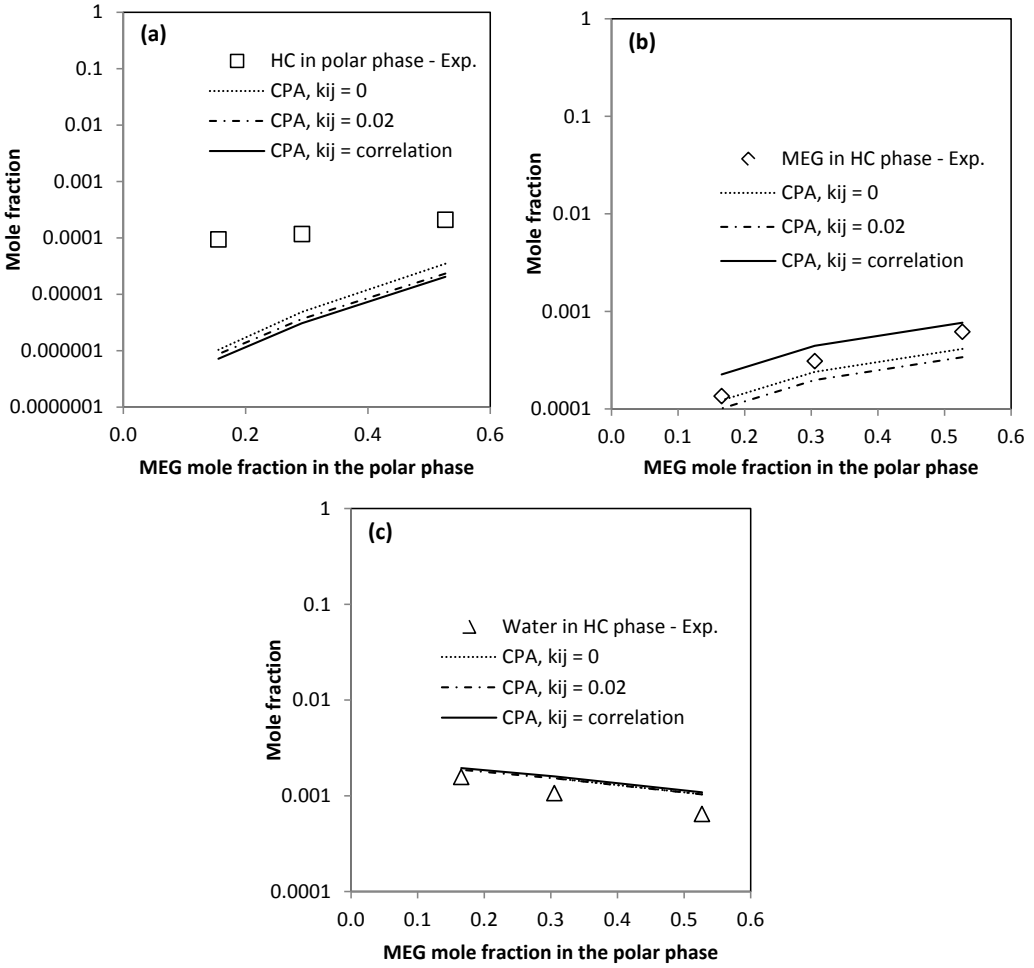

Figure 7.24: Modeling of the mutual solubility (in mole fraction, x) of Fluid – 2, MEG and water at temperature 323.15 K and pressure 1 atm.: (a) Hydrocarbons in polar phase (b) MEG in organic phase (c) water in organic phase. The points are experimental data and the lines are modeling results with the CPA EoS using k_{ij} for MEG-water=-0.115 and HC-water from correlation given in Eq. 7.2. For MEG-HC there are used a k_{ij} = 0, k_{ij} = 0.02 and k_{ij} from correlation given in eq. 7.3.

7.3.8 Comparison of results

All the experimental data available for oil systems with MEG/water have been modelled in this work with the CPA EoS, using three different approaches (using $k_{ij} = 0$, $k_{ij} = 0.02$ and k_{ij} from developed correlations for all MEG-HC pairs). All experimental data, along with the calculated vales from the CPA EoS can be seen in Appendix B. Binary interaction parameters between Water-HC are estimated using the correlation presented in this work (Equation 7.2).

The results presented in this section are the average deviations after modelling all the experimental data for all temperatures and pressures. Table 7.27 presents the results obtained for the hydrocarbon systems + MEG/water, using a $k_{ij} = 0$ for all MEG-HC pairs.

Table 7.27: %AAD for oil systems + MEG/water using a $k_{ij} = 0$ for all MEG-HC pairs

System (HC) + MEG/water	HC in polar phase %AAD	MEG in HC phase %AAD	Water in HC phase %AAD
Condensate-1	34	73	21
Condensate-2	56	38	28
Condensate-3	11	48	17
Light Oil – 1	30	47	14
Light Oil – 2	38	38	27
Fluid – 1	38	25	11
Fluid – 2	93	41	19
Average	43	44	20

Table 7.28 presents the results obtained for the hydrocarbon systems + MEG/water, using a single temperature independent k_{ij} = 0.02 for all MEG-HC pairs.

Table 7.28: Average deviations for all oil systems with MEG and water, using a single temperature independent k_{ij} = 0.02 for all MEG-HC pairs

System (HC) + MEG/water	HC in polar phase %AAD	MEG in HC phase %AAD	Water in HC phase %AAD
Condensate-1	21	47	21
Condensate-2	67	14	28
Condensate-3	18	21	17
Light Oil – 1	41	57	14
Light Oil – 2	26	40	27
Fluid – 1	46	39	11
Fluid – 2	95	52	19
Average	45	39	20

Table 7.29 presents the results obtained for the hydrocarbon systems + MEG/water, using the correlations given in equation 7.3 for k_{ij} between all MEG-HC pairs. Table 7.30 presents average deviations for well-defined hydrocarbons with MEG and water.

Table 7.29: Average deviations for all oil systems with MEG and water, using correlations given in equation 7.3 for k_{ij} between all MEG-HC pairs

System (HC) + MEG/water	HC in polar phase %AAD	MEG in HC phase %AAD	Water in HC phase %AAD
Condensate-1	23	55	21
Condensate-2	66	21	28
Condensate-3	23	18	17
Light Oil – 1	54	19	14
Light Oil – 2	28	37	27
Fluid – 1	50	15	12
Fluid – 2	96	25	18
Average	49	27	20

Table 7.30: Average deviations for well-defined hydrocarbons with MEG and water

System (HC) + MEG/water	HC in polar phase %AAD	MEG in HC phase %AAD	Water in HC phase %AAD
n-hexane	44	42	44
Benzene	71	14	4
2,2,4 trimethylC5	82	83	43
n-nonane	35	50	9
Ethylbenzene	33	35	20
C1/C3/C7 or toluene	50	26	31
C3/toluene	16	8	12
Average	47	37	23

In table 7.31 we show the average of all the deviations, using different approaches for the binary interaction parameters, and compare it against the results for well-defined systems.

Table 7.31: Average deviations with the CPA EoS, using different approaches for binary interaction parameter between all MEG-HC pair.

k_{ij} between MEG-HC	HC in polar phase	MEG in HC phase	Water in HC phase
	%AAD	%AAD	%AAD
k_{ij} = 0.00	43	44	20
k_{ij} = 0.02	45	39	20
k_{ij} from correlation (eq. 7.3)	49	27	20
Well-defined systems	47	37	23

Overall the predictive performance of the model is satisfactory. CPA can satisfactorily describe the temperature dependency of mutual solubility for condensates/oils + MEG systems. In the condensates/oil + MEG + water systems CPA can describe both the temperature and composition dependency of solubility and these trends are consistent for all the systems investigated in this work. Finally the results with condensates and oil related systems are as good as for well-defined hydrocarbon systems.

Using the CPA EoS with the current oil characterization method are struggling with predicting the hydrocarbon content in the polar phase for the more heavy oils. Using a correlation for the binary interaction parameters between MEG-HC, provides very good prediction for both phases, and is seen to give overall better results, than using an average k_{ij} (k_{ij} = 0 or k_{ij} = 0.02). Especially predictions of water and glycol content in the organic phase are improved. This is seen in high degree for the heavy oils, such as Light oil – 1 and the new Fluid 1 + 2.

Having correlations for binary interaction parameters between water-HC and MEG-HC as a function of molecular weight works very well with oil characterization and modeling of oil systems, since molecular weight is a direct output of the characterization, and it is therefore possible to directly estimate/predict all k_{ij}'s needed, making the modeling procedure much more predictive.

The major issue with predictions is capturing the heavy hydrocarbon solubility in the polar phase, which has a significant impact on the mutual solubility. The polar chemicals have an increased solubility in the organic phase, when more heavy hydrocarbons and aromatic components are present.

Further improvements might be gained by tuning the correlations; however, experimental data are hard to come by. Further work on the MEG-HC correlations should be done, by investigating few systems of MEG and C_{10+} hydrocarbons, in order to verify/optimize the correlations.

7.4 Conclusions

In this work the cubic plus association (CPA) equation of state (EoS) has been applied to the modeling of the mutual solubility of reservoir fluids, monoethylene-glycol (MEG) and water. The reservoir fluid consists of seven different hydrocarbons fluids from different offshore fields in the North Sea. For characterization of the reservoir fluids, the correlations of Yan et al. [5] are applied.

New correlations for estimating binary interaction parameters between MEG-water and MEG-HC have been proposed. The CPA EoS is applied to the liquid-liquid equilibrium of reservoir-fluid + MEG and reservoir-fluid + MEG + water systems in a temperature range 275-326 K and atmospheric pressure. For reservoir-fluid + MEG systems excellent correlations are obtained for the mutual solubility of reservoir fluid and MEG as a function of temperature, using correlation for estimating all k_{ij} between MEG and hydrocarbons. In the case of light oil - 1 satisfactory correlation is obtained for the solubility of hydrocarbons in MEG phase, but the solubility of MEG in hydrocarbons is underestimated. This is partially due to uncertainty in the data and naphthenic nature of the oil. More investigations are required for the data and the modeling of light oil - 1.

For the reservoir-fluid + MEG + water systems satisfactory predictions are obtained using correlation for estimating all k_{ij} between MEG and hydrocarbons and water-HC k_{ij} from the developed correlation presented. CPA can satisfactorily describe the trends in solubilities of reservoir fluids, MEG and water as a function of MEG mole fraction in the polar phase and as a function of temperature. The results are generally correct in order of magnitude. Interestingly the modeling results for light oil - 1 + MEG + water systems are equally good in contrast to light oil - 1 + MEG system where the solubility of MEG in light oil - 1 was under estimated.

It was generally found, that using the new developed correlation (eq. 7.3) for estimating all binary interaction parameters between MEG-HC, greatly increases the accuracy in predictions of MEG content in the hydrocarbon phase. This is achieved at the cost of some accuracy of predicted hydrocarbon content in the polar phase. The hydrocarbon content in the polar phase is, however, expected to be under-predicted, as we do not explicitly account of the aromaticity of the mixture. In order to enhance the predictions, effort should be done to account for the cross-association volume and energy for MEG and aromatic hydrocarbons (i.e. benzene, toluene and xylene) present in the oil.

Finally a comparison of CPA calculations is made between reservoir fluid and well-defined hydrocarbons in presence of polar chemicals such as water and MEG. It has been seen that modeling results for reservoir fluid systems are as good as for well-defined hydrocarbon systems. In some cases the modeling results for the systems with reservoir fluid are better than those of the systems with well-defined hydrocarbons.

The deviations from experimental data are attributed to the complexity of the systems with associating and non-associating components and the challenges involved in the measurements and the modeling of very low solubilities on the order of part per million level. In case of reservoir fluid, systems are even more complex as we have numerous well-defined components (about 90 components in C_2-C_9 carbon fractions) and hundreds of ill-defined components in decane plus fraction. The components are paraffinic, naphthenic and aromatic in nature and of a wide range of molar mass and density.

References

[1] Fink, J. *Oil Field Chemicals*. 1st ed. Gulf Professional Publishing, **2003**.

[2] Aas, N. Knudsen, B. Sæten, J. O. Nordstad, E. In *Proceedings of SPE International Conference on Health, Safety and Environment in Oil and Gas Exploration and Production*, **2002**.

[3] Oliveira, M. B. Coutinho, J. A. P. Queimada, A. J. *Fluid Phase Equilibria* 258 **(2007)** 58-66.

[4] Pedersen, K. S. Michelsen, M. L. Fredheim, A. O. *Fluid Phase Equilibria* 126 **(1996)** 13-28.

[5] Yan, W. Kontogeorgis, G. M. Stenby, E. H. *Fluid Phase Equilibria* 276 (**2009)** 75-85.

[6] Kontogeorgis, G. M. Voutsas, E. C. Yakoumis, I. V. Tassios, D. P. *Industrial & Engineering Chemistry Research* 35 (**1996)** 4310-4318.

[7] Wei, Y. S. Sadus, R. J. *AIChE Journal* 46 (**2000)** 169-196.

[8] Kontogeorgis, G. M. Folas, G. K. *Thermodynamic Models for Industrial Applications: From Classical and Advanced Mixing Rules to Association Theories*, 1st ed. Wiley, **2010**.

[9] Kontogeorgis, G. M. Michelsen, M. L. Folas, G. K. Derawi, S. von Solms, N. Stenby, E. H. *Industrial & Engineering Chemistry Research* 45 (**2006)** 4855-4868.

[10] Kontogeorgis, G. M. Michelsen, M. L. Folas, G. K. Derawi, S. von Solms, N. Stenby, E. H. *Industrial & Engineering Chemistry Research* 45 (**2006)** 4869-4878.

[11] Pedersen, K. S. Thomassen, P. Fredenslund, A. *Advances in Thermodynamics, C_{7+} Fraction Characterization*, Taylor & Francis: New York, **1989**, Vol. 1.

[12] Riaz, M.. PhD Thesis, Technical University of Denmark, **2010**

[13] Frost, M. *Measurement and modelling of phase equilibrium in Oil-MEG-Water mixtures. MSc Thesis,* DTU: 2800 Kgs Lyngby, Denmark, **2010**.

[14] Yussuf, M. *Measurement of Phase Equilibria for Oil-Water-MEG Mixtures. MSc Thesis*, DTU: 2800 Kgs Lyngby, Denmark, **2011**.

[15] Riaz, M. Kontogeorgis, G. M. Stenby, E. H. Yan, W. Haugum, T. Christensen, K. O. Solbraa, E. Løkken, T. V. *Fluid Phase Equilibria* 300 (**2011)** 172-181.

[16] Riaz, M. Kontogeorgis, G. M. Stenby, E. H. Yan, W. Haugum, T. Christensen, K. O. Løkken, T. V. Solbraa, E. *Journal of Chemical & Engineering Data***,** 56 **(2011)** 4342-4351.

[17] M. Riaz, M. A. Yussuf, M. Frost, G.M. Kontogeorgis, E.H. Stenby, W. Yan, E. Solbraa, *Energy and Fuels*, 28 (**2014**), 5, p. 3530-3538

[18] M. Frost, G.M. Kontogeorgis, E.H. Stenby, M.A. Yussuf, T. Haugum, K.O. Christensen, E. Solbraa, T.V. Løkken*, Fluid phase Equilibria*, (**2013**) 1-6

[19] A. Chapoy, S. Mokraoui, A.Valtz, D. Richon, A.H. Mohammadi, B. Tohidi, *Fluid Phase Equilib.* 226 (**2004**) 213–220.

[20] W.R. Parrish, A.G. Pollin, T.W. Schidt, *Proceedings of the 61st Gas Process, Assoc. Annual Convention*, **1982**, pp. 164–170.

[21] A. Dhima, J.C. de Hemptinne, G. Moracchini, *Fluid Phase Equilib.* 145 (**1998**) 129–150.

[22] J.J. Carroll, F.Y. Jou, A.E. Mather, *Fluid Phase Equilib.* 140 (**1997**) 157–169.

[23] A.H. Mohammadi, A. Chapoy, B. Tohidi, D. Richon, *Ind. Eng. Chem. Res.* 43 (**2004**) 5418–5424.

[24] H.H. Reamer, B.H. Sage,W.N. Lacey, *Ind. Eng. Chem.* 44 (**1952**) 609–615.

[25] Gillespie, P.C.; Wilson, G.M., *Gas Processors Association Research Report RR-48*; Gas Processors Association: Tulsa, OK **1982**.

[26] Tsonopoulos, C.; Wilson, G. M., *AIChE Journal* 29 (**1983)** 990.

[27] Heidman, J.L.; Tsonopoulos, C.; Brady, C.J.; Wilson, G.M., *AIChE Journal* 31 **(1985)** 376.

[28] Economou, I.G.; Heidman, J.D.; Tsonopoulos, C, Wilson GM., *AIChE Journal* 43 (**1997)** 535.

[29] P. Schatzberg, *J. Phys. Chem.* 67 *(***1963***)***,** 776-779

[30] A. L. Ferguson, P. G. Debenedetti, and A. Z. Panagiotopoulos*, J. Phys. Chem. B* 113 (**2009)** 6405–6414

[31] C. Tsonopoulos*, Fluid Phase Equilibria,* 156 (**1999**) 21–33

[32] Folas, G. K. Berg, O. J. Solbraa, E. Fredheim, A. O. Kontogeorgis, G. M. Michelsen, M. L. Stenby, E. H. *Fluid Phase Equilibria* 251 **(2007)** 52-58.

[33] Derawi, S. O. Michelsen, M. L. Kontogeorgis, G. M. Stenby, E. H. *Fluid Phase Equilibria* 209 (**2003)** 163-184.

[34] Derawi, S. O. Kontogeorgis, G. M. Michelsen, M. L. Stenby, E. H. *Industrial & Engineering Chemistry Research* 42 (**2003)** 1470-1477.

Chapter 8 – Conclusions and future work

8.1 Conclusions

As it is expensive to measure phase equilibrium for oil systems with all production chemicals used by oil industry, it is of interest to investigate alternative approaches to predict them using an equation of state. On the basis of the amount of chemicals used, MEG and methanol are among the most important chemicals and it was decided that the study should focus on these two gas-hydrate inhibitors.

The main purpose of this project is to produce new experimental data, for phase equilibrium of both oil systems and well-defined systems with water and gas hydrate inhibitors (MEG/methanol). Experimental work is naturally time consuming, as it involves many elements and stages, which are out of your control. Especially, as in this work, when design and construction of new and innovative equipment are involved. Although the new experimental equipment was built in the workshop of the department, it took over one year to have the main body of the cell finished, and an additional period of six more months to get it equipped with all the necessary connections.

One of the main purposes of this work was achieved, with the successful development of two new high-quality experimental set-ups of a considerable complexity, capable of producing reliable results, characterized by a superior precision and accuracy. Both experimental set-ups presented in this work, should be regarded as an important and solid contribution to the future, constituting a basis that will simplify the implementation of future research projects with an experimental component. An effort to fully describe the developed equipment, including the optimization of existing equipment, was done in this dissertation, in an attempt to illustrate the type of problems that often occur in experimental work, but that very seldom get published.
Designing and constructing a completely new type of experimental equipment, allowed a high degree of customization, making it more accurate for the immediate needs. The quality of the experimental equipment was confirmed by the extensive testing performed to all the systems involved, from the temperature and pressure measurements to the analytical aspects. These tests revealed the high precision and accuracy of the results which can be achieved with the equipment.

New VLLE experimental results was presented for the system of methane + n-hexane + water + methanol at T = 298.6 K and pressures of 9.2 MPa and 6.8 MPa. This contributes to the high quality of the constructed equipment, which has proven to be able to produce highly accurate results, within a reasonable timeframe.

New experimental data have been presented, using both an existing VLE cell described in chapter 2 and a completely new VLLE cell developed and constructed in this work (Chapter 3). The experimental data covers phase equilibrium (VLE and VLLE) of hydrocarbons with polar chemicals, such as water and MEG/methanol.

For thermodynamic modeling using the CPA EoS, methanol is described as two-site (2B) molecule whereas the four-site (4C) scheme is used for both MEG and water throughout in this work in accordance to previous studies [1,2]. In the process of extending the CPA EoS to reservoir fluids in presence of polar chemicals, it is of interest to investigate the phase equilibrium of systems of well-defined hydrocarbons and polar chemicals. CPA has therefore been applied to VLE, LLE and VLLE of binary systems containing well-defined hydrocarbons (i.e. methane, n-alkanes) and polar chemicals such as water or MEG/methanol.

CPA was successfully applied to different types of equilibrium, in a relatively wide range of both pressures and temperatures, with the need for only small corrections, as indicated by the low values for the binary interaction parameter, k_{ij}, used in most cases.

Satisfactory modeling results are obtained for the mutual solubility of methane + water and methane + methanol by using a single temperature independent binary interaction parameter. Prediction of the water content in the gas phase is comparable to other models, such as the semiempirical GERG-water method, which is based on the Peng−Robinson equation of state with a modified energy parameter. The CPA EoS can satisfactory predict the mutual solubility of aromatic hydrocarbons (ethylbenzene) with MEG and MEG/water, when the cross association is taken into account, using a single temperature independent $k_{ij} = 0.0254$ and $\beta_{cross} = 0.02$.

For the ternary system of methane + water + methanol, overall, the lowest deviations were found for the methanol solubility in the gas phase, while the model generally overestimates the methane solubility in the liquid phase and underestimates the water vapor content. The results are satisfactory, using k_{ij} adopted from binary systems.

Accurate predictions are made for VLLE of a quaternary system of methane + n-hexane + methanol + water, using the CPA EoS with binary interaction parameters adopted from binary systems. The predictions are in good agreement with the experimental data, even for very low solubility, such as n-hexane in aqueous phase. In conclusion, the CPA EoS predicts satisfactorily the multiphase equilibrium of multicomponent water – alcohol – aliphatic hydrocarbon systems, based solely on the binary interaction parameters taken from binary systems, using the 2B association scheme for methanol and the 4C association scheme for water. Overall CPA is a powerful tool for predictions of mutual solubility in hydrocarbon systems containing water and gas hydrate inhibitors (MEG/methanol).

To investigate the distribution of MEG in oil-water systems using the CPA EoS, experimental data are required, however, such data are very rare. In this work, an experimental study of phase equilibrium was carried out for oil, MEG and water systems at Statoil R&D, Norway. Experimental data for the mutual solubility of North Sea Oil + MEG and North Sea Oil + MEG + water are presented. The systems were investigated in the temperature range of 303.15 to 323.15 K at atmospheric pressure. In the systems of oil + MEG, the mutual solubility increases with increasing temperature, with the solubility of aromatic hydrocarbons being higher than that of naphthenic and paraffinic hydrocarbons in each carbon fraction. Detailed investigation of hydrocarbon solubility in the polar phase show, that benzene and toluene contribute a major part to the solubility of reservoir fluids in MEG. In the reservoir-fluid + MEG + water system, the mutual solubility of MEG and oil decreases with increasing water content in the polar phase and the solubility of some hydrocarbon components become negligible. The mutual solubility increases with increasing temperature. The data presented in this project are new data, with good reproducibility of the data.

The CPA EoS have been applied to the modeling of the mutual solubility of reservoir fluids, MEG and water. The reservoir fluid consists of seven different hydrocarbons fluids [3-6, this work] from different offshore fields in the North Sea. For characterization of the reservoir fluids, the correlations of Yan et al. [7] are applied.

New correlations for estimating binary interaction parameters between MEG-water and MEG-HC have been proposed. The CPA EoS is applied to the liquid-liquid equilibrium of reservoir-fluid + MEG and reservoir-fluid + MEG + water systems in a temperature range 275-326 K and

atmospheric pressure. For reservoir-fluid + MEG systems excellent correlations are obtained for the mutual solubility of reservoir fluid and MEG as a function of temperature, using correlation for estimating all k_{ij} between MEG and hydrocarbons and water-hydrocarbons. In the case of light oil - 1 satisfactory results are obtained for the solubility of hydrocarbons in MEG phase, but the solubility of MEG in hydrocarbons is underestimated.

For the reservoir-fluid + MEG + water systems satisfactory predictions are obtained using correlations for estimating all k_{ij} between MEG and hydrocarbons and water-HC. CPA can satisfactorily describe the trends in solubilities of reservoir fluids, MEG and water as a function of MEG mole fraction in the polar phase and as a function of temperature. The results are generally correct in order of magnitude.

It was generally found, that using the new developed correlation (eq. 7.3) for estimating all binary interaction parameters between MEG-HC, greatly increases the accuracy in predictions of MEG content in the hydrocarbon phase. This is achieved at the cost of some accuracy of predicted hydrocarbon content in the polar phase. The hydrocarbon content in the polar phase is, however, expected to be under-predicted, as we do not explicitly account of the aromaticity of the mixture. In order to enhance the predictions, effort should be done to account for the cross-association volume and cross-association energy for MEG and aromatic hydrocarbons (i.e. benzene, toluene and xylene) present in the oil.

Finally a comparison of CPA calculations is made between reservoir fluid and well-defined hydrocarbons in presence of polar chemicals such as water and MEG. It has been seen that modeling results for reservoir fluid systems are as good as for well-defined hydrocarbon systems. In some cases the modeling results for the systems with reservoir fluid are better than those of the systems with well-defined hydrocarbons. The deviations from experimental data are attributed to the complexity of the systems with associating and non-associating components and the challenges involved in the measurements and the modeling of very low solubilities, which are in the order of part per million. In case of reservoir fluid, systems are even more complex as we have numerous well-defined components (about 90 components in C_2-C_9 carbon fractions) and hundreds of ill-defined components in decane plus fraction. The components are paraffinic, naphthenic and aromatic in nature and of a wide range of molar mass and density. It has been shown that the CPA EoS is a flexible model by applying to a variety of phase equilibria, such as VLE, LLE and VLLE

of binary, multicomponent and reservoir fluid mixtures in presence of polar associating, non-associating and solvating compounds.

8.2 Future work

The work presented had a focus on the study of hydrocarbon systems containing gas hydrate inhibitor. The nature of the work was characterized by a rather broad perspective. From an experimental point of view, it is possible to provide a set of advices for the future experimental work with the equilibrium cells in the laboratories of the group, which have been presented in this dissertation.

Rather than pointing a specific path, the commissioning of these two experimental set-ups can be regarded as the opening of a new range of opportunities, for different projects, since the applicability of these experimental set-ups is not limited to the type of systems under consideration in the particular areas focused on this work. It is important to take into account however, that as versatile as the existing equipment may be, often there is the need for new customized set-ups, as recently pointed out by Richon [8]. Of extreme importance is the continuity in the use of the equipment, which tends to suffer a precocious ageing, leading to malfunctions, sometimes of an irreversible character, when not used, as demonstrated with the equilibrium cell recovered in the present work. New experimental equipment constitutes an investment whose profitability in terms of results is time limited, before it becomes obsolete, which in these days might happen relatively fast due to the constant technological development placed at the service of instrumentation.
As the equipment have shown great promise in the measurement of VLLE for complex systems, such as hydrocarbons with polar chemicals (water/methanol), it is advised to continue analyzing these types of systems. There is still a high demand for high quality experimental data, and as many research groups are moving away from experimental work, it is even more important to continue in this direction that has been started.

The developed correlation for binary interaction parameters between MEG-HC and water-HC come with some limitations, since there is a lack of experimental data for binary systems containing heavy hydrocarbons. More binary data for MEG + alkane and MEG + aromatic hydrocarbons is required in order to develop a fully predictive model for distribution of complex chemicals in oil-

water systems. Experimental data are also required for water + heavy aromatics and MEG + heavy aromatic in order to investigate the influence of solvation in the C_{10+} fractions. These type of experimental data are difficult to measure, as the solubility are very low, however, in order to continue and overcome the current limitations, experimental data for well-defined systems are needed.

In this project, reservoir fluids are characterized using Yan et al. [7] correlations with a characterization method similar to one proposed by Pedersen et al. [9,10], however other characterization methods should also be tested such as Whitson et al. [11] method. In order to investigate the effect PNA distribution in the C_{10+} fraction of oil, TBP data with experimental density and molar mass of each cut are required. The density and molar mass of a carbon fraction may then be correlated to PNA distribution. However, improvements in the predicted solubility of oil with polar chemicals could be improved by explicitly accounting for benzene and toluene. The light aromatics have the largest impact, on the solubility of hydrocarbon in the polar phase. Again, in order to make the best correlations and assumption, experimental data should be acquired for the well-defined systems of heavy hydrocarbons with the polar chemicals.
In the experimental work with reservoir fluids, distilled water is used. It would be of great interest, to use actual formation water, as to evaluate the effect of ions on the mutual solubility. This provides a serious test of the chemical analysis, as salts are very difficult to handle by normal means (GC). Such investigations would provide a more realistic picture, of the distribution of chemicals and hydrocarbons.

Based on the authors personal opinion and the concluding remark to the recommendations; there is still a great need for experimental data. However, more than ever, there is a requirement for data with high accuracy. Theory and models are becoming more and more accurate, so in order to move further ahead, the data that the theory is tested against needs to be improved. The new equipment for measurement of VLLE is a step in that direction.

References

[1] S.O. Derawi, G.M. Kontogeorgis, M.L. Michelsen, E.H. Stenby, *Ind. Eng. Chem. Res.* 42 (**2003**) 1470-1477

[2] G.M. Kontogeorgis, I.V. Yakoumis, H. Meijer, E. Hendriks, T. Moorwood, *Fluid Phase Equilibr.* 201 (**1999**) 158-160

[3] Frost, M. Kontogeorgis, G. M. Stenby, E. H. Yan, W. Haugum, T. Christensen, K. O. Solbraa, E. Løkken, T. V. *Fluid Phase Equilibria* (**2013**) 1-6

[4] Riaz, M. Kontogeorgis, G. M. Stenby, E. H. Yussuf, A. M. Haugum, T. Christensen, K. O. Solbraa, E. Løkken, T. V. *Fluid Phase Equilibria* (**2013)**, *340*, 1-6.

[5] Riaz, M. Kontogeorgis, G. M. Stenby, E. H. Yan, W. Haugum, T. Christensen, K. O. Løkken, T. V. Solbraa, E. *Journal of Chemical & Engineering Data 56* (**2011)** 4342-4351

[6] Riaz, M. Yussuf, A. M. Frost, M. Kontogeorgis, G. M. Stenby, E. H. Yan, W. Solbraa, E. *Energy and Fuels 28 (***2014)** 3530-3538.

[7] Yan, W. Kontogeorgis, G. M. Stenby, E. H. *Fluid Phase Equilibria* 276 (**2009)** 75-85.

[8] D. Richon, *Pure Appl. Chem.* 81 (**2009**) 1769-1782.

[9] Pedersen, K. S. Thomassen, P. Fredenslund, A. *Advances in Thermodynamics, C7+ Fraction Characterization*, Taylor & Francis: New York, **1989**, Vol. 1.

[10] Soave, G. *Fluid Phase Equilibria* 31 (**1986)** 203-207.

[11] Whitson, C. H. Søreide, I. Chorn, L. G. Mansoori, G. A. *Advances in Thermodynamics, C7+ Fraction Characterization*, Taylor & Francis: New York, **1989**, Vol. 1.

List of Symbols

a_0	Parameter in the energy term of CPA
$\alpha(T)$	Energy parameter of the mixture
b	Co-volume parameter of the mixture
c_1	Pure component parameter for Soave's $\alpha(T)$-function
$g(\rho)$	Radial distribution function
k_{ij}	Binary interaction parameter in the CPA Equation of State
MW	Molecular Weight
P	Pressure
P_c	Critical Pressure
P_{cm}	CPA "monomer" critical pressure
R	Gas Constant
SG	Specific Gravity
SG_0	Specific gravity of n-alkanes
T	Temperature
T_b	Boiling point temperature
T_c	Critical temperature
T_{cm}	CPA "monomer" critical temperature
v	Molar volume
w_i	Mass fraction of component *i*

X_{A_i}	Fraction of site *A* on component *i* not bonded to any other component
x_i	Mole fraction of component *i*

Greek letters

$\beta^{A_iB_j}$	Association volume
$\Delta^{A_iB_j}$	Association strength between site *A* on molecule *i* and site *B* on molecule *j*
$\varepsilon^{A_iB_j}$	Association energy
ρ	Density
ω	Acentric factor
ω_m	CPA "monomer" acentric factor

List of abbreviations

ASTM	American society of testing and materials
CAS Number	(a unique numerical identifier assigned by) chemical abstracts service (to each chemical)
CPA	Cubic-Plus-Association
ECR	Elliott combining rule
EoS	Equation of State
FID	fluid ionization detector
GCs	gas chromatographs
HC	hydrocarbon
LLE	liquid-liquid equilibrium
MEG	monoethylene glycol
NRTL	non-random two liquid
NP	number of points
PNA	paraffinic, naphthenic and aromatic (content of condensate or oil)

PR	Peng Robinson (equation of state)
RF	response factor
R & D	research and development
RRF	relative response factor
SAFT	statistical associating fluid theory
SARA	saturates, asphaltenes, resins and aromatic (analysis method)
SCN	single carbon number
SimDist	simulated distillation (GC)
SRK	Soave-Redlich-Kwong (EoS)
TBP	true boiling point (distillation)
UNIFAC	universal quasi-chemical functional group activity coefficient (model)
UNIQUAQ	universal quasi-chemical (model)
VLE	vapor-liquid equilibrium
VLLE	vapor-liquid-liquid equilibrium

List of Tables

List of Figures

APPENDICES

Appendix A: GC Analysis

In this appendix temperature programs used for gas chromatographs are shown in figures A.1 and A 2. The temperature profile for GC 1 (Glycol) is standard. A short upstart period and then a temperature increase the glycol has evaporated. The maximum temperature is kept for a while to ensure that the column is clean. This is presented in figure A1.

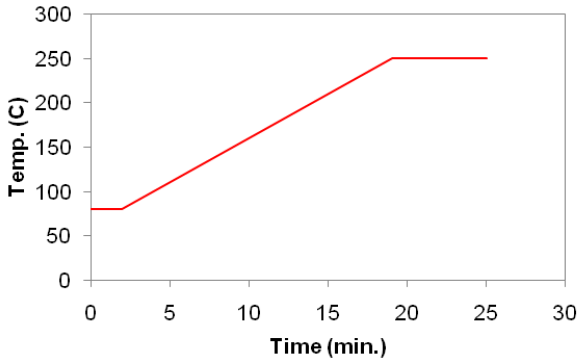

Figure A1: Temperature profile for the GC 1, which was used for analysis of glycol content in oil.

The temperature profile for the SimDist (GC) used in this work is much like that of GC1. The SimDist has a very long period at maximum temperature, which is because of the distillation simulation that takes place.

This is presented in figure A2.

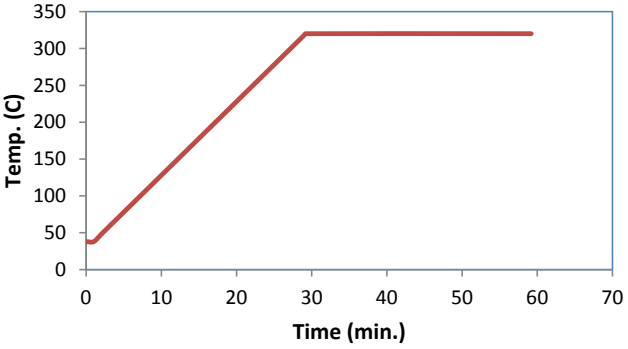

Figure A2: Temperature profile for the GC 2 (SimDist), which was used for analysis of hydrocarbons (oils) in polar phase.

Appendix B: Experimental data and predictions with the CPA EoS

In appendix B modeling work related to the phase behavior of reservoir fluid systems in presence of polar chemicals is presented. It presents all the experimental data and predictions made with the CPA EoS for oil systems with MEG + water.

B1: Condensate – 1

***kij* = 0 for all MEG-HC pairs**

Table B1: Experimental solubility and predicted values for Condensate – 1 + MEG + water at T = 303.15 K and atmospheric pressure. k_{ij} = 0 for all MEG-HC pair and k_{ij} are estimated from correlation in equation 7.2 for all water-HC.

Temperature 303.15K							
		Polar phase Mole ppm			Hydrocarbon phase Mole ppm		
Component	Feed mole fraction	Exp.	Calc.	%AAD	Exp.	Calc.	%AAD
MEG	0.3901	0.5367	0.5365	0.04	147	164	11.41
Water	0.3365	0.4628	0.4627	0.01	388	262	32.36
Hydrocarbon	0.2735	510	748	46.65	99.95	99.96	0.01
MEG	0.2314	0.3005	0.3005	0.01	80	91	13.78
Water	0.5385	0.6994	0.6993	0.01	607	398	34.42
Hydrocarbon	0.2301	90	131	45.62	99.93	99.95	0.02
MEG	0.1321	0.1635	0.1636	0.05	18	46	153.50
Water	0.6755	0.8364	0.8364	0.00	800	488	39.03
Hydrocarbon	0.1924	53	33	37.62	99.92	99.95	0.03

Table B2: Experimental solubility and predicted values for Condensate – 1 + MEG + water at T = 323.15 K and atmospheric pressure. k_{ij} = 0 for all MEG-HC pair and k_{ij} are estimated from correlation in equation 7.2 for all water-HC.

Temperature 323.15K							
		Polar phase Mole ppm			Hydrocarbon phase Mole ppm		
Component	**Feed mole fraction**	**Exp.**	**Calc.**	**%AAD**	**Exp.**	**Calc.**	**%AAD**
MEG	0.4992	0.7222	0.7216	0.09	381	591	55.24
Water	0.1909	0.2765	0.2759	0.23	402	390	2.88
Hydrocarbon	0.3098	1793	2562	42.88	99.92	99.90	0.02
MEG	0.3041	0.4037	0.4038	0.02	172	338	96.55
Water	0.4488	0.5960	0.5958	0.03	946	817	13.62
Hydrocarbon	0.2472	417	426	2.15	99.89	99.88	0.00
MEG	0.1324	0.1621	0.1621	0.02	61	127	107.67
Water	0.6843	0.8378	0.8378	0.00	1218	1174	3.58
Hydrocarbon	0.1833	69	51	26.25	99.87	99.87	0.00

***kij* = 0.02 for all MEG-HC pairs**

Table B3: Experimental solubility and predicted values for Condensate – 1 + MEG + water at T = 303.15 K and atmospheric pressure. k_{ij} = 0.02 for all MEG-HC pair and k_{ij} are estimated from correlation in equation 7.2 for all water-HC.

Temperature 303.15K							
		Polar phase Mole ppm			Hydrocarbon phase Mole ppm		
Component	**Feed mole fraction**	**Exp.**	**Calc.**	**%AAD**	**Exp.**	**Calc.**	**%AAD**
MEG	0.3901	0.5367	0.5366	0.02	147	131	10.92
Water	0.3365	0.4628	0.4628	0.01	388	261	32.73
Hydrocarbon	0.2735	510	553	8.43	99.95	99.96	0.02
MEG	0.2314	0.3005	0.3005	0.01	80	73	8.98
Water	0.5385	0.6994	0.6993	0.01	607	397	34.55
Hydrocarbon	0.2301	90	106	17.93	99.93	99.95	0.02
MEG	0.1321	0.1635	0.1636	0.05	18	37	102.89
Water	0.6755	0.8364	0.8364	0.00	800	487	39.09
Hydrocarbon	0.1924	53	29	45.62	99.92	99.95	0.03

Table B4: Experimental solubility and predicted values for Condensate – 1 + MEG + water at T = 323.15 K and atmospheric pressure. k_{ij} = 0.02 for all MEG-HC pair and k_{ij} are estimated from correlation in equation 7.2 for all water-HC.

Temperature 323.15K							
		Polar phase Mole ppm			Hydrocarbon phase Mole ppm		
Component	**Feed mole fraction**	**Exp.**	**Calc.**	**%AAD**	**Exp.**	**Calc.**	**%AAD**
MEG	0.4992	0.7222	0.7221	0.01	381	483	26.69
Water	0.1909	0.2765	0.2761	0.16	402	387	3.73
Hydrocarbon	0.3098	1793	1846	2.93	99.92	99.91	0.01
MEG	0.3041	0.4037	0.4038	0.03	172	277	60.93
Water	0.4488	0.5960	0.5958	0.03	946	814	13.98
Hydrocarbon	0.2472	417	337	19.23	99.89	99.89	0.00
MEG	0.1324	0.1621	0.1621	0.02	61	104	69.74
Water	0.6843	0.8378	0.8378	0.00	1218	1173	3.72
Hydrocarbon	0.1833	69	45	34.78	99.87	99.87	0.00

MEG-HC kij = Correlation

Table B5: Experimental solubility and predicted values for Condensate – 1 + MEG + water at T = 303.15 K and atmospheric pressure. k_{ij} for all MEG-HC pairs are estimated from correlation in equation 7.3 and k_{ij} are estimated from correlation in equation 7.2 for all water-HC.

Temperature 303.15K							
		Polar phase Mole ppm			Hydrocarbon phase Mole ppm		
Component	**Feed mole fraction**	**Exp.**	**Calc.**	**%AAD**	**Exp.**	**Calc.**	**%AAD**
MEG	0.3901	0.5367	0.5366	0.02	147	150	2.28
Water	0.3365	0.4628	0.4628	0.00	388	262	32.48
Hydrocarbon	0.2735	510	575	12.75	99.95	99.96	0.01
MEG	0.2314	0.3005	0.3005	0.01	80	84	4.50
Water	0.5385	0.6994	0.6993	0.01	607	398	34.48
Hydrocarbon	0.2301	90	108	19.63	99.93	99.95	0.02
MEG	0.1321	0.1635	0.1636	0.05	18	37	104.11
Water	0.6755	0.8364	0.8364	0.00	800	487	39.09
Hydrocarbon	0.1924	53	29	45.79	99.92	99.95	0.03

Table B6: Experimental solubility and predicted values for Condensate – 1 + MEG + water at T = 323.15 K and atmospheric pressure. k_{ij} for all MEG-HC pairs are estimated from correlation in equation 7.3 and k_{ij} are estimated from correlation in equation 7.2 for all water-HC.

Temperature 323.15K							
		Polar phase Mole ppm			Hydrocarbon phase Mole ppm		
Component	**Feed mole fraction**	**Exp.**	**Calc.**	**%AAD**	**Exp.**	**Calc.**	**%AAD**
MEG	0.4992	0.7222	0.7220	0.02	381	547	43.57
Water	0.1909	0.2765	0.2760	0.17	402	389	3.33
Hydrocarbon	0.3098	1793	1913	6.70	99.92	99.91	0.02
MEG	0.3041	0.4037	0.4038	0.03	172	313	81.91
Water	0.4488	0.5960	0.5958	0.03	946	816	13.78
Hydrocarbon	0.2472	417	344	17.61	99.89	99.89	0.00
MEG	0.1324	0.1621	0.1621	0.02	61	117	92.39
Water	0.6843	0.8378	0.8378	0.00	1218	1174	3.64
Hydrocarbon	0.1833	69	45	35.06	99.87	99.87	0.00

B2: Condensate – 2

***kij* = 0 for all MEG-HC pairs**

Table B7: Experimental solubility and predicted values for Condensate – 2 + MEG + water at T = 303.15 K and atmospheric pressure. k_{ij} = 0 for all MEG-HC pair and k_{ij} are estimated from correlation in equation 7.2 for all water-HC.

Temperature 303.15K							
		Polar phase Mole ppm			Hydrocarbon phase Mole ppm		
Component	**Feed mole fraction**	**Exp.**	**Calc.**	**%AAD**	**Exp.**	**Calc.**	**%AAD**
MEG	0.3865	0.5370	0.5370	0.00	103	157	52.46
Water	0.3329	0.4625	0.4625	0.00	394	252	36.13
Hydrocarbon	0.2805	508	472	7.12	99.95	99.96	0.01
MEG	0.2345	0.3033	0.3033	0.01	73	88	20.59
Water	0.5386	0.6966	0.6966	0.00	635	380	40.09
Hydrocarbon	0.2269	189	68	63.97	99.93	99.95	0.02
MEG	0.1312	0.1621	0.1621	0.01	36	43	20.03
Water	0.6783	0.8378	0.8379	0.01	806	469	41.78
Hydrocarbon	0.1905	67	14	79.54	99.92	99.95	0.03

Table B8: Experimental solubility and predicted values for Condensate – 2 + MEG + water at T = 323.15 K and atmospheric pressure. k_{ij} = 0 for all MEG-HC pair and k_{ij} are estimated from correlation in equation 7.2 for all water-HC.

Temperature 323.15K							
		Polar phase Mole ppm			Hydrocarbon phase Mole ppm		
Component	**Feed mole fraction**	**Exp.**	**Calc.**	**%AAD**	**Exp.**	**Calc.**	**%AAD**
MEG	0.3865	0.5366	0.5369	0.06	328	429	30.67
Water	0.3329	0.4622	0.4624	0.04	784	617	21.33
Hydrocarbon	0.2805	1181	666	43.58	99.89	99.90	0.01
MEG	0.2345	0.3032	0.3033	0.04	158	243	53.54
Water	0.5386	0.6965	0.6966	0.01	1119	926	17.22
Hydrocarbon	0.2269	311	108	65.40	99.87	99.88	0.01
MEG	0.1312	0.1621	0.1621	0.01	82	122	48.30
Water	0.6783	0.8378	0.8379	0.01	1309	1136	13.25
Hydrocarbon	0.1905	91	24	74.13	99.86	99.87	0.01

***kij* = 0.02 for all MEG-HC pairs**

Table B9: Experimental solubility and predicted values for Condensate – 2 + MEG + water at T = 303.15 K and atmospheric pressure. k_{ij} = 0.02 for all MEG-HC pair and k_{ij} are estimated from correlation in equation 7.2 for all water-HC.

Temperature 303.15K							
		Polar phase Mole ppm			Hydrocarbon phase Mole ppm		
Component	**Feed mole fraction**	**Exp.**	**Calc.**	**%AAD**	**Exp.**	**Calc.**	**%AAD**
MEG	0.3865	0.537	0.5371	0.02	103	126	22.74
Water	0.3329	0.4625	0.4626	0.01	394	251	36.36
Hydrocarbon	0.2805	508	329	35.16	99.95	99.96	0.01
MEG	0.2345	0.3033	0.3033	0.01	73	71	2.75
Water	0.5386	0.6966	0.6966	0.00	635	380	40.19
Hydrocarbon	0.2269	189	52	72.26	99.93	99.95	0.03
MEG	0.1312	0.1621	0.1621	0.01	36	35	3.08
Water	0.6783	0.8378	0.8379	0.01	806	469	41.83
Hydrocarbon	0.1905	67	12	82.78	99.92	99.95	0.03

Table B10: Experimental solubility and predicted values for Condensate – 2 + MEG + water at T = 323.15 K and atmospheric pressure. k_{ij} = 0.02 for all MEG-HC pair and k_{ij} are estimated from correlation in equation 7.2 for all water-HC.

Temperature 323.15K							
		Polar phase Mole ppm			Hydrocarbon phase Mole ppm		
Component	**Feed mole fraction**	**Exp.**	**Calc.**	**%AAD**	**Exp.**	**Calc.**	**%AAD**
MEG	0.3865	0.5366	0.5371	0.09	328	352	7.28
Water	0.3329	0.4622	0.4625	0.06	784	613	21.76
Hydrocarbon	0.2805	1181	480	59.34	99.89	99.90	0.01
MEG	0.2345	0.3032	0.3033	0.05	158	200	26.38
Water	0.5386	0.6965	0.6966	0.01	1119	924	17.45
Hydrocarbon	0.2269	311	85	72.73	99.87	99.89	0.02
MEG	0.1312	0.1621	0.1621	0.00	82	100	22.29
Water	0.6783	0.8378	0.8379	0.01	1309	1134	13.37
Hydrocarbon	0.1905	91	20	77.87	99.86	99.88	0.02

MEG-HC kij = Correlation

Table B11: Experimental solubility and predicted values for Condensate – 2 + MEG + water at T = 303.15 K and atmospheric pressure. k_{ij} for all MEG-HC pairs are estimated from correlation in equation 7.3 and k_{ij} are estimated from correlation in equation 7.2 for all water-HC.

Temperature 303.15K							
		Polar phase Mole ppm			Hydrocarbon phase Mole ppm		
Component	**Feed mole fraction**	**Exp.**	**Calc.**	**%AAD**	**Exp.**	**Calc.**	**%AAD**
MEG	0.3865	0.537	0.5371	0.02	103	137	32.98
Water	0.3329	0.4625	0.4626	0.01	394	251	36.29
Hydrocarbon	0.2805	508	333	34.36	99.95	99.96	0.01
MEG	0.2345	0.3033	0.3033	0.01	73	77	5.29
Water	0.5386	0.6966	0.6966	0.00	635	380	40.16
Hydrocarbon	0.2269	189	53	71.83	99.93	99.95	0.03
MEG	0.1312	0.1621	0.1621	0.01	36	38	4.86
Water	0.6783	0.8378	0.8379	0.01	806	469	41.81
Hydrocarbon	0.1905	67	12	82.57	99.92	99.95	0.03

Table B12: Experimental solubility and predicted values for Condensate – 2 + MEG + water at T = 323.15 K and atmospheric pressure. k_{ij} for all MEG-HC pairs are estimated from correlation in equation 7.3 and k_{ij} are estimated from correlation in equation 7.2 for all water-HC.

Temperature 323.15K							
		Polar phase Mole ppm			Hydrocarbon phase Mole ppm		
Component	**Feed mole fraction**	**Exp.**	**Calc.**	**%AAD**	**Exp.**	**Calc.**	**%AAD**
MEG	0.3865	0.5366	0.5371	0.08	328	379	15.40
Water	0.3329	0.4622	0.4625	0.06	784	614	21.63
Hydrocarbon	0.2805	1181	480	59.34	99.89	99.90	0.01
MEG	0.2345	0.3032	0.3033	0.05	158	215	35.79
Water	0.5386	0.6965	0.6966	0.01	1119	925	17.37
Hydrocarbon	0.2269	311	85	72.57	99.87	99.89	0.01
MEG	0.1312	0.1621	0.1621	0.00	82	108	31.30
Water	0.6783	0.8378	0.8379	0.01	1309	1135	13.33
Hydrocarbon	0.1905	91	20	77.75	99.86	99.88	0.01

B3: Condensate – 3

***kij* = 0 for all MEG-HC pairs**

Table B13: Experimental solubility and predicted values for Condensate – 3 + MEG + water at T = 313.15 K and atmospheric pressure. k_{ij} = 0 for all MEG-HC pair and k_{ij} are estimated from correlation in equation 7.2 for all water-HC.

Temperature 313.15K							
		Polar phase Mole ppm			Hydrocarbon phase Mole ppm		
Component	**Feed mole fraction**	**Exp.**	**Calc.**	**%AAD**	**Exp.**	**Calc.**	**%AAD**
MEG	0.3534	0.5063	0.5059	0.07	178	253	42.12
Water	0.3446	0.4937	0.4933	0.09	480	392	18.31
Hydrocarbon	0.3019	679	813	19.76	99.93	99.94	0.00
MEG	0.2238	0.2957	0.2956	0.02	91	147	61.34
Water	0.5331	0.7042	0.7042	0.00	673	561	16.71
Hydrocarbon	0.243	170	169	0.76	99.98	99.93	0.05
MEG	0.1279	0.1628	0.1628	0.01	53	75	41.91
Water	0.6578	0.8371	0.8372	0.01	796	680	14.57
Hydrocarbon	0.2143	52	45	13.58	99.99	99.92	0.07

***kij* = 0.02 for all MEG-HC pairs**

Table B14: Experimental solubility and predicted values for Condensate – 3 + MEG + water at T = 313.15 K and atmospheric pressure. k_{ij} = 0.02 for all MEG-HC pair and k_{ij} are estimated from correlation in equation 7.2 for all water-HC.

Temperature 313.15K							
		Polar phase Mole ppm			Hydrocarbon phase Mole ppm		
Component	**Feed mole fraction**	**Exp.**	**Calc.**	**%AAD**	**Exp.**	**Calc.**	**%AAD**
MEG	0.3534	0.5063	0.5060	0.05	178	205	15.44
Water	0.3446	0.4937	0.4934	0.07	480	390	18.70
Hydrocarbon	0.3019	679	611	10.06	99.93	99.94	0.01
MEG	0.2238	0.2957	0.2957	0.01	91	120	31.32
Water	0.5331	0.7042	0.7042	0.00	673	559	16.92
Hydrocarbon	0.243	170	138	19.10	99.98	99.93	0.05
MEG	0.1279	0.1628	0.1628	0.00	53	61	15.70
Water	0.6578	0.8371	0.8372	0.01	796	679	14.67
Hydrocarbon	0.2143	52	39	24.31	99.99	99.93	0.07

MEG-HC kij = Correlation

Table B15: Experimental solubility and predicted values for Condensate – 3 + MEG + water at T = 313.15 K and atmospheric pressure. k_{ij} for all MEG-HC pairs are estimated from correlation in equation 7.3 and k_{ij} are estimated from correlation in equation 7.2 for all water-HC.

Temperature 313.15K							
		Polar phase Mole ppm			Hydrocarbon phase Mole ppm		
Component	**Feed mole fraction**	**Exp.**	**Calc.**	**%AAD**	**Exp.**	**Calc.**	**%AAD**
MEG	0.3534	0.5063	0.5061	0.05	178	200	12.49
Water	0.3446	0.4937	0.4934	0.07	480	390	18.75
Hydrocarbon	0.3019	679	572	15.74	99.93	99.94	0.01
MEG	0.2238	0.2957	0.2957	0.01	91	116	28.00
Water	0.5331	0.7042	0.7042	0.00	673	559	16.94
Hydrocarbon	0.243	170	129	23.94	99.98	99.93	0.05
MEG	0.1279	0.1628	0.1628	0.00	53	60	12.79
Water	0.6578	0.8371	0.8372	0.01	796	679	14.69
Hydrocarbon	0.2143	52	37	28.25	99.99	99.93	0.07

B4: Light Oil – 1

***kij* = 0 for all MEG-HC pairs**

Table B16: Experimental solubility and predicted values for Light Oil – 1 + MEG + water at T = 313.15 K and atmospheric pressure. k_{ij} = 0 for all MEG-HC pair and k_{ij} are estimated from correlation in equation 7.2 for all water-HC.

Temperature 313.15K							
		Polar phase Mole ppm			Hydrocarbon phase Mole ppm		
Component	**Feed mole fraction**	**Exp.**	**Calc.**	**%AAD**	**Exp.**	**Calc.**	**%AAD**
MEG	0.4511	0.5229	0.5229	0.01	493	258	47.58
Water	0.4115	0.4769	0.4769	0.00	722	655	9.23
Hydrocarbon	0.1374	230	238	3.48	99.88	99.91	0.03
MEG	0.2421	0.2701	0.2701	0.02	270	132	50.94
Water	0.6544	0.7298	0.7299	0.01	908	1012	11.44
Hydrocarbon	0.1035	117	49	57.71	99.88	99.89	0.00

Table B17: Experimental solubility and predicted values for Light Oil – 1 + MEG + water at T = 323.15 K and atmospheric pressure. k_{ij} = 0 for all MEG-HC pair and k_{ij} are estimated from correlation in equation 7.2 for all water-HC.

Temperature 323.15K							
		Polar phase Mole ppm			Hydrocarbon phase Mole ppm		
Component	**Feed mole fraction**	**Exp.**	**Calc.**	**%AAD**	**Exp.**	**Calc.**	**%AAD**
MEG	0.4348	0.4919	0.4920	0.02	568	397	30.11
Water	0.4488	0.5078	0.5078	0.01	1023	1044	2.07
Hydrocarbon	0.1164	239	229	4.01	99.84	99.86	0.01
MEG	0.2673	0.2982	0.2983	0.03	363	147	59.42
Water	0.6288	0.7016	0.7016	0.01	1443	969	32.82
Hydrocarbon	0.1039	129	61	53.00	99.82	99.89	0.07

***kij* = 0.02 for all MEG-HC pairs**

Table B18: Experimental solubility and predicted values for Light Oil – 1 + MEG + water at T = 313.15 K and atmospheric pressure. k_{ij} = 0.02 for all MEG-HC pair and k_{ij} are estimated from correlation in equation 7.2 for all water-HC.

Temperature 313.15K							
		Polar phase Mole ppm			Hydrocarbon phase Mole ppm		
Component	**Feed mole fraction**	**Exp.**	**Calc.**	**%AAD**	**Exp.**	**Calc.**	**%AAD**
MEG	0.4511	0.5229	0.5229	0.00	493	210	57.38
Water	0.4115	0.4769	0.4769	0.00	722	654	9.44
Hydrocarbon	0.1374	230	189	17.82	99.88	99.91	0.04
MEG	0.2421	0.2701	0.2701	0.01	270	108	60.05
Water	0.6544	0.7298	0.7299	0.01	908	1011	11.32
Hydrocarbon	0.1035	117	43	63.17	99.88	99.89	0.01

Table B19: Experimental solubility and predicted values for Light Oil – 1 + MEG + water at T = 323.15 K and atmospheric pressure. k_{ij} = 0.02 for all MEG-HC pair and k_{ij} are estimated from correlation in equation 7.2 for all water-HC.

Temperature 323.15K							
		Polar phase Mole ppm			Hydrocarbon phase Mole ppm		
Component	**Feed mole fraction**	**Exp.**	**Calc.**	**%AAD**	**Exp.**	**Calc.**	**%AAD**
MEG	0.4348	0.4919	0.4920	0.03	568	326	42.64
Water	0.4488	0.5078	0.5078	0.00	1023	1041	1.80
Hydrocarbon	0.1164	239	185	22.40	99.84	99.86	0.02
MEG	0.2673	0.2982	0.2983	0.03	363	120	66.97
Water	0.6288	0.7016	0.7016	0.01	1443	968	32.90
Hydrocarbon	0.1039	129	52	59.55	99.82	99.89	0.07

MEG-HC kij = Correlation

Table B20: Experimental solubility and predicted values for Light Oil – 1 + MEG + water at T = 313.15 K and atmospheric pressure. k_{ij} for all MEG-HC pairs are estimated from correlation in equation 7.3 and k_{ij} are estimated from correlation in equation 7.2 for all water-HC.

Temperature 313.15K							
		Polar phase Mole ppm			Hydrocarbon phase Mole ppm		
Component	Feed mole fraction	Exp.	Calc.	%AAD	Exp.	Calc.	%AAD
MEG	0.4511	0.5229	0.5229	0.00	493	431	12.54
Water	0.4115	0.4769	0.4770	0.01	722	660	8.59
Hydrocarbon	0.1374	230	148	35.69	99.88	99.89	0.01
MEG	0.2421	0.2701	0.2701	0.02	270	220	18.62
Water	0.6544	0.7298	0.7299	0.02	908	1016	11.86
Hydrocarbon	0.1035	117	33	71.55	99.88	99.88	0.01

Table B21: Experimental solubility and predicted values for Light Oil – 1 + MEG + water at T = 323.15 K and atmospheric pressure. k_{ij} for all MEG-HC pairs are estimated from correlation in equation 7.3 and k_{ij} are estimated from correlation in equation 7.2 for all water-HC.

Temperature 323.15K							
		Polar phase Mole ppm			Hydrocarbon phase Mole ppm		
Component	Feed mole fraction	Exp.	Calc.	%AAD	Exp.	Calc.	%AAD
MEG	0.4348	0.4919	0.4920	0.03	568	648	14.05
Water	0.4488	0.5078	0.5078	0.00	1023	1053	2.92
Hydrocarbon	0.1164	239	148	38.18	99.84	99.83	0.01
MEG	0.2673	0.2982	0.2983	0.03	363	244	32.65
Water	0.6288	0.7016	0.7017	0.01	1443	973	32.54
Hydrocarbon	0.1039	129	40	68.86	99.82	99.88	0.06

B5: Light Oil – 2

***kij* = 0 for all MEG-HC pairs**

Table B22: Experimental solubility and predicted values for Light Oil – 2 + MEG + water at T = 313.15 K and atmospheric pressure. k_{ij} = 0 for all MEG-HC pair and k_{ij} are estimated from correlation in equation 7.2 for all water-HC.

Temperature 313.15K							
		Polar phase Mole ppm			Hydrocarbon phase Mole ppm		
Component	**Feed mole fraction**	**Exp.**	**Calc.**	**%AAD**	**Exp.**	**Calc.**	**%AAD**
MEG	0.4104	0.5389	0.5386	0.06	207	265	28.14
Water	0.351	0.461	0.4606	0.10	788	467	40.70
Hydrocarbon	0.2386	647	862	33.26	99.94	99.93	0.01

Table B23: Experimental solubility and predicted values for Light Oil – 2 + MEG + water at T = 323.15 K and atmospheric pressure. k_{ij} = 0 for all MEG-HC pair and k_{ij} are estimated from correlation in equation 7.2 for all water-HC.

Temperature 323.15K							
		Polar phase Mole ppm			Hydrocarbon phase Mole ppm		
Component	**Feed mole fraction**	**Exp.**	**Calc.**	**%AAD**	**Exp.**	**Calc.**	**%AAD**
MEG	0.4074	0.5374	0.5369	0.09	549	430	21.63
Water	0.3507	0.4626	0.4621	0.11	917	716	21.87
Hydrocarbon	0.2418	686	974	42.05	99.93	99.89	0.05
MEG	0.2459	0.3023	0.3022	0.02	529	243	54.02
Water	0.5676	0.6976	0.6975	0.01	1351	1079	20.10
Hydrocarbon	0.1864	270	207	23.42	99.97	99.87	0.11
MEG	0.1377	0.1633	0.1633	0.01	234	124	47.15
Water	0.7055	0.8367	0.8366	0.01	1744	1320	24.31
Hydrocarbon	0.1567	125	59	52.47	99.99	99.86	0.13

***kij* = 0.02 for all MEG-HC pairs**

Table B24: Experimental solubility and predicted values for Light Oil – 2 + MEG + water at T = 313.15 K and atmospheric pressure. k_{ij} = 0.02 for all MEG-HC pair and k_{ij} are estimated from correlation in equation 7.2 for all water-HC.

Temperature 313.15K							
		Polar phase Mole ppm			Hydrocarbon phase Mole ppm		
Component	Feed mole fraction	Exp.	Calc.	%AAD	Exp.	Calc.	%AAD
MEG	0.4104	0.5389	0.5387	0.04	207	216	4.23
Water	0.351	0.461	0.4606	0.08	788	465	40.94
Hydrocarbon	0.2386	647	660	2.02	99.94	99.93	0.00

Table B25: Experimental solubility and predicted values for Light Oil – 2 + MEG + water at T = 323.15 K and atmospheric pressure. k_{ij} = 0.02 for all MEG-HC pair and k_{ij} are estimated from correlation in equation 7.2 for all water-HC.

Temperature 323.15K							
		Polar phase Mole ppm			Hydrocarbon phase Mole ppm		
Component	Feed mole fraction	Exp.	Calc.	%AAD	Exp.	Calc.	%AAD
MEG	0.4074	0.5374	0.5371	0.06	549	353	35.66
Water	0.3507	0.4626	0.4622	0.09	917	713	22.25
Hydrocarbon	0.2418	686	754	9.86	99.93	99.89	0.04
MEG	0.2459	0.3023	0.3023	0.01	529	200	62.17
Water	0.5676	0.6976	0.6976	0.01	1351	1077	20.30
Hydrocarbon	0.1864	270	173	35.84	99.97	99.87	0.10
MEG	0.1377	0.1633	0.1633	0.01	234	102	56.46
Water	0.7055	0.8367	0.8366	0.01	1744	1318	24.40
Hydrocarbon	0.1567	125	53	57.54	99.99	99.86	0.13

MEG-HC kij = Correlation

Table B26: Experimental solubility and predicted values for Light Oil – 2 + MEG + water at T = 313.15 K and atmospheric pressure. k_{ij} for all MEG-HC pairs are estimated from correlation in equation 7.3 and k_{ij} are estimated from correlation in equation 7.2 for all water-HC.

Temperature 313.15K							
		Polar phase Mole ppm			Hydrocarbon phase Mole ppm		
Component	Feed mole fraction	Exp.	Calc.	%AAD	Exp.	Calc.	%AAD
MEG	0.4104	0.5389	0.5387	0.03	207	284	36.98
Water	0.351	0.461	0.4607	0.07	788	468	40.67
Hydrocarbon	0.2386	647	614	5.04	99.94	99.92	0.01

Table B27: Experimental solubility and predicted values for Light Oil – 2 + MEG + water at T = 323.15 K and atmospheric pressure. k_{ij} for all MEG-HC pairs are estimated from correlation in equation 7.3 and k_{ij} are estimated from correlation in equation 7.2 for all water-HC.

Temperature 323.15K							
		Polar phase Mole ppm			Hydrocarbon phase Mole ppm		
Component	Feed mole fraction	Exp.	Calc.	%AAD	Exp.	Calc.	%AAD
MEG	0.4074	0.5374	0.5371	0.06	549	459	16.46
Water	0.3507	0.4626	0.4622	0.08	917	717	21.81
Hydrocarbon	0.2418	686	705	2.71	99.93	99.88	0.05
MEG	0.2459	0.3023	0.3023	0.01	529	259	51.07
Water	0.5676	0.6976	0.6976	0.00	1351	1080	20.05
Hydrocarbon	0.1864	270	158	41.34	99.97	99.87	0.11
MEG	0.1377	0.1633	0.1633	0.01	234	131	43.82
Water	0.7055	0.8367	0.8366	0.01	1744	1321	24.28
Hydrocarbon	0.1567	125	49	61.03	99.99	99.85	0.13

B6: Fluid – 1

***kij* = 0 for all MEG-HC pairs**

Table B28: Experimental solubility and predicted values for Fluid – 1 + MEG + water at T = 303.15 K and atmospheric pressure. k_{ij} = 0 for all MEG-HC pair and k_{ij} are estimated from correlation in equation 7.2 for all water-HC.

Temperature 303.15K							
		Polar phase Mole ppm			Hydrocarbon phase Mole ppm		
Component	**Feed mole fraction**	**Exp.**	**Calc.**	**%AAD**	**Exp.**	**Calc.**	**%AAD**
MEG	0.3952	0.5264	0.5265	0.01	239	151	36.94
Water	0.3551	0.4730	0.4730	0.00	382	334	12.34
Hydrocarbon	0.2497	571	503	11.93	99.94	99.95	0.01
MEG	0.2356	0.2965	0.2966	0.03	124	84	31.92
Water	0.5586	0.7033	0.7033	0.00	558	501	10.35
Hydrocarbon	0.2058	166	94	43.63	99.93	99.94	0.01
MEG	0.1345	0.1605	0.1606	0.04	44	42	3.56
Water	0.7031	0.8394	0.8394	0.00	722	613	15.09
Hydrocarbon	0.1624	88	24	72.31	99.92	99.93	0.01

Table B29: Experimental solubility and predicted values for Fluid – 1 + MEG + water at T = 313.15 K and atmospheric pressure. k_{ij} = 0 for all MEG-HC pair and k_{ij} are estimated from correlation in equation 7.2 for all water-HC.

Temperature 313.15K							
		Polar phase Mole ppm			Hydrocarbon phase Mole ppm		
Component	**Feed mole fraction**	**Exp.**	**Calc.**	**%AAD**	**Exp.**	**Calc.**	**%AAD**
MEG	0.3453	0.4546	0.4546	0.01	375	221	41.18
Water	0.4140	0.5450	0.5450	0.00	523	601	14.93
Hydrocarbon	0.2407	408	371	9.12	99.91	99.92	0.01
MEG	0.2345	0.2921	0.2921	0.01	189	141	25.60
Water	0.5682	0.7077	0.7078	0.00	713	785	10.09
Hydrocarbon	0.1974	166	109	34.44	99.91	99.91	0.00
MEG	0.1354	0.1611	0.1611	0.00	88	72	18.18
Water	0.7053	0.8388	0.8389	0.01	936	952	1.70
Hydrocarbon	0.1592	87	31	64.95	99.90	99.90	0.00

Table B30: Experimental solubility and predicted values for Fluid – 1 + MEG + water at T = 323.15 K and atmospheric pressure. k_{ij} = 0 for all MEG-HC pair and k_{ij} are estimated from correlation in equation 7.2 for all water-HC.

Temperature 323.15K							
		Polar phase Mole ppm			Hydrocarbon phase Mole ppm		
Component	**Feed mole fraction**	**Exp.**	**Calc.**	**%AAD**	**Exp.**	**Calc.**	**%AAD**
MEG	0.4031	0.5418	0.5418	0.00	586	426	27.33
Water	0.3404	0.4576	0.4574	0.04	647	770	18.99
Hydrocarbon	0.2565	573	732	27.64	99.88	99.88	0.00
MEG	0.2363	0.2989	0.2990	0.02	275	236	14.13
Water	0.5541	0.7009	0.7009	0.00	1068	1178	10.38
Hydrocarbon	0.2096	186	138	25.57	99.87	99.86	0.01
MEG	0.1417	0.1665	0.1665	0.01	164	124	24.35
Water	0.7095	0.8335	0.8335	0.00	1575	1428	9.33
Hydrocarbon	0.1489	86	40	53.19	99.83	99.84	0.02

***kij* = 0.02 for all MEG-HC pairs**

Table B31: Experimental solubility and predicted values for Fluid – 1 + MEG + water at T = 303.15 K and atmospheric pressure. k_{ij} = 0.02 for all MEG-HC pair and k_{ij} are estimated from correlation in equation 7.2 for all water-HC.

Temperature 303.15K							
		Polar phase Mole ppm			Hydrocarbon phase Mole ppm		
Component	**Feed mole fraction**	**Exp.**	**Calc.**	**%AAD**	**Exp.**	**Calc.**	**%AAD**
MEG	0.3952	0.5264	0.5266	0.03	239	122	49.11
Water	0.3551	0.4730	0.4731	0.01	382	334	12.57
Hydrocarbon	0.2497	571	374	34.50	99.94	99.95	0.02
MEG	0.2356	0.2965	0.2967	0.04	124	68	44.99
Water	0.5586	0.7033	0.7033	0.00	558	500	10.47
Hydrocarbon	0.2058	166	76	54.06	99.93	99.94	0.01
MEG	0.1345	0.1605	0.1606	0.04	44	34	22.01
Water	0.7031	0.8394	0.8394	0.00	722	613	15.15
Hydrocarbon	0.1624	88	21	75.68	99.92	99.94	0.01

Table B32: Experimental solubility and predicted values for Fluid – 1 + MEG + water at T = 313.15 K and atmospheric pressure. k_{ij} = 0.02 for all MEG-HC pair and k_{ij} are estimated from correlation in equation 7.2 for all water-HC.

Temperature 313.15K							
		Polar phase Mole ppm			Hydrocarbon phase Mole ppm		
Component	**Feed mole fraction**	**Exp.**	**Calc.**	**%AAD**	**Exp.**	**Calc.**	**%AAD**
MEG	0.3453	0.4546	0.4547	0.02	375	180	52.03
Water	0.4140	0.5450	0.5450	0.01	523	599	14.62
Hydrocarbon	0.2407	408	286	29.96	99.91	99.92	0.01
MEG	0.2345	0.2921	0.2921	0.02	189	115	39.26
Water	0.5682	0.7077	0.7078	0.00	713	784	9.91
Hydrocarbon	0.1974	166	90	46.03	99.91	99.91	0.00
MEG	0.1354	0.1611	0.1611	0.00	88	59	33.13
Water	0.7053	0.8388	0.8389	0.01	936	951	1.62
Hydrocarbon	0.1592	87	27	69.11	99.90	99.90	0.00

Table B33: Experimental solubility and predicted values for Fluid – 1 + MEG + water at T = 323.15 K and atmospheric pressure. k_{ij} = 0.02 for all MEG-HC pair and k_{ij} are estimated from correlation in equation 7.2 for all water-HC.

Temperature 323.15K							
		Polar phase Mole ppm			Hydrocarbon phase Mole ppm		
Component	Feed mole fraction	Exp.	Calc.	%AAD	Exp.	Calc.	%AAD
MEG	0.4031	0.5418	0.5420	0.02	586	350	40.23
Water	0.3404	0.4576	0.4575	0.02	647	766	18.50
Hydrocarbon	0.2565	573	554	3.45	99.88	99.89	0.01
MEG	0.2363	0.2989	0.2990	0.02	275	195	29.24
Water	0.5541	0.7009	0.7009	0.00	1068	1176	10.15
Hydrocarbon	0.2096	186	114	38.48	99.87	99.86	0.00
MEG	0.1417	0.1665	0.1665	0.02	164	103	37.58
Water	0.7095	0.8335	0.8335	0.00	1575	1427	9.42
Hydrocarbon	0.1489	86	35	58.65	99.83	99.85	0.02

MEG-HC kij = Correlation

Table B34: Experimental solubility and predicted values for Fluid – 1 + MEG + water at T = 303.15 K and atmospheric pressure. k_{ij} for all MEG-HC pairs are estimated from correlation in equation 7.3 and k_{ij} are estimated from correlation in equation 7.2 for all water-HC.

Temperature 303.15K							
		Polar phase Mole ppm			Hydrocarbon phase Mole ppm		
Component	Feed mole fraction	Exp.	Calc.	%AAD	Exp.	Calc.	%AAD
MEG	0.3952	0.5264	0.5266	0.03	239	178	25.78
Water	0.3551	0.4730	0.4731	0.02	382	335	12.21
Hydrocarbon	0.2497	571	339	40.59	99.94	99.95	0.01
MEG	0.2356	0.2965	0.2967	0.04	124	99	20.02
Water	0.5586	0.7033	0.7033	0.00	558	501	10.25
Hydrocarbon	0.2058	166	69	58.64	99.93	99.94	0.01
MEG	0.1345	0.1605	0.1606	0.04	44	49	13.17
Water	0.7031	0.8394	0.8394	0.00	722	614	15.05
Hydrocarbon	0.1624	88	20	77.88	99.92	99.93	0.01

Table B35: Experimental solubility and predicted values for Fluid – 1 + MEG + water at T = 313.15 K and atmospheric pressure. k_{ij} for all MEG-HC pairs are estimated from correlation in equation 7.3 and k_{ij} are estimated from correlation in equation 7.2 for all water-HC.

Temperature 313.15K							
		Polar phase Mole ppm			Hydrocarbon phase Mole ppm		
Component	**Feed mole fraction**	**Exp.**	**Calc.**	**%AAD**	**Exp.**	**Calc.**	**%AAD**
MEG	0.3453	0.4546	0.4547	0.02	375	258	31.33
Water	0.4140	0.5450	0.5451	0.01	523	602	15.14
Hydrocarbon	0.2407	408	259	36.40	99.91	99.91	0.00
MEG	0.2345	0.2921	0.2921	0.01	189	164	13.29
Water	0.5682	0.7077	0.7078	0.01	713	786	10.23
Hydrocarbon	0.1974	166	81	51.10	99.91	99.90	0.00
MEG	0.1354	0.1611	0.1611	0.00	88	84	4.75
Water	0.7053	0.8388	0.8389	0.01	936	952	1.77
Hydrocarbon	0.1592	87	25	71.66	99.90	99.90	0.00

Table B36: Experimental solubility and predicted values for Fluid – 1 + MEG + water at T = 323.15 K and atmospheric pressure. k_{ij} for all MEG-HC pairs are estimated from correlation in equation 7.3 and k_{ij} are estimated from correlation in equation 7.2 for all water-HC.

Temperature 323.15K							
		Polar phase Mole ppm			Hydrocarbon phase Mole ppm		
Component	**Feed mole fraction**	**Exp.**	**Calc.**	**%AAD**	**Exp.**	**Calc.**	**%AAD**
MEG	0.4031	0.5418	0.5420	0.02	586	494	15.65
Water	0.3404	0.4576	0.4575	0.01	647	772	19.30
Hydrocarbon	0.2565	573	505	11.88	99.88	99.87	0.00
MEG	0.2363	0.2989	0.2990	0.02	275	273	0.62
Water	0.5541	0.7009	0.7009	0.00	1068	1180	10.56
Hydrocarbon	0.2096	186	104	43.94	99.87	99.85	0.01
MEG	0.1417	0.1665	0.1665	0.01	164	144	12.58
Water	0.7095	0.8335	0.8335	0.00	1575	1430	9.25
Hydrocarbon	0.1489	86	33	61.88	99.83	99.84	0.02

B7: Fluid – 2

***kij* = 0 for all MEG-HC pairs**

Table B37: Experimental solubility and predicted values for Fluid – 2 + MEG + water at T = 303.15 K and atmospheric pressure. k_{ij} = 0 for all MEG-HC pair and k_{ij} are estimated from correlation in equation 7.2 for all water-HC.

Temperature 303.15K							
		Polar phase Mole ppm			Hydrocarbon phase Mole ppm		
Component	**Feed mole fraction**	**Exp.**	**Calc.**	**%AAD**	**Exp.**	**Calc.**	**%AAD**
MEG	0.4109	0.5322	0.5324	0.03	223	151	32.36
Water	0.3610	0.4676	0.4676	0.00	679	447	34.23
Hydrocarbon	0.2281	191	30	84.32	99.91	99.94	0.03
MEG	0.2435	0.3090	0.3090	0.02	98	87	11.13
Water	0.5446	0.6909	0.6910	0.01	913	665	27.21
Hydrocarbon	0.2118	120	5	96.23	99.90	99.92	0.03
MEG	0.1339	0.1650	0.1650	0.04	40	43	6.90
Water	0.6775	0.8349	0.8350	0.00	1076	825	23.36
Hydrocarbon	0.1886	98	1	99.09	99.89	99.91	0.02

Table B38: Experimental solubility and predicted values for Fluid – 2 + MEG + water at T = 313.15 K and atmospheric pressure. k_{ij} = 0 for all MEG-HC pair and k_{ij} are estimated from correlation in equation 7.2 for all water-HC.

Temperature 313.15K							
		Polar phase Mole ppm			Hydrocarbon phase Mole ppm		
Component	**Feed mole fraction**	**Exp.**	**Calc.**	**%AAD**	**Exp.**	**Calc.**	**%AAD**
MEG	0.4060	0.5265	0.5266	0.03	269	253	6.19
Water	0.3650	0.4733	0.4733	0.00	943	694	26.43
Hydrocarbon	0.2290	209	35	83.38	99.88	99.91	0.03
MEG	0.2273	0.2920	0.2921	0.02	123	140	13.81
Water	0.5511	0.7079	0.7079	0.01	1270	1044	17.74
Hydrocarbon	0.2216	117	5	95.85	99.86	99.88	0.02
MEG	0.1245	0.1554	0.1555	0.06	55	69	25.98
Water	0.6764	0.8445	0.8445	0.00	1359	1276	6.08
Hydrocarbon	0.1991	94	1	98.89	99.86	99.87	0.01

Table B39: Experimental solubility and predicted values for Fluid – 2 + MEG + water at T = 323.15 K and atmospheric pressure. k_{ij} = 0 for all MEG-HC pair and k_{ij} are estimated from correlation in equation 7.2 for all water-HC.

Temperature 323.15K							
		Polar phase Mole ppm			Hydrocarbon phase Mole ppm		
Component	**Feed mole fraction**	**Exp.**	**Calc.**	**%AAD**	**Exp.**	**Calc.**	**%AAD**
MEG	0.4054	0.5268	0.5270	0.04	309	412	33.54
Water	0.3640	0.4730	0.4730	0.00	1214	1035	14.74
Hydrocarbon	0.2306	243	42	82.64	99.85	99.86	0.01
MEG	0.2372	0.3052	0.3053	0.03	154	240	55.43
Water	0.5400	0.6947	0.6947	0.01	1390	1525	9.66
Hydrocarbon	0.2228	145	7	95.10	99.85	99.82	0.02
MEG	0.1322	0.1654	0.1655	0.05	68	123	81.49
Water	0.6670	0.8345	0.8345	0.00	1669	1870	12.04
Hydrocarbon	0.2009	107	2	98.54	99.83	99.80	0.03

***kij* = 0.02 for all MEG-HC pairs**

Table B40: Experimental solubility and predicted values for Fluid – 2 + MEG + water at T = 303.15 K and atmospheric pressure. k_{ij} = 0.02 for all MEG-HC pair and k_{ij} are estimated from correlation in equation 7.2 for all water-HC.

Temperature 303.15K							
		Polar phase Mole ppm			Hydrocarbon phase Mole ppm		
Component	**Feed mole fraction**	**Exp.**	**Calc.**	**%AAD**	**Exp.**	**Calc.**	**%AAD**
MEG	0.4109	0.5322	0.5324	0.03	223	122	45.38
Water	0.3610	0.4676	0.4676	0.00	679	446	34.32
Hydrocarbon	0.2281	191	20	89.71	99.91	99.94	0.03
MEG	0.2435	0.3090	0.3090	0.02	98	71	28.17
Water	0.5446	0.6909	0.6910	0.01	913	664	27.27
Hydrocarbon	0.2118	120	3	97.23	99.90	99.93	0.03
MEG	0.1339	0.1650	0.1650	0.04	40	35	13.55
Water	0.6775	0.8349	0.8350	0.00	1076	825	23.38
Hydrocarbon	0.1886	98	1	99.26	99.89	99.91	0.03

Table B41: Experimental solubility and predicted values for Fluid – 2 + MEG + water at T = 313.15 K and atmospheric pressure. k_{ij} = 0.02 for all MEG-HC pair and k_{ij} are estimated from correlation in equation 7.2 for all water-HC.

Temperature 313.15K							
		Polar phase Mole ppm			Hydrocarbon phase Mole ppm		
Component	**Feed mole fraction**	**Exp.**	**Calc.**	**%AAD**	**Exp.**	**Calc.**	**%AAD**
MEG	0.4060	0.5265	0.5267	0.04	269	206	23.51
Water	0.3650	0.4733	0.4733	0.00	943	693	26.56
Hydrocarbon	0.2290	209	23	88.86	99.88	99.91	0.03
MEG	0.2273	0.2920	0.2921	0.02	123	114	7.09
Water	0.5511	0.7079	0.7079	0.01	1270	1043	17.81
Hydrocarbon	0.2216	117	4	96.87	99.86	99.88	0.02
MEG	0.1245	0.1554	0.1555	0.06	55	56	2.91
Water	0.6764	0.8445	0.8445	0.00	1359	1276	6.12
Hydrocarbon	0.1991	94	1	99.07	99.86	99.87	0.01

Table B42: Experimental solubility and predicted values for Fluid – 2 + MEG + water at T = 323.15 K and atmospheric pressure. k_{ij} = 0.02 for all MEG-HC pair and k_{ij} are estimated from correlation in equation 7.2 for all water-HC.

Temperature 323.15K							
		Polar phase Mole ppm			Hydrocarbon phase Mole ppm		
Component	**Feed mole fraction**	**Exp.**	**Calc.**	**%AAD**	**Exp.**	**Calc.**	**%AAD**
MEG	0.4054	0.5268	0.5270	0.05	309	339	9.86
Water	0.3640	0.4730	0.4730	0.01	1214	1033	14.92
Hydrocarbon	0.2306	243	29	88.16	99.85	99.86	0.02
MEG	0.2372	0.3052	0.3053	0.03	154	198	28.04
Water	0.5400	0.6947	0.6947	0.01	1390	1523	9.53
Hydrocarbon	0.2228	145	5	96.32	99.85	99.83	0.02
MEG	0.1322	0.1654	0.1655	0.05	68	101	49.65
Water	0.6670	0.8345	0.8345	0.00	1669	1869	11.97
Hydrocarbon	0.2009	107	1	98.79	99.83	99.80	0.02

MEG-HC kij = Correlation

Table B43: Experimental solubility and predicted values for Fluid – 2 + MEG + water at T = 303.15 K and atmospheric pressure. k_{ij} for all MEG-HC pairs are estimated from correlation in equation 7.3 and k_{ij} are estimated from correlation in equation 7.2 for all water-HC.

Temperature 303.15K							
		Polar phase Mole ppm			Hydrocarbon phase Mole ppm		
Component	**Feed mole fraction**	**Exp.**	**Calc.**	**%AAD**	**Exp.**	**Calc.**	**%AAD**
MEG	0.4109	0.5322	0.5323	0.03	447	297	33.51
Water	0.3610	0.4676	0.4676	0.01	679	450	33.80
Hydrocarbon	0.2281	191	18	90.54	99.91	99.93	0.02
MEG	0.2435	0.3090	0.3090	0.01	197	171	13.02
Water	0.5446	0.6909	0.6910	0.01	913	667	26.93
Hydrocarbon	0.2118	120	3	97.47	99.90	99.92	0.02
MEG	0.1339	0.1650	0.1650	0.03	80	84	4.30
Water	0.6775	0.8349	0.8350	0.01	1076	826	23.21
Hydrocarbon	0.1886	98	1	99.32	99.89	99.91	0.02

Table B44: Experimental solubility and predicted values for Fluid – 2 + MEG + water at T = 313.15 K and atmospheric pressure. k_{ij} for all MEG-HC pairs are estimated from correlation in equation 7.3 and k_{ij} are estimated from correlation in equation 7.2 for all water-HC.

Temperature 313.15K							
		Polar phase Mole ppm			Hydrocarbon phase Mole ppm		
Component	Feed mole fraction	Exp.	Calc.	%AAD	Exp.	Calc.	%AAD
MEG	0.4060	0.5265	0.5266	0.03	538	482	10.41
Water	0.3650	0.4733	0.4734	0.01	943	728	22.84
Hydrocarbon	0.2290	209	20	90.23	99.88	99.88	0.00
MEG	0.2273	0.2920	0.2920	0.01	246	266	8.14
Water	0.5511	0.7079	0.7080	0.01	1270	1092	14.01
Hydrocarbon	0.2216	117	3	97.38	99.86	99.86	0.00
MEG	0.1245	0.1554	0.1555	0.05	109	131	19.31
Water	0.6764	0.8445	0.8445	0.00	1359	1331	2.03
Hydrocarbon	0.1991	94	1	99.23	99.86	99.85	0.00

Table B45: Experimental solubility and predicted values for Fluid – 2 + MEG + water at T = 323.15 K and atmospheric pressure. k_{ij} for all MEG-HC pairs are estimated from correlation in equation 7.3 and k_{ij} are estimated from correlation in equation 7.2 for all water-HC.

Temperature 323.15K							
		Polar phase Mole ppm			Hydrocarbon phase Mole ppm		
Component	Feed mole fraction	Exp.	Calc.	%AAD	Exp.	Calc.	%AAD
MEG	0.4054	0.5268	0.5270	0.04	617	766	24.12
Water	0.3640	0.4730	0.4730	0.01	1214	1086	10.57
Hydrocarbon	0.2306	243	26	89.48	99.85	99.81	0.03
MEG	0.2372	0.3052	0.3052	0.02	309	443	43.63
Water	0.5400	0.6947	0.6947	0.01	1390	1593	14.59
Hydrocarbon	0.2228	145	5	96.88	99.85	99.80	0.05
MEG	0.1322	0.1654	0.1654	0.04	135	226	67.06
Water	0.6670	0.8345	0.8345	0.01	1669	1949	16.77
Hydrocarbon	0.2009	107	1	99.00	99.83	99.78	0.04

Appendix C: Academic activities

Peer reviewed journal articles

1. M. Frost, G.M. Kontogeorgis, E.H. Stenby, M.A. Yussuf, T. Haugum, K.O. Christensen, E. Solbraa, T.V. Løkken, , Fluid phase Equilibria, (2013) 1-6
2. M. Frost, E. Karakatsani, N. von Solms, D. Richon, G.M. Kontogeorgis, Journal of Chemical Engineering Data, Grant Wilson Special issue 2013, 59 (2014) 961-96
3. M. Riaz, M. A. Yussuf, M. Frost, G.M. Kontogeorgis, E.H. Stenby, W. Yan, E. Solbraa, Energy and Fuels, 28 (2014), 5, p. 3530-3538

Conference presentations

1. M. Frost, G.M. Kontogeorgis, N. von Solms, Measurements and Modeling of Phase Equilibrium of oil-water-polar Chemicals (**Poster**), Study Trip, Houston TX, USA, March 17-23, 2012
2. M. Frost, G.M. Kontogeorgis, N. von Solms, New PhD project: Measurements and modeling of phase equilibrium of oil-water-polar chemicals (**Poster**), CERE Annual Discussion Meeting, Hillerød, Denmark, 2011
3. M. Frost, G.M. Kontogeorgis, N. von Solms, Measurements and Modeling of Oil systems with Water and Polar Chemicals (**Oral**), CERE Annual Discussion Meeting, Hillerød, Denmark, June 13-15, 2012
4. M. Frost, G.M. Kontogeorgis, N. von Solms, Measurements and Modeling of Phase Equilibrium of oil-water-polar Chemicals (**Poster**), 26th ESAT, Potsdam, Germany, Oct. 7-10, 2012
5. M. Frost, G.M. Kontogeorgis, N. von Solms, Experimental method for measurements of VLE/VLLE – equipment and results (**Oral**), CERE Annual Discussion Meeting, Snekkersten, Denmark, June 19-21, 2013

6. M. Frost, G.M. Kontogeorgis, N. von Solms, Measurement and Modeling of Phase Equilibrium of systems containing Polar Chemicals (**Oral**), Thermodynamics 2013, Manchester, UK, Sept. 3-6, 2013
7. M. Frost, G.M. Kontogeorgis, N. von Solms, Oil Characterization with CPA – Modeling and New Experimental Data (**Oral**), CERE Annual Discussion Meeting, Snekkersten, Denmark, June 25-27, 2014

Center for Energy Resources Engineering
Department of Chemical and
Biochemical Engineering
Technical University of Denmark
Søltofts Plads, Building 229
DK-2800 Kgs. Lyngby
Denmark

Phone: +45 4525 2800
Fax: +45 4525 4588
Web: www.cere.dtu.dk

ISBN : 978-87-93054-63-9